Vol. 51 · No. 3 · August 2026

# RDE
Restorative Dentistry & Endodontics



The Korean Academy of Conservative Dentistry

www.rde.ac

RDE Restorative Dentistry & Endodontics Vol. 51 · No. 3 · August 2026 The Korean Academy of Conservative Dentistry

eISSN 2234-7666

Vol. 51 · No. 3 · August 2026

# RDE
Restorative Dentistry & Endodontics

The Korean Academy of Conservative Dentistry

www.rde.ac

RDE Restorative Dentistry & Endodontics

Vol. 51 · No. 3 · August 2026

eISSN 2234-7666

## Aims and Scope

The *Restorative Dentistry and Endodontics* (officially abbreviated as Restor Dent Endod; RDE) is a peer-reviewed and open access journal providing up-to-date information regarding the research and developments on new knowledge and innovations pertinent to the field of contemporary clinical operative dentistry, restorative dentistry, and endodontics. In the field of operative and restorative dentistry, the journal deals with diagnosis, treatment planning, treatment concepts and techniques, adhesive dentistry, esthetic dentistry, tooth whitening, dental materials and implant restoration. In the field of endodontics, the journal deals with a variety of topics such as etiology of periapical lesions, outcome of endodontic treatment, surgical endodontics including replantation, transplantation and implantation, dental trauma, intracanal microbiology, endodontic materials (MTA, nickel-titanium instruments, etc), molecular biology techniques, and stem cell biology. RDE publishes original articles, review articles and case reports dealing with aforementioned topics from all over the world.

RDE is indexed/tracked/covered by Web of Science-Emerging Sources Citation Index (ESCI), Scopus, PubMed, PubMed Central, EBSCO, KoreaMed, Synapse, KCI, Crossref, DOAJ, and Google Scholar.

This Journal was supported by the Korean Federation of Science and Technology Societies Grant funded by the Korean Government (MEST).

## History

RDE (eISSN 2234-7666) is the official journal of the Korean Academy of Conservative Dentistry and was renamed from the *Journal of Korean Academy of Conservative Dentistry* (pISSN 1225-0864; eISSN 2093-8179), which was first published in 1975. It was initially published once a year but became a biannual journal in 1986, a quarterly journal in 1999, and then a bimonthly journal in 2001. From 2012, the journal name was renamed, the official language of the journal was changed to English, and it is currently published quarterly. This journal is supported in part by a Grant from the Korean Federation of Science and Technology Societies funded by the Korean Government (MEST).

## Distribution

Restor Dent Endod is not for sale, but is distributed to members of Korean Academy of Conservative Dentistry and relevant researchers and institutions world-widely on the last day of February, May, August, and November of each year. Full text PDF files are also available at the official website (https://www.rde.ac; http://www.kacd.or.kr), KoreaMed Synapse (https://synapse.koreamed.org), and PubMed Central. To report a change of mailing address or for further information contact the academy office through the editorial office listed below.

## Open Access



**Official Publication of Korean Academy of Conservative Dentistry**
Published on August 31, 2026

**Publisher**
**The Korean Academy of Conservative Dentistry**
B163, Seoul National University Dental Hospital, 101 Daehak-ro, Jongno-gu, Seoul, Korea
Tel: +82-2-763-3818
Fax: +82-2-763-3819
Email: kacd@kacd.or.kr

**Editorial Office**
**The Korean Academy of Conservative Dentistry**
B163 Seoul National University Dental Hospital, 101 Daehak-ro, Jongno-gu, Seoul 03080, Korea
Tel: +82-2-763-3818
Fax: +82-2-763-3819
Email: editor@rde.ac

**Publishing Office**
**M2PI**
#805, 26 Sangwon 1-gil, Seongdong-gu, Seoul 04779, Korea
Tel: +82-2-6966-4930
Fax: +82-2-6966-4945
Email: support@m2-pi.com

RDE Restorative Dentistry & Endodontics

# Editorial Board

RDE Restorative Dentistry & Endodontics

# Contents

Vol. 51 · No. 3 · August 2026

Restorative Dentistry & Endodontics

Review Article

eISSN 2234-7666
Restor Dent Endod. 2026 August;51(3):e28
https://doi.org/10.5395/rde.2026.51.e28

# Educational implications of a novel system for classifying root and canal anatomy in the human dentition: a narrative review

Hany Mohamed Aly Ahmed[1,*], Paul Michael Howell Dummer[2]

[1]Department of Restorative Dentistry, Faculty of Dentistry, Universiti Malaya, Kuala Lumpur, Malaysia
[2]School of Dentistry, College of Biomedical and Life Sciences, Cardiff University, Cardiff, United Kingdom

## ABSTRACT

A comprehensive understanding of both the external and internal anatomy of teeth is fundamental for the effective diagnosis and management of pulp and periapical pathoses. Recent progress in noninvasive, high-resolution imaging modalities, including cone-beam computed tomography and micro-computed tomography, has significantly enhanced the ability to examine the complex morphology of dental structures. These technological advancements have facilitated a level of anatomical detail that was previously unattainable, particularly in the assessment of crown, root, and canal systems. In response to this wealth of new anatomical data, a novel classification framework has been developed, enabling the systematic coding of root and canal configurations across all tooth types. This system offers a more nuanced and comprehensive representation of root canal anatomy compared to earlier classification models. This narrative review explores the implementation of this contemporary classification scheme in education, with a particular focus on its utility in recognizing anatomical variations and accessory canals for the benefit of undergraduate and postgraduate dental students as well as general dental practitioners.

**Keywords:** Ahmed coding system; Classification; Dentition; Education; Root canal anatomy

## INTRODUCTION

A comprehensive knowledge of root and canal morphology in the human dentition is essential for the success of endodontic therapies [1]. Over time, a variety of diagnostic modalities, including staining and clearing techniques, two-dimensional (2D) radiographic imaging, scanning electron microscopy, cone-beam computed tomography (CBCT), and micro-computed tomography (micro-CT), have been utilized in both research and clinical contexts to investigate dental anatomy [2–7]. It is widely recognized that considerable variation exists in root and canal configuration, depending on the type of tooth and the population studied [1,7].

The purpose of classification within scientific disciplines is to systematically organize knowledge and

**Received:** September 15, 2025 **Revised:** January 21, 2026 **Accepted:** February 2, 2026
**Citation**
Ahmed HMA, Dummer PMH. Educational implications of a novel system for classifying root and canal anatomy in the human dentition: a narrative review. Restor Dent Endod 2026;51(3):e28.
***Correspondence to**
**Hany Mohamed Aly Ahmed, PhD**
Department of Restorative Dentistry, Faculty of Dentistry, Universiti Malaya, Jalan Universiti, Kuala Lumpur 50603, Malaysia
Email: hany_endodontist@hotmail.com

to delineate the defining features of the entities being classified [8]. From the pioneering investigations by Hess and Zürcher [2] to contemporary research, there has been a growing recognition of the need for a comprehensive system to describe root and canal morphology across all tooth types and anatomical variations. The Vertucci classification [3] has historically been the most commonly adopted framework for categorizing canal configurations. However, its limitations have been increasingly highlighted in recent studies, which demonstrate that the system does not adequately accommodate the full spectrum of anatomical diversity encountered in clinical practice [9,10]. In light of this shortcoming, a new coding system has been introduced to standardize the classification of root and canal anatomy [9]. This contemporary approach has demonstrated accuracy in both laboratory-based and clinical observational studies [10]. The present article aims to summarize the structure and utility of this novel system, with particular emphasis on its implications for dental education.

## WHY WAS A NEW SYSTEM FOR CLASSIFYING TOOTH ANATOMY NEEDED?

Using tooth sectioning and 2D radiographic techniques, Weine *et al.* [4,11] initially classified root canal configurations (RCCs) into four distinct types (Figure 1A). Vertucci *et al.* [12] subsequently described eight canal types (Figure 1B) with further reports [13–16] identifying 15 other canal configurations to complement Vertucci's original classification [3] (Figure 1C). Later, a range of canal configurations that could not be classified within the existing systems were introduced [17].

The classification system introduced by Vertucci *et al.* [12], along with its supplementary categories, has been the most widely adopted and has proven useful in categorizing numerous canal configurations. However, there are significant limitations within the system, including:

### Lack of information on the root number and location in anterior and premolar teeth

The classification of Vertucci *et al.* [12] organizes RCCs into distinct types; however, it does not provide codes or descriptions for the number of roots or their specific location in anterior and premolar teeth. This limitation leads to several issues.

a) It is impossible to distinguish between a Vertucci type IV canal (which has two separate root canals) in a single-rooted or a double-rooted tooth (Figure 2 [18]), as the number of roots is not specified.
b) Vertucci type V canals (which can have one or two canals) may occur in either single-rooted or double-rooted teeth, but this distinction is not addressed in the system.
c) Maxillary (or mandibular) premolars (or anterior teeth) with three canals are classified as Vertucci type VIII, without accounting for the number of roots or the position of the canal bifurcations along the root.

This lack of detail reduces the accuracy and thus the utility of canal classifications in these specific tooth types.

The absence of this critical information on the num-

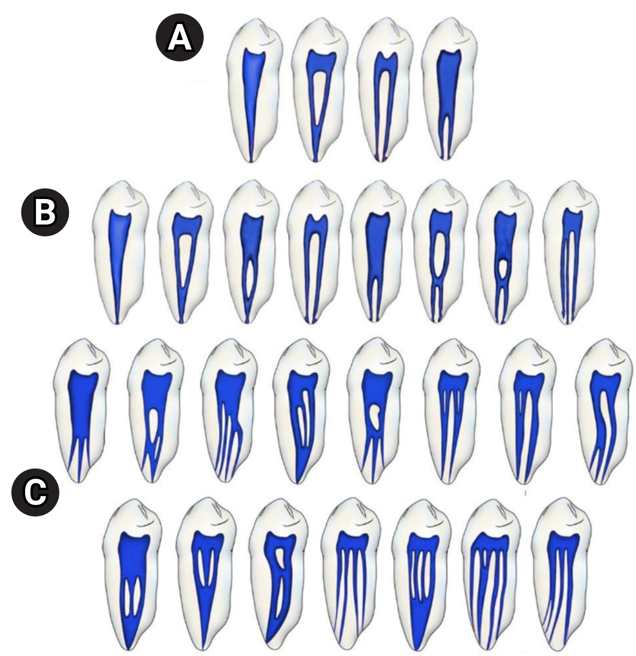


**Figure 1.** Common classifications of root canal configurations. (A) Weine *et al.*'s classification [11]: types I (1), II (2-1), III (2), and IV (1-2). (B) Vertucci *et al.*'s classification [12]: types I (1), II (2-1), III (1-2-1), IV (2), V (1-2), VI (2-1-2), VII (1-2-1-2), and VIII (3). (C) Supplemental configurations of the Vertucci classification [13–16]: types IX (1-3), X (1-2-3-2), XI (1-2-3-4), XII (2-3-1), XIII (1-2-1-3), XIV (4-2), XV (3-2), XVI (2-3), XVII (1-3-1), XVIII (3-1), XIX (2-1-2-1), XX (4), XXI (4-1), XXII (5-4), and XXIII (3-4).


https://doi.org/10.5395/rde.2026.51.e28

ber of roots has significant implications for the clinical management of teeth undergoing root canal treatment and endodontic surgery. One key area affected is access cavity preparation, where premolar teeth with varying root numbers typically have canal orifices located in different positions [19]. Additionally, root canal instrumentation and the preparation for intracanal posts differ in double-rooted maxillary premolars, particularly because of the reduced dentine thickness near the furcation groove on the palatal aspect of the buccal root [19] (Figure 3). In certain cases, the buccal root of double-rooted maxillary premolars may feature deep grooves on both the buccal and palatal surfaces (Figure 3C), further complicating treatment planning.

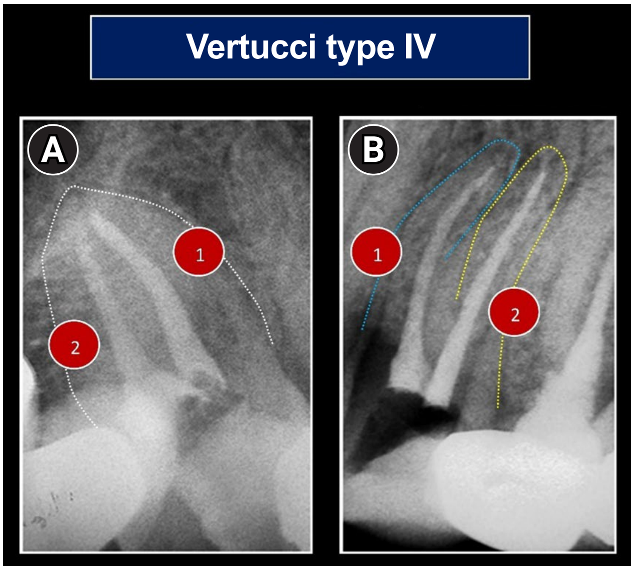


Figure 2. Periapical radiographs of a single-rooted (A) and double-rooted (B) maxillary premolar which are classified the same using the Vertucci classification, that is, type IV (two separate canals). Reproduced and modified from Ahmed *et al.* [18], according to the Creative Commons License.

In addition to the number of roots, the location of the roots is also a crucial factor that the Vertucci system does not define. This lack of information can lead to difficulties in accurately classifying certain tooth configurations. Examples where root location is important include:

a) Anterior teeth with two roots can occur in two forms: either as mesial and distal or buccal and palatal/lingual roots [20].
b) Double-rooted mandibular premolars can present with two variations: either with mesial and distal

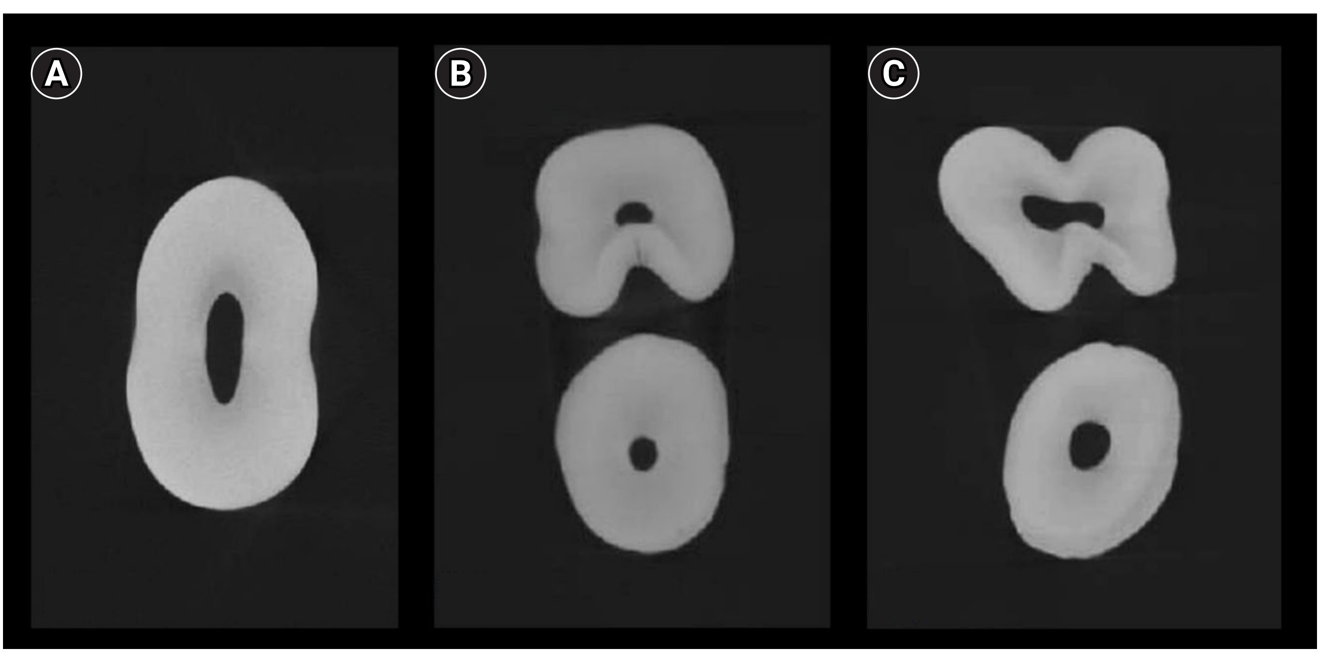


Figure 3. Micro-computed tomography images showing the morphological variations in the axial sections of maxillary premolars: (A) single-rooted; (B) double-rooted with a furcation groove in the palatal aspect of the buccal root; and (C) double-rooted with developmental grooves in the buccal and palatal aspects of the root.

root locations or with buccal and lingual root locations [10] (Figure 4).

c) Maxillary premolars with three roots can appear in a range of configurations, such as having two buccal roots and one palatal root or one buccal root and two palatal roots [19,21].

These variations in root location are important for treatment planning but are not adequately addressed by the Vertucci classification system.

### Absence of clear definitions for root canal components

The Vertucci classification lacks precise definitions for key root canal components, such as the canal orifice. In a subsequent publication, Vertucci [1] described the canal orifice as "a root canal begins as a funnel-shaped canal orifice generally present at or slightly apical to the cervical line." However, this definition lacks clarity regarding what is meant by "slightly apical" to the cervical line. One possible reason for this ambiguity is that the Vertucci classification was based on decalcified, stained teeth, where the preparation process and immersion in strong acids can significantly degrade a tooth's normal anatomical features, including the cementoenamel junction (CEJ). As a result, accurately identifying the CEJ on such specimens is challenging [22].

It is also important to note that, in multi-rooted teeth, the location of the pulp chamber floor may not align with the CEJ [1,23], further complicating the Vertucci system's applicability in such cases.

### Intercanal communications—are they a fundamental component of root canal configurations or not?

An intercanal communication has been defined by the American Association of Endodontists [24] as "a thin communication between two or more canals in the same root or between vascular elements in tissues." However, there is ongoing confusion and a lack of consensus regarding whether such a communication should be considered an integral part of the RCC, influencing its classification, or whether it should be regarded as a minor feature that does not affect the anatomical classification of the main canal system. This issue has been discussed in the literature, with differing views on its significance [25] (Figure 5).

Classifying root canals using the Vertucci classification becomes more complex when intercanal communications are considered as part of the main canal configuration (Figure 5). Since Vertucci [3] did not specify criteria for defining intercanal communications, this leads to further confusion, especially when micro-CT studies report many canal configurations as "Vertucci non-classifiable types" [26,27]. Several observational CBCT clin-

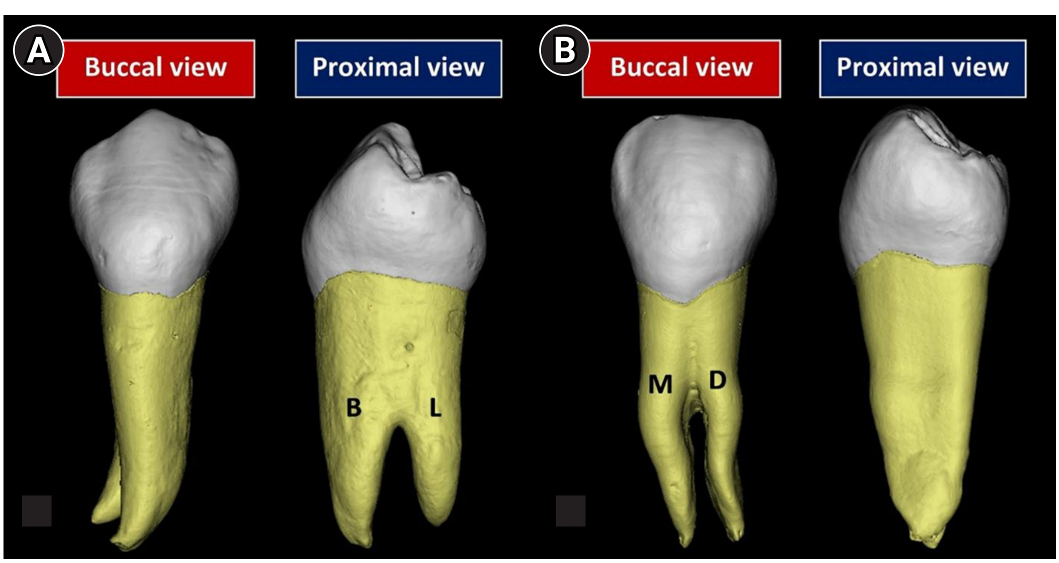


Figure 4. Micro-computed tomography reconstructed images of double-rooted mandibular premolars with (A) buccal and lingual roots and (B) mesial and distal roots. B, buccal; L, lingual; M, mesial; D, distal. Reproduced from Ahmed *et al.* [10], according to the Creative Commons License.


https://doi.org/10.5395/rde.2026.51.e28

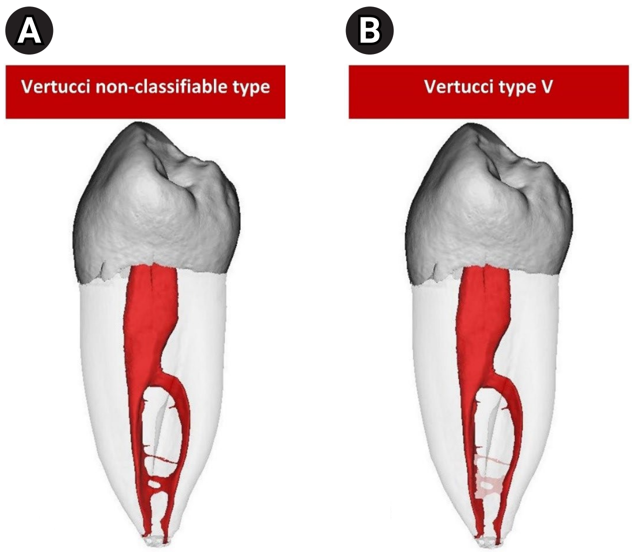


**Figure 5.** A micro-computed tomography image of a mandibular right first premolar, classified using the Vertucci classification [3]: (A) when intercanal communication is included, Vertucci non-classifiable (1-2-1-2-1-2-1-2); (B) when intercanal communication is not included, Vertucci type V.

ical studies either have not included transverse canals as part of the RCC or have failed to clarify the criteria for defining transverse canals when they are not meant to be considered [6,28,29]. This variation in interpretation has led to conflicts when comparing studies, not only due to the use of different diagnostic tools and study models, but also because the same classification system is being applied inconsistently [10].

Classifying a transverse canal anastomosis separately from the main RCC raises concerns due to its clinical significance during various stages of conventional root canal treatment. These stages include canal preparation, filling, as well as root-end cavity preparation and filling during surgery [30–32]. Additionally, a transverse canal anastomosis may communicate with the external root surface, potentially allowing microorganisms and their associated toxins to come into contact with the lateral periodontal and periapical tissues [33]. This highlights the importance of considering such anatomical features in diagnosis and treatment planning.

### Defining root canal configurations using Roman numerals

Defining RCCs using a simple scheme of Roman numerals as done with the Vertucci system has proven to be inadequate, as numerous studies have highlighted the complexity of root canal anatomy in human teeth with many canal configurations being identified as "Vertucci non-classifiable types" [27,34–36]. This underscores the impracticality of using a limited set of Roman numerals to accurately describe the wide variety of canal configurations, making it clear that a more comprehensive system is needed.

## INTRODUCTION TO THE NOVEL SYSTEM FOR ROOT AND CANAL MORPHOLOGY

A novel coding system for classifying root and canal morphology was introduced by Ahmed *et al.* [9], offering comprehensive details on tooth notation, the number of roots, and RCCs. The purpose of this novel system was to establish an accurate and practical framework for use by undergraduate and postgraduate students, clinicians, and researchers. It enables the classification of root and canal configurations when using various methods of tooth examination, ensuring greater consistency and clarity in the assessment of tooth anatomy.

The Ahmed *et al.*'s classification system [9] comprises codes for three distinct components: tooth number (TN), number of roots, and RCC (Figures 6, 7).

### Tooth number

The TN can be expressed using any standard numbering system. In cases where a tooth cannot be identified using one of these systems (e.g., extracted teeth of unknown origin), an appropriate abbreviation may be used. For example, the upper (maxillary) central incisor may be abbreviated as UCI.

### Number of roots

The number of roots (R) is indicated as a superscript before TN ($^{R}$TN). For example, $^{1}$TN means that tooth 'TN' has one root; $^{2}$TN means that the tooth has two roots and so on.

### Root canal configuration

The RCC for each root is indicated as a superscript number(s) following the TN. This defines the continuous course of the root canal system, starting from the

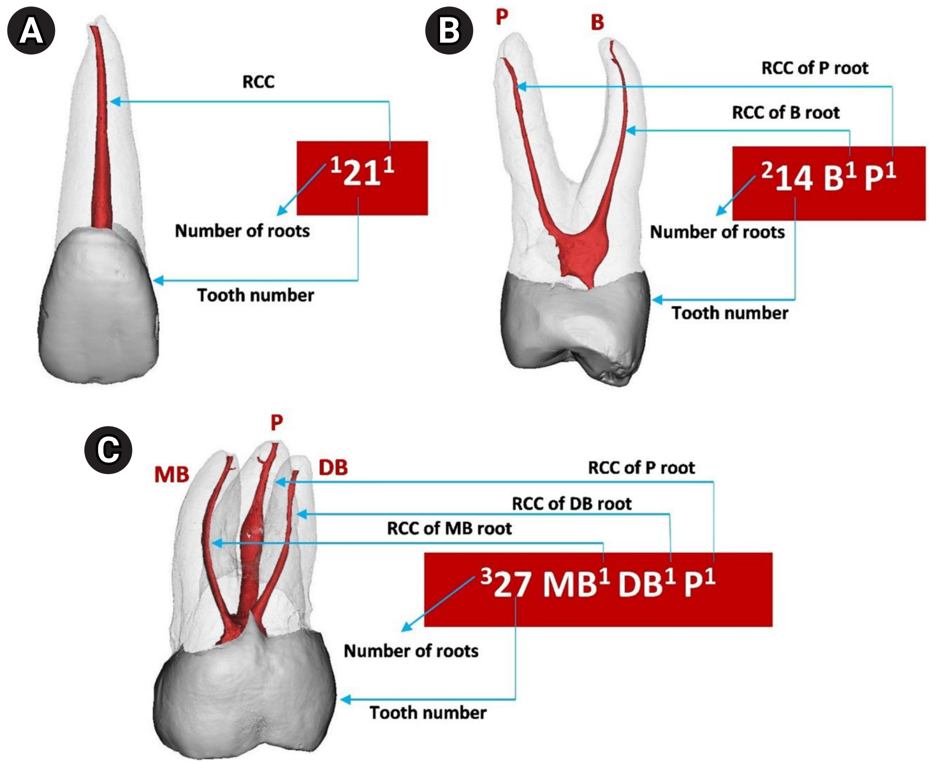


Figure 6. Micro-computed tomography reconstructed images showing the application of the Ahmed *et al.*'s coding system [9] in a range of teeth. (A) $^{1}21^{1}$ refers to a single rooted tooth 21 with a single root canal configuration, (B) $^{2}14$ B$^{1}$ P$^{1}$ refers to a double-rooted tooth 14 in which each of the B and P roots has one root canal, (C) $^{3}27$ MB$^{1}$ DB$^{1}$ P$^{1}$ refers to a three-rooted tooth 27 in which each of the MB, DB and P roots has a single root canal configuration. RCC, root canal configuration; P, palatal; B, buccal; MB, mesio-buccal; DB, disto-buccal.

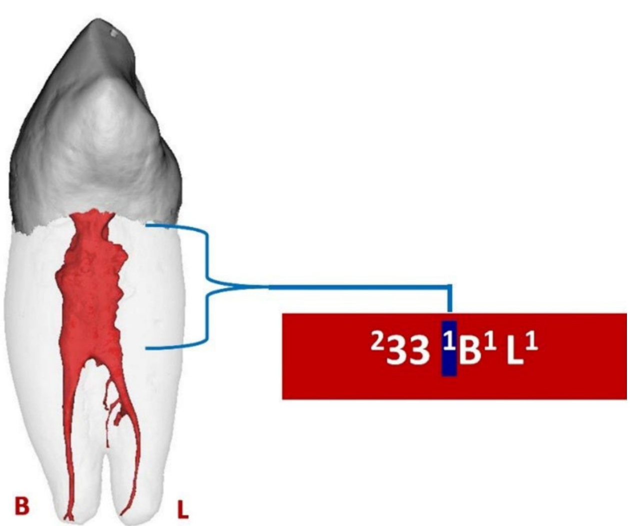


Figure 7. Three-dimensional reconstructed double-rooted mandibular canine with a common canal coronally identified by a superscript number (highlighted in blue) before the buccal (B) and lingual (L) roots.

root canal orifice (O), passing through the canal (C), and ending at the foramen (F) (or foramina). The system specifies that the root canal orifice begins at the CEJ in single-rooted teeth and at the level of bifurcation in multi-rooted teeth.

In certain cases, the root bifurcation in multi-rooted teeth occurs in the middle or apical third of the root. In these instances, a common canal may be present coronally, starting at the level of the CEJ, similar to single-rooted teeth. This common canal is indicated as a superscript before describing the canal configuration for each of the roots (Figure 7). Recently, the coding system has been further applied in the primary dentition [37].

## INVOLVEMENT OF COMPLEMENTARY CODES FOR ACCESSORY CANALS

When necessary, the coding system can also be used to


https://doi.org/10.5395/rde.2026.51.e28

classify accessory canals in conjunction with main canal configurations within a single code. The root length is divided into three sections: coronal third (C), starting from an imaginary line at the most apical portion of the pulp chamber; middle third (M); and apical third (A). Each of these thirds is identified as a superscript within parentheses following the RCC. In some cases, an accessory canal may not terminate in a foramen. In such instances, the code (1-0) indicates a blind accessory canal, and the code (2-1-0) denotes a looped accessory canal. Figure 8 illustrates the application of the new coding system for accessory canals.

## COMPLEMENTARY CODES FOR DENTAL ANOMALIES

The coding system can be adapted to classify root anomalies and their subtypes. The abbreviation for each anomaly (A) can be added within brackets. For example, (DE) refers to "dens evaginatus" affecting a specific tooth (Figure 9).

- When a tooth has two or more different developmental anomalies, a comma (,) should be placed between the initials of each anomaly (A1, A2). For example, (DI, RD) refers to a tooth with both dens invaginatus (DI) and root dilaceration (RD).

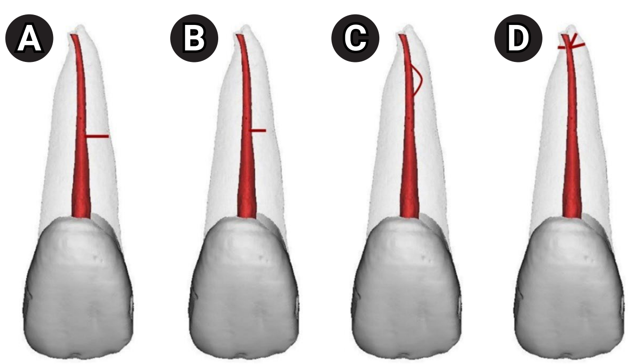


**Figure 8.** Application of the Ahmed *et al.* system [9] to classify root canal configuration and accessory canals in a single code. (A) $^{1}21^{1(M1)}$: Single-rooted tooth 21 with one canal and one patent accessory canal in the middle third. (B) $^{1}21^{1(M1\text{-}0)}$: Single-rooted tooth 21 with one canal and one blind accessory canal in the middle third. (C) $^{1}21^{1(M2\text{-}1\text{-}0)}$: Single-rooted tooth 21 with one canal and one loop accessory canal in the middle third. (D) $^{1}21^{1(MD)}$: Single-rooted tooth 21 with one canal and apical delta.

- A slash (/) should be used to describe fused teeth, such as when one tooth is fused to a supernumerary tooth, or when roots are fused in double-rooted teeth. Two slashes (//) should be used to indicate fused teeth or roots with intercommunications in the root canals.
- The subtype of each anomaly (if applicable) should be written as a superscript following the anomaly abbreviation. For instance, ($D^{II}$) refers to a tooth with dens invaginatus type II [38,39].

## APPLICATIONS OF THE AHMED CODING SYSTEM IN DENTAL EDUCATION

Understanding the external and internal anatomical variations of tooth roots is essential for successful root canal treatment and a range of other endodontic therapies [40,41]. Dental anatomy plays a pivotal role in the endodontic curriculum and serves as the foundation for students to grasp the complexities of root canal systems before progressing to clinical practice. Survey studies are valid research tools that provide information on feedback and behaviors of respondents [42], and they enable continued assessment and evaluation of new trends in endodontic education [43].

### Survey studies examined the coding system in dental education

To date, four survey studies compared the Ahmed coding system to the Vertucci system [44–47]. Three of

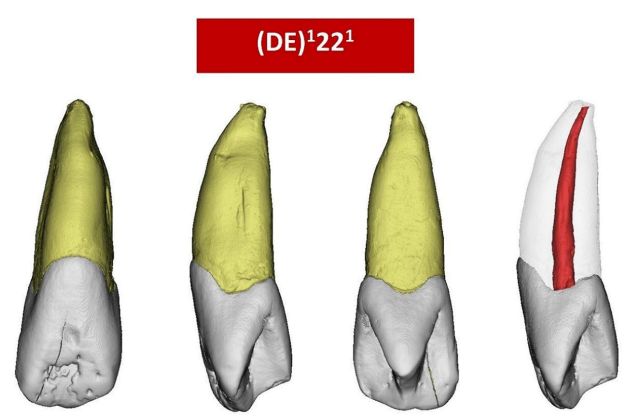


**Figure 9.** Application of the Ahmed *et al.* system [9] to classify a maxillary left lateral incisor with dens evaginatus (DE).

these studies used a validated questionnaire [44–46], in which a Microsoft PowerPoint (PPT) presentation (35 slides; Microsoft Corp., Redmond, WA, USA) was prepared with three components: (i) introduction; (ii) Vertucci classification (and its supplemental configuration types); and (iii) Ahmed coding system together with examples of teeth interpreted using both systems. For consistency, the description of the two classification systems had the same number of slides, font size, slide background, and transition animations; however, since the new system comprises codes with superscripts, the font size of the codes to define root and canal morphology was made larger to allow better visibility. To ensure transparency, the presenters of the PPT presentations in the three studies were independent and did not contribute to the development of the Ahmed coding system.

The fourth study [47] examined the incorporation of small-group practical seminars into a traditional lecture format to improve the understanding of both systems in addition to the Weine classification. The three systems were supported by a brief PPT presentation showing schematic and radiographic images of different canal configurations. This was followed by a practical exercise that included a template showing the external anatomy of the different dental groups, in which the student was requested to draw several internal anatomies based on the different classifications. Table 1 shows the details of the four studies included in this review.

### Preferences of students and general dental practitioners

The first survey conducted among 382 undergraduate dental students from eight Malaysian dental schools revealed that over 90% of students reported that the Ahmed system was more accurate and practical compared to the Vertucci system and its supplemental configurations [44]. More than 95% of students reported that the new coding system improved their understanding of root canal morphology and that they would recommend its inclusion in both preclinical and clinical courses. The positive feedback observed among undergraduate students was similarly echoed by postgraduate dental students in the same study, emphasizing the system's utility in advanced learning [44], similar to the second study done in Peru [45]. The large-scale study in India

**Table 1.** A list of the survey studies that examined the preference of students when using the Ahmed *et al.* coding system [9]

| Study | Year | Country | Teaching method used | Participants | Types of questions | Criteria of the presenter(s) |
|---|---|---|---|---|---|---|
| Ahmed *et al.* [44] | 2020 | Malaysia | PowerPoint presentation (physical lecture) (English) | Undergraduates ($n$ = 382) | Multi-choice questions ($n$ = 5) followed by an open-ended question ($n$ = 1) | Two calibrated presenters graduated from a dental school not less than 10 years ago, had at least 3 years of teaching experience, and did not contribute to the development of the classification systems involved |
| Salas *et al.* [45] | 2021 | Peru | PowerPoint presentation (online lecture) (Spanish) | General dental practitioners and endodontic specialists (82%), members of the Peru Society of Endodontics and dental students (18%) (n = 239) | Multi-choice questions ($n$ = 5) followed by an open-ended question ($n$ = 1) | The presentation was delivered by the first author in an online lecture |
| Karobari *et al.* [46] | 2023 | India | PowerPoint presentation (physical and online lecture) (English) | Undergraduates, interns, and postgraduates ($n$ = 1,082) | Multi-choice questions ($n$ = 5) followed by an open-ended question ($n$ = 1) | A trained and calibrated presenter who did not contribute to the development of the classification systems involved |
| Pérez-Higueras *et al.* [47] | 2024 | Spain | PowerPoint presentation (physical lecture followed by a seminar) (Spanish) | Undergraduates ($n$ = 81)<br>The students were then divided into small groups (10–12 each) | Multi-choice questions ($n$ = 6) followed by open-ended questions ($n$ = 2) | A facilitator with teaching experience in undergraduate endodontics of at least 10 years |


https://doi.org/10.5395/rde.2026.51.e28

involving 1,082 participants from 13 dental schools reported that 93% of participants found the Ahmed classification system to be more practical and accurate compared to the Vertucci system [46].

Figure 10 summarizes the survey results from various studies that used the same questionnaire, comparing

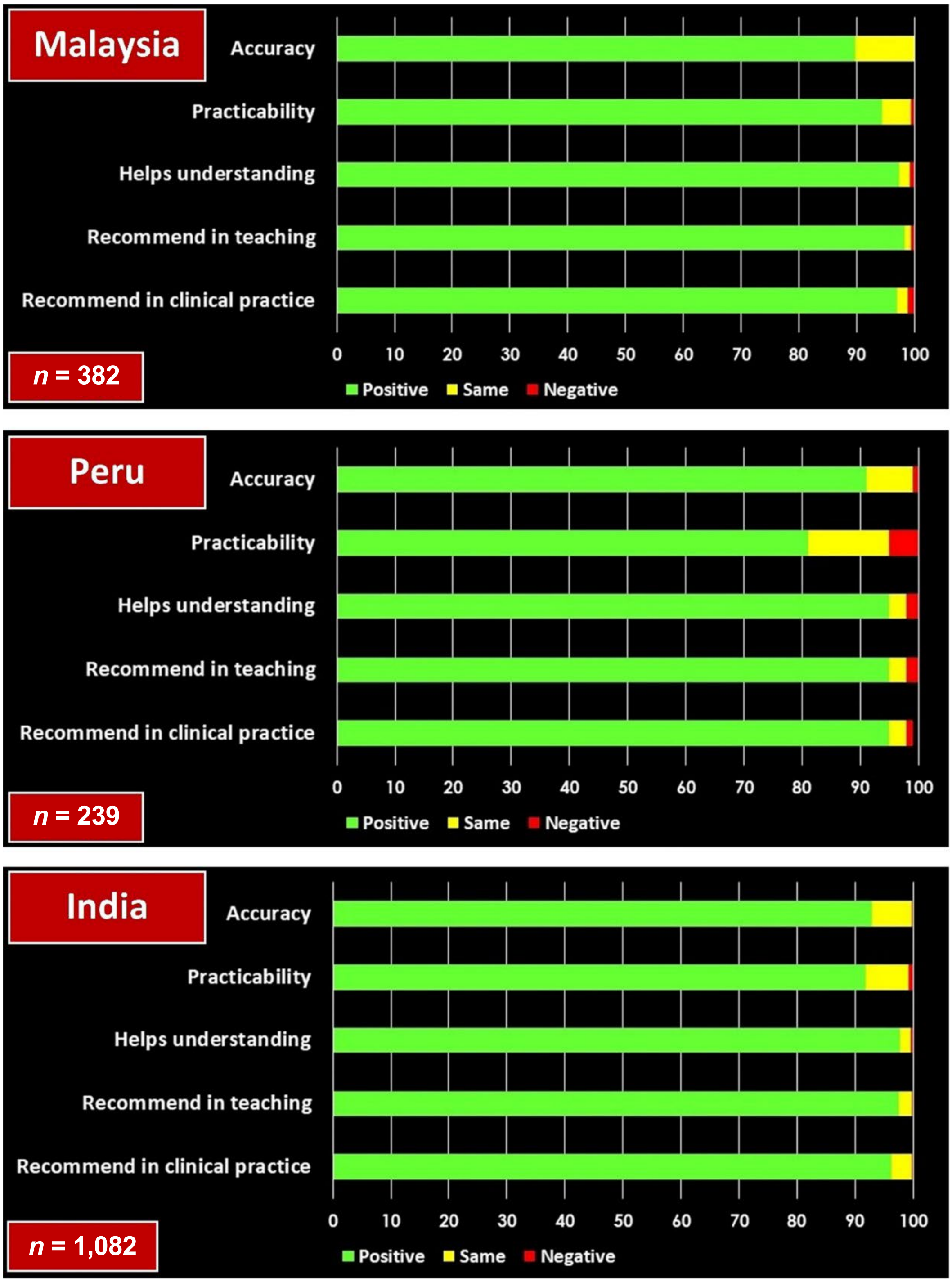


**Figure 10.** Summary of the results obtained from the three surveys that compared the feedback from students and dentists on the Ahmed *et al.* coding system [9] compared to the Vertucci classification [3] in terms of accuracy, practicability, help in understanding of root canal anatomy, and recommendations in teaching and clinical practice.

the responses from dental students, postgraduate students, and practitioners about the practicality and accuracy of the Ahmed coding system versus the Vertucci classification. The results indicate a clear preference for the Ahmed system, which supports its potential for widespread implementation in dental education worldwide.

In the fourth survey study [47], 98.8% of students agreed that the Ahmed classification system was the most complete, and 84% of students found it to be the most intuitive. However, 67% of students reported that the Ahmed system was the most difficult to understand. Despite this difficulty, all students believed that the small-group practical seminars helped them better understand the Ahmed coding system. This study demonstrates that, while the Ahmed system may initially seem complex, the use of interactive seminars significantly enhanced students' comprehension and application of the system, reinforcing the concept that hands-on learning can be an effective tool for understanding complex dental anatomy.

### Reasons behind the favorable reports on the Ahmed coding system

The positive feedback regarding the Ahmed coding system can be attributed to several key factors.

**1. Open system for comprehensive classification**

The coding system is an "open system," meaning it is flexible and adaptable. It is capable of accurately classifying the number of roots and their canal configurations for all teeth, whether simple or complex. This flexibility allows for a more comprehensive approach to classifying root canal systems, offering a greater level of detail than other systems that may be limited to specific types of canal configurations.

**2. No memorization of Roman numerals**

Unlike the Vertucci classification, which relies on Roman numerals for categorizing RCCs, the Ahmed system does not require users to memorize a set of predefined categories. This user-friendly approach simplifies the learning process, as it allows for a more intuitive and flexible method to describe RCCs without being constrained by a rigid classification system. This flexibility makes it easier for both students and clinicians to apply the system in practice.

**3. Student reflections and expanding possibilities**

The survey conducted among Malaysian dental students focused primarily on RCCs; however, students expressed interest in extending the system's application to classify other anatomical features such as accessory canals and anomalies [44]. This feedback highlights the ability of students to think critically about how the system can be adapted to other areas of dental anatomy. Such reflections indicate that students are not only grasping the principles of the system but also developing a deeper understanding of the subject. They are able to apply, analyze, and extend their knowledge in line with Bloom's taxonomy, which emphasizes the importance of learners creating and expanding on existing knowledge [48].

In conclusion, the Ahmed coding system is favored for its flexibility, simplicity, and ability to accurately describe complex anatomical features. Its "open system" structure makes it an effective educational tool that is applicable to the entire range of RCCs, accessory canals, and anomalies. Student feedback and the potential of the system for further expansion underscore its value in enhancing both dental education and clinical practice. This adaptability and the possibility of future improvements suggest that the system can evolve as new anatomical knowledge is acquired, making it a dynamic tool for understanding and classifying dental anatomy. The widespread positive feedback supports its integration into dental curricula across the globe, with students and practitioners recognizing its value in accurately diagnosing and classifying complex root canal systems. These findings, however, should not undermine the value of previous classification systems. Dental practitioners should remain aware of the advantages and limitations of each system. Despite its limitations, the Vertucci classification has been widely used for more than four decades. Its eight canal configuration types can describe many root canal configurations in the human dentition and facilitate comparison with previous studies.


https://doi.org/10.5395/rde.2026.51.e28

### Limitations and technical challenges of the Ahmed coding system

While the Ahmed coding system has demonstrated significant advantages in classifying complex root canal anatomies and providing greater detail compared to other systems, it is important to recognize its limitations, which need to be considered by dental professionals, educators, and researchers when applying this classification in practice.

**1. Increased number of groupings**

One of the limitations of the Ahmed system is that it often results in a larger number of groupings for teeth with more intricate canal anatomical features, especially in cases involving multi-rooted teeth (maxillary and mandibular premolars and molars), examined using highly accurate devices such as micro-CT which allows the visualization of fine canal branchings and even the smallest accessory canals that may not be visible with other methods [10,49–52].

This increased number of groups has also been documented in previous CBCT studies [53–55]. A recent study [56] compared root and canal anatomy in maxillary first premolars in 22 countries using both the Ahmed and Vertucci systems and concluded that the Ahmed coding system was more accurate and comprehensive than the Vertucci system. However, a larger number of groups was observed when using the Ahmed system because it takes into account the number of roots (so each single, double, and three-rooted variant will have separate codes) in addition to the complex canal anatomy that was allocated with separate codes corresponding to the large number of non-classifiable Vertucci types.

This expanded number of tooth groups in micro-CT and CBCT anatomy studies might appear overwhelming to some users, particularly those unfamiliar with the finer details of tooth anatomy. While this increased granularity may seem complex, it allows for a more precise categorization of complex canal configurations, providing clinicians with specific and accurate information to plan treatments accordingly [10]. This is also important for accurate comparisons between research studies.

Traditional 2D radiographs can be helpful for basic canal classification, but often lack the detail required for identifying complex anatomical features or subtle canal variations. As a result, the classification of canal anatomy using 2D images leads to fewer groups but is less accurate than those obtained using more advanced three-dimensional (3D) imaging techniques [57].

**2. Learning curve**

Given the detailed nature of the Ahmed coding system, it requires a learning curve for dental students and practitioners who are new to this approach, especially when classifying multi-rooted teeth with common canals (Figure 7), and when the complementary codes are used to classify teeth with multiple roots, canal configurations, accessory canals, and anomalies [44]. As mentioned above, the use of interactive seminars enhances the comprehension and understanding of root canal anatomy classifications [47].

## DIRECTIONS FOR FUTURE RESEARCH

### Integration of the system with case difficulty assessment tools

The Ahmed coding system plays an essential role not only in classifying root canal anatomy but also in determining the difficulty level of a particular case scheduled for root canal treatment. This is particularly important in clinical practice, especially when the operator is an undergraduate dental student, a postgraduate student, or a general dental practitioner (GDP).

Taking into account the inherent limitations of diagnostic 2D periapical imaging, it is crucial that each case be appropriately assessed according to the operator's level of knowledge and skill, so the level of complexity is tackled at the appropriate stage of their education or career. This would provide them with a structured approach to anticipate challenges and plan accordingly, and also ensure optimal patient care and minimize the risk of errors or complications during treatment. For example, a tooth code of $^{2}$14 B$^{1}$ P$^{1}$ refers to a double-rooted maxillary molar tooth (tooth 14), where each root (B and P) has a single canal. This is a relatively straightforward case and most likely suitable for an undergraduate dental student or a GDP. A tooth code of (RE) $^{3}$46 M$^{2}$ D$^{1}$ DL$^{1}$ refers to a three-rooted mandibular molar tooth (tooth 46) (RE refers to radix entomolaris), where the mesial root (M) has two separate canals and each of the distal root (D) and disto-lingual root (DL) has a single canal. Given the usual buccal curvature of the DL root, the case would be more challenging for a dental student or GDP and would be more suitable for an endodontic specialist. Indeed, the availability of CBCT data would provide more detailed codes and thus a more accurate case difficulty assessment process.

### Evaluation of the effectiveness in improving students' understanding of root canal morphology

Future studies should also assess the effectiveness of the system in improving students' understanding of root and canal morphology and the consistency of students' ability to apply the system, especially in identifying different canal configurations across various tooth types. The evaluation of the coding system by researchers in different countries with various educational backgrounds and teaching models is needed. The implementation of calibration sessions, particularly for undergraduate and postgraduate students, as well as for practitioners unfamiliar with the system, would be beneficial to ensure that the Ahmed coding system is applied consistently by different users. This would help ensure that the system is used in a uniform manner across different clinical and educational settings.

### Integration of the system with virtual reality in teaching root canal anatomy

Several studies have explored innovative teaching methods to improve the understanding of root canal anatomy by dental students. Reymus *et al.* [58] reported favorable feedback from third-year undergraduate students who were taught root canal anatomy using virtual reality (VR). The VR application incorporated the Ahmed coding system for classifying the CBCT scanned teeth where the Digital Imaging and Communications in Medicine (DICOM) files were converted to Standard Tessellation Language (STL) files imported into a VR software and viewed in a head-mounted VR device. The VR environment helped students to interact with 3D models of teeth and visualize RCCs in a more engaging and dynamic way. The immersive experience of VR likely helped students grasp complex anatomical concepts more effectively.

Another study [59] utilized STL files from DICOM files of micro-CT scanned teeth classified using the Vertucci and Ahmed coding system; the researchers used a software application that was designed to be compatible with Android handheld devices for augmented reality and VR devices. By combining interactive digital technologies with traditional teaching methods, this approach allowed students to visualize and manipulate root canal systems in a highly interactive environment. The use of this technology further enhanced students' understanding of root canal anatomy and the various classification systems. Future studies can use micro-CT scanned models for the development of a VR environment presenting the complementary codes of the Ahmed *et al.* system, thus integrating the main and accessory canals in a single code, as shown in Figure 11. This can also be applied to dental anomalies and the anatomical variations in the primary dentition.

### Integration of the system with deep learning models

A recent review discussed potential applications of artificial intelligence (AI) in root canal anatomy education [60]. The use of real-time AI-assisted analysis of 2D and CBCT imaging is a promising platform for root canal anatomy education of dental students and classifications of root and canal configurations using the novel coding system. Deep learning models that guide students to focus on certain landmarks on enhanced 2D radiographic images may help improve their skills and their ability during case difficulty assessment. The AI platform can also provide guidelines to help students navigate through the steps involved in the management (including access cavity preparation, instrumentation plan, and root canal filling) of different canal types, ranging from simple to more complex codes. However, it has to be acknowledged that the development of accurate AI models suitable for educational purposes requires large, diverse datasets for training and validation. Clinical exploration of canals remains an important step for the identification and classification of roots and canals. At present, AI applications should be used in root and canal anatomy education with caution, since they may generate incorrect recommendations if there is an over-reliance on technology based on limited patient data [61]. AI applications for the use of the Ahmed


https://doi.org/10.5395/rde.2026.51.e28

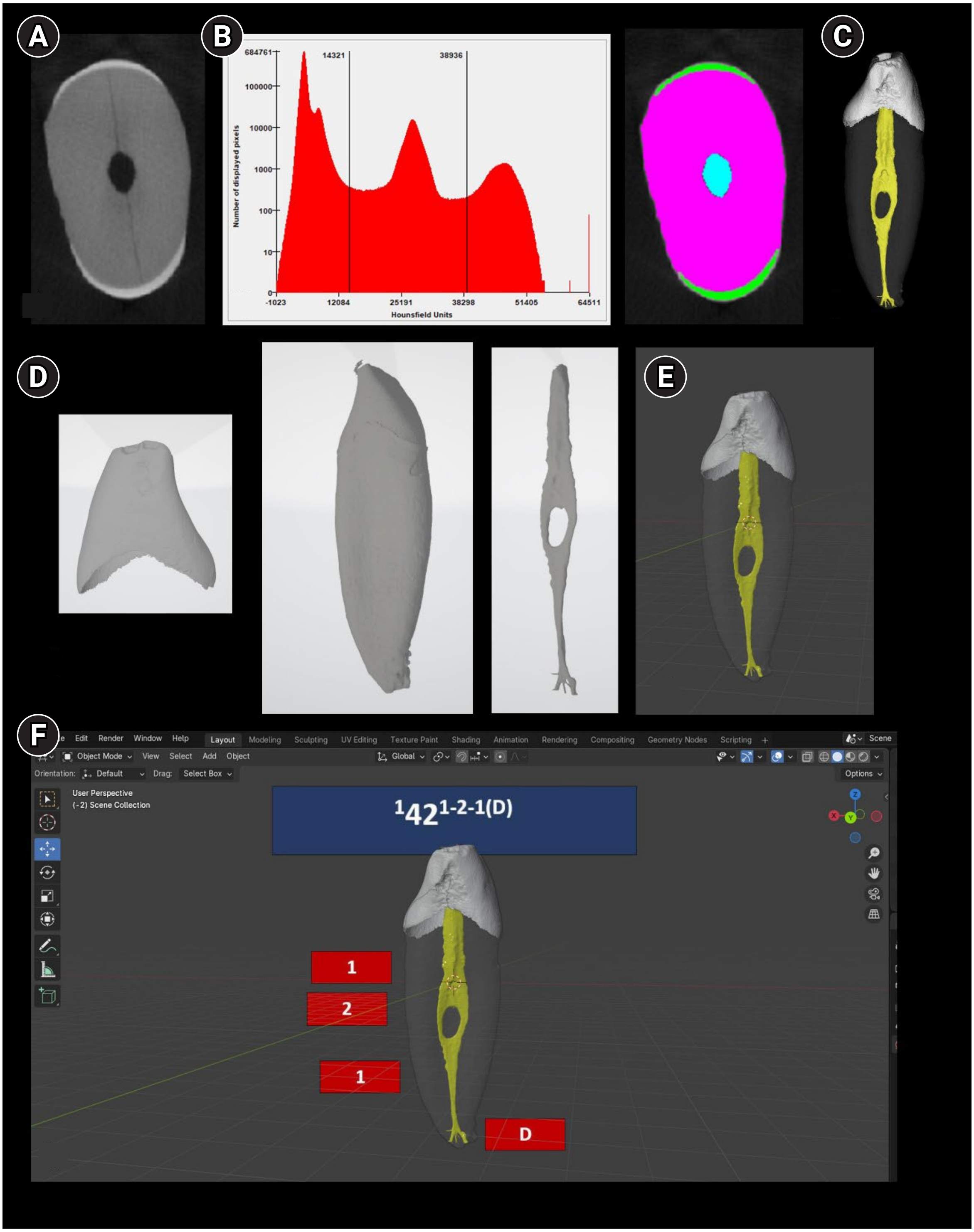


**Figure 11.** Potential application of micro-computed tomography (micro-CT) scanned teeth for virtual reality (VR) applications using complementary codes of the Ahmed *et al.*'s system [9]. (A) After micro-CT scanning (axial section) and the use of Mimics software (DICOM files). (B) After segmentation of the enamel, dentine, and pulp space. (C) After three-dimensional (3D) reconstruction. (D) Conversion to STL (Standard Tessellation Language) files. (E) Using Blender (version 4.4.3; Blender Foundation, Amsterdam, Netherlands) for 3D reconstruction. (F) After the addition of complementary codes for main and accessory canals for a single-rooted tooth 42 with canal configuration 1-2-1 and an apical delta (D). This can be used with a VR device.

coding system in different imaging and education tools require further research.

## CONCLUSIONS

The Ahmed coding system has shown considerable promise for classifying root and canal anatomy, particularly in teeth with multiple roots and/or complex canal anatomy. The integration of technology-enhanced educational approaches, such as 3D imaging and interactive learning platforms, significantly enhances comprehension of root and canal anatomy when interpreted using contemporary classification systems. However, dental students, educators, and clinicians must be aware of the strengths and limitations of these systems. Future research is needed to explore AI applications in improving the interpretation and classification of root and canal anatomy.

### CONFLICT OF INTEREST

No potential conflict of interest relevant to this article was reported.

### FUNDING/SUPPORT

The authors have no financial relationships relevant to this article to disclose.

### AUTHOR CONTRIBUTIONS

Conceptualization, Methodology: Ahmed HMA, Dummer PMH. Writing - original draft: Ahmed HMA. Writing - review & editing: Ahmed HMA, Dummer PMH. All authors read and approved the final manuscript.

### DATA SHARING STATEMENT

The datasets are not publicly available but are available from the corresponding author upon reasonable request.

### DISCOLURE OF GENERATIVE AI IN SCIENTIFIC WRITING

An AI tool was used solely to edit selected paragraphs of the manuscript.

## REFERENCES

1. Vertucci FJ. Root canal morphology and its relationship to endodontic procedures. Endod Topics 2005;10:3-29.
2. Hess W, Zürcher E. The anatomy of the root-canals of the teeth of the permanent dentition. New York: William Wood & Co; 1925.
3. Vertucci FJ. Root canal anatomy of the human permanent teeth. Oral Surg Oral Med Oral Pathol 1984;58:589-599.
4. Weine FS, Hayami S, Hata G, Toda T. Canal configuration of the mesiobuccal root of the maxillary first molar of a Japanese sub-population. Int Endod J 1999;32:79-87.
5. Morfis A, Sylaras SN, Georgopoulou M, Kernani M, Prountzos F. Study of the apices of human permanent teeth with the use of a scanning electron microscope. Oral Surg Oral Med Oral Pathol 1994;77:172-176.
6. Martins JN, Marques D, Mata A, Caramês J. Root and root canal morphology of the permanent dentition in a Caucasian population: a cone-beam computed tomography study. Int Endod J 2017;50:1013-1026.
7. Versiani MA, Ordinola-Zapata R, Keleş A, Alcin H, Bramante CM, Pécora JD, *et al.* Middle mesial canals in mandibular first molars: a micro-CT study in different populations. Arch Oral Biol 2016;61:130-137.
8. Stains M, Talanquer V. Classification of chemical reactions: stages of expertise. J Res Sci Teaching 2008;45:771-793.
9. Ahmed HM, Versiani MA, De-Deus G, Dummer PM. A new system for classifying root and root canal morphology. Int Endod J 2017;50:761-770.
10. Ahmed HM, Rossi-Fedele G, Dummer PM. Critical analysis of a new system to classify root and canal morphology: a systematic review. Aust Endod J 2023;49:750-768.
11. Weine FS, Healey HJ, Gerstein H, Evanson L. Canal configuration in the mesiobuccal root of the maxillary first molar and its endodontic significance. Oral Surg Oral Med Oral Pathol 1969;28:419-425.
12. Vertucci F, Seelig A, Gillis R. Root canal morphology of the human maxillary second premolar. Oral Surg Oral Med Oral Pathol 1974;38:456-464.
13. Gulabivala K, Aung TH, Alavi A, Ng YL. Root and canal morphology of Burmese mandibular molars. Int Endod J 2001;34:359-370.
14. Gulabivala K, Opasanon A, Ng YL, Alavi A. Root and canal morphology of Thai mandibular molars. Int Endod J 2002;35:56-62.
15. Ng YL, Aung TH, Alavi A, Gulabivala K. Root and canal morphology of Burmese maxillary molars. Int Endod J 2001;34:620-630.
16. Sert S, Bayirli GS. Evaluation of the root canal configurations


https://doi.org/10.5395/rde.2026.51.e28

of the mandibular and maxillary permanent teeth by gender in the Turkish population. J Endod 2004;30:391-398.
17. Versiani MA, Ordinola-Zapata R. Root canal anatomy: implications in biofilm disinfection. In: Chávez de Paz L, Sedgley C, Kishen A, editors. Root canal biofilms. Cham: Springer; 2015.
18. Ahmed HM, Hashem AA, Dummer PM. Application of a new system for classifying root and canal anatomy in clinical practice: explanation and elaboration. Eur Endod J 2021;6:132-142.
19. Ahmed HM, Cheung GS. Accessory roots and root canals in maxillary premolar teeth: a review of a critical endodontic challenge. ENDO (Lond Engl) 2012;6:7-18.
20. Ahmed HM, Hashem AA. Accessory roots and root canals in human anterior teeth: a review and clinical considerations. Int Endod J 2016;49:724-736.
21. Neelakantan P, Subbarao C, Ahuja R, Subbarao CV. Root and canal morphology of Indian maxillary premolars by a modified root canal staining technique. Odontology 2011;99:18-21.
22. Ahmed HM, Ibrahim N, Mohamad NS, Nambiar P, Muhammad RF, Yusoff M, *et al*. Application of a new system for classifying root and canal anatomy in studies involving micro-computed tomography and cone beam computed tomography: explanation and elaboration. Int Endod J 2021;54:1056-1082.
23. Ahmed HM, Keleş A, Wolf TG, Nagendrababu V, Duncan HF, Peters OA, *et al*. Controversial terminology in root and canal anatomy: a comprehensive review. Eur Endod J 2024;9:308-334.
24. American Association of Endodontists. Glossary of endodontic terms [Internet]. Chicago: American Association of Endodontists; 2020 [cited 2024 Oct 18]. Available from: https://www.aae.org/specialty/download/glossary-of-endodontic-terms/
25. Karobari MI, Noorani TY, Halim MS, Dummer PM, Ahmed HM. Should inter-canal communications be included in the classification of root canal systems? Int Endod J 2019;52:917-919.
26. Filpo-Perez C, Bramante CM, Villas-Boas MH, Húngaro Duarte MA, Versiani MA, Ordinola-Zapata R. Micro-computed tomographic analysis of the root canal morphology of the distal root of mandibular first molar. J Endod 2015;41:231-236.
27. Leoni GB, Versiani MA, Pécora JD, Damião de Sousa-Neto M. Micro-computed tomographic analysis of the root canal morphology of mandibular incisors. J Endod 2014;40:710-716.
28. Arslan H, Ertas H, Ertas ET, Kalabalık F, Saygılı G, Capar ID. Evaluating root canal configuration of mandibular incisors with cone-beam computed tomography in a Turkish population. J Dent Sci 2015;10:359-364.
29. da Silva EJ, de Castro RW, Nejaim Y, Silva AI, Haiter-Neto F, Silberman A, *et al*. Evaluation of root canal configuration of maxillary and mandibular anterior teeth using cone beam computed tomography: an in-vivo study. Quintessence Int 2016;47:19-24.
30. von Arx T. Frequency and type of canal isthmuses in first molars detected by endoscopic inspection during periradicular surgery. Int Endod J 2005;38:160-168.
31. Endal U, Shen Y, Knut A, Gao Y, Haapasalo M. A high-resolution computed tomographic study of changes in root canal isthmus area by instrumentation and root filling. J Endod 2011;37:223-227.
32. Wu MK, Dummer PM, Wesselink PR. Consequences of and strategies to deal with residual post-treatment root canal infection. Int Endod J 2006;39:343-356.
33. Villegas JC, Yoshioka T, Kobayashi C, Suda H. Frequency of transverse anastomoses with and without apical communication in Japanese population teeth. Aust Endod J 2004;30:50-52.
34. Verma P, Love RM. A Micro CT study of the mesiobuccal root canal morphology of the maxillary first molar tooth. Int Endod J 2011;44:210-217.
35. Lee KW, Kim Y, Perinpanayagam H, Lee JK, Yoo YJ, Lim SM, *et al*. Comparison of alternative image reformatting techniques in micro-computed tomography and tooth clearing for detailed canal morphology. J Endod 2014;40:417-422.
36. Kim Y, Chang SW, Lee JK, Chen IP, Kaufman B, Jiang J, *et al*. A micro-computed tomography study of canal configuration of multiple-canalled mesiobuccal root of maxillary first molar. Clin Oral Investig 2013;17:1541-1546.
37. Ahmed HM, Musale PK, El Shahawy OI, Dummer PM. Application of a new system for classifying tooth, root and canal morphology in the primary dentition. Int Endod J 2020;53:27-35.
38. Oehlers FA. Dens invaginatus (dilated composite odontome): I. Variations of the invagination process and associated anterior crown forms. Oral Surg Oral Med Oral Pathol 1957;10:1204-1218.
39. Oehlers FA. Dens invaginatus (dilated composite odon-

tome): II. Associated posterior crown forms and pathogenesis. Oral Surg Oral Med Oral Pathol 1957;10:1302-1316.
40. Cantatore G, Berutti E, Castellucci A. Missed anatomy: frequency and clinical impact. Endod Top 2006;15:3-31.
41. Ahmed HM, El-Karim I, Duncan HF, Krastl G, Galler K. Implications of root, pulp chamber, and canal anatomy on pulpotomy and revitalization procedures. Clin Oral Investig 2023;27:6357-6369.
42. Lydeard S. The questionnaire as a research tool. Fam Pract 1991;8:84-91.
43. Mala S, Lynch CD, Burke FM, Dummer PM. Attitudes of final year dental students to the use of rubber dam. Int Endod J 2009;42:632-638.
44. Ahmed HM, Che Ab Aziz ZA, Azami NH, Farook MS, Khan AA, Mohd Noor NS, *et al*. Application of a new system for classifying root canal morphology in undergraduate teaching and clinical practice: a national survey in Malaysia. Int Endod J 2020;53:871-879.
45. Salas H, Torres J, Pauro J, Ahmed HM. A new coding system for root and canal morphology: an online survey from Peru. Int Endod J 2021;54:147-149.
46. Karobari MI, Ahmed HM, Khamis MF, Ibrahim N, Noorani TY. Application of two systems to classify the root and canal morphology in the human dentition: a national survey in India. J Dent Educ 2023;87:1089-1098.
47. Pérez-Higueras JJ, Oteo B, Gancedo-Caravia L, Arias A. Influence of the incorporation of small-group practical seminars to a traditional lecture for the understanding of root canal morphology classification systems. Eur J Dent Educ 2024;28:371-376.
48. Krathwohl DR. A revision of Bloom's taxonomy: an overview. Theory Pract 2002;41:212-218.
49. Aljawhar AM, Ibrahim N, Abdul Aziz A, Ahmed HM, Azami NH. Micro-computed tomographic evaluation of root and canal anatomy of maxillary first premolars in Iraqi sub-population. Sci Rep 2025;15:10821.
50. Ahmed HM, Noor NS, Hasanusi HF, Khalid PN, Nabhan MS, Noorani TY, *et al*. Characterisation of root canal configurations and accessory canals in mandibular incisors: a micro-computed tomography study on a Malaysian subpopulation. Aust Endod J 2025;51:258-266.
51. Villa N, Weissheimer T, Vier-Pelisser FV, Alcalde MP, Vivan RR, Duarte MA, *et al*. Comparative study of Vertucci and Ahmed classifications to evaluate the main root canal configuration of mandibular incisors in a Brazilian population. Aust Endod J 2022;48:409-414.
52. Saber SM, Elashiry MM, Sadat SM, Nawar NN. A microcomputed tomographic analysis of the morphological variabilities and incidence of extra canals in mandibular first molar teeth in an Egyptian subpopulation. Sci Rep 2023;13:8985.
53. Olczak K, Pawlicka H, Szymański W. Root form and canal anatomy of maxillary first premolars: a cone-beam computed tomography study. Odontology 2022;110:365-375.
54. Buchanan GD, Gamieldien MY, Fabris-Rotelli I, van Schoor A, Uys A. A study of mandibular premolar root and canal morphology in a Black South African population using cone-beam computed tomography and two classification systems. J Oral Sci 2022;64:300-306.
55. Buchanan GD, Gamieldien MY, Fabris-Rotelli I, Van Schoor A, Uys A. Root and canal morphology of maxillary second molars in a Black South African subpopulation using cone-beam computed tomography and two classifications. Aust Endod J 2023;49 Suppl 1:217-227.
56. Pertek Hatipoğlu F, Magat G, Karobari MI, Madarati AA, Tulegenova I, Hatipoğlu Ö, *et al*. Root and canal configurations of maxillary first premolars in 22 countries using two classification systems: a multinational cross-sectional study. Sci Rep 2025;15:19290.
57. Ahmed HM. A critical analysis of laboratory and clinical research methods to study root and canal anatomy. Int Endod J 2022;55 Suppl 2:229-280.
58. Reymus M, Liebermann A, Diegritz C. Virtual reality: an effective tool for teaching root canal anatomy to undergraduate dental students: a preliminary study. Int Endod J 2020;53:1581-1587.
59. Diegritz C, Fotiadou C, Fleischer F, Reymus M. Tooth anatomy inspector: a comprehensive assessment of an extended reality (XR) application designed for teaching and learning of root canal anatomy by students. Int Endod J 2024;57:1682-1688.
60. Ahmed HM, Al-Maswary A, Habaebi M, Tasdelen A, Al Husaini MA, Elnawawy H, *et al*. Artificial intelligence in the study of root and canal anatomy: a comprehensive review on applications, advantages, challenges and future directions. Eur Endod J 2025;10:343-364.
61. Aminoshariae A, Nosrat A, Nagendrababu V, Dianat O, Mohammad-Rahimi H, O'Keefe AW, *et al*. Artificial intelligence in endodontic education. J Endod 2024;50:562-578.


https://doi.org/10.5395/rde.2026.51.e28

RDE Restorative Dentistry & Endodontics

Research Article

eISSN 2234-7666
Restor Dent Endod. 2026 August;51(3):e29
https://doi.org/10.5395/rde.2026.51.e29

# Diagnostic accuracy of ChatGPT-5 in evaluating root canal treatment and periapical pathosis on periapical radiographs

**Waleed Almutairi[1,*], Mujahid Alnasser[2], Hanan Alharbi[1], Obadah Austah[3]**

[1]Division of Endodontics, Department of Conservative Dental Sciences, College of Dentistry, Qassim University, Qassim, Saudi Arabia
[2]General Practitioner, Dr. Tooth Private Clinics, Qassim, Saudi Arabia
[3]Department of Endodontics, Faculty of Dentistry, King Abdulaziz University, Jeddah, Saudi Arabia

## ABSTRACT

**Objectives:** Artificial intelligence (AI) chatbots such as ChatGPT-5 (OpenAI) are increasingly used for dental radiograph interpretation, especially among patients seeking self-assessment. However, their diagnostic accuracy in endodontics remains unclear.
**Methods:** This cross-sectional STARD-AI-compliant study analyzed 271 anonymized periapical radiographs of endodontically treated posterior teeth, classified as straightforward ($n = 167$) or complex ($n = 104$), using standardized ChatGPT-5 prompts. Diagnostic criteria included obturation length (short, adequate, long), presence of voids, and periapical pathosis. Results were compared to those of a panel of general dentists and a reference standard from endodontic specialists. Sensitivity, specificity, and accuracy were calculated using the McNemar test ($p < 0.05$).
**Results:** ChatGPT-5 demonstrated high specificity (up to 99.3%) for normal or adequately treated findings but low sensitivity for short (13.7%) or long (0.0%) obturations, voids (9.0%–22.7%), and periapical lesions (10.5%–28.6%). Overall accuracy (54.0%–63.2%) was significantly lower than that of general dentists (76.0%–85.6%) ($p < 0.001$).
**Conclusions:** Although ChatGPT-5 achieved high specificity, its low sensitivity and overall accuracy limit diagnostic reliability. Expert clinician oversight remains essential for accurate interpretation and treatment planning.

**Keywords:** Artificial intelligence; Dental radiography; Diagnostic accuracy; Endodontics; Generative artificial intelligence

## INTRODUCTION

Artificial intelligence (AI) chatbots have transformed digital communication by enabling people to ask targeted, individualized inquiries and receive precise, context-specific answers [1]. This is accomplished by mimicking the neural networks found in the human brain. One of the most prominent examples is ChatGPT-5 (OpenAI, San Francisco, CA, USA), a multimodal AI system capable of processing both textual and visual inputs

**Received:** November 8, 2025 **Revised:** January 16, 2026 **Accepted:** January 20, 2026

**Citation**
Almutairi W, Alnasser M, Alharbi H, Austah O. Diagnostic accuracy of ChatGPT-5 in evaluating root canal treatment and periapical pathosis on periapical radiographs. Restor Dent Endod 2026;51(3):e29.

***Correspondence to**
**Waleed Almutairi, BDS, MS**
Division of Endodontics, Department of Conservative Dental Sciences, College of Dentistry, Qassim University, Qassim, Saudi Arabia
Email: wgm1410@gmail.com

[2]. In this context, 'multimodal' refers to the model's ability to process and integrate both textual input and visual data, such as radiographic images, within a single analytical framework.

ChatGPT-5 has become deeply integrated into modern daily life, with applications extending from education and business to healthcare clinical decision support [3]. This expanding scope of use has naturally extended into healthcare contexts, where patients increasingly upload medical and dental images to AI platforms in search of preliminary interpretations or reassurance [4]. This trend reflects the rising influence of AI as an auxiliary source of information that allows patients to engage more actively in health-related decision-making [5]. In dentistry, ChatGPT-5 can provide valuable insights and descriptive assessment of radiographic density patterns, quality of root canal treatment, and pathological changes [6,7]. However, it is important to acknowledge that the diagnostic reliability of general-purpose AI models in radiographic interpretation has not been scientifically validated [8,9].

Despite the widespread use of ChatGPT-5 in healthcare-related contexts, its diagnostic accuracy in dental radiography, particularly in endodontics, remains largely unexplored. Only a few preliminary studies have evaluated AI models' performance in dental imaging [10], and most have focused on domain-specific algorithms rather than generalist large language models. The lack of validation raises concerns regarding potential misinterpretations when patients or clinicians rely on these systems for diagnostic insights.

Therefore, this study aimed to evaluate the diagnostic accuracy of ChatGPT-5 in interpreting periapical radiographs of endodontically treated teeth and to compare its performance with that of practicing general dentists and an expert endodontic reference standard. To our knowledge, this is the first investigation to benchmark a general-purpose AI chatbot against human clinicians using real radiographic data in endodontics.

## METHODS

This diagnostic accuracy study was conducted in accordance with the Standards for Reporting Diagnostic Accuracy Studies 2015 (STARD 2015) and the STARD-Artificial Intelligence (STARD-AI) extension for studies involving AI-based diagnostic systems [11]. The study protocol was retrospectively registered and made publicly available on the Open Science Framework (https://osf.io/kmsqx). All key methodological components of the study, including design, participant selection, index test, reference standard, and statistical analysis, were reported in compliance with these guidelines to ensure transparency and reproducibility. STARD-compliant flow diagrams are presented in Figures 1 to 3.

Ethical approval was granted by the Institutional Review Board of the Ministry of Health, Qassim Province, Saudi Arabia (H-040Q-001), and the study complied with the principles of the Declaration of Helsinki. Because the study used anonymized retrospective data,

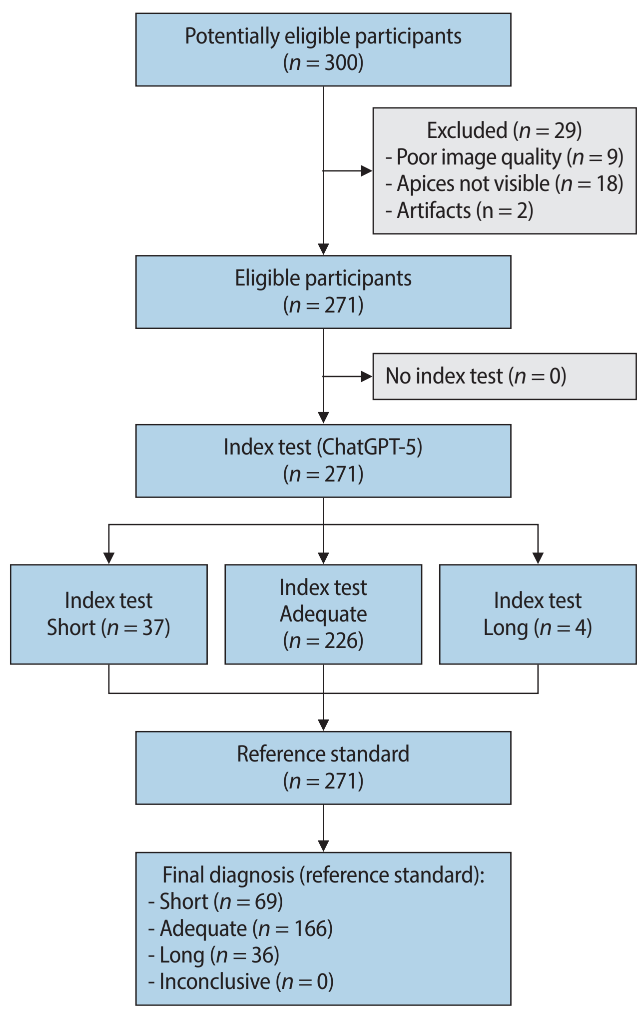


Figure 1. STARD (Standards for Reporting of Diagnostic Accuracy Studies) flow diagram for obturation length evaluation.


https://doi.org/10.5395/rde.2026.51.e29

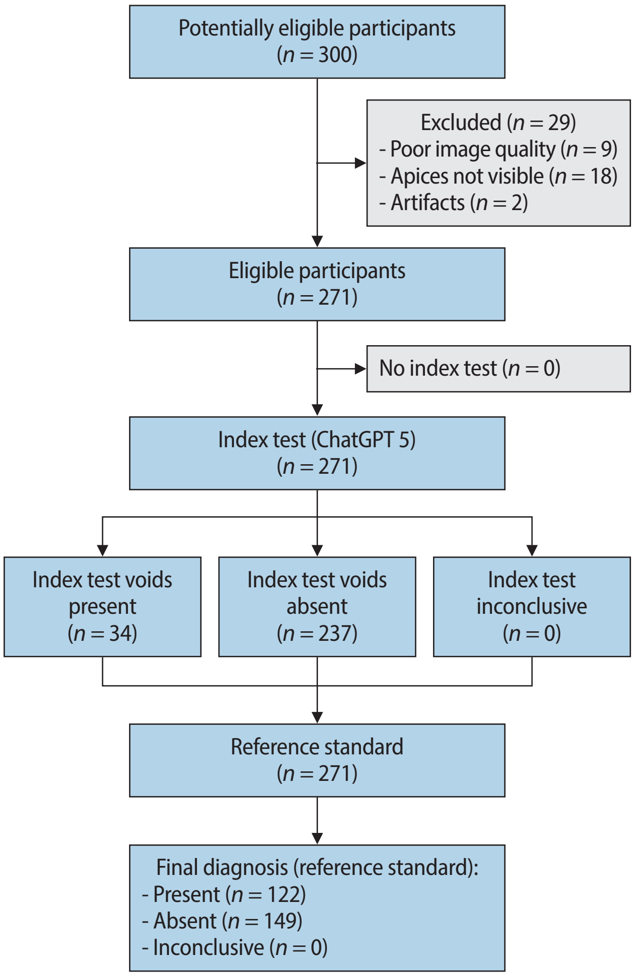


**Figure 2.** STARD (Standards for Reporting of Diagnostic Accuracy Studies) flow diagram for void detection in root canal fillings.

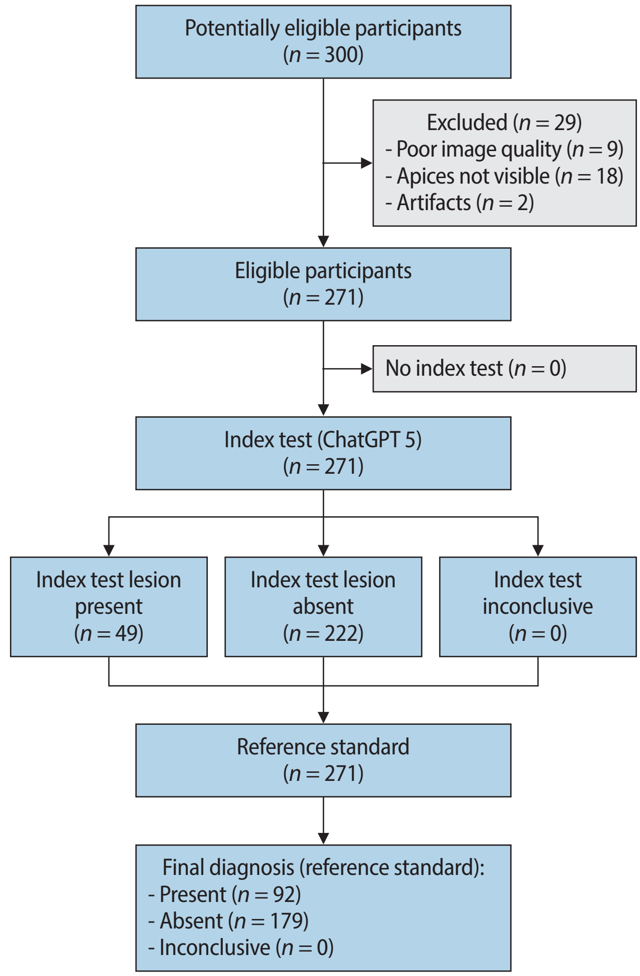


**Figure 3.** STARD (Standards for Reporting of Diagnostic Accuracy Studies) flow diagram for pathology detection in the apical area.

informed consent was waived.

### Radiographic data collection

Periapical radiographs were retrospectively obtained from a private dental clinic archive. Imaging was performed using a standardized digital intraoral X-ray unit (Planmeca ProX; Planmeca Oy, Helsinki, Finland) with consistent exposure parameters (70 kVp, 8 mA, and an exposure time of 0.2 seconds). All images were exported as high-resolution, uncompressed JPEG files. Two trained independent investigators, who were not involved in the diagnostic assessment phase, anonymized and pre-classified the radiographs into two categories: straightforward or complex.

A radiograph was classified "complex" if it met any of the following criteria:

1. Overlapping or superimposed anatomical structures (e.g., zygomatic arch or maxillary sinus shadow obstructing apex visibility).
2. Evidence of procedural complications (e.g., ledges, perforations, separated instruments), or
3. Fuzzy or blurred radiographic apex.

This classification was designed to reflect real-world diagnostic conditions, as radiographic complexity may differentially affect both human interpretation and AI-based assessment, thereby influencing diagnostic accuracy. Radiographs that did not meet any of these criteria and showed clearly interpretable root canal fillings and apices were classified as "straightforward." Inter-rater agreement was reached through discussion. Radio-

https://doi.org/10.5395/rde.2026.51.e29

graphs of posterior teeth were included; anterior teeth and non-endodontically treated cases were excluded. Inclusion criteria consisted of periapical radiographs of endodontically treated teeth that provided clear visualization of the root apex and extended at least 2 mm beyond the radiographic apex. Images with artifacts, poor contrast, or incomplete apical capture were omitted.

### Diagnostic evaluation

The diagnostic assessment involved three evaluators grouped into two categories: the AI-based model (ChatGPT-5) and a consensus panel of two licensed general dentists, each with at least five years of clinical experience. The general dentists jointly reviewed the radiographs and reached a consensus through discussion.

ChatGPT-5 independently evaluated the same radiographs using the platform's image input interface. To simulate realistic public-facing use, radiographs were submitted using the platform's visual input functionality. Following multiple preliminary tests to optimize prompt clarity, the model was provided with the following prompt: "As a professional dentist, assess the uploaded radiographs using these criteria: (1) length of obturation—short, adequate, or long; (2) presence of voids—yes or no; and (3) presence of periapical pathosis—yes or no." The same standardized prompt was applied uniformly to all 271 radiographs. While ChatGPT-5 generally provided definitive categorical outputs, responses in complex cases frequently included uncertainty modifiers such as 'appears to be' or 'may suggest,' indicating reduced confidence in visually ambiguous scenarios.

For human evaluators, standardized diagnostic definitions were applied:

- Root canal filling length:
  - Short: obturation ending >2 mm short of the radiographic apex.
  - Adequate: obturation terminating within 0–2 mm of the apex.
  - Long: obturation extending beyond the apex.
- A void was defined as a radiolucent gap within the filling material, and a periapical lesion as a radiolucency exceeding twice the width of the normal periodontal ligament space at the apex; both were evaluated as a binary variable (yes or no).

Diagnostic criteria were intentionally withheld from ChatGPT-5 to simulate typical real-world public usage, where users commonly upload images without structured clinical definitions. This approach was adopted to enhance the external validity of the findings.

### Reference standard

The reference standard was established by two board-certified endodontists, each with more than 5 years of clinical experience in endodontic diagnosis and treatment. All radiographs were reviewed independently on a calibrated 24-inch LCD monitor (1,920 × 1,080 resolution) under standardized lighting in a quiet environment without knowledge of the ChatGPT or general dentists' assessments. Disagreements between the endodontists were resolved by discussion to establish the reference standard.

### Sample size calculation

The required sample size was estimated using an expected agreement proportion of 0.80 (based on prior AI-dentist diagnostic concordance studies [12,13]), a 95% confidence level (Z = 1.96), and a 5% margin of error (E = 0.05). The calculation indicated a minimum of 246 radiographs. The following formula was used:

$$n = \frac{Z^2\, P\left(1 - P\right)}{E^2}$$

where, $n$ = required sample size; $Z$ = Z value corresponding to 95% confidence level (1.96); $P$ = expected proportion of agreement between AI model and dentists. Based on the initial estimates, $P$ was set to 80% (0.8 agreement); $E$ = acceptable margin of error, which was set to 5% (0.05).

The calculation was performed under a two-tailed test assumption, aiming to detect any statistically significant difference—either higher or lower—in agreement between the AI model and human evaluators. A two-sided 95% confidence interval was thus applied.

The values were substituted into the formula as follows:

$$n = \frac{(1.96)^2\, 0.8\, (1 - 0.8)}{(0.05)^2} \approx 246$$

 https://doi.org/10.5395/rde.2026.51.e29

### Statistical analysis

Sensitivity, specificity, and overall accuracy were calculated for ChatGPT-5 and general dentists relative to the reference standard. Sensitivity reflected the ability to detect inadequate obturations, voids, or apical lesions; specificity reflected the correct identification of normal findings of the apical area and adequate root canal filling. The McNemar test was used to compare diagnostic proportions ($\alpha = 0.05$). Statistical analyses were performed using IBM SPSS Statistics version 29.0 (IBM Corp., Armonk, NY, USA).

## RESULTS

A total of 271 anonymized periapical radiographs met the inclusion criteria and were analyzed. Of these, 167 (61.6%) were classified as straightforward and 104 (38.4%) as complex based on radiographic interpretability.

### Root canal filling length

Assessment of obturation length revealed notable variability among evaluators (Table 1). The reference standard identified 69 cases (25.5%) as short, 166 (61.3%) as adequate, and 36 (13.3%) as long. ChatGPT-5 identified fewer short (13.7%, $n = 37$) and long fillings (1.5%, $n = 4$) while overestimating adequate cases (83.4%, $n = 226$). In contrast, general dentists' classifications were more closely aligned with the reference standard (short, 28.8%; adequate, 58.7%; and long, 12.5%).

In straightforward radiographs, ChatGPT-5 achieved high sensitivity for adequate fillings (92.7%) but markedly low sensitivity for short (13.3%) and long (0.0%) fillings. Specificity ranged from 10.4% (adequate) to 99.3% (long), yielding an overall accuracy of 58.9%. In complex radiographs, sensitivity for short fillings increased to 39.1%, with accuracy reaching 61.5%.

General dentists demonstrated consistently superior diagnostic performance. For straightforward radiographs, their overall accuracy was 85.6%, with high sensitivity for all filling categories (≥81.8%). In complex cases, accuracy remained high (81.7%). Statistical analysis confirmed significant differences in sensitivity and overall accuracy between ChatGPT-5 and general dentists for both radiograph types ($p = 0.003$ and $p < 0.001$, respectively), while specificity differences were not significant ($p = 0.239$ and $p = 0.427$, respectively) (Table 1, Figure 1).

### Detection of voids in root canal fillings

The reference standard detected voids in 122 radiographs (45.0%), whereas ChatGPT-5 identified only 34 (12.5%), indicating frequent under-detection. The general dentists recognized voids in 80 cases (29.5%), closely approximating the reference standard.

For straightforward radiographs, ChatGPT-5 demonstrated a sensitivity of 9%, specificity of 91%, and overall accuracy of 54%. In complex radiographs, sensitivity improved to 22.7% and accuracy to 58.7%, with specificity of 85%. In contrast, the general dentists achieved sensitivity values of 57.7% (straightforward) and 56.8% (complex), with overall accuracies of 76% and 78.8%, respectively. Differences in sensitivity and accuracy between ChatGPT-5 and the dentists were statistically significant ($p = 0.01$ and $p < 0.001$), while specificity differences were not ($p = 0.781$ and $p = 0.149$) (Table 2, Figure 2).

### Detection of periapical lesions

The reference standard classified 92 radiographs (33.9%) as having periapical lesions. ChatGPT-5 detected only

**Table 1.** Performance of ChatGPT-5 and general dentists in detecting root canal filling length

| Evaluator | Length | Straightforward radiographs | | | Complex radiographs | | |
|---|---|---|---|---|---|---|---|
| | | Sensitivity (%) | Specificity (%) | Accuracy (%) | Sensitivity (%) | Specificity (%) | Accuracy (%) |
| ChatGPT-5 | Short | 13.3 | 94.1 | 71.8 | 39.1 | 81.5 | 72.1 |
| | Adequate | 92.7 | 10.4 | 58.9 | 77.6 | 32.4 | 61.5 |
| | Long | 0.0 | 99.3 | 85.9 | 7.1 | 97.8 | 85.6 |
| General dentists | Short | 84.8 | 91.7 | 89.8 | 91.3 | 90.1 | 90.4 |
| | Adequate | 86.9 | 83.8 | 85.6 | 82.1 | 81.1 | 81.7 |
| | Long | 81.8 | 97.9 | 95.8 | 57.1 | 94.4 | 89.4 |

https://doi.org/10.5395/rde.2026.51.e29

**Table 2.** Performance of ChatGPT-5 and general dentists in detecting voids in root canal fillings

| | Straightforward radiographs | | Complex radiographs | |
|---|---|---|---|---|
| | ChatGPT-5 (%) | General dentists (%) | ChatGPT-5 (%) | General dentists (%) |
| Sensitivity | 9.0 | 57.7 | 22.7 | 56.8 |
| Specificity | 91.0 | 92.1 | 85.0 | 95.0 |
| Accuracy | 54.0 | 76.0 | 58.7 | 78.8 |

**Table 3.** Performance of ChatGPT-5 and general dentists in detecting periapical lesions

| | Straightforward radiographs | | Complex radiographs | |
|---|---|---|---|---|
| | ChatGPT-5 (%) | General dentists (%) | ChatGPT-5 (%) | General dentists (%) |
| Sensitivity | 10.5 | 93.0 | 28.6 | 80.0 |
| Specificity | 88.2 | 79.1 | 71.0 | 87.0 |
| Accuracy | 63.2 | 83.8 | 56.7 | 84.6 |

49 (18.1%), showing limited sensitivity but high specificity. For straightforward radiographs, sensitivity was 10.5%, specificity 88.2%, and overall accuracy 63.2%. For complex radiographs, sensitivity rose to 28.6%, specificity declined to 71.0%, and accuracy was 56.7%.

General dentists demonstrated markedly higher diagnostic performance, with sensitivity of 93.0% and specificity of 79.1% in straightforward radiographs, and 80.0% and 87.0%, respectively, in complex radiographs. Their overall accuracy exceeded 83% across all conditions. Statistical comparisons confirmed significantly higher sensitivity and accuracy for general dentists ($p < 0.001$ for straightforward, $p = 0.002$ for complex), with specificity differences significant only in complex cases ($p = 0.029$) (Table 3, Figure 3).

In summary, across all diagnostic parameters, ChatGPT-5 demonstrated high specificity but consistently low sensitivity, particularly in detecting voids and periapical lesions. General dentists maintained balanced sensitivity and specificity, achieving accuracies above 80% in all assessments, whereas ChatGPT-5's performance ranged between 54% and 63%.

## DISCUSSION

This study evaluated the diagnostic accuracy of ChatGPT-5 as a public source of medical information in interpreting periapical radiographs of endodontically treated teeth. As of February 2025, ChatGPT-5 had over 400 million weekly active users, reflecting its rapid growth and widespread adoption [12]. A recent Cleveland Clinic survey reported that a significant portion of the public turns to AI chatbots, such as ChatGPT-5, for medical information, with 72% of Americans believing the health advice they received from these chatbots is accurate [13]. Moreover, four out of five AI users considered information obtained from ChatGPT-5 to be at least as reliable as that provided by their physicians [14]. This growing trust in AI-driven health guidance raises concerns, particularly regarding the accuracy and reliability of the medical advice provided by AI chatbots.

In this study, the model demonstrated high specificity but consistently low sensitivity across all diagnostic parameters, indicating that while it could correctly identify normal findings, it frequently failed to detect pathological or suboptimal conditions. These results align with the study's initial hypothesis and emphasize that generalist large-language-model systems, although capable of image recognition, remain unreliable for clinical diagnostic purposes.

The overall accuracy of ChatGPT-5 (54%–63%) was significantly lower than that of general dentists (76%–86%), reaffirming that professional human judgment remains essential for radiographic interpretation. The pattern of high specificity but poor sensitivity is characteristic of untrained or nonspecialized classifiers that default to "normal" findings when diagnostic confidence is low. This outcome is in agreement with previous AI radiology investigations, where general-purpose models underperformed compared with domain-trained algorithms designed specifically for dental imaging [15].

The limited diagnostic performance of ChatGPT-5 can be attributed to its architecture and training paradigm. Although the model is multimodal, its foundational structure is language-oriented, optimized for text generation rather than pixel-based image analysis. It lacks supervised exposure to annotated dental radiographs and thus cannot accurately recognize subtle endodontic features such as obturation length deviations, apical radiolucencies, or voids. Dedicated deep-learning networks trained on labeled datasets—such as convolutional neural networks or transformer-based vision mod-


https://doi.org/10.5395/rde.2026.51.e29

els—have achieved sensitivities above 85% in similar diagnostic tasks [16,17], underscoring the gap between purpose-built systems and generalist AI. Although domain-specific fine-tuning of large language models may improve performance, such adaptations may not fully overcome the inherent limitations of language-first architectures. Diagnostic tasks in endodontic radiology likely require purpose-built vision models trained on large, annotated dental imaging datasets, rather than general-purpose AI systems adapted post hoc.

Clinically, these findings have practical implications. With the increasing use of ChatGPT-based platforms by patients seeking self-assessment, there is a risk that misinterpretation of radiographs may lead to delayed professional consultation, unwarranted anxiety, or misplaced reassurance. Endodontists and general practitioners should be aware of these limitations and proactively educate patients on the boundaries of AI-generated health information. The ChatGPT-5 evaluation was intentionally conducted using natural language prompts that simulate realistic public-facing interactions, without embedding detailed operational definitions. Future research may explore whether incorporating standardized diagnostic definitions into AI prompts enhances interpretive reliability.

Several factors may explain the observed discrepancies between ChatGPT-5 and human evaluators. The lack of diagnostic calibration, absence of case-specific context (such as patient symptoms or clinical notes), and the inherent ambiguity of radiographic features contribute to performance variability [18,19]. Despite standardized training, dental professionals may interpret radiographic features differently due to variations in clinical experience, perceptual sensitivity, and diagnostic thresholds for pathology. Factors such as contrast perception, anatomical variations, and subjective assessment of radiolucencies contribute to these discrepancies, particularly in complex cases where the pathological findings are subtle or ambiguous [20]. Although expert disagreement reinforces the inherent subjectivity of human evaluation, the collective accuracy of the included dentists remained superior to that of the AI model. The persistence of interobserver variability suggests that AI should not replace expert interpretation but rather serve as an adjunct tool. Additionally, the model's reliance on a single image per case contrasts with the multi-image or three-dimensional (3D) datasets often available to clinicians, further reducing diagnostic precision.

This study has limitations inherent to retrospective radiographic designs. The dataset comprised periapical radiographs from a single clinical setting, which may limit generalizability. The ChatGPT-5 prompt was standardized to simulate public usage; however, different phrasing or context could influence responses. Moreover, the model's outputs were not repeated across sessions to test reproducibility, as image-based stochastic variation may exist. Future research should explore incorporating multiple AI systems, larger multicenter datasets, and prospective designs that evaluate human-AI collaborative workflows. Developing specialized, dentistry-trained multimodal models may substantially enhance diagnostic accuracy and clinical reliability. Additionally, this study relied on static two-dimensional periapical radiographs, whereas 3D imaging modalities such as cone-beam computed tomography are increasingly used in endodontic practice and may yield different diagnostic performance profiles.

Overall, ChatGPT-5's performance in this study underscores that general-purpose AI remains an adjunctive tool rather than a diagnostic substitute. While it demonstrated a capacity for identifying normal cases, it failed to match the diagnostic precision of trained clinicians. Continuous refinement of domain-specific AI frameworks, combined with clinician oversight, is essential to ensure safe and effective integration of AI into endodontic practice.

## CONCLUSIONS

ChatGPT-5 demonstrated high specificity but low sensitivity in interpreting periapical radiographs of endodontically treated teeth, limiting its diagnostic reliability. While the model can recognize normal findings, it frequently fails to identify inadequate root canal fillings, voids, and periapical pathoses. These findings underscore that general-purpose AI systems remain unsuitable for autonomous diagnostic use in endodontics. Clinician expertise and critical interpretation remain indispensable, and ongoing development of domain-specific, dentistry-trained AI models is essential to enhance diagnostic accuracy, patient safety, and the responsible integration of AI into clinical practice.

## CONFLICT OF INTEREST

No potential conflict of interest relevant to this article was reported.

## FUNDING/SUPPORT

This study received no specific grant from any funding agency in the public, commercial, or not-for-profit sectors.

## ACKNOWLEDGMENTS

The authors thank the IT department from Dr. Tooth Private Clinics for their help in retrieving radiographs.

## AUTHOR CONTRIBUTIONS

Conceptualization: Almutairi W, Alharbi H. Data curation: Alnasser M, Alharbi H, Austah O. Formal analysis: Almutairi W, Austah O. Investigation: Almutairi W, Alnasser M, Alharbi H. Methodology: Almutairi W, Alharbi H. Project administration: Almutairi W, Alnasser M. Validation: Austah O, Alharbi H. Writing - original draft: Almutairi W, Alharbi H. Writing - review & editing: Austah O.

## DATA SHARING STATEMENT

The datasets are available upon reasonable request from the corresponding author.

## DISCLOSURE OF GENERATIVE AI IN SCIENTIFIC WRITING

We confirm that generative AI (specifically ChatGPT-5) was indeed central to the conduct of this study, as detailed in the methodology section, which investigates its accuracy. Regarding the preparation of the manuscript, generative AI tools were used only for grammar checking. All content was originally written by the authors and fully reviewed and edited for accuracy and originality.

# REFERENCES


1. Goodfellow I, Bengio Y, Courville A. Deep learning. Cambridge, MA: MIT Press; 2016.
2. Vaswani A, Shazeer N, Parmar N, *et al*. Attention is all you need. In: Proceedings of the 31st Annual Conference on Neural Information Processing Systems (NeurIPS 2017); December 4–9, 2017; Long Beach, CA, USA. Red Hook, NY: Curran Associates, Inc; 2017. p. 5998–6008.
3. Rutledge GW. Diagnostic accuracy of GPT-4 on common clinical scenarios and challenging cases. Learn Health Syst 2024;8:e10438.
4. Amin K, Khosla P, Doshi R, Chheang S, Forman HP. Artificial intelligence to improve patient understanding of radiology reports. Yale J Biol Med 2023;96:407-417.
5. Bickmore TW, Pfeifer LM, Jack BW. Taking the time to care: empowering low-health-literacy hospital patients with virtual nurse agents. In: Proceedings of the SIGCHI Conference on Human Factors in Computing Systems. Boston (MA): ACM Press; 2009. p. 126–35.
6. Asgary S. Artificial intelligence in endodontics: a scoping review. Iran Endod J 2024;19:85-98.
7. Sadr S, Mohammad-Rahimi H, Motamedian SR, Zahedrozegar S, Motie P, Vinayahalingam S, *et al*. Deep learning for detection of periapical radiolucent lesions: a systematic review and meta-analysis of diagnostic test accuracy. J Endod 2023;49:248-261.
8. Ghaffari M, Zhu Y, Shrestha A. A review of advancements of artificial intelligence in dentistry. Dent Rev 2024;4:100081.
9. Keshavarz P, Bagherieh S, Nabipoorashrafi SA, Chalian H, Rahsepar AA, Kim GHJ, *et al*. Chatgpt in radiology: a systematic review of performance, pitfalls, and future perspectives. Diagn Interv Imaging 2024;105:251-265.
10. Stephan D, Bertsch A, Burwinkel M, Vinayahalingam S, Al-Nawas B, Kämmerer PW, *et al*. AI in dental radiology-improving the efficiency of reporting with ChatGPT: comparative study. J Med Internet Res 2024;26:e60684.
11. Sounderajah V, Ashrafian H, Golub RM, Shetty S, De Fauw J, Hooft L, *et al*. Developing a reporting guideline for artificial intelligence-centred diagnostic test accuracy studies: the STARD-AI protocol. BMJ Open 2021;11:e047709.
12. Singh S. ChatGPT statistics 2024 - 300 million active users (December) [Internet]. San Francisco, CA: DemandSage; 2024 [cited 2025 May 23]. Available from: https://www.demandsage.com/ChatGPT-statistics
13. Cleveland Clinic. Cleveland Clinic survey: most Americans using health-monitoring technology are experiencing significant physical and mental benefits [Internet]. Cleveland, OH: Cleveland Clinic; 2024 Feb 1 [cited 2025 May 23]. Available from: https://newsroom.clevelandclinic.org/2024/02/01/cleveland-clinic-survey-most-americans-using-health-monitoring-technology-are-experiencing-significant-physical-and-mental-benefits
14. Ayo-Ajibola O, Davis RJ, Lin ME, Riddell J, Kravitz RL. Char-


 https://doi.org/10.5395/rde.2026.51.e29

acterizing the adoption and experiences of users of artificial intelligence-generated health information in the United States: cross-sectional questionnaire study. J Med Internet Res 2024;26:e55138.
15. Baza R. Evaluating artificial intelligence in dental radiography: an experimental study and a comparative analysis of AI ability in diagnosing panoramic X-ray infections [master's thesis]. Stockholm (Sweden): KTH Royal Institute of Technology; 2024.
16. Jurafsky D, Martin JH. Speech and language processing. 3rd ed. London: Pearson; 2021.
17. Moor M, Banerjee O, Abad ZS, Krumholz HM, Leskovec J, Topol EJ, *et al*. Foundation models for generalist medical artificial intelligence. Nature 2023;616:259-265.
18. Goldman M, Pearson AH, Darzenta N. Endodontic success: who's reading the radiograph? Oral Surg Oral Med Oral Pathol 1972;33:432-437.
19. Goldman M, Pearson AH, Darzenta N. Reliability of radiographic interpretations. Oral Surg Oral Med Oral Pathol 1974;38:287-293.
20. Hegde S, Gao J, Vasa R, Cox S. Factors affecting interpretation of dental radiographs. Dentomaxillofac Radiol 2023;52:20220279.

RDE Restorative Dentistry & Endodontics

Research Article

eISSN 2234-7666
Restor Dent Endod. 2026 August;51(3):e30
https://doi.org/10.5395/rde.2026.51.e30

# The influence of various adhesive applicators on the bond strength to dentin: an *in vitro* experimental study

**Ahmed Alshawi[1,*], Benin Dikmen[2], Fadimeana Lal[1], Sevda Ozel Yildiz[3], Ugur Erdemir[1]**

[1]Department of Restorative Dentistry, Faculty of Dentistry, Istanbul University, Istanbul, Türkiye
[2]Department of Restorative Dentistry, Faculty of Dentistry, Istanbul Medipol University, Istanbul, Türkiye
[3]Department of Biostatistics, Faculty of Medicine, Istanbul University, Istanbul, Türkiye

## ABSTRACT

**Objectives:** The aim of this *in vitro* study was to evaluate the influence of various adhesive applicators on the microshear bond strength (μSBS) of flowable resin composite to dentin.
**Methods:** Forty-two extracted molars were prepared as disks and divided into two groups. In the first group, GLUMA Bond Universal (Heraeus Kulzer GmbH) was applied to the tooth surface for 20 seconds using a bristle brush, while in the second group, the same adhesive was applied by the same operator using a microbrush. Photopolymerization was performed for 10 seconds using a Valo light-curing unit (Ultradent Products Inc.). Microcylindrical silicone tubes (2 mm long, 0.8 mm inner diameter) were used as molds on the bonded dentin surfaces, and Charisma Bulk Flow ONE resin composite (Heraeus Kulzer GmbH) was injected and cured for 20 seconds. Both groups underwent a μSBS test, and the failure modes were examined microscopically. Student's *t*-test compared the failure stress between the groups ($p < 0.05$).
**Results:** The bristle brush group had the highest mean stress at failure (49.09 ± 8.76 MPa) compared to the microbrush group (37.20 ± 6.77 MPa), which also had the highest percentage of adhesive failure (95.24%).
**Conclusions:** The choice of adhesive applicator plays a significant role in determining the μSBS of flowable resin composite to dentin. It is advisable to use a bristle brush applicator when applying adhesive.

**Keywords:** Adhesive; Applicators; Dentin

## INTRODUCTION

In recent years, adhesive dentistry has made considerable progress, particularly in improving the mechanical properties and bond strength of resin-based adhesive systems [1,2]. Nevertheless, these procedures remain

**Received:** November 25, 2025 **Revised:** January 26, 2026 **Accepted:** February 4, 2026

**Citation**
Alshawi A, Dikmen B, Lal F, Ozel Yildiz S, Erdemir U. The influence of various adhesive applicators on the bond strength to dentin: an *in vitro* experimental study. Restor Dent Endod 2026;51(3):e30.

***Correspondence to**
**Ahmed Alshawi, DDS**
Department of Restorative Dentistry, Faculty of Dentistry, Istanbul University, Prof. Dr. Cavit Orhan Tütengil Street No: 4, Fatih, Istanbul 34116, Türkiye
Email: a.alshawi@ogr.iu.edu.tr

Portions of this work were presented at the 2024 FDI World Dental Congress and published as an abstract in the *International Dental Journal* (Vol. 74, Suppl. 1, Oct 2024, p. S116-S117).

highly technique-dependent due to the many steps involved, making them susceptible to operator-induced variations. Consequently, the success of an adhesive system depends not only on its inherent material properties but also on the clinician's technique and the tools used during application [3,4].

As dental adhesives are increasingly used in restorative treatments, the application method has become a crucial factor influencing bond strength and clinical results. There are several techniques for applying adhesives, each of which can impact the final result. These include: (a) direct application followed by immediate light-curing; (b) application with removal of excess adhesive with a gentle air stream; (c) removal of excess adhesive with a dry microapplicator; and (d) removal with both a dry microapplicator and a gentle air stream. A thin and uniform layer of adhesive is considered essential for achieving optimal bond strength [5,6].

To minimize the technique's sensitivity, newer adhesive formulations have been developed that are easier to apply and require fewer steps, making them more suitable for routine clinical use [1]. Universal adhesives, for example, contain water as a key component that enables ionization of the acidic monomers and promotes adequate bonding with both dentin and enamel surfaces [7,8].

Accordingly, solvent evaporation is a crucial step during application. It has been shown that extending the air-drying time to 10–15 seconds, as recommended by the manufacturer, significantly improves the bond strength to dentin after 24 hours [9,10]. Other approaches to improve adhesion include applying multiple layers of universal adhesive, which can enhance hybrid-layer formation and resin penetration [11–13]. During application, clinicians also need to control critical parameters, such as active rubbing and air-drying, which together increase the adhesive's contact time and the pressure exerted on the tooth surface, thereby promoting a stronger micromechanical bond to both enamel and dentin [6,14,15].

Initially, dental adhesives were applied using simple tools, such as cotton pellets, tissue, sponge tips, or disposable brushes with elongated bristles [16]. The introduction of the microbrush in the early 2000s represented a significant advance in the application of adhesives [17]. This tool, a flexible, hand-held, disposable applicator with a fine nylon tip, allows for more precise placement and handling of adhesive materials. It is commonly used to apply, rub, or clean various substances, such as etchants, disclosant dyes, and resins [15], and is usually made from fibers such as nylon, cotton, or synthetic polymers [18]. Comparative studies have shown that the use of microbrushes can produce a more uniform, micromechanically stable bond than conventional brushes, especially when placing endodontic posts [19,20].

Scanning electron microscopy (SEM) is often used in such investigations to identify defects and assess the integrity of the adhesive layer. In one study, Alshawi *et al*. [15] used SEM to examine the residual contaminants on adhesive surfaces of different applicators. Their results showed that microbrushes consistently left fiber residues on the bonded surfaces, while bristle brush applicators left no visible residues. Although Alshawi *et al*. [15] did not explicitly investigate the mechanical effects of these residues, the presence of microfibers could weaken the bond between the restorative material and dentin, leading to microleakage, secondary caries, or restoration failure.

A review of the literature shows that previous studies have found differences in bond strength between different applicator types when used on root dentin [4]. In contrast, the effects of the different applicator types on bond strength to crown dentin during adhesive application in the prepared cavity remain uninvestigated.

The aim of this *in vitro* study is to evaluate the influence of different applicator types (specifically, bristle brush vs microbrush) on the microshear bond strength (μSBS) of a universal adhesive applied to crown dentin when used with a flowable resin composite. Previous microscopic investigations have indicated that microbrush applicators consistently leave fiber residues on bonded surfaces, whereas bristle brush applicators do not leave visible contaminants [15]. Based on the premise that residual contaminants at the adhesive interface can compromise bonding integrity, the research hypothesis is that the use of bristle brush applicators will result in significantly higher μSBS values to crown dentin compared to microbrush applicators.


https://doi.org/10.5395/rde.2026.51.e30

## METHODS

### Determination of the specimen size

The specimen size was determined based on a pilot study with both groups ($n$ = 21), which resulted in a large effect size (f = 0.89) based on the calculated means and standard deviations. At least 30 specimens (15 per group) were required to achieve 95% significance at a significance level of 0.05. To improve reliability, the total specimen size was increased to 42 ($n$ = 21 per group).

### Preparation of the specimens

The study protocol was approved by the Clinical Research Ethics Committee of the Faculty of Dentistry, Istanbul University (project number: 2024/10).

A total of 42 sound human molars that had been extracted for periodontal reasons and showed neither caries nor structural damage were used for this study. Informed consent was obtained from all patients prior to extraction, and they were informed that their teeth would be used for research purposes. After extraction, the teeth were stored in sterile saline solution (0.9% NaCl, w/v) at 4°C for up to 14 days. All visible calculus, discoloration, and biological debris were removed with manual curettes. Each tooth was then embedded in a 16 × 16 × 28 mm self-curing acrylic resin block (Varidur; Buehler, Lake Bluff, IL, USA).

The occlusal enamel of each molar was removed with a slow-speed diamond saw (Isomet, Buehler) under constant water cooling to a depth of 3 mm from the highest cusp, exposing a flat dentin surface to produce a disk-shaped specimen. All specimens were prepared by a single examiner (AA) and examined at ×3.5 magnification to ensure smooth margins and no sharp edges. To simulate an artificial smear layer, the exposed dentin was polished with 150- and 320-µm grit silicon carbide abrasive papers [20]. The surfaces were then rinsed with sterile deionized water for 10 seconds and carefully air-dried.

### Adhesive procedure

Specimens were randomly assigned to two experimental groups using a computer-generated randomization table created by an independent researcher not involved in the laboratory procedures. All bonding procedures were performed by a single calibrated operator (AA) according to the manufacturer's instructions for GLUMA Bond Universal (Heraeus Kulzer GmbH, Hanau, Germany).

To ensure standardization of the adhesive volume, the specific 'drop control' nozzle design of the adhesive bottle GLUMA Bond Universal was used. According to the manufacturer, this system ensures a consistent, precise, and clean dosage for every application. Only one drop of the adhesive was dispensed and applied strictly in accordance with these manufacturer's instructions for each applicator [21]. Following application, the adhesive was air-dried carefully with a gentle stream of oil-free air until the adhesive film was immobile. This step was performed strictly according to the manufacturer's instructions to ensure solvent evaporation and prevent the formation of excessive puddles or variations in film thickness [21].

### Group 1 ($n$ = 21): bristle brush applicator

In this group, GLUMA Bond Universal was actively applied to the prepared dentin surfaces in self-etch mode using a bristle brush applicator (Ultrabrush; Young Innovations, Algonquin, IL, USA) (Figure 1).

The adhesive was rubbed over the surface for 20 seconds with a manual pressure of approximately 0.35 N (35 gf) [19,22,23]. This was followed by air drying with an oil-free air stream of increasing intensity, directed from the periphery to the center, until the adhesive layer stopped moving. A new disposable applicator was used for each specimen. The adhesive was light-cured for 10

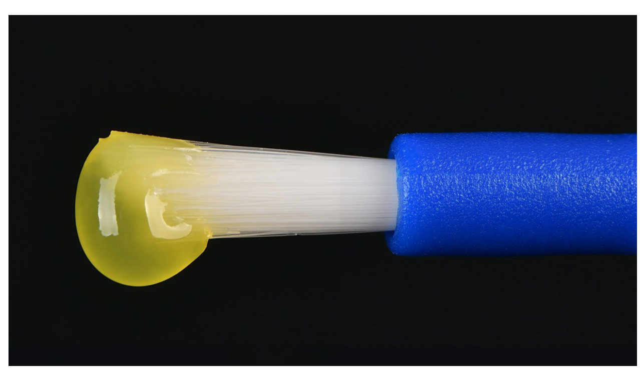

**Figure 1.** Photograph of the disposable bristle brush applicator (Ultrabrush fine ± 100 fibers; Young Innovations, Algonquin, IL, USA) moistened with GLUMA Bond Universal (Heraeus Kulzer GmbH, Hanau, Germany) for application to dentin specimens.

https://doi.org/10.5395/rde.2026.51.e30

seconds using a multi-LED light-curing unit (Valo LED Cordless; Ultradent Products Inc., South Jordan, UT, USA) at a standard mode of 1,000 mW/cm$^2$.

For the microshear strength test, silicone tubes with an inner diameter of 0.8 mm were cut into 2 mm long pieces that served as molds [24]. A tube was placed on the bonded dentin surface, and Charisma Bulk Flow ONE (Heraeus Kulzer GmbH) flowable resin composite was injected into the tube from bottom to top to prevent bubble entrapment. The filled tube was covered with a transparent Mylar strip and light-cured for 20 seconds. The silicone molds were then carefully removed by cutting vertically with a sharp lancet to avoid failure before testing.

### Group 2 ($n$ = 21): microbrush applicator

In the second group, the same adhesive system was applied with a microbrush applicator (Microbrush, Young Innovations) (Figure 2).

The operator (AA) used the same technique, time, and pressure parameters as in group 1. Similarly, four resin composite microcylinders (0.8 mm diameter and 2 mm height) were fabricated on each dentin surface using the same materials and procedures as described in group 1.

After placement of the adhesive and resin composite, all specimens were stored in distilled water at 37°C in an incubator for 24 hours prior to mechanical testing.

### Bond strength testing

The μSBS testing was performed using a universal testing machine (Instron 3365; Instron Corp., Norwood, MA, USA) at a crosshead speed of 1 mm/min. A chisel-shaped loading device applied force until fracture occurred. The fracture stress was calculated from the measured specimen diameter.

Figure 2. Photograph of the disposable Microbrush applicator (Microbrush Plus, regular 2.0 mm, green; Young Innovations, Algonquin, IL, USA) moistened with GLUMA Bond Universal (Heraeus Kulzer GmbH, Hanau, Germany) for application to dentin specimens.

### Failure mode analysis

After the test, both the fractured resin composite cylinders and the corresponding dentin substrates were collected for fractographic analysis. Each specimen was examined under an optical microscope at ×50 magnification (Olympus BX51 SM Analysis System; Olympus Corporation, Tokyo, Japan).

### Scanning electron microscopy surface analysis

Representative specimens ($n$ = 11 per group) were randomly selected for SEM analysis. Specimens were dehydrated in an ascending series of acetone concentrations (70%, 80%, 90%, and 100%) and then stored in 100% acetone. Specimens were dried using a critical point dryer (Leica EM CPD300; Leica Microsystems, Wetzlar, Germany). After drying, a gold-palladium coating was applied using a sputter coater (Leica EM SCD500) in diffuse mode for 10 seconds. The SEM images were taken with a GeminiSEM 500 (Carl Zeiss, Jena, Germany) equipped with an Inlens electron detector and operated at 10 kV with different magnifications.

All the steps of specimen preparation, along with the materials, instruments, and devices employed in this study, are illustrated in Figure 3.

### Statistical analysis

Data normality was assessed using the Shapiro-Wilk test. As the μSBS data followed a parametric distribution, comparisons between groups were performed using Student's $t$-test. Statistical significance was set at $p < 0.05$. All analyses were performed using IBM SPSS Statistics for Windows, version 26.0 (IBM Corp., Armonk, NY, USA).

## RESULTS

### Microshear bond strength

The comparison of the μSBS between the two groups showed statistically significant differences (Table 1 and


https://doi.org/10.5395/rde.2026.51.e30

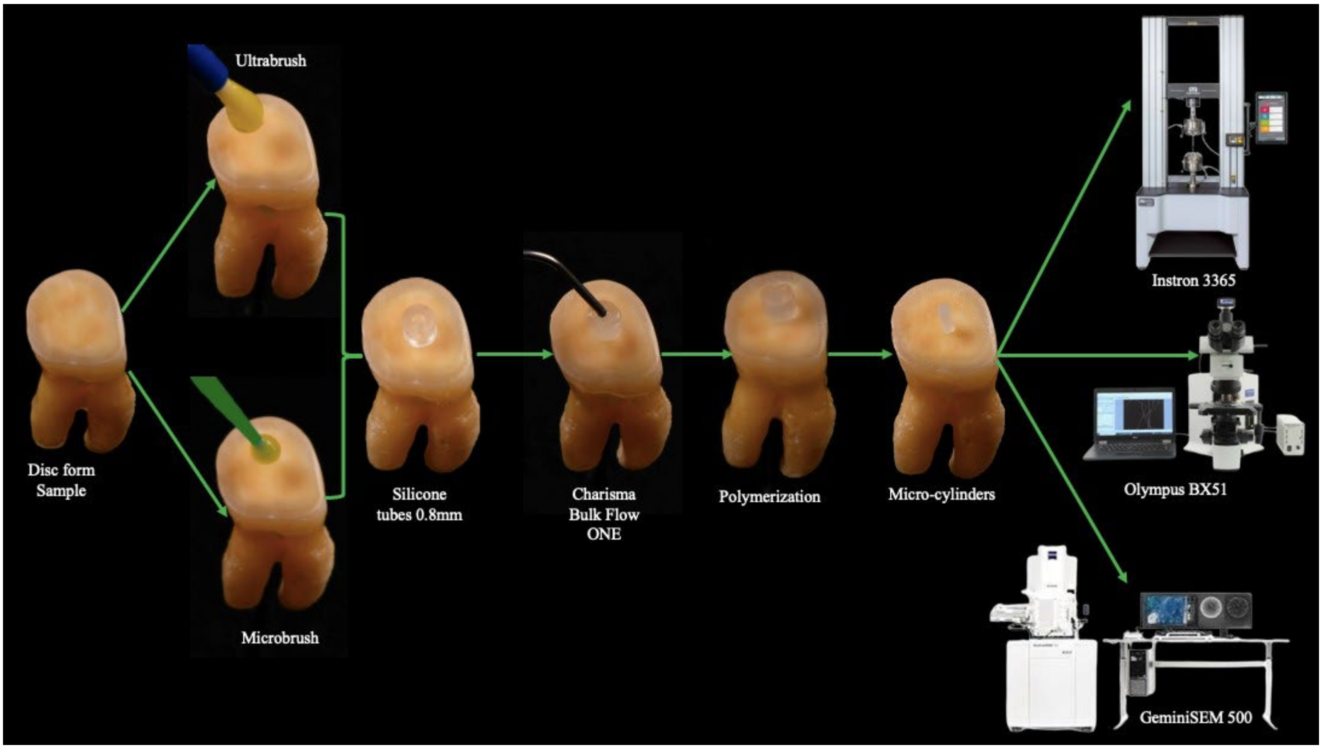


**Figure 3.** Schematic representation of the specimen preparation, materials, and equipment used in the individual phases of this study.

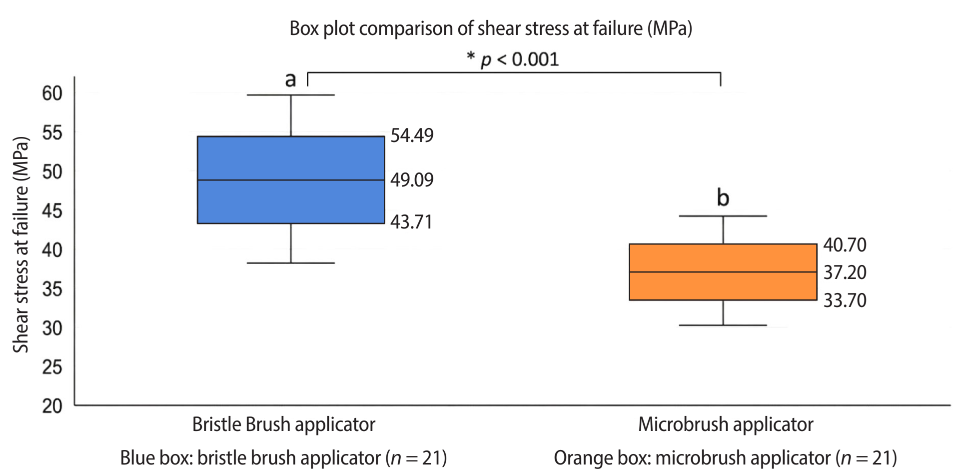


**Figure 4.** Comparison of microshear bond strength between the two groups. Box plots are schematic representations based on mean and standard deviation, as raw data were not provided. Different lowercase letters indicate statistically significant differences ($p < 0.05$), with $p < 0.001$ between groups.

Figure 4). The group in which the universal adhesive was applied with the bristle brush applicator (group 1) had a significantly higher mean shear stress at failure (49.09 ± 8.76 MPa) than the group with the microbrush applicator (group 2), which had a mean value of 37.20 ± 6.77 MPa. The difference in mean bond strength between the two groups was statistically significant ($p < 0.001$, Student's *t*-test).

These results indicate that the bristle brush applicator resulted in a stronger adhesive bond to dentin under the same experimental conditions, supporting the hypothesis that the applicator type may influence adhesive performance. The lower standard deviation in the microbrush group (± 3.50) compared to the bristle brush group (± 5.39) also indicates a more consistent but weaker adhesive performance when using the microbrush.

### Failure mode analysis

Analyzing the distribution of failure modes provides additional support for the mechanical data. In the bristle brush group, 71.40% of the specimens showed adhesive failure, while 28.60% exhibited cohesive failure within the resin composite substrate. In contrast, the microbrush group showed a higher proportion of adhesive failures (95.24%) and a lower proportion of cohesive failures (4.76%) (Table 2 and Figure 5).

The higher rate of adhesive failures in the microbrush group indicates a weaker adhesive interface, which is consistent with the lower μSBS values in this group. Conversely, the higher frequency of cohesive failures in the bristle brush group suggests that the bond between the adhesive and the dentin was strong enough that failures occurred more frequently within the restorative material rather than at the adhesive interface.

### Scanning electron microscopy observations (descriptive)

Qualitative SEM analysis of representative specimens from both groups revealed remarkable differences in surface characteristics after application. The bristle brush group exhibited a more uniform and homogeneous adhesive layer with minimal surface contamination (Figure 6).

In contrast, there is a widespread distribution of fiber residues within the microbrush group. Fiber residues were identified embedded at the adhesive interface in 100% of the examined specimens, with fiber diameters ranging between 14.7 and 19.7 μm (minimum–maximum) (Figure 7). The consistent presence of these inclusions confirms that fiber shedding is a systematic

**Table 1.** Comparison of micro-shear bond strength between the two groups

| Variable | Bristle brush applicator group ($n = 21$) | Microbrush applicator group ($n = 21$) | $p$-value |
|---|---|---|---|
| Shear stress at failure (MPa) | 49.09 ± 8.76[a] | 37.20 ± 6.77[b] | <0.001 |

Values are presented as mean ± standard deviation.
Means with different lowercase letters indicate statistically significant differences between groups ($p < 0.05$).

**Table 2.** Comparison of failure modes between the two groups

| Variable | Bristle brush applicator group ($n = 21$) | Microbrush applicator group ($n = 21$) |
|---|---|---|
| Adhesive failure (%) | 71.40 | 95.24 |
| Cohesive failure (%) | 28.60 | 4.76 |

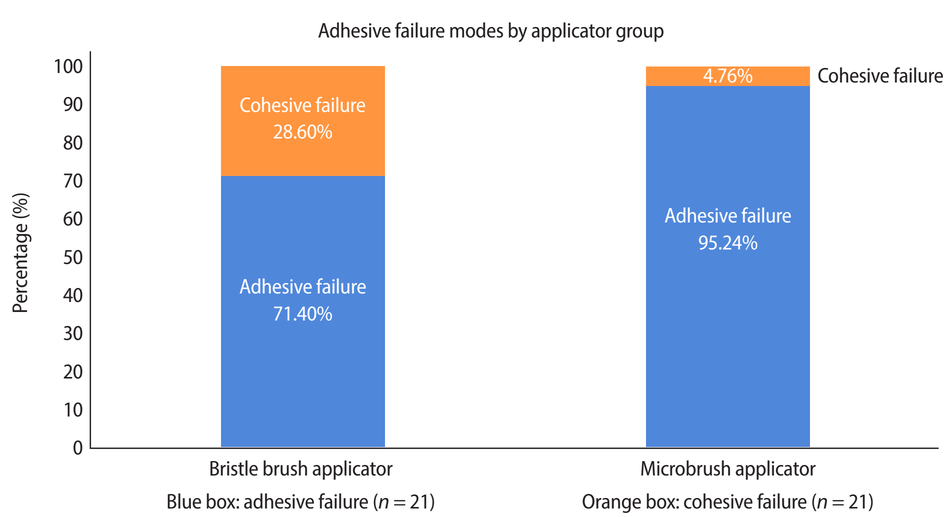


**Figure 5.** A graphic compares the adhesive failure modes observed in both groups.


https://doi.org/10.5395/rde.2026.51.e30

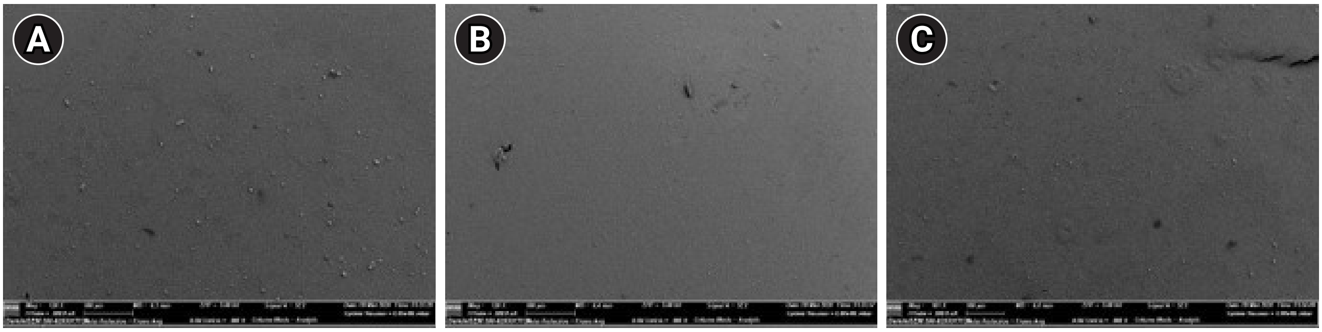

**Figure 6.** (A–C) Scanning electron microscopy images of the examined specimens from the disposable bristle brush applicator group. They show a more consistent and uniform adhesive layer with no surface contamination (residue-free) on the adhesive surface.

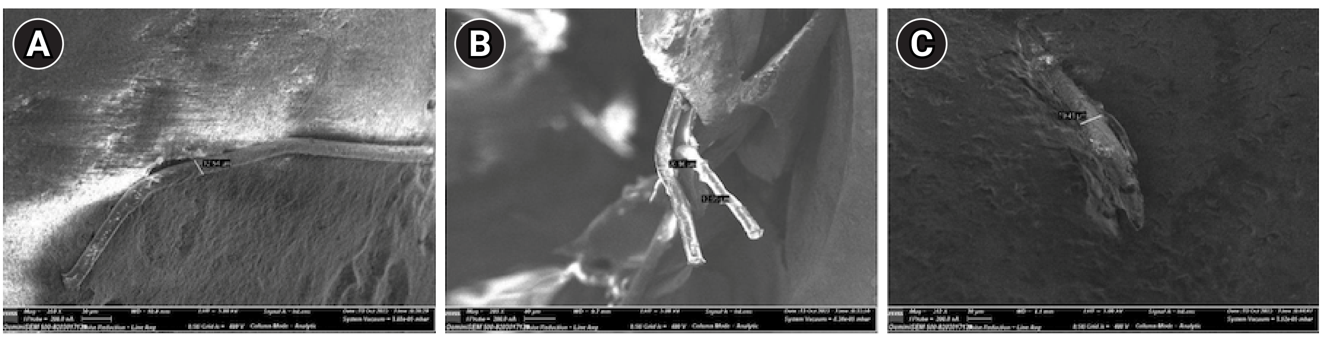

**Figure 7.** (A–C) Scanning electron microscopy images of the examined specimens from the microbrush group, displaying the fiber residues embedded on the surface, and showing the diametric measurements of the embedded fiber residues. The analysis confirmed that fiber diameters ranged from 14.67 to 19.66 µm (minimum–maximum).

occurrence rather than a stochastic defect. These embedded fibers created visible interfacial discontinuities that appeared to act as stress concentrators, initiating adhesive failure.

## DISCUSSION

The present study showed that the type of applicator used to apply a universal adhesive significantly affected the µSBS to dentin. The bristle brush applicator resulted in a significantly higher mean bond strength than the microbrush, with the difference confirmed by both failure mode analysis and SEM observations. These results support the research hypothesis that the use of bristle brush applicators will yield significantly higher µSBS values to crown dentin than microbrush applicators. Our results are consistent with previous findings that application technique variables, such as the rubbing action and mechanical contact between the applicator and the substrate, directly influence the quality of the bonding surface [25]. In our study, the bristle brush group not only achieved higher µSBS values but also exhibited a greater proportion of cohesive failures, suggesting that the bond to dentin was strong enough to shift the failure site to the resin composite substrate rather than the adhesive interface. In contrast, the microbrush group showed mainly adhesive failures, indicating a weaker interfacial bond.

An important factor influencing these results could be the presence of fiber residues from the microbrush applicator. SEM examination revealed visible nylon fiber residues embedded in the adhesive layer of all examined microbrush specimens, while no such residues were found in the bristle brush specimen. This observation of fiber residues in 100% of the examined microbrush specimens is consistent with findings from previous studies, which similarly reported contamination of the adhesive interface when fibrous microbrushes were employed [15,16]. Embedded fibers may act as stress concentrators or barriers to resin infiltration, reducing the cohesive strength of the adhesive layer and resulting in lower μSBS values.

This is consistent with the findings of Alshawi *et al.* [15], who reported that microbrushes consistently left fiber residues on the bonding surfaces in Class I cavities, whereas this was not the case with bristle brushes. Similarly, Berton *et al.* [16] observed fiber residues in both Class I and Class II cavities when adhesives were applied with microbrushes.

A potential causal link between fiber embedding and reduced bond strength is supported by the fractographic data. The microbrush group demonstrated a distinct pattern of adhesive failures (95.24%) that corresponded directly to the interface, with SEM analysis confirming 100% fiber contamination. This suggests that the embedded fibers may have acted as stress concentrators or flaws at the interface, potentially preventing intimate contact and likely contributing to premature adhesive failure. The fiber residues appear to act as mechanical discontinuities, potentially interfering with polymerization and reducing bond strength by creating weak zones within the adhesive layer. Microbrushes are widely used, accounting for approximately 76% of all applicators sold in Italy in August 2022 [16]. Despite their popularity, their design leads to fiber shedding. To avoid this, non-absorbent, lint-free nylon fibers have been developed that allow for practical adhesive application [17]. However, these fibers are not always firmly attached to the plastic handle, leading to fiber shedding during heavy scrubbing [15]. Since most adhesive manufacturers recommend active application with firm rubbing and multilayer application can improve adhesive performance [25], mechanical stress during application probably increases the likelihood of fiber loss from the microbrush tips. Interestingly, a group of Italian researchers from the College of Siena published numerous papers on post-cementation in endodontic canals between 2001 and 2002. They reported better resin tag formation and higher bond strength when the adhesives were applied with microbrushes rather than small plastic bristle brushes [26–30]. These differences are probably due to the particular anatomical challenges of intracanal application, where microbrushes are better able to adapt to narrow, deep spaces compared to bristle brushes. However, for preparations in shallow cavities - as in the present study - the risk of fiber contamination by microbrushes might outweigh the ergonomic advantages. Another factor that could affect these results is the angle of the fiber tips of the bristle brushes, which may be at 90° to the dentin surface in the specimens used in this study. However, it is unlikely that the bristle tips were oriented at exactly 90° to the root dentin. This study hypothesizes that the active application protocol (scrubbing) employed on a flat surface exerts direct compressive and shear forces on the microbrush fibers against the hard dentin substrate. Unlike the lateral friction in a canal, this direct perpendicular scrubbing likely accelerates fiber detachment and embedment. Consequently, in the absence of anatomical constraints, the material stability of the applicator becomes the dominant factor, explaining why the fiber-free bristle brush performed significantly better.

From a clinical perspective, our results suggest that bristle brush applicators are a more reliable option for applying adhesives to accessible dentin surfaces, thereby reducing the likelihood of interface contamination and improving bond strength. Nevertheless, microbrushes may be valuable in endodontics, as their flexibility and reach are advantageous, provided that potential problems with residue are avoided through improved manufacturing or adapted application protocols [4,26,28,29].

This study employed GLUMA Bond Universal exclusively, a singular adhesive system. Variations among universal adhesives in solvent composition—such as acetone, ethanol, and water—and viscosity can influence their interaction with applicator fibers and shedding. Consequently, the findings may not be generalizable to all universal adhesives, particularly those with differing solvents or viscosities. Further research should quantify the clinical impact of microbrush fiber residues on the longevity of restorations and evaluate alternative applicator designs or materials. It would also be helpful to investigate whether preconditioning of microbrushes (e.g., pre-rinsing or fiber inspection) could reduce the transfer of residues. Until such findings are available, clinicians should be aware of the potential for fiber contamination and consider applicator choice as a variable


https://doi.org/10.5395/rde.2026.51.e30

that may impact adhesive performance and ultimately the success of bonded restorations.

## CONCLUSIONS

Overall, the results indicate that the bristle brush applicator can achieve a higher and more uniform dentin bond strength than the disposable microbrush when used with the tested universal adhesive under the experimental conditions. The persistent presence of microbrush fiber residue, confirmed by SEM examination, appears to contribute to lower mechanical performance. These results emphasize the importance of applicator choice as a controllable variable in adhesive dentistry and highlight the need for greater awareness of potential applicator-induced contamination.

From a restorative perspective, the results suggest that bristle brush applicators may work better when bonding cavity walls, especially when the bonding surface is fully accessible. The absence of fiber residue reduces the risk of interface contamination, which could otherwise affect polymerization or cause microcracks. In contrast, the microbrush remains useful in narrow spaces, such as root canals, due to its geometry, which provides better access and adaptation, though fiber detachment may occur. Therefore, the applicator used should be tailored to the clinical situation, balancing ease of access with potential risks to the adhesive's integrity.

This *in vitro* study was conducted on flat dentin surfaces under controlled conditions that may not fully reflect the clinical environment. Variables such as saliva contamination, cavity shape, and operator variability could influence residue deposition and bond strength. In addition, only one brand of each applicator type was tested, and differences in manufacturing could influence the tendency for residue detachment.

Furthermore, to definitively isolate the effect of fiber shedding from other applicator mechanics, future studies should include a fiber-free silicone microbrush as a control group. This would help clarify the specific contribution of fiber inclusion to the reduction in bond strength. Further investigations should explore the following aspects: the effect of fiber residues on polymerization kinetics and nano-leakage; the influence of various adhesive formulations on residue adhesion; and strategies to modify the design of microbrushes or fiber anchoring to mitigate contamination risks.

### CONFLICT OF INTEREST

No potential conflict of interest relevant to this article was reported.


### FUNDING/SUPPORT

The authors have no financial relationships relevant to this article to disclose.


### AUTHOR CONTRIBUTIONS

Conceptualization, Funding acquisition, Resources: Alshawi A. Data curation, Validation: Erdemir U, Alshawi A, Lal F. Formal analysis: Ozel Yildiz S, Lal F, Alshawi A. Investigation: Dikmen B, Alshawi A, Lal F. Methodology: Erdemir U, Alshawi A. Project administration: Erdemir U. Software: Ozel Yildiz S, Lal F. Supervision: Erdemir U. Visualization: Dikmen B, Alshawi A. Writing - original draft: Alshawi A, Dikmen B, Ozel Yildiz S, Lal F. Writing - review & editing: Erdemir U, Alshawi A. All authors read and approved the final manuscript.

### DATA SHARING STATEMENT

The datasets are available from the corresponding author upon reasonable request.

### DISCLOSURE OF GENERATIVE AI IN SCIENTIFIC WRITING

Generative AI was utilized solely to improve the language, readability, and grammar of the manuscript. It was not used in data collection, data analysis, or the generation of scientific content or conclusions. The authors take full responsibility for the final content of the publication.

## REFERENCES


1. Cadenaro M, Josic U, Maravić T, Mazzitelli C, Marchesi G, Mancuso E, *et al*. Progress in dental adhesive materials. J Dent Res 2023;102:254-262.
2. Alshawi A, Dikmen B, Ozel Yildiz S, Erdemir U. Effect of modeling liquids on Vickers microhardness, flexural strength and color stability of resin-based composites. Mater Res Express 2025;12:115402.
3. Ueda M, Mine A, De Munck J, Hakogi T, Van Meerbeek B, Kuboki T. The effect of clinical experience on dentine bonding effectiveness: students versus trained dentists. J Oral Rehabil 2010;37:653-657.
4. Souza RO, Lombardo GH, Michida SM, Galhano G, Botti-

no MA, Valandro LF. Influence of brush type as a carrier of adhesive solutions and paper points as an adhesive-excess remover on the resin bond to root dentin. J Adhes Dent 2007;9:521-526.
5. de Menezes FC, da Silva SB, Valentino TA, Oliveira MA, Rastelli AN, Conçalves Lde S. Evaluation of bond strength and thickness of adhesive layer according to the techniques of applying adhesives in composite resin restorations. Quintessence Int 2013;44:9-15.
6. Araújo-Neto VG, Silvestre FA, Lomonaco D, Sauro S, Feitosa VP, Giannini M. Effect of multi-layer applications of self-etch universal bonding agents on the adhesion of resin composite to enamel. Odontology 2025;113:252-260.
7. Catel Y, Fischer UK, Moszner N. Monomers for adhesive polymers, 13.1 synthesis, radical photopolymerization and adhesive properties of polymerizable 2-substituted 1, 3-propylidenediphosphonic acids. Des Monomers Polym 2014;17:286-299.
8. Fujita K, Nishiyama N. Degradation of single bottle type self-etching primer effectuated by the primer's storage period. Am J Dent 2006;19:111-114.
9. Perdigão J, Swift EJ. Universal adhesives. J Esthet Restor Dent 2015;27:331-334.
10. Thitthaweerat S, Nakajima M, Foxton RM, Tagami J. Effect of solvent evaporation strategies on regional bond strength of one-step self-etch adhesives to root canal dentine. Int Endod J 2013;46:1023-1031.
11. Zecin-Deren A, Sokolowski J, Szczesio-Wlodarczyk A, Piwonski I, Lukomska-Szymanska M, Lapinska B. Multi-layer application of self-etch and universal adhesives and the effect on dentin bond strength. Molecules 2019;24:345.
12. Nagarkar S, Theis-Mahon N, Perdigão J. Universal dental adhesives: current status, laboratory testing, and clinical performance. J Biomed Mater Res B Appl Biomater 2019;107:2121-2131.
13. Zecin-Deren A, Lukomska-Szymanska M, Szczesio-Wlodarczyk A, Piwonski I, Sokolowski J, Lapinska B. The influence of application protocol of simplified and universal adhesives on the dentin bonding performance. Appl Sci 2019;10:124.
14. Van Meerbeek B, Yoshihara K, Yoshida Y, Mine A, De Munck J, Van Landuyt KL. State of the art of self-etch adhesives. Dent Mater 2011;27:17-28.
15. Alshawi A, Lal F, Dikmen B, Erdemir U. Do applicator residues remain on the cavity surface during the adhesive application process? Malays Dent J 2025;48:9-15.
16. Berton F, Rapani A, Zotti M, Stacchi C, Berton T, Porrelli D. Presence of microbrush remnants on the adhesion surface: a microscopical analysis. J Dent 2022;127:104320.
17. Generali P. Microbrush X-extended reach applicator [Internet]. Style Italiano Endodontics; 2019 [cited 2025 Nov 25]. Available from: https://endodontics.styleitaliano.org/microbrush-x-extended-reach-applicator/
18. Mitthra S, Sujatha V, Mahalaxmi S. Nano in micro: the role of nanobrush in dentistry. Drug Invent Today 2019;11:2159-2161.
19. Loguercio AD, Muñoz MA, Luque-Martinez I, Hass V, Reis A, Perdigão J. Does active application of universal adhesives to enamel in self-etch mode improve their performance? J Dent 2015;43:1060-1070.
20. Botta SB, Vieira SN, Cordon R, Marques MM, Matos AB. Can the method of primer application influence adhesion to Er:YAG-laser irradiated dentin? J Contemp Dent Pract 2009;10:49-57.
21. Kulzer. GLUMA Bond Universal dental science: scientific compendium [Internet]. Hanau (Germany): Kulzer; 2018 [cited 2025 Nov 25]. Available from: https://www.kulzer.com/media/product-downloads/international-en-int2/gluma/gluma-bond-universal/gluma-bond-universal-compendium-en.pdf
22. Loguercio AD, Stanislawczuk R, Mena-Serrano A, Reis A. Effect of 3-year water storage on the performance of one-step self-etch adhesives applied actively on dentine. J Dent 2011;39:578-587.
23. Reis A, Pellizzaro A, Dal-Bianco K, Gones OM, Patzlaff R, Loguercio AD. Impact of adhesive application to wet and dry dentin on long-term resin-dentin bond strengths. Oper Dent 2007;32:380-387.
24. Ismail AM, Bourauel C, ElBanna A, Salah Eldin T. Micro versus macro shear bond strength testing of dentin-composite interface using chisel and wireloop loading techniques. Dent J (Basel) 2021;9:140.
25. Breschi L, Mazzoni A, Ruggeri A, Cadenaro M, Di Lenarda R, De Stefano Dorigo E. Dental adhesion review: aging and stability of the bonded interface. Dent Mater 2008;24:90-101.
26. Vichi A, Grandini S, Ferrari M. Comparison between two clinical procedures for bonding fiber posts into a root canal: a microscopic investigation. J Endod 2002;28:355-360.
27. Ferrari M, Vichi A, Grandini S. Efficacy of different adhesive techniques on bonding to root canal walls: an SEM investi-


https://doi.org/10.5395/rde.2026.51.e30

gation. Dent Mater 2001;17:422-429.
28. Ferrari M, Grandini S, Simonetti M, Monticelli F, Goracci C. Influence of a microbrush on bonding fiber post into root canals under clinical conditions. Oral Surg Oral Med Oral Pathol Oral Radiol Endod 2002;94:627-631.
29. Ferrari M, Vichi A, Grandini S, Geppi S. Influence of microbrush on efficacy of bonding into root canals. Am J Dent 2002;15:227-231.
30. Fonseca TS, Alfredo E, Vansan LP, Silva RG, Sousa YT, Saquy PC, *et al*. Retention of radicular posts varying the application technique of the adhesive system and luting agent. Braz Oral Res 2006;20:347-352.

RDE Restorative Dentistry & Endodontics

Research Article

eISSN 2234-7666
Restor Dent Endod. 2026 August;51(3):e31
https://doi.org/10.5395/rde.2026.51.e31

# Microbial leakage and marginal adaptation of alkasite restorative material in Class II cavities: an *in vitro* study

**Kah Hup Chew[1], Norhayati Yusop[2], Kasmawati Mokhtar[1], Hafizah Ibrahim[1,*]**

[1]Conservative and Endodontic Unit, School of Dental Sciences, Health Campus, Universiti Sains Malaysia, Kota Bharu, Malaysia
[2]Basic Science Unit, School of Dental Sciences, Health Campus, Universiti Sains Malaysia, Kota Bharu, Malaysia

## ABSTRACT

**Objectives:** This study aimed to determine the relationship between the interfacial properties of proximal cavities (microbial leakage and marginal adaptation) and restorative materials (alkasite, resin composite, and glass hybrid).
**Methods:** This study involved 66 human third molars that were left intact. Standardized Class II cavities were done on the mesial surface. The samples were then divided into five groups: (i) Cention N (CN, Ivoclar Vivadent), (ii) Filtek Z350XT (FZ, 3M ESPE), (iii) EQUIA Forte (GC Corporation), and (iv) two controls. For 40 days, a dual-chamber model containing *Streptococcus mutans* was used to study microbial leakage. Qualitative assessments of the sectioned samples were also carried out using a scanning electron microscope (SEM). Moreover, this study employed descriptive and Kaplan-Meier analyses, alongside a one-way analysis of variance for additional descriptive comparisons ($p < 0.05$).
**Results:** Across different restorative materials, notable variations in microbial leakage were recorded. From the supplementary analysis between CN and FZ, a statistically significant difference was demonstrated ($p = 0.037$). In comparison to other restorative systems, CN also produced a prolonged mean time before microbial leakage occurred. For the interfacial properties of the restorative systems, illustrative information was offered via the SEM images.
**Conclusions:** Regarding microbial leakage, all restorative systems presented their occurrence (despite the constraints of this study). When assessing CN and FZ restorative systems, a slower rate of microbial leakage was also concluded for CN. For the tooth-restoration interface, qualitative data were verified through SEM observations.

**Keywords:** Dental materials; Marginal adaptation; Leakage

## INTRODUCTION

Within the vicinity or adjacent to restorative materials and existing sealants, secondary caries (or recurrent caries) is typically observed [1]. At the restoration margin, this process has a higher likelihood of occurring, causing dental restorations to possess lower durability and effectiveness. For resin composite and amalgam restorations, failure and the need for replacement may then be necessary. Regarding the development of sec-

**Received:** August 24, 2025 • **Revised:** January 23, 2026 • **Accepted:** February 20, 2026
**Citation**
Chew KH, Yusop N, Mokhtar K, Ibrahim H. Microbial leakage and marginal adaptation of alkasite restorative material in Class II cavities: an *in vitro* study. Restor Dent Endod 2026;51(3):e31.
***Correspondence to**
**Hafizah Ibrahim, DDS**
Conservative and Endodontic Unit, School of Dental Sciences, Health Campus, Universiti Sains Malaysia, Kubang Kerian, 16150 Kota Bharu, Kelantan, Malaysia
Email: hafizahibrahim@usm.my

ondary caries, a prevalent factor contributing to this outcome is polymerization shrinkage. In this process, *Streptococcus mutans*, which thrives in conditions favorable to plaque accumulation, can cause bacterial infiltration and the progression of caries via marginal discrepancies [2]. Other factors have also been identified as worsening secondary caries. For example, within the resin matrices for resin composite restoration, contraction stress and hydrolytic degradation can take place [3]. Hence, optimal marginal adaptation in restorative materials must be attained to minimize microbial leakage, alongside improving clinical outcomes (lower incidence of secondary caries).

The movement or infiltration of fluids, bacteria, or molecules at the junction between restorative materials and tooth structure is denoted as microleakage. In restorative dentistry, this process is a considerable issue, in which several impacts (pulpal inflammation, tooth hypersensitivity, and restorative failure) from secondary caries may occur [4]. For resin composite-based restorative systems, antibacterial characteristics are insufficient. If the marginal sealing is compromised, these systems can be more susceptible to microbial colonization [5]. As such, viable alternatives for restorative applications have been created in response to these concerns.

For the efficient placement of materials in dental restorations, alkasite restorative materials (such as Cention N [CN]; Ivoclar Vivadent, Schaan, Liechtenstein) integrating mechanical with bioactive advantages are an optimal choice. Due to its highly reactive fillers, CN is conducive to the ion exchange of fluoride, calcium, and hydroxyl ions. With these ions, demineralization and remineralization can then be hindered, along with demonstrating antibacterial properties, as a result of pH stabilization blocking the acid [6]. For deeper cavities, polymerization can also be promoted via their dual-cure features. Thus, for resin composites that primarily necessitate incremental layering approaches, this step can be removed [7].

In earlier studies, various methods for measuring microbial leakage were established that contained both benefits and limitations. A longstanding and economical technique for visualizing microbial leakage was pioneered by Alani and Toh [8]. Under a stereomicroscope, methylene blue for dye penetration was used to detect leakage. Nonetheless, several constraints have been indicated with this approach. As partial information for assessing microbial leakage is delivered, an underestimation of leakage can occur. Compared to other bacteria (*S. mutans*), an overestimation of microbial leakage can also happen owing to the smaller dye size [9,10]. In a separate investigation, Bagherian *et al*. [11] proposed the method of bacterial penetration. This strategy was based on *S. mutans* as a significant contributor to the development of dental caries. Given that it closely resembles the conditions found in the human oral cavity, it is currently regarded as the most clinically relevant approach. Nevertheless, this method is extremely slow, as it may take between 40 and 60 days to generate results [12].

The most effective seals are usually the most difficult to achieve. On the other hand, these seals are critical in preventing the occurrence of secondary caries for Class II restorations. Hence, this *in vitro* study examined the correlation between the interfacial properties of proximal cavities (microbial leakage and marginal adaptation) and various restorative materials. Based on the microbial leakage assessment technique, a comparison was made among CN, Filtek Z350XT (FZ; 3M ESPE, St. Paul, MN, USA), EQUIA Forte (EF; GC Corporation, Tokyo, Japan), and two control groups (positive and negative) concerning Class II restorations. Hence, the deficiency in research regarding microbiological methods for bacterial penetration in CN restorations could be addressed when conducting a comparative analysis for these materials on actual clinical sealing performance. Through this comparison, information concerning clinical performance and restoration longevity could then be obtained for CN, FZ, and EF. In this study, the null hypothesis ($H_o$) was posited as follows:

$H_o$: There would be no significant differences in the time to microbial leakage and marginal adaptation across Class II restorations restored with alkasite (CN), resin composite (FZ), and glass hybrid restorative systems (EF).

## METHODS

### Experimental materials

In Table 1, the materials, manufacturers, curing meth-


https://doi.org/10.5395/rde.2026.51.e31

**Table 1.** Types of materials evaluated

| Material | Manufacturer | Type and method of curing | Resin | Filler | Filler content (wt%/vol%) |
|---|---|---|---|---|---|
| Cention N (bulk-fill) | Ivoclar Vivadent, Schaan, Liechtenstein | Alkasite (self-curing powder/liquid with optional additional light curing) | UDMA<br>DCP<br>Aromatic aliphatic-UDMA<br>PEG-400 DMA | Br-Al-Si glass filler, ytterbium trifluoride, and Isofiller (copolymer), a calcium barium aluminum fluorosilicate glass filler and a calcium fluorosilicate (alkaline) glass filler (0.1–35 µm) | 75/61 |
| Filtek Z350XT | 3M ESPE, St. Paul, MN, USA | Nano-hybrid composite (light-cured) | Bis-GMA<br>Bis-EMA<br>UDMA | Non-aggregated 20 nm Silica filler, non-aggregated 4–11 nm zirconia filler and aggregated silica/zirconia cluster filler | 78.5/63.3 |
| EQUIA Forte (EQUIA Forte Fil + EQUIA Forte Coat) | GC Corporation, Tokyo, Japan | Glass ionomer with glass hybrid technology | Polyacrylic acid, distilled water, polybasic carboxylic acid | Strontium fluoro-alumino-silicate glass, polyacrylic acid powder, pigments | - |

UDMA, urethane dimethacrylate; DCP, tricyclodecane dimethanol dimethacrylate; PEG-400 DMA, polyethylene glycol-400 dimethacrylate; bis-GMA, bisphenol glycol dimethacrylate; bis-EMA, bisphenol ethylmethacrylate.

ods, types of resin, and fillers utilized for each restorative material are listed. To restore Class II cavities in the third molars, the restorative materials were employed. Examinations concerning microbial leakage and marginal adaptation were then carried out.

### Teeth preparation

In this study, ethical approval from Jawatankuasa Etika Penyelidikan Manusia (JEPeM) Universiti Sains Malaysia was received in accordance with the Helsinki Declaration (USM/JEPeM/KK/23070568). Using strict inclusion criteria, 66 human third molars with no caries, restorations, or cracks were selected. All third molars were also kept in a 0.02% thymol solution for 1 day to prevent bacterial contamination, alongside maintaining hydration. Regarding the mesial aspect, every tooth was subjected to Class II cavity preparation. For the gingival wall cavities, the buccolingual and mesiodistal widths were 4 mm and 2 mm, respectively.

To preserve the remaining enamel width of 0.5 mm to 1.0 mm, the gingival wall was situated within the enamel, which was above the cementoenamel junction. The preparations also incorporated rounded internal line angles, and to maintain uniformity, retentive grooves were omitted. A high-speed straight fissure diamond point friction grip bur with water coolant was also utilized for the cavity preparation. To maintain optimum cutting quality and uniformity, a bur was changed after five cavity preparations. Lastly, to ensure uniformity in the dimensions of the prepared cavities, one trained operator, using a digital vernier calliper, conducted all the cavity preparations.

### Grouping of teeth

Once the third molar teeth were prepared, they were divided into five groups (three experimental [$n = 20$] and two control groups [$n = 3$]). In Groups 1 to 3, restoration involved employing an alkasite restorative material (CN), nanohybrid resin composite (FZ), and bulk-filled glass hybrid restorative material (EF), respectively. For bacterial penetration (positive control), Group 4 comprised unrestored teeth following cavity preparation. To prevent bacterial ingress (negative control), Group 5 consisted of unrestored teeth with all surfaces entirely covered in nail varnish. The teeth restoration process

https://doi.org/10.5395/rde.2026.51.e31 

also included the use of a matrix to simulate natural contact points. The prepared teeth were secured in place on green stone, along with adjacent non-carious teeth. A sectional matrix band (Halo Sectional Matrix System Kit; Ultradent Products, Inc., South Jordan, UT, USA) was also used to assure proper contouring and adaptation during the restoration process.

### Tooth restoration and sealing

Group 1 samples were subjected to 20 seconds of acid etching with 37% phosphoric acid gel (Scotchbond; 3M ESPE), which was accompanied by a water rinse to remove residual etchant. A microbrush was also used to apply the bonding agent (Tetric N-Bond; Ivoclar Vivadent) and was light-cured for 20 seconds. In addition, to create a uniform CN mixture, 15 g of powder with 4 mL of liquid was combined. Subsequently, an incremental technique and a 20-second light-curing process were sequentially used. During the curing, a light-cured unit tip (3M Elipar DeepCure-S LED curing light; 3M ESPE) was brought close to the restorative material (wavelength, 430–480 nm). In order to achieve consistent polymerization, the curing light unit was recharged after every 10 samples.

The same procedure (37% phosphoric acid gel for 20 seconds and followed by water rinse) was done for Group 2. In this group, a single-bond universal adhesive bonding agent (3M ESPE) was applied using a microbrush. For optimal adhesion to the tooth structure, a 20-second light-curing process was performed on the material. Subsequently, the incremental layering technique was used to apply FZ (40-second light-curing for each layer). Polishing was done on the same day to achieve a smooth surface finish via a composite resin polishing kit (AZDENT RA 0309; AZDENT Dental Co., Ltd., Zhengzhou, China) and a slow-speed handpiece (PTL-CL-LED; NSK Ltd., Kanuma, Japan).

In Group 3, the GC Cavity Conditioner (GC Corporation) was applied for 10 seconds, after which it was rinsed off and gently dried without desiccation prior to the placement of EQUIA Forte Fil. The capsule was then initiated and triturated for 10 seconds, after which it was promptly positioned with a capsule applicator. Subsequently, the material was molded. Once prepared, improved mechanical characteristics were accomplished by applying EQUIA Forte Coat and then light-cured for 20 seconds. Likewise, bacterial penetration was permitted for the positive control group, which contained unrestored teeth following cavity preparation. Conversely, for completely preventing bacterial penetration, the negative control group had all tooth surfaces coated with nail varnish.

### Thermocycling

Within a 37°C incubator (Memmert GmbH, Schwabach, Germany), all samples were kept in distilled water after restoration for 24 hours. In order to replicate oral conditions, the samples were also subjected to 1,000 thermal cycles (5°C–55°C, 30 seconds dwell time per cycle) [13]. For enhancing the consistency of specimen preparation, each sample underwent derooting, after which the dentin between the pulp chamber floor and the furcation area was removed. Across all surfaces, nail varnishes were finally applied. In this study, to ensure the margins were properly isolated, a 2-mm perimeter around the restoration was created.

### Disinfection and sterilization

Using epoxy resin (Araldite; Huntsman Advanced Materials, Basel, Switzerland), the samples were firmly affixed at the ends of plastic tubes to establish a stable interface. Each sample was assigned a code that corresponded to its group number before being packed and sterilized by gamma irradiation (eliminating microbial contamination). In guaranteeing aseptic conditions, the glass tubes were also sterilized for 15 minutes through an autoclave (Systec GmbH, Wettenberg, Germany) at 121°C.

### Sample preparation

For assessing microbial penetration, Figure 1 depicts the employed modified two-chamber microbial leakage model [11]. A sterile glass tube filled with brain-heart infusion broth (BHI; Oxoid Ltd., Basingstoke, UK) was used. For each sample, an immersion in the medium covering 2–3 mm was also ensured. An initial suspension of *S. mutans* (ATCC 25175; concentration, $1.5 \times 10^8$ colony-forming units [CFU]/mL) was then prepared to introduce the bacterial challenge. Subsequently, to ensure that the restorative margin was continuously


https://doi.org/10.5395/rde.2026.51.e31

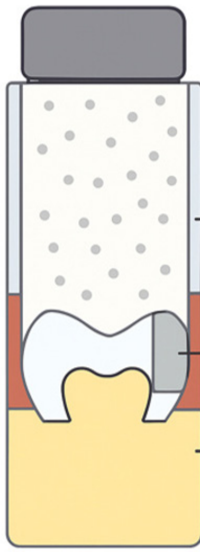


**Figure 1.** Schematic diagram of the modified dual-chamber model used for microbial leakage assessment. BHI, brain-heart infusion.

exposed to *S. mutans*, 8 mL of the bacterial suspension was utilized to fill the upper chamber of the experimental setup. To maintain a sterile environment and prevent unintended contamination, along with preserving the integrity of the experiment, all procedures were also conducted with great care within a biosafety cabinet field (Heraeus HS-12; Heraeus, Hanau, Germany).

### Incubation and bacterial penetration monitoring

A 37°C incubator was utilized for placing all the samples for 40 days. For turbidity (bacterial penetration and microbial leakage), the lower chamber was monitored on a daily basis. When turbidity was detected, a broth sample was streaked onto blood agar plates in duplicate to incubate for 24 hours. The isolated bacteria were then examined using an Axioplan 2 imaging system (Carl Zeiss Pte. Ltd., Singapore, Singapore) with Gram staining and microscopic examination to identify *S. mutans* and to check for the presence of other microorganisms. To maintain a constant bacterial challenge, 8 mL of fresh *S. mutans* suspensions (concentration, $1.5 \times 10^8$ CFU/mL) were also added to the upper chamber every day. The occurrence of turbidity (microbial leakage) was then recorded for each sample. Lastly, data collection was conducted in a systematic manner over a span of 40 days. Statistical analysis was also performed using IBM SPSS Statistics ver. 29.0 (IBM Corp., Armonk, NY, USA) in evaluating the microbial leakage patterns, alongside comparing the efficacy of the restorative materials under study.

### Marginal adaptation analysis

Each experimental group sample was sectioned mesiodistally using a hard tissue cutter (EXAKT Apparatebau GmbH & Co. KG, Norderstedt, Germany) through the middle of the restoration. This method ensured precision of cut while minimizing thermal damage. For the scanning electron microscopy (SEM) analysis, the proximal surface of the cut samples was examined using a SEM (JEOL JSM-IT100; JEOL Ltd., Tokyo, Japan). Both low and high magnifications of the SEM (500× and 1,000×) were also used to assess the quality of the sample, along with the presence and continuity of the interface between the enamel and restoration. Through this process, data regarding microgaps and interfacial discontinuities (microbial leakage and secondary caries) were obtained [14]. During the SEM assessment, a single calibrated examiner who was unaware of the group assignments was also present. There were no repeated quantitative measurements or statistical analyses due to the SEM analysis being primarily descriptive.

### Statistical analysis

Using IBM SPSS Statistics ver. 29.0, data analysis was performed. In assessing the occurrence of microbial leakage throughout the 40-day observation period, the Kaplan-Meier product-limit survival analysis was employed. The mean leakage times were also described descriptively. For providing a descriptive comparison of mean leakage times across the group, one-way analysis of variance (ANOVA) with the Games-Howell *post hoc* test was utilized. In this study, the threshold for statistical significance was then established at $p < 0.05$.

## RESULTS

### Microbial leakage

Regarding the microbial leakage assessments of the three experimental groups, descriptive and Kaplan-Meier survival analyses were used, along with a supplementary descriptive comparison (ANOVA, $p < 0.05$). The minimum duration for microbial leakage in CN, FZ, and EF groups was then computed to be 3, 2, and 3 days, respectively. On the contrary, the maximum durations recorded were 36, 17, and 23 days, respectively. Concerning the mean values (± standard deviation), Table 2 reveals a decreasing value order as follows: CN (16.30 ± 9.465) > EF (12.50 ± 6.692) > FZ (10.15 ± 4.522). In Figure 2, the survival probabilities for microbial leakage over a 40-day period are also measured via the Kaplan-Meier product-limit method. Another finding that should be interpreted with caution was that across the three groups, the one-way ANOVA revealed a statistically significant difference in mean leakage times ($p = 0.030$). In comparing CN with FZ, the Games-Howell *post hoc* analysis computed a significant difference ($p = 0.037$). Conversely, when comparing CN with EF and EF with FZ, no significant differences were recorded ($p = 0.320$ and $p = 0.404$) (Table 2).

### Marginal adaptation

From the SEM assessment, qualitative differences in marginal adaptation and interfacial morphology were presented for all the restorative materials (Figure 3). Notably, a more consistent enamel-restoration interface was indicated for CN. Nonetheless, a higher occurrence of interfacial discontinuities was implied in FZ and EF.

## DISCUSSION

In this study, based on a bacterial penetration method to assess microbial leakage, both microbial leakage and marginal adaptation of various restorative materials were successfully examined. What could then be observed was that CN, FZ, and EF produced notable disparity in microbial leakage. In this case, a partial rejection of the null hypothesis concerning microbial leakage was suggested. This study also only performed a qualitative evaluation of the marginal adaptation. As such, for the corresponding null hypothesis, statistical rejection was precluded.

In dentistry, microleakage in dental restorations has consistently raised concerns. Specifically, several processes in the tooth have been demonstrated to cause issues via dimensional alterations of restorative materials. Such examples of these processes entail polymerization shrinkage, thermal contraction, and mechanical stress, alongside tooth-related dimensional changes [15]. For polymerization shrinkage, contraction forces are generated within the resin composite. Microbial leakage can then occur when the bonds to the cavity walls are disrupted [16]. Microbial leakage following the polymerization of resin composites can also be observed when inner cracks develop in the enamel [17].

Regarding the coefficient of thermal expansion, it has been mainly deemed as a factor causing microbial leakage [18]. In an investigation documented by McCabe and Walls [19], the authors reported that differences in this coefficient between restorative materials and teeth

**Table 2.** Microbial leakage in the three experimental groups over a 40-day period

| Group | No. of samples | Leakage day | | $p$-value[a)] | Post hoc GH |
|---|---|---|---|---|---|
| | | Range | Mean ± SD | | |
| CN | 20 | 3–36 | 16.30 ± 9.46 | 0.030* | a |
| FZ | 20 | 2–17 | 10.15 ± 4.52 | | a |
| EF | 20 | 3–23 | 12.50 ± 6.69 | | b |

SD, standard deviation; GH, Games-Howell test.
Groups with same letter are significantly different from each other.
CN, Cention N (Ivoclar Vivadent, Schaan, Liechtenstein); FZ, Filtek Z350XT (3M ESPE, St. Paul, MN, USA); EF, EQUIA Forte (GC Corporation, Tokyo, Japan).
[a)]Analyzed by analysis of variance.
*$p < 0.05$, statistically significant difference.

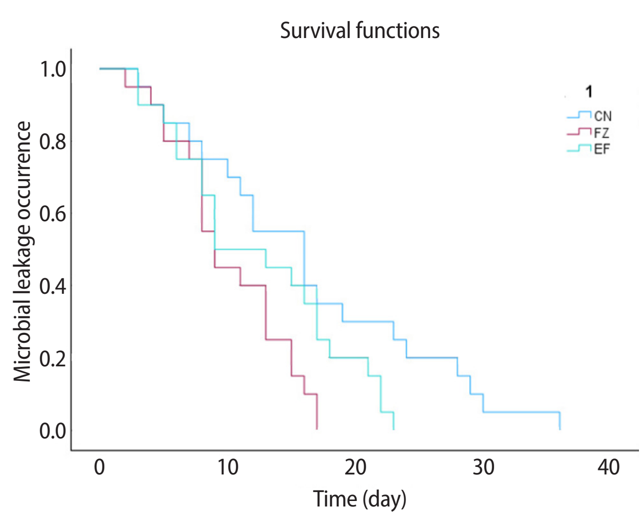


**Figure 2.** Microbial leakage occurrence rates over 40 days among different restorative materials. CN, Cention N (Ivoclar Vivadent, Schaan, Liechtenstein); FZ, Filtek Z350XT (3M ESPE, St. Paul, MN, USA); EF, EQUIA Forte (GC Corporation, Tokyo, Japan).


https://doi.org/10.5395/rde.2026.51.e31

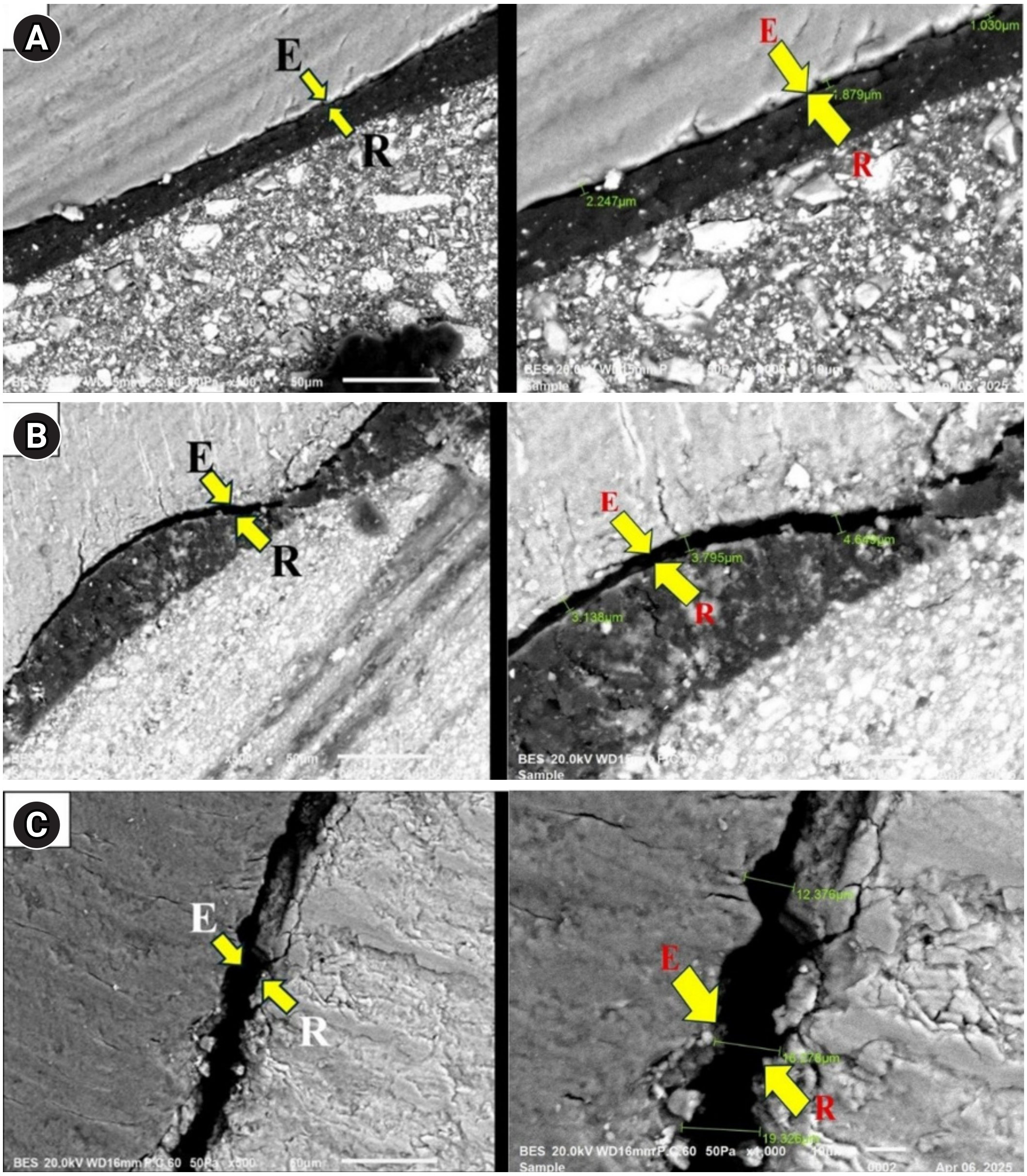


**Figure 3.** Scanning electron microscope images of the enamel–restoration interface for three materials (A, Cention N [Ivoclar Vivadent, Schaan, Liechtenstein]; B, Filtek Z350XT [3M ESPE, St. Paul, MN, USA]; and C, EQUIA Forte [GC Corporation, Tokyo, Japan]) at 500× (left) and 1,000× (right) magnifications. Yellow arrows indicate the marginal gap between enamel (E) and restorative material (R).

could produce this leakage type. This leakage has also been observed to occur under bond failure, as the restorations along cavity walls promote micromovements due to elastic modulus disparities [20]. For the samples undergoing thermocycling in this study, it was then expected that microbial leakage might be generated when repetitive contraction and expansion stress occurred on the tooth and restoration interfaces. Specifically, earlier onset of microbial leakage could occur under higher interfacial stress and gap formation owing to the rising thermal expansion of the resin composite.

In examining microbial leakage for Class II cavities, various restorative materials were employed in this study. Nevertheless, there are currently no restorative techniques or materials that can achieve an ideal marginal seal with cavity walls, along with completely pre-

https://doi.org/10.5395/rde.2026.51.e31 

venting microbial leakage [21]. At the interface between tooth structure and restorative materials, microsurfaces are also invariably present. Thus, if the penetration of bacteria and fluids takes place, secondary caries can occur [22]. When examining the results of this study, an elevated C-factor in Class II restorations was assumed to demonstrate a larger microbial leakage than Class I restorations. In utilizing comparable restorative materials, a significant correlation was then indicated between this factor and microbial leakage [23].

Looking through earlier studies, there were multiple techniques for assessing microbial leakage (SEM, dual-chamber modification, and dye penetration). Historically, the earliest strategy employed to assess microbial leakage was dye penetration. In most investigations, the ease and practicality of this approach have rendered it frequently utilized as a gold standard [8,11,24-26]. Some dye examples that are primarily used include methylene blue, eosin, hematoxylin, aniline red, fluorescent dye, and crystal violet red [8]. Nonetheless, a number of limitations have been documented with this method.

To effectively demonstrate the adaptation of restorations, another strategy for the assessment of microbial leakage involves the SEM tool [21]. As a detailed visualization of the enamel-restoration interface (high magnification) can be obtained through this tool, a qualitative evaluation of interfacial continuity can be presented, alongside the presence of observable gaps. Therefore, the microbial leakage and bacterial infiltration along the margins can be placed in detail [27]. In readily navigating through marginal gaps, the small size of *S. mutans* (0.5–1 μm) also makes this process easily achieved [28]. Secondary caries can then form when bacterial infiltration is allowed, along with the movement of enzymes and saliva. For deep cavities, this outcome is evident when enamel is compromised, alongside the edges consisting of dentin and cementum (or both) [29].

For Class II restoration, this study employed a dual-chamber modification in evaluating microbial leakage. Typically, a documented count of the days during which turbidity is observed is necessary for assessing microbial leakage (quantitative data). Given that *S. mutans* more accurately reflects oral conditions (more reliable data), they are mainly applied via this approach [30]. Conversely, this process remains time-consuming (40–60 days) concerning the microbial penetration method. Daily observations of samples are conducted, alongside the replacement of fresh bacteria if there is no turbidity.

In the event of turbidity, it is essential to confirm the presence of bacteria through culturing, morphology assessment of the bacterial colony, Gram staining, and microscopic observation. Through these steps, no contamination from other bacterial species, aside from *S. mutans*, can then be confirmed. For assessing the movement of bacteria across the tooth-restoration interface, the microbial penetration method is also highly capable. Nevertheless, in understanding microbial leakage, information concerning bacterial metabolites, fluids, toxins, or ions is lacking [30]. For this study, mimicking the chemical composition of saliva within the oral cavity is another challenge, as the employed BHI broth could not completely achieve this environment [11].

For all restorations assessed in this study, microbial leakage was detected within 40 days, aligning with the outcomes reported by Nematollahi *et al.* [30]. What could be inferred from this observation was that at the marginal gaps at the tooth-restoration interface, the daily replacement and exposure to large fresh bacteria levels caused them to infiltrate. Further examination of the results also revealed a correlation between restorative materials and microbial leakage rates, in which a delayed onset or an earlier occurrence of this leakage was observed for CN and FZ, respectively. For the CN restorative system, the formation of an acid-resistant interface and resin-dentin interdiffusion zone might be the factors lowering the leakage when utilized alongside the suggested bonding protocol (strong sealing) [31]. Yoo *et al.* [32] also published similar trends.

In reducing shrinkage stress, CN powder was suitable based on its isofiller. On the contrary, the liquid formulation contained four dimethacrylates (DMAs), along with initiators and various additives. Improved mechanical strength and durability over time were also demonstrated when tricyclodecan-dimethanol dimethacrylate (DCP), urethane dimethacrylate (UDMA), aromatic aliphatic-UDMA, and polyethylene glycol 400 (PEG-400) DMA were present to produce cross-links during polymerization. Likewise, straightforward handling was offered by DCP, alongside its low viscosity. For UDMA,


https://doi.org/10.5395/rde.2026.51.e31

it acted as the main component of the monomer matrix to improve mechanical characteristics while preserving moderate viscosity. A lower likelihood of discoloration could also be attained through the aliphatic features of aromatic aliphatic-UDMA. In enhancing stiffness, aromatic diisocyanates were pivotal. Better flowability and adaptation to the smear layer could then be accomplished using PEG-400 DMA [33,34]. For both polymerization and low shrinkages, they could also be lowered via CN (containing patented filler partially functionalized with silane) and the organic/inorganic ratio with monomer composition, respectively [31].

Regarding marginal adaptation, varying interfacial morphology was observed from the SEM images for different materials. At the enamel-restoration interface, fewer noticeable discontinuities were denoted for CN, agreeing with the data published by Samanta *et al.* [35] and Firouzmandi *et al.* [36]. In another article by Mehesen *et al.* [14] concerning glass ionomer-based restorations, greater marginal gaps were reported. Nonetheless, qualitative observations were only presented in this study for the SEM analysis. Interestingly, the microbial leakage characteristics of CN for both this study and Sujith *et al.* [37] were identical, who examined the hybrid composite restorative materials and glass ionomer cement, alongside their corresponding mechanical and microbial leakage performances.

In this study, the experiment was performed under *in vitro* conditions for the alkasite restorative material and glass hybrid restorative materials. Conversely, other clinical studies have reported positive *in vivo* outcomes in posterior restorations. For alkasite restorative materials concerning stress-bearing posterior teeth, several benefits have been documented (satisfactory marginal integrity, periodontal response, and short- to medium-term survival). As such, regular clinical use can benefit from this design [7]. In terms of nanohybrid resin composites, favorable aesthetic results and mechanical strength have also been noted within long-term clinical studies. Nevertheless, issues with secondary caries and restoration replacement over time can still occur due to polymerization shrinkage and marginal degradation [22]. Regarding posterior restorations in atraumatic restorative treatment and high-caries-risk populations, glass hybrid restorative materials still remain popular owing to their fluoride release and chemical adhesion to tooth structure [38]. All these clinical observations have then suggested that under controlled laboratory conditions, microbial leakage and interfacial behavior examinations are vital, which this study successfully addressed.

From this study, the chemical composition and ion-releasing ability of CN were thoroughly explained. Still, to provide context for the current findings, a comparative analysis with FZ and EF properties must be carried out. When using FZ, enhanced polishability, aesthetics, and mechanical strength can generally be observed, as this nanohybrid resin composite contains high filler loading and nanoscale filler technology. Nevertheless, being a methacrylate-based composite, it is naturally prone to polymerization shrinkage stress, along with insufficient intrinsic ion release. Thus, the formation of marginal gaps, alongside a heightened vulnerability to microbial penetration as time progresses, can occur [15,16].

For EF, it represents a glass hybrid restorative system, which consists of high-viscosity glass ionomer cement and a resin-based surface coating. Based on its chemical adhesion to tooth structure and the release of fluoride, EF can diminish the risk of caries. In contrast, the marginal integrity of Class II restorations when exposed to occlusal loading can be jeopardized due to the sensitivity to moisture (initial setting phase), alongside lower fracture toughness [38]. Therefore, as the CN restorative system integrates resin-based mechanical properties and alkaline ion release, superior microbial sealing restorative systems can be attained (demonstrated in this study). It was also crucial to note that for each material, the bonding and conditioning protocols recommended by the manufacturer were followed. Thus, the results should be interpreted with respect to the system containing the materials.

From a clinical standpoint, scenarios involving critical marginal sealing and caries prevention could highly benefit from alkasite restorative systems (CN), as demonstrated in this study. In particular, in scenarios where optimal moisture control proved difficult, individuals with a high risk of caries, deep proximal cavities, or clinical circumstances could employ these Class II restorations. As this study also revealed good ion-releas-

https://doi.org/10.5395/rde.2026.51.e31

ing ability and qualitative interfacial properties, a more stable tooth-restoration interface, alongside minimized bacterial infiltration at the margins of the restoration, could be accomplished. Nonetheless, the differences observed were dependent on the material system used, which clinicians must take into account. Significant relationships were also exhibited between long-term clinical success, cavity design, occlusal loading, oral hygiene, and patient-related risk factors.

It was important to note that between restorative materials and the authentic oral environment, actual conditions or interactions that occurred in this study were not completely represented by the data. Some constraints observed in this methodology involved inadequate causatives (salivary enzymes, bacterial plaque, and pH fluctuations) within the oral environment. Accordingly, to confirm the clinical advantages of alkasite restorative systems in dynamic oral environments, a long-term randomized controlled clinical trial was necessary. The inferential comparisons of microbial leakage times also denoted another limitation, as they were not solely reliant on survival-specific statistical tests. Thus, it is advisable for future research to utilize survival-based comparative methods.

## CONCLUSIONS

Albeit with variations in both the extent and timing of the leakage observed, this *in vitro* study revealed that all restorative systems demonstrated microbial leakage. Compared to FZ, delayed microbial leakage was presented by the CN restorative system. For the qualitative illustrative information on the tooth-restoration interface, it was demonstrated through the SEM observations.

### CONFLICT OF INTEREST

No potential conflict of interest relevant to this article was reported.

### FUNDING/SUPPORT

This research project was supported by a short-term grant from Universiti Sains Malaysia (304/PPSG/6315781).

### AUTHOR CONTRIBUTIONS

Conceptualization: Ibrahim H, Yusop N. Data curation, Formal analysis, Investigation, Software, Visualization: Chew KH. Funding acquisition, Project administration, Supervision: Ibrahim H. Methodology, Validation: Mokhtar K. Resources: Yusop N. Writing - original draft: Chew KH. Writing - review & editing: Ibrahim H, Mokhtar K, Yusop N. All authors read and approved the final manuscript.

### DATA SHARING STATEMENT

The datasets are not publicly available but are available from the corresponding author upon reasonable request.

### DISCLOSURE OF GENERATIVE AI IN SCIENTIFIC WRITING

During the preparation of this manuscript, the authors used AI to assist with language editing, grammar refinement, and improvement of sentence clarity. The authors reviewed and edited all AI-generated content and take full responsibility for the accuracy, integrity, and originality of the manuscript.

## REFERENCES

1. Askar H, Krois J, Göstemeyer G, Bottenberg P, Zero D, Banerjee A, *et al*. Secondary caries: what is it, and how it can be controlled, detected, and managed? Clin Oral Investig 2020;24:1869-1876.
2. Patel MU, Punia SK, Bhat S, Singh G, Bhargava R, Goyal P, *et al*. An in vitro evaluation of microleakage of posterior teeth restored with amalgam, composite and Zirconomer: a stereomicroscopic study. J Clin Diagn Res 2015;9:ZC65-ZC67.
3. Bourbia M, Finer Y. Biochemical stability and interactions of dental resin composites and adhesives with host and bacteria in the oral cavity: a review. J Can Dent Assoc 2018;84:i1.
4. Breschi L, Mazzoni A, Ruggeri A, Cadenaro M, Di Lenarda R, De Stefano Dorigo E. Dental adhesion review: aging and stability of the bonded interface. Dent Mater 2008;24:90-101.
5. Park C, Park H, Lee J, Seo H, Lee S. Surface roughness and microbial adhesion after finishing of alkasite restorative material. J Korean Acad Pediatr Dent 2020;47:188-195.
6. Ruengrungsom C, Burrow MF, Parashos P, Palamara JE. Evaluation of F, Ca, and P release and microhardness of eleven ion-leaching restorative materials and the recharge efficacy using a new Ca/P containing fluoride varnish. J Dent 2020;102:103474.
7. Mustafa K, Alfakhry G, Milly H. Periodontal evaluation for a new alkasite restorative material in noncarious cervical


https://doi.org/10.5395/rde.2026.51.e31

lesions: a randomized-controlled clinical trial. Clin Exp Dent Res 2024;10:e70025.
8. Alani AH, Toh CG. Detection of microleakage around dental restorations: a review. Oper Dent 1997;22:173-185.
9. Wimonchit S, Timpawat S, Vongsavan N. A comparison of techniques for assessment of coronal dye leakage. J Endod 2002;28:1-4.
10. Memarpour M, Derafshi R, Razavi M. Comparison of microleakage from stainless steel crowns margins used with different restorative materials: an in vitro study. Dent Res J (Isfahan) 2016;13:7-12.
11. Bagherian A, Ahmadkhani M, Sheikhfathollahi M, Bahramabadinejad R. Microbial microleakage assessment of a new hydrophilic fissure sealant: a laboratory study. Pediatr Dent 2013;35:194-198.
12. Erdilek N, Ozata F, Sepetcioglu F. Microleakage of glass ionomer cement composite resin and glass ionomer resin cement. J Clin Pediatr Dent 1997;21:311-314.
13. Moosavi H, Mohammadipour HS, Ghavamnasiri M, Alizadeh S. Effect of bleaching and thermocycling on resin-enamel bond strength. Int J Biomater 2015;2015:921425.
14. Mehesen R, Jazar H, Sheta N, Montaser M. Scan electron microscope evaluation of marginal adaptation of alkasite, bulk-fil resin composite, resin modified glass ionomer, and high viscosity glass ionomer restorative materials. Egypt Dent J 2022;68:1859-1866.
15. Staninec M, Mochizuki A, Tanizaki K, Jukuda K, Tsuchitani Y. Interfacial space, marginal leakage, and enamel cracks around composite resins. Oper Dent 1986;11:14-24.
16. Davidson CL, de Gee AJ, Feilzer A. The competition between the composite-dentin bond strength and the polymerization contraction stress. J Dent Res 1984;63:1396-1399.
17. Han L, Okamoto A, Iwaku M. The effects of various clinical factors on marginal enamel micro-cracks produced around composite restoration. Dent Mater J 1992;11:26-37.
18. Yazici AR, Baseren M, Dayangaç B. The effect of flowable resin composite on microleakage in class V cavities. Oper Dent 2003;28:42-46.
19. McCabe JF, Walls AWG. Properties used to characterise materials. In: McCabe JF, Walls AWG, editors. Applied dental materials. 8th ed. Oxford, UK: Blackwell Science; 1998. p. 4-28.
20. Lundin SA, Norén JG. Marginal leakage in occlusally loaded, etched, class-II composite resin restorations. Acta Odontol Scand 1991;49:247-254.
21. Ian AT, Muttlib NA, Bakar WZ, Alam MK. Comparison between microleakage of composite and porcelain in Class V restoration: an in vitro study. Int Med J 2013;20:359-362.
22. Rai N, Shetty S, Gupta R. Comparative evaluation of the microleakage of Cention N and glass ionomer cements in open-sandwich class II restorations: an in vitro study. J Int Oral Health 2023;15:113-118.
23. Kalmowicz J, Phebus JG, Owens BM, Johnson WW, King GT. Microleakage of class I and II composite resin restorations using a sonic-resin placement system. Oper Dent 2015;40:653-661.
24. Chen X, Cuijpers VM, Fan MW, Frencken JE. Validation of micro-CT against the section method regarding the assessment of marginal leakage of sealants. Aust Dent J 2012;57:196-199.
25. Parolia A, Adhauliya N, de Moraes Porto IC, Mala K. A comparative evaluation of microleakage around class V cavities restored with different tooth colored restorative materials. Oral Health Dent Manag 2014;13:120-126.
26. Taylor MJ, Lynch E. Microleakage. J Dent 1992;20:3-10.
27. Gunjal S, Nagesh L, Raju HG. Comparative evaluation of marginal integrity of glass ionomer and resin based fissure sealants using invasive and non-invasive techniques: an in vitro study. Indian J Dent Res 2012;23:320-325.
28. Schmalz G, Ergücü Z, Hiller KA. Effect of dentin on the antibacterial activity of dentin bonding agents. J Endod 2004;30:352-358.
29. Visuttiwattanakorn P, Suputtamongkol K, Angkoonsit D, Kaewthong S, Charoonanan P. Microtensile bond strength of repaired indirect resin composite. J Adv Prosthodont 2017;9:38-44.
30. Nematollahi H, Bagherian A, Ghazvini K, Esmaily H, Mehr MA. Microbial microleakage assessment of class V cavities restored with different materials and techniques: a laboratory study. Dent Res J (Isfahan) 2017;14:344-350.
31. Meshram P, Meshram V, Palve D, Patil S, Gade V, Raut A. Comparative evaluation of microleakage around Class V cavities restored with alkasite restorative material with and without bonding agent and flowable composite resin: an in vitro study. Indian J Dent Res 2019;30:403-407.
32. Yoo HM, Oh TS, Pereira PN. Effect of saliva contamination on the microshear bond strength of one-step self-etching adhesive systems to dentin. Oper Dent 2006;31:127-134.
33. Ivoclar Vivadent. Scientific documentation: Cention N [Internet]. Schaan, Liechtenstein: Ivoclar Vivadent; c2016 [cited

2025 Aug 24]. Available from: https://www.ivoclar.com/en_eme/products/filling-materials/cention-n
34. Moszner N, Fischer UK, Angermann J, Rheinberger V. A partially aromatic urethane dimethacrylate as a new substitute for Bis-GMA in restorative composites. Dent Mater 2008;24:694-699.
35. Samanta S, Das UK, Mitra A. Comparison of microleakage in Class V cavity restored with flowable resin composite, glass ionomer cement and Cention N. Imp J Interdiscip Res 2017;3:180-183.
36. Firouzmandi M, Alavi AA, Jafarpour D, Sadatsharifee S. Fracture strength and marginal adaptation of conservative and extended MOD cavities restored with Cention N. Int J Dent 2021;2021:5599042.
37. Sujith R, Yadav TG, Pitalia D, Babaji P, Apoorva K, Sharma A. Comparative evaluation of mechanical and microleakage properties of Cention-N, composite, and glass ionomer cement restorative materials. J Contemp Dent Pract 2020;21:691-695.
38. Czarnecka B, Kruszelnicki A, Kao A, Strykowska M, Nicholson JW. Adhesion of resin-modified glass-ionomer cements may affect the integrity of tooth structure in the open sandwich technique. Dent Mater 2014;30:e301-e305.


https://doi.org/10.5395/rde.2026.51.e31

RDE Restorative Dentistry & Endodontics

Research Article

eISSN 2234-7666
Restor Dent Endod. 2026 August;51(3):e32
https://doi.org/10.5395/rde.2026.51.e32

# Classification proposal of obliterated canals based on the position of the target point and the caliber of the root canal

Gustavo Adolfo Castillo Barrios[1], Patricia Rodríguez Sánchez[1], Anuar Elian Barona Triviño[1], Carlos Humberto Martínez Cajas[2,*]

[1]Department of Endodontics, Universidad del Valle, Cali, Colombia
[2]Clinical Specialization Programs in Dentistry, Institución Universitaria Colegios de Colombia (UNICOC), Cali, Colombia

## ABSTRACT

**Objectives:** This study aimed to propose a classification system for calcified root canals based on the location of the target point or canal starting point and root canal lumen caliber to facilitate the evaluation of dynamically guided techniques in endodontic treatment.
**Methods:** A retrospective analysis of eight cases with calcified root canals was conducted. Periapical radiographs and cone-beam computed tomography were used to classify cases based on root location and degree of obliteration. Clinical and radiographic outcomes were evaluated.
**Results:** Eight classification types are identified, ranging from non-obliteration and partial obliteration to total obliteration. The location of the root canal lumen varies from the pulp chamber to the apical third of the root. Guided endodontics with dynamic navigation has been demonstrated to be an effective treatment modality in cases of advanced obliteration, thereby substantiating its efficacy in complex scenarios.
**Conclusions:** The proposed classification system provides a framework to understand the complexity of calcified root canals. Guided endodontics with dynamically guided techniques can be valuable in managing these challenging cases, particularly when the root canal lumen is in the apical third. Further studies are needed to validate the classification system and evaluate the long-term outcomes of the different treatment approaches.

**Keywords:** Cone-beam computed tomography; Dental pulp; Dental pulp calcification; Dental radiography; Tooth injuries

## INTRODUCTION

Conventional endodontic treatment involves shaping, cleaning, and disinfecting the root canal system due to inflammation or pulp necrosis [1] caused by extensive caries, dental trauma, and dental procedures such as extensive restorations and crowns. Low- or moderate-intensity dental trauma can stimulate the cells of

**Received:** October 17, 2025 **Revised:** January 17, 2026 **Accepted:** February 20, 2026

**Citation**
Castillo Barrios GA, Rodríguez Sánchez P, Barona Triviño AE, Martínez Cajas CH. Classification proposal of obliterated canals based on the position of the target point and the caliber of the root canal. Restor Dent Endod 2026;51(3):e32.
***Correspondence to**
**Carlos Humberto Martínez Cajas, DDS, MSc**
Clinical Specialization Programs in Dentistry, Institución Universitaria Colegios de Colombia (UNICOC), Cl. 13N No. 3N-13, Santiago de Cali, Valle del Cauca 760046, Colombia
Email: cmartinezc@unicoc.edu.co

the pulp tissue, causing calcification or obliteration of the root canal in response to this noxious stimulus [1,2]. These obliterations, caused by trauma, can occur in 40% of cases, and the need for endodontic treatment varies between 7% and 27% due to the presence of symptoms, crown discoloration, or radiographic findings with the presence of periapical pathology [3]. Other causes of pulp canal obliteration include orthodontic treatment, revascularization, and advanced age [4].

In 2000, Bastone *et al.* [5] reported that the frequency of dentoalveolar trauma was high among school and university students. Subluxation and low-intensity luxation such as extrusion and lateral luxation are the main causes of calcification in the root canal [2]. Andreasen *et al.* [1] reported a 15% rate of root canal obliteration after observing 637 injured teeth; similarly, Bastos and Côrtes [6] in 2018 reported a percentage of pulpal obliteration ranging from 3.7% to 40% in these cases. The mechanism by which pulp canal obliteration or calcific metamorphosis occurs remains unknown, and in efforts to explain it, the approach of Siddiqui and Mohamed [7] is highlighted, who propose that it may be produced by an injury to the neurovascular supply of the pulp. The presence of obliteration of the canal system can be identified through changes in tooth color or during a routine dental examination. Oginni *et al.* [4] in 2009, evaluated teeth with pulpal canal obliteration and reported that 79.71% of teeth presented a coronal discoloration (yellow or gray) and 33.3% with an apical lesion. However, endodontic treatment is not always indicated until a complete clinical evaluation of the patient's signs and symptoms is performed [8]. According to Jain *et al.* [3], endodontic therapy is indicated in 7%–27% of cases if they present with symptoms or radiographic evidence of apical periodontitis.

Conventional canal treatments are commonly accompanied by periapical radiographs because of their low radiation doses and low costs. However, endodontic treatments in the presence of obliterations, which are considered to have a higher degree of difficulty, require the use of high-resolution tomography because of the greater amount of information they provide about root anatomy and morphology. Currently, the European Society of Endodontics supports the use of tomographic images for the assessment and resolution of complex cases, in addition to being necessary for any type of dynamic or static navigation [9]. Due to this reduction in the canal lumen, the execution of endodontic treatments becomes more complex because of the difficulty of locating and negotiating the root canals correctly and conservatively. Connert *et al.* [10] report high percentages of deviation (success in only 41.7% of cases) with the freehand technique, even with the aid of tomography and magnification; currently, computer-assisted navigation techniques (static and/or dynamic navigation) are much more precise for performing these procedures [11,12]. Even with the use of these navigation systems, the location of the root canals is complex and varies depending on the degree of pulp obliteration and the location at the beginning of the root canal lumen (target point) [13]. These anatomical characteristics are normally observed with the help of periapical radiography, especially using high-resolution cone-beam computed tomography (CBCT), which is indicated in cases of greater complexity [14].

Radiographically, the obliteration of the pulp canals can be classified into two types: partial obliteration, in which the pulp chamber is not observed and the canal is considerably calcified; and total obliteration, in which the pulp chamber and root canal are practically imperceptible radiographically [7,8].

## MAIN SUBJECTS

### Classification of calcified canals

High-quality periapical radiographs and a high-resolution CBCT (ranging from 75 to 100 μm) are recommended to assess the presence of the root canal lumen and its subsequent classification. This classification comprises eight categories as follows (Figure 1).

**1. Type Ia: Partial obliteration with predominant vertical constriction (coronal initiation)**

Presence of discernible canal lumen above the cement-enamel junction (CEJ) with progressive corono-apical calcification. The root canal maintains radiographic visibility throughout its length despite marked coronal narrowing. Radiographically, the intracanal radiolucency (representing the patent canal lumen) measures >50% of the estimated normal canal width at the


https://doi.org/10.5395/rde.2026.51.e32

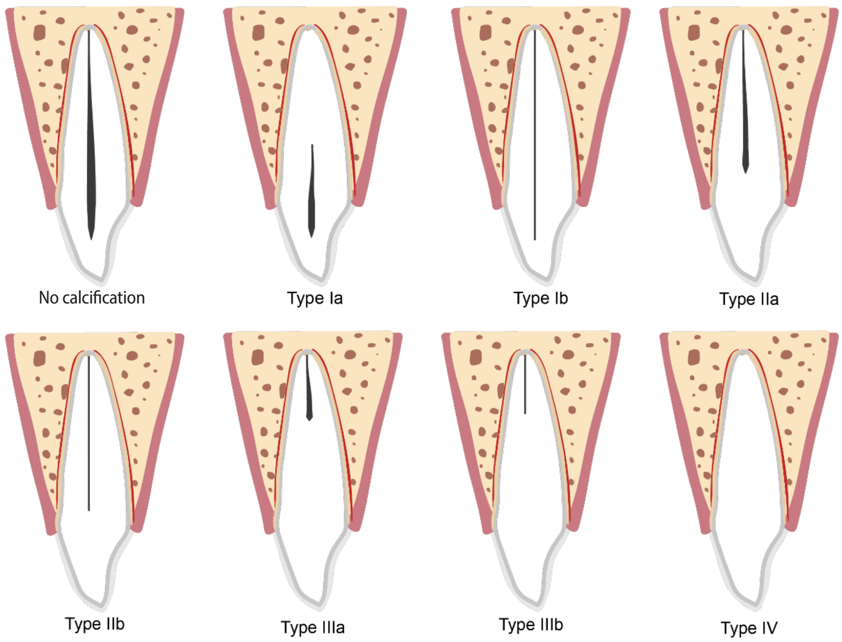


**Figure 1.** Classification proposal of calcified canals.

cervical third, with constriction predominantly affecting the vertical (corono-apical) dimension. The target point (canal orifice) remains clearly locatable on radiographic examination.

Distinguishing feature: minimal to absent horizontal (circumferential) constriction of the canal walls.

**2. Type Ib: Advanced obliteration with vertical and horizontal constriction (coronal initiation)**

Advanced calcification beginning above the CEJ, demonstrating both significant vertical (corono-apical) and horizontal (circumferential) constriction of the root canal. The visible intracanal radiolucency is reduced to ≤50% of the normal canal width, with radiodensity approaching but not identical to surrounding dentin. The canal lumen remains discernible on radiographs, though requiring careful examination. Apical patency of the canal is maintained.

Distinguishing features: pronounced bilateral constriction patterns and substantially reduced lumen visibility compared to Type Ia, while lumen identification remains feasible.

**3. Type IIa: Partial obliteration with minimal horizontal constriction (cervical-middle initiation)**

Partial calcification beginning between the CEJ and the middle third of the root. The pulp chamber remains visible, though reduced in volume. The intracanal radiolucency exceeds 50% of the estimated normal canal width at the level of obliteration onset, indicating predominant vertical constriction with minimal horizontal (circumferential) involvement. The radiodensity differential between the calcified zone and surrounding dentin remains evident, allowing clear delineation of the obliterated region. Apical to the calcified zone, canal patency is evident.

Distinguishing feature: preserved circumferential canal wall outline and relatively open apical anatomy.

**4. Type IIb: Advanced obliteration with concurrent vertical and horizontal constriction (cervical-middle initiation)**

Advanced calcification originating between the CEJ and the middle third of the root, characterized by severe bilateral constriction (both corono-apical and circumferential). The visible canal lumen is reduced to ≤50% of the normal estimated diameter. Radiographic visualization reveals a marked reduction in radiodensity differential (approaching dentin equivalence), making canal identification challenging. The transition zone between obliterated and patent canal is distinct but narrow.

Distinguishing feature: pronounced 360º circumferential constriction combined with significant vertical narrowing; increased difficulty in lumen identification without magnification or three-dimensional imaging.

**5. Type IIIa: Partial obliteration with preserved apical patency (middle-third or apical initiation)**

Partial calcification with onset in the middle third of the root or apical region, leaving the coronal two-thirds patent. The intracanal radiolucency in the non-obliterated zones exceeds 50% of normal canal width. Horizontal (circumferential) constriction is minimal to absent. The calcified zone is clearly distinguishable radiographically from surrounding dentin by virtue of maintained radiodensity differential. Considerable patent canal space remains accessible for negotiation both coronally and apically.

Distinguishing feature: obliteration limited to specific root thirds with well-preserved access anatomy and target point identification.

**6. Type IIIb: Advanced obliteration with severe constriction (middle-third or apical initiation)**

Advanced calcification beginning in the middle third or apical region, featuring pronounced vertical and horizontal constriction within the obliterated zone. The visible canal lumen is ≤50% of normal width within the calcified region. Radiodensity approaches dentin equivalence, substantially reducing the radiographic differential. While obliteration is localized, the calcified zone presents severe bilateral constriction, necessitating advanced diagnostic imaging (CBCT) or magnification for precise lumen identification. Patent canal anatomy is preserved both coronally and apically, yet access through the constricted zone is substantially compromised.

Distinguishing feature: high-grade constriction (>50% volume reduction) within a localized calcification zone, combined with radiodensity near equivalence to dentin.

**7. Type IV: Total obliteration with complete radiodensity equivalence**

Complete obliteration of the root canal throughout its entire length from the pulp chamber to the apical foramen. Radiographically, the entire pulp space demonstrates radiodensity equivalent to or exceeding surrounding dentin, rendering the intracanal lumen non-discernible on conventional radiography. No visible radiolucency representing patent canal space remains at any level. The distinction between the canal space and surrounding dentin is absent or imperceptible.

Distinguishing feature: absolute absence of radiographic canal visibility and uniform radiodensity throughout the canal path.

## Classification proposal and case examples

**1. Classification Type Ia: Partial obliteration with predominant vertical constriction (coronal initiation)**

- Example 1: A 52-year-old female patient with no medical history was referred for endodontic treatment of the upper right lateral incisor without presenting any symptoms. A clinical examination was conducted, which revealed a negative sensitivity test result. Radiographic analysis revealed the presence of a radiolucent area in the apical region, indicative of a periapical osteolytic lesion. The root canal lumen was found to be obliterated, resulting in a reduced lumen within the root canal system within the pulp chamber. The diagnosis was confirmed as asymptomatic apical periodontitis. Subsequent tomographic analysis guided the decision to perform root canal treatment with magnification and freehand techniques, owing to the presence of a small periapical radiolucent area. The infiltration of anesthesia was facilitated using a 2% lidocaine solution with 1:80,000 epinephrine, and the procedure was conducted under the guidance of a microscope and a #3 round diamond bur. The canal was then prepared using a #10 hand file and irrigated with 5.25% sodium hypochlorite (NaOCl). A WaveOne Gold primary system (Dentsply Maillefer Instruments Holding Sàrl, Ballaigues, Switzerland) was then utilized. Subsequently, the canal was obturated using WaveOne Gold cone and AH Plus root canal sealer (Dentsply


https://doi.org/10.5395/rde.2026.51.e32

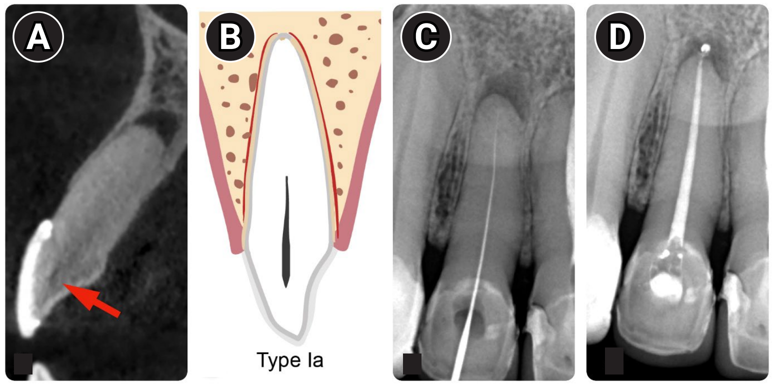


Figure 2. Characteristics of Type Ia root canal classification. (A) Tomographic image. The red arrow indicates the target point (start of the canal) without any change from its original position. It is clearly visible in the sagittal cone-beam computed tomography view. The root canal disappears at the start of the cervical third of the root. (B) Type Ia classification scheme. (C) Initial root canal negotiation with a file to determine the temporary working length. (D) Filled canal.

DeTrey GmbH, Konstanz, Germany) (Figure 2).

**2. Classification Type Ib: Advanced obliteration with vertical and horizontal constriction (coronal initiation)**

- Example 2: A 72-year-old female patient with a history of controlled hypertension was referred for intermittent symptoms and canal obliteration in the lower right central incisor. The patient reported positive vertical and horizontal percussion and a negative sensitivity test during the clinical examination. Radiographically, a radiolucent area was observed apically, compatible with a lesion of pulpal origin, and a decrease in the lumen throughout the root canal, with the beginning of the canal lumen in the pulp chamber. Apical periodontitis was defined as a diagnosis, and conventional endodontics was the ideal treatment. Due to the tomographic analysis, it was decided to perform the treatment with magnification and a 1 mm Steco bur (Steco-system-technik GmbH & Co. KG, Lemgo, Germany) freehand. A palatal access was made near the incisal edge to have an access path perpendicular to the long axis of the tooth. Canal patency occurred in the coronal third with little wear of the remaining tooth within a few minutes. Subsequently, the canal was instrumented with a medium WaveOne Gold file, copiously irrigated, activated with 5.25% sodium hypochlorite, and filled with a gutta-percha cone of the same system and Bio-C Sealer cement. Finally, the patient was referred for lingual resin (Figure 3).

**3. Classification Type IIa: Partial obliteration with minimal horizontal constriction (cervical-middle initiation)**

- Example 3: A 46-year-old female patient was referred for locating the canal and performing conventional endodontic treatment on the lower right central incisor, with a diagnosis of asymptomatic apical periodontitis. A CBCT image was obtained to establish the diagnosis and treatment plan. The results established obliteration of the pulp chamber and partial calcification of the canal, with the beginning of the canal lumen above the middle third of the root. A periapical radiolucent area compatible with a lesion was also observed. Subsequently, the DICOM files from the tomography were used to perform digital planning in the software Navident dynamic navigation system (ClaroNav Inc., Toronto, ON, Canada). A Steco bur endodontic guided bur (Steco-system-technik GmbH & Co. KG) was used to achieve patency. The target point of the tooth was located between the middle and cervical thirds with a pre-curved #10 file. Subsequently, the canal was instrumented using the HyFlex CM rotary NiTi files #30 (Coltene/Whaledent AG, Altstätten, Switzerland), irrigated with sodium hypochlorite, and obturated using the lateral condensation technique with AH Plus (Figure 4).

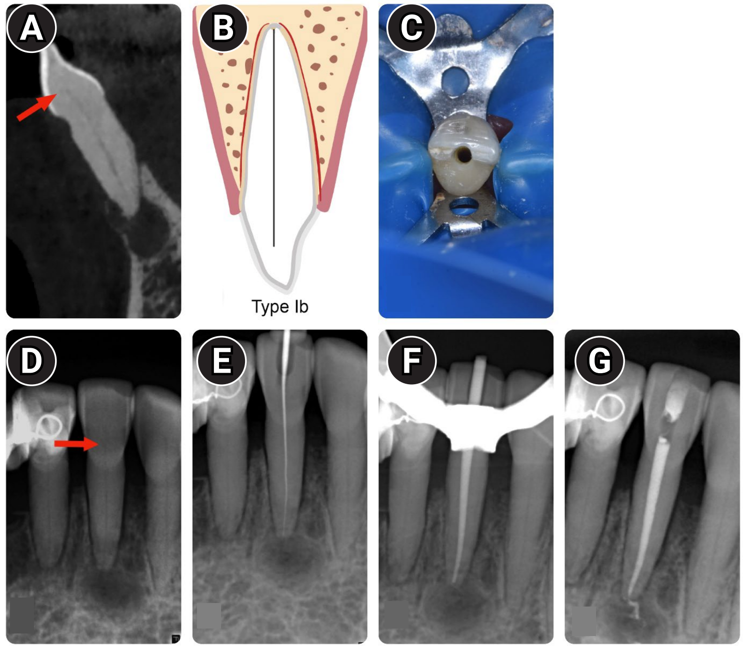


Figure 3. Characteristics of Type Ib root canal classification. (A) Tomographic image. The red arrow indicates the target point (start of the canal), which is located in its original position; however, narrowing of the canal lumen is observed along the entire root. (B) Type Ib classification scheme. (C) Access to pulp chamber/root canal. (D) Initial radiograph. The red arrow indicates narrowing of the root canal along the entire root. (E) Initial root canal negotiation with a file to determine the temporary working length. (F) Gutta-percha master point fitting before root canal filling. (G) Filled canal.

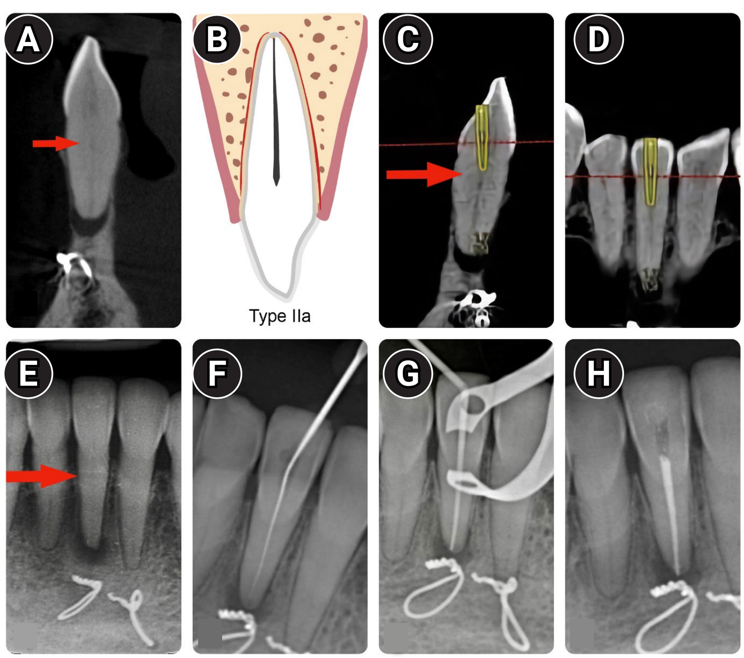


Figure 4. Characteristics of Type IIa root canal classification. (A) Tomographic image. The red arrow indicates the start of the canal lumen (target point). (B) Type IIa classification scheme. (C) Planning access to the pulp chamber/root canal in a sagittal slice. The red arrow indicates the target point for planning (start of the canal lumen). (D) Planning for pulp chamber/root canal access coronal slice. (E) Initial radiograph. The red arrow indicates the start of the root canal. (F) Initial root canal negotiation with a file to determine the temporary working length. (G) Gutta-percha master point fitting before root canal filling. (H) Filled canal.


https://doi.org/10.5395/rde.2026.51.e32

**4. Classification Type IIb: Advanced obliteration with concurrent vertical and horizontal constriction (cervical-middle initiation)**

- Example 4: A 27-year-old man presented with pain in the upper right central incisor upon percussion. With no significant medical history, clinical examination revealed a negative response to cold testing and a positive reaction to vertical percussion. Radiographic findings showed a periapical radiolucency, indicative of a periapical lesion, along with partial obliteration of the root canal and no visible canal orifice in the pulp chamber. A diagnosis of symptomatic apical periodontitis was made, and conventional endodontic treatment was planned.

Access preparation began with the removal of enamel using a #2 round diamond bur. The opening was extended towards the incisal edge to ensure a straight-line access parallel to the long axis of the tooth. A pencil mark was placed on the vestibular surface for orientation. A 1-mm Steco bur was used in a low-speed handpiece to locate the canal orifice. The canal was then cleaned and shaped with a #10 file and a WaveOne Gold primary file (size 25) and obturated with a corresponding gutta-percha cone and Bio-C Sealer. The patient was referred for restorative treatment and scheduled for a 6-month follow-up (Figure 5).

**5. Classification Type IIIa: Partial obliteration with preserved apical patency (middle-third or apical initiation)**

- Example 5: A 25-year-old female patient was referred by an endodontist to locate the canal and obturate the upper right central incisor. The patient had no systemic medical conditions. She had a history of orthodontic treatment 2 years ago. A clinical examination revealed a negative sensitivity test. Radiographically, a decrease in the canal lumen was observed up to the middle-third of the root. A diagnosis of pulpal necrosis was made, and guided endodontics was determined to be the ideal treatment. The initial tomography was performed after creating a small opening with a #2 round diamond bur. These DICOM files from the tomography were import-

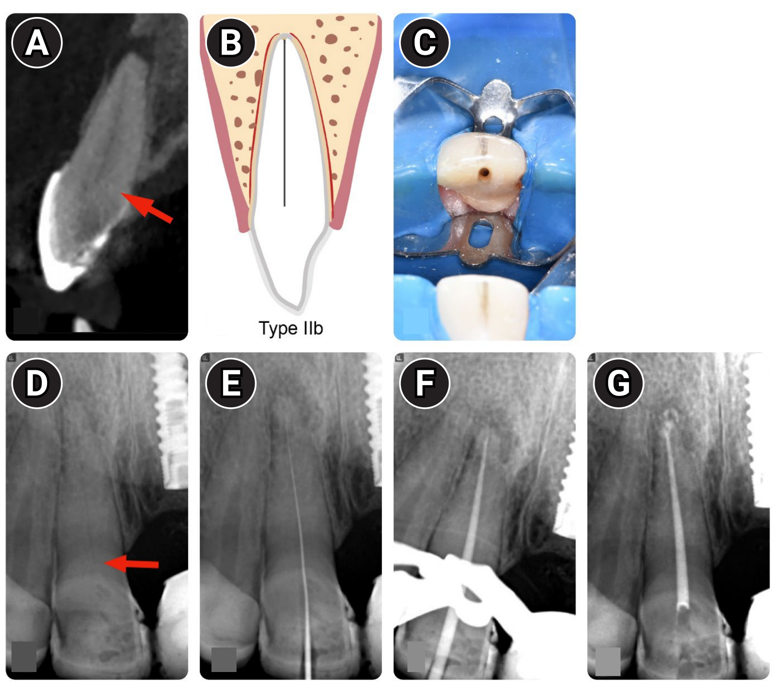


**Figure 5.** Characteristics of Type IIb root canal classification. (A) Tomographic image. The red arrow indicates the start of the canal lumen (target point). (B) Type IIb classification scheme. (C) Access to pulp chamber/root canal. (D) Initial radiograph. The red arrow indicates the start of the root canal. (E) Initial root canal negotiation with a file to determine the temporary working length. (F) Gutta-percha master point fitting before root canal filling. (G) Filled canal.

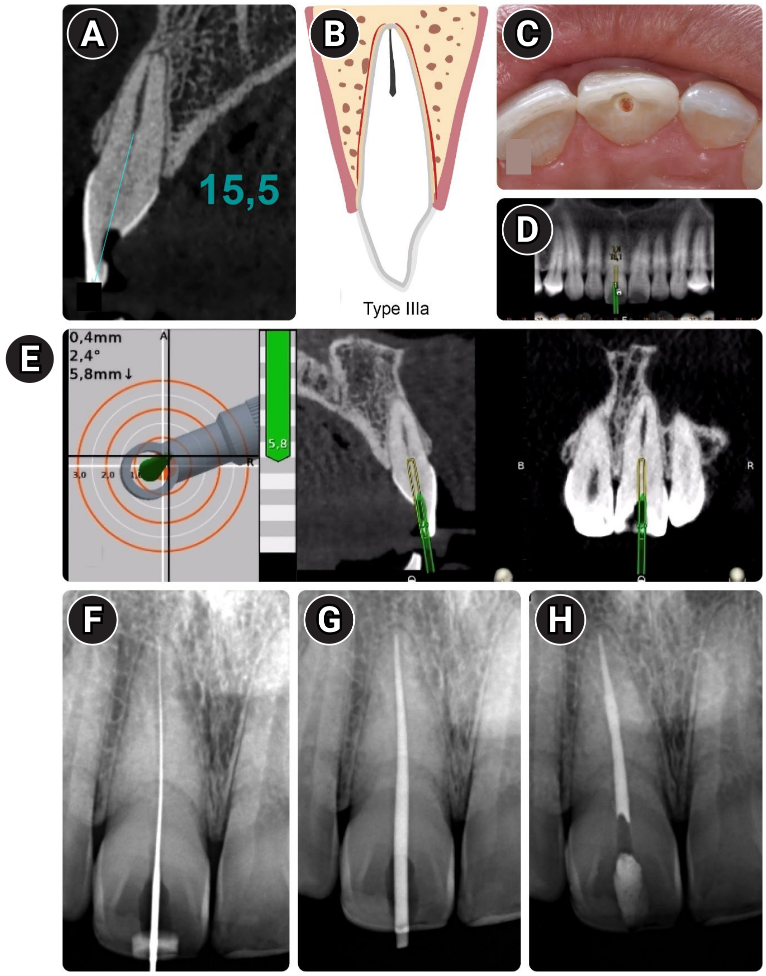


Figure 6. Characteristics of Type IIIa root canal classification. (A) Tomographic image. (B) Type IIIa classification scheme. (C) Access to pulp chamber/root canal. (D) Planning for pulp chamber/root canal access coronal slice. (E) Navident (ClaroNav Inc., Toronto, ON, Canada) graphical interface for root canal access planning. (F) Initial radiograph. (G) Gutta-percha master point fitting before root canal filling. (H) Filled canal.

ed into Navident software to create the respective plan and alignment. Lidocaine 2% with epinephrine 1:80,000 was administered, and canal patency was achieved with a 0.75-mm Tivoli bur (Gebr. Brasseler GmbH & Co. KG, Lemgo, Germany). The target point was located 16 mm from the incisal edge. The estimated time to locate the target point was 5 minutes. Mechanical instrumentation was performed using a WaveOne Gold medium file system, and obturation was performed with a cone of the same caliber from the same system and Bio-C Sealer (Figure 6).

**6. Classification Type IIIb: Advanced obliteration with severe constriction (middle-third or apical initiation)**

• Example 6: A 63-year-old woman with no significant medical history was referred for mild to moderate pain in the upper left central incisor. The clinical examination revealed positive vestibular palpation and percussion, normal periodontal probing, and an adapted crown. Radiographically, the lumen of the partially obliterated canal and apical hypodense area compatible with a periapical lesion are observed. A diagnosis of symptomatic apical periodontitis was made, and apical microsurgery was proposed to the patient as treatment due to an adapted crown and advanced obliteration of the root canal with a high degree of difficulty.

Initially, the area of tooth 11 was anesthetized with two carpules of 2% lidocaine with epinephrine 1:80,000, and a triangular flap was made from tooth 12 to tooth 21. Subsequently, the inflamed tissue was removed, an


https://doi.org/10.5395/rde.2026.51.e32

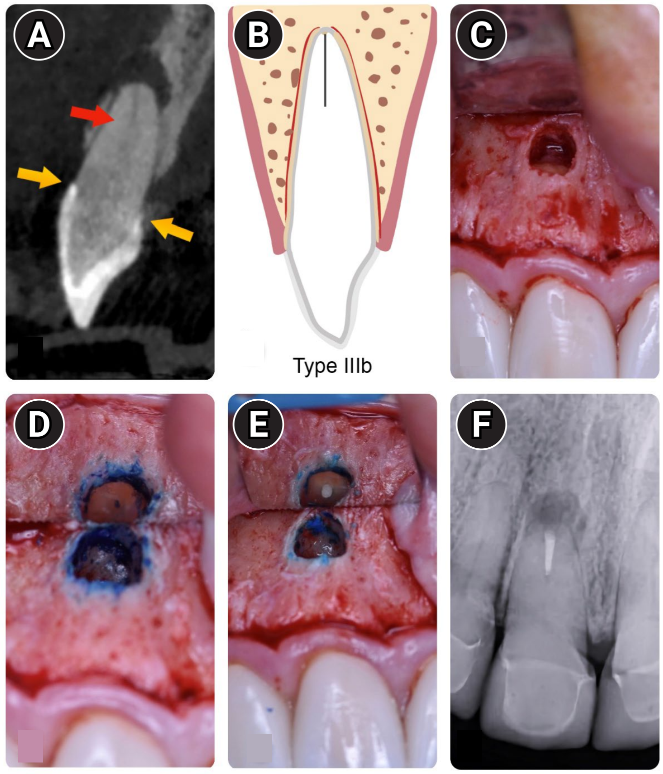


**Figure 7.** Characteristics of Type IIIb root canal classification. (A) Tomographic image, target point (red arrow), adapted crown (yellow arrows). (B) Type IIIb classification scheme. (C) Access to apex. (D) Root apex outline (methylene blue). (E) Filled root canal with the retrograde filling material. (F) Postoperative periapical radiograph showing root-end fillings.

apicoectomy (3 mm) was performed, and apical retro-preparation was made with a diamond ultrasound tip. Finally, the apex was filled with Bio-C® Repair bioceramic reparative material (Angelus Indústria e Comércio Ltda, Londrina, Paraná, Brazil), and the flap was sutured with 5-zero DemeCAPRONE™ synthetic absorbable monofilament suture (DemeTECH Corporation, Miramar, Florida, USA) (Figure 7).

- Example 7: A 36-year-old male patient with intermittent pain in the left lower central incisor with a history of trauma; no medical history. Clinical examination revealed positive vertical percussion and a negative sensitivity test. A CBCT image revealed advanced obliteration of the root canal with diffuse light between the middle and apical thirds. A diagnosis of symptomatic apical periodontitis was made. Due to the level of obliteration and the difficulty of treatment, guided endodontics were performed with dynamic navigation. The DICOM files from diagnostic tomography were imported into the navigation device software Navident, where the orientation and depth of the access path were planned at 15.4 mm from the cervical margin to the beginning of the root canal lumen. Canal patency was achieved using a 1-mm Steco bur. Instrumentation was performed with a large file from the WaveOne Gold, and subsequent obturation was performed with a size 45 cone from the same system and Bio-C Sealer (Figure 8).

**7. Classification Type IV: Total obliteration with complete radiodensity equivalence**

- Example 8: A 40-year-old female patient with no systemic medical history was referred for evaluation and treatment planning for the upper left lateral incisor. The patient had a history of orthodontic treatment. Clinical examination revealed a color change, a negative sensitivity test, and positive horizontal percussion.

Radiographically, a completely obliterated canal and a healthy periapical region were observed. Pulp necrosis was diagnosed, and the patient was informed of

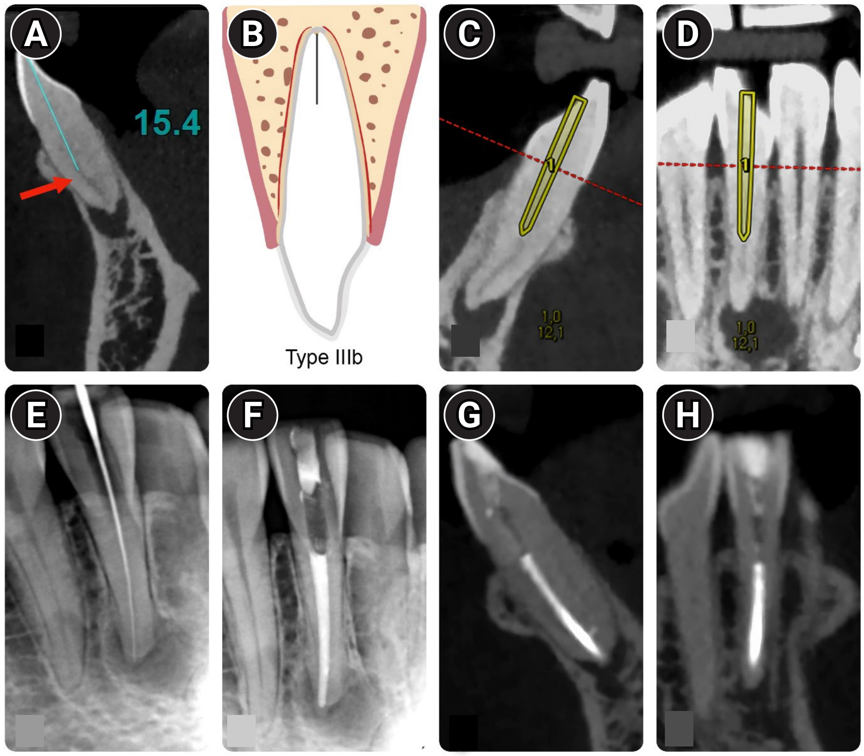


**Figure 8.** Characteristics of Type IIIb root canal classification. (A) Tomographic image. The red arrow indicates the target point located in the apical third. (B) Type IIIb classification scheme. (C) Planning for pulp chamber/root canal access sagittal oblique slice. (D) Planning for pulp chamber/root canal access coronal slice. (E) Initial root canal negotiation with a file to determine the temporary working length. (F) Filled canal. (G) Filled canal sagittal oblique slice. (H) Filled canal coronal slice.

the treatment options (apical microsurgery and guided endodontics). The patient preferred conventional endodontics; therefore, it was decided to perform computer-assisted endodontic treatment. Initially, the DICOM files from the tomography were entered into the Navident for subsequent planning. An access pathway was established along the tooth's long axis to negotiate the root canal lumen at any level, in the absence of a predefined orifice target point. A 0.75 mm Tivoli endodontic bur (Gebr. Brasseler GmbH & Co. KG) on a low-speed handpiece was used to initiate the opening. The canal lumen was in the cervical third, and the absence of pulpal vitality was confirmed. The canal was instrumented with a primary file from the WaveOne Gold and obturated with a cone of the same system and AH Plus. The patient was then referred for restorative treatment (Figure 9).

## DISCUSSION

The cases presented above propose an exhaustive and exclusive classification of the state of obliterated or calcified root canals based on the location of the target-point and the visible caliber on radiographs and/or tomography with a clinical focus and negotiation of ducts by guided endodontics. In this context, it is important to highlight that Lima *et al.* [15], in 2024 in a bibliometric review, mention that from the first publication on this topic in 2016 by Krastl *et al.* [16], the prevalent focus of research has been the static navigation technique and that it was the negotiation of calcified ducts that has given rise and development of the technique.

The documentary collection on the effectiveness and efficiency of guided techniques is constituted, for the most part, by numerous case reports whose evidence indicates that guided endodontics is a technique with high precision and with the capacity to predict the out-


https://doi.org/10.5395/rde.2026.51.e32

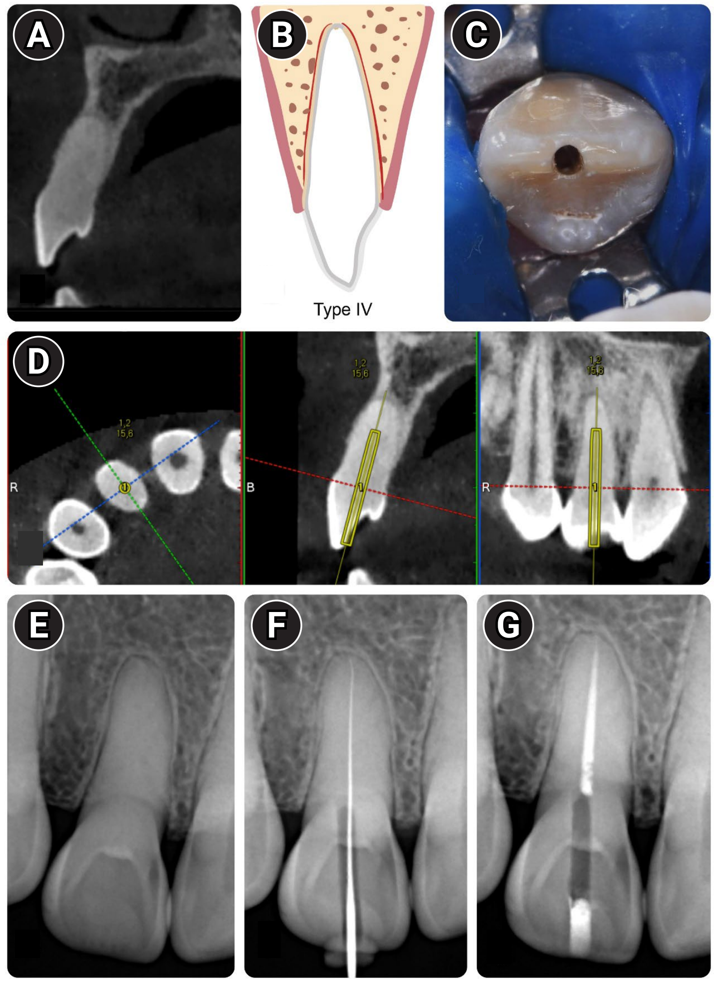


**Figure 9.** Characteristics of Type IV root canal classification. (A) Tomographic image. (B) Type IV classification scheme. (C) Access to pulp chamber/root canal. (D) Navident (ClaroNav Inc., Toronto, ON, Canada) graphical interface for root canal access planning. (E) Initial radiograph. (F) Initial root canal negotiation with a file to determine the temporary working length. (G) Filled canal.

come of the intervention [17]. However, there is a gap in the evaluation of efficacy given the limited number of high-quality clinical trials with long-term follow-up [15,17]; the available studies are affected by the heterogeneity of the outcomes [17,18], absence of standardized protocols, the difficulty in the proper selection of cases with particular indications for each technique [15] and lack of consensus in essential aspects of endodontic therapy [18]. It is in this sense that the scientific community has directed efforts in the determination of taxonomies that allow us to define in a precise and practical way characteristic aspects of the conditions and outcomes in health [19,20].

In 2024, Terán-Miranda [21] makes a very detailed classification proposal of the level and degree of calcification where ten levels are recognized according to the identification zone of the calcification (pulpar, cervical, middle, apical, pulpar + cervical, cervical + middle, middle apical, pulpar + cervical + middle, cervical + middle + apical and total) and four degrees (permeable, obliterated, intermittent, closed), which in the context of studies with an analytical approach can favor type II error due to the number of subgroups resulting from the combination of its two components. In contrast, the current proposal defines a total of eight categories on an ordinal scale because of the challenge of reaching the target point and the negotiation of the root canals according to the caliber.

| 3D Diagram | Description | Adaptation |
|---|---|---|
|  | Left maxillary central incisor, uniradicular with pulp canal obliteration classification IIa (Partial obliteration of the root canal that begins between the CEJ and the middle third of the root) | $(PCo)^{IIa}\ {}^{1}21^{1}$ |
|  | Right maxillary first premolar, biradicular with obliteration of the buccal pulp canal, classification Ia (Presence of canal lumen above the CEJ with obliteration in the cervical, middle and apical root thirds) in buccal root Ib. (Advanced obliteration of the root canal that begins in the crown above the CEJ) | $(PCo)^{2}$ 14 $B^{1(Ib)}$ $P1^{(Ia}$) |
|  | Lower right second molar, biradicular with distal root dilaceration and obliteration in mesial pulp canal with classification IV. (Total obliteration of the root canal) | $(PCo)^{2}$ 47 $M^{(RD)}$ $D^{(IV)}$ |

*International tooth numbering system (FDI)

**Figure 10.** Adaptation to the nomenclature of classification of morphological anomalies. 3D, three-dimensional; CEJ, cementoenamel junction; FDI, Fédération Dentaire Internationale; PCo, pulp canal obliteration.

Another important aspect is the easy adaptation to the nomenclature of classification of morphological anomalies proposed by Ahmed and Dummer [22] by prefixing pulp canal obliteration (PCo) and classification in superscript to the number of the dental piece, in those uniradicular and/or multiradicular teeth in which the classification of the root canal coincides. In case of disagreement, PCo is prefixed to the tooth number and the classification in superscript is added for calcified root canals present [20,22–25] (Figure 10).

While the limitations of images obtained via CBCT should be considered (difficulty in detecting accessory canals and minor anatomical variations), their use is recommended for applying the classification, as their influence on the decision regarding the complexity or difficulty of endodontic therapy is recognized [26], especially in cases where the morphological characteristics of the root canal system pose a challenge for diagnosis, prognosis, and therapeutic approach; their use is even recommended for the evaluation of clinical results [27,28]; however, it is important to emphasize the possibility of using high-quality radiographic images, which favors the implementation of the classification in regions where the availability of obtaining CBCT images is limited; furthermore, the simplicity and conciseness in the definition, as well as the adaptation to the Ahmed scheme, can be taught and adopted from undergraduate and postgraduate professional training [24,29].

The conventional technique for locating canals allows the location of the root canals, but requires excellent spatial location, magnification, and ultrasonic tips [8]. Recent reports have shown that new navigation techniques in endodontics are usually more accurate and require less clinical working time [11,30–34]. Connert *et al.* [10] in 2019 report the results of an *in vitro* study that indicates that static navigation was significantly superior to the conventional technique, even considering that it was used by operators with different levels of


https://doi.org/10.5395/rde.2026.51.e32

experience; similarly, clinical cases have been reported to have been performed with static navigation with high accuracy for locating calcified canals [35,36].

Villa *et al.* [34] reported two clinical cases approached with dynamic navigation in anterior teeth, achieving a high degree of precision and conservative accesses with the use of the Navident; in 2020, Jain *et al.* [37] performed an *in vitro* study with 40 upper and lower anterior teeth printed in three-dimensional, where the dynamic navigation technique proved to be more efficient and faster for locating obliterated canals. Gambarini *et al.* [38] also reported a case of apical surgery in an upper anterior tooth with the help of the Navident system, achieving optimal precision. Zubizarreta-Macho *et al.* [11] conducted a study comparing the conventional technique with the two types of navigation (static and dynamic) and observed that the latter had better performance when comparing the previous planning versus the execution, locating the lumen of the root canals. They concluded that although dynamic navigation is more precise than static navigation, there was no statistically significant difference in loss of dental tissue after opening.

Geo *et al.* [12] reported that the main advantages of dynamic navigation are greater accuracy, no need for patient scanning, simpler planning process, better instrument access due to the absence of guides, visualization of the access path in real-time, and the possibility of changing or correcting the plan at any time.

It can therefore be concluded that, according to the results presented, the two techniques present very similar results in terms of accuracy and predictability for locating obliterated canals [11,12]; however, the complexity of these treatments with any type of navigation can vary depending on the location of the target point or the beginning of the root canal lumen and their caliber. Clinically, a narrow canal located in the apical third of the root could be much more complex to locate than a canal that starts above the middle third of the root. Studies that analyze and compare the complexity of the procedures according to these clinical characteristics have not been conducted.

## CONCLUSIONS

A classification system comprising eight types of calcified root canals was proposed, categorized by the degree of obliteration and the anatomical location of the canal's "target point" along the root axis. This taxonomy offers significant clinical utility for the planning and execution of endodontic treatment protocols, particularly concerning access and exploration of the root canal system.

Furthermore, the analysis of the presented clinical cases elucidates the distinct characteristics of each category while simultaneously highlighting the effectiveness of guided techniques (static and dynamic) as preferred strategies for managing obliterated canals.

This framework is positioned to serve as a valuable didactic resource in both undergraduate and postgraduate training, enabling students to grasp the inherent complexities of these cases and facilitating informed decision-making regarding referral and counter-referral pathways. Moreover, this system contributes substantially to the taxonomic resources available for future research concerning the prevalence, prognosis, and treatment strategies associated with this variant of the root canal system.

### CONFLICT OF INTEREST

No potential conflict of interest relevant to this article was reported.

### FUNDING/SUPPORT

The authors have no financial relationships relevant to this article to disclose.

### AUTHOR CONTRIBUTIONS

Conceptualization: Castillo Barrios GA, Rodríguez Sánchez P, Barona Triviño AE; Formal analysis, Investigation: all authors; Supervision, Visualization: Martínez Cajas CH; Writing - original draft: all authors; Writing - review & editing: all authors. All authors read and approved the final manuscript.

### DATA SHARING STATEMENT

The datasets are not publicly available but are available from the corresponding author upon reasonable request.

### DISCLOSURE OF GENERATIVE AI IN SCIENTIFIC WRITING

The authors used DeepL (DeepL SE, Cologne, Germany) and Claude (Anthropic PBC, San Francisco, CA, USA) to check the grammatical structure of the English in the draft while preparing this paper. After using these tools, the authors reviewed and edited the content as necessary and assume full responsibility for the content of the publication.

## REFERENCES

1. Andreasen FM, Zhijie Y, Thomsen BL, Andersen PK. Occurrence of pulp canal obliteration after luxation injuries in the permanent dentition. Endod Dent Traumatol 1987;3:103-115.
2. Bourguignon C, Cohenca N, Lauridsen E, Flores MT, O'Connell AC, Day PF, *et al*. International Association of Dental Traumatology guidelines for the management of traumatic dental injuries: 1. Fractures and luxations. Dent Traumatol 2020;36:314-330.
3. Jain SD, Carrico CK, Bermanis I. 3-Dimensional accuracy of dynamic navigation technology in locating calcified canals. J Endod 2020;46:839-845.
4. Oginni AO, Adekoya-Sofowora CA, Kolawole KA. Evaluation of radiographs, clinical signs and symptoms associated with pulp canal obliteration: an aid to treatment decision. Dent Traumatol 2009;25:620-625.
5. Bastone EB, Freer TJ, McNamara JR. Epidemiology of dental trauma: a review of the literature. Aust Dent J 2000;45:2-9.
6. Bastos JV, Côrtes MIS. Pulp canal obliteration after traumatic injuries in permanent teeth: scientific fact or fiction? Braz Oral Res 2018;32:e75.
7. Siddiqui SH, Mohamed AN. Calcific metamorphosis: a review. Int J Health Sci (Qassim) 2016;10:437-442.
8. McCabe PS, Dummer PM. Pulp canal obliteration: an endodontic diagnosis and treatment challenge. Int Endod J 2012;45:177-197.
9. Patel S, Brown J, Pimentel T, Kelly RD, Abella F, Durack C. Cone beam computed tomography in endodontics: a review of the literature. Int Endod J 2019;52:1138-1152.
10. Connert T, Krug R, Eggmann F, Emsermann I, ElAyouti A, Weiger R, *et al*. Guided endodontics versus conventional access cavity preparation: a comparative study on substance loss using 3-dimensional-printed teeth. J Endod 2019;45:327-331.
11. Zubizarreta-Macho Á, Muñoz AP, Deglow ER, Agustín-Panadero R, Álvarez JM. Accuracy of computer-aided dynamic navigation compared to computer-aided static procedure for endodontic access cavities: an in vitro study. J Clin Med 2020;9:129.
12. D GT, Saxena P, Gupta S. Static vs. dynamic navigation for endodontic microsurgery: a comparative review. J Oral Biol Craniofac Res 2022;12:410-412.
13. Martinho FC, Griffin IL, Corazza BJ. Current applications of dynamic navigation system in endodontics: a scoping review. Eur J Dent 2023;17:569-586.
14. Reddy S, Prakash V, Tamilselvi R, Karthick A. Morphologic aberrations of mandibular premolar with two and three canals: case report. Indian J Forensic Med Toxicol 2020;14:1184-1188.
15. Lima TO, Rocha AO, Dos Anjos LM, Meneses Júnior NS, Hungaro Duarte MA, Alcalde MP, *et al*. A global overview of guided endodontics: a bibliometric analysis. J Endod 2024;50:10-16.
16. Krastl G, Zehnder MS, Connert T, Weiger R, Kühl S. Guided endodontics: a novel treatment approach for teeth with pulp canal calcification and apical pathology. Dent Traumatol 2016;32:240-246.
17. Puri A, Abraham D, Gupta A. Impact of guided endodontics on the success of endodontic treatment: an umbrella review of systematic reviews and meta-analyses. Cureus 2024;16:e68853.
18. El-Karim I, Duncan HF, Nagendrababu V, Clarke M. The importance of establishing a core outcome set for endodontic clinical trials and outcomes studies. Int Endod J 2023;56 Suppl 2:200-206.
19. Ahmed HM, Rossi-Fedele G, Dummer PM. Critical analysis of a new system to classify root and canal morphology: a systematic review. Aust Endod J 2023;49:750-768.
20. Ahmed HM, Hashem AA, Dummer PM. Application of a new system for classifying root and canal anatomy in clinical practice: explanation and elaboration. Eur Endod J 2021;6:132-142.
21. Terán-Miranda ME. Classification of the level and degree of calcification of root canals by cone-beam computed tomography. Rev Cient Odontol (Lima) 2024;12:e219.
22. Ahmed HM, Dummer PM. A new system for classifying tooth, root and canal anomalies. Int Endod J 2018;51:389-404.
23. Ahmed HM, Che Ab Aziz ZA, Azami NH, Farook MS, Khan AA, Mohd Noor NS, *et al*. Application of a new system for classifying root canal morphology in undergraduate teaching and clinical practice: a national survey in Malaysia. Int Endod J 2020;53:871-879.
24. Ahmed HM, Dummer PM. Advantages and applications of a new system for classifying roots and canal systems in re-


https://doi.org/10.5395/rde.2026.51.e32

search and clinical practice. Eur Endod J 2017;3:9-17.
25. Ahmed HM, Ibrahim N, Mohamad NS, Nambiar P, Muhammad RF, Yusoff M, *et al*. Application of a new system for classifying root and canal anatomy in studies involving micro-computed tomography and cone beam computed tomography: explanation and elaboration. Int Endod J 2021;54:1056-1082.
26. Rodríguez G, Abella F, Durán-Sindreu F, Patel S, Roig M. Influence of cone-beam computed tomography in clinical decision making among specialists. J Endod 2017;43:194-199.
27. Alzamzami ZT, Abulhamael AM, Talim DJ, Khawaji H, Barzanji S, Roges RA. Cone-beam computed tomographic usage: survey of American endodontists. J Contemp Dent Pract 2019;20:1132-1137.
28. Chan F, Brown LF, Parashos P. CBCT in contemporary endodontics. Aust Dent J 2023;68 Suppl 1:S39-S55.
29. Karobari MI, Parveen A, Mirza MB, Makandar SD, Nik Abdul Ghani NR, Noorani TY, *et al*. Root and root canal morphology classification systems. Int J Dent 2021;2021:6682189.
30. Buchgreitz J, Buchgreitz M, Bjørndal L. Guided root canal preparation using cone beam computed tomography and optical surface scans: an observational study of pulp space obliteration and drill path depth in 50 patients. Int Endod J 2019;52:559-568.
31. Casadei BA, Lara-Mendes ST, Barbosa CF, Araújo CV, de Freitas CA, Machado VC, *et al*. Access to original canal trajectory after deviation and perforation with guided endodontic assistance. Aust Endod J 2020;46:101-106.
32. Connert T, Zehnder MS, Weiger R, Kühl S, Krastl G. Microguided endodontics: accuracy of a miniaturized technique for apically extended access cavity preparation in anterior teeth. J Endod 2017;43:787-790.
33. Connert T, Zehnder MS, Amato M, Weiger R, Kühl S, Krastl G. Microguided endodontics: a method to achieve minimally invasive access cavity preparation and root canal location in mandibular incisors using a novel computer-guided technique. Int Endod J 2018;51:247-255.
34. Villa-Machado PA, Restrepo-Restrepo FA, Sousa-Dias H, Tobón-Arroyave SI. Application of computer-assisted dynamic navigation in complex root canal treatments: report of two cases of calcified canals. Aust Endod J 2022;48:187-196.
35. Lara-Mendes ST, Barbosa CF, Machado VC, Santa-Rosa CC. A new approach for minimally invasive access to severely calcified anterior teeth using the guided endodontics technique. J Endod 2018;44:1578-1582.
36. Fonseca Tavares WL, Diniz Viana AC, de Carvalho Machado V, Feitosa Henriques LC, Ribeiro Sobrinho AP. Guided endodontic access of calcified anterior teeth. J Endod 2018;44:1195-1199.
37. Jain SD, Saunders MW, Carrico CK, Jadhav A, Deeb JG, Myers GL. Dynamically navigated versus freehand access cavity preparation: a comparative study on substance loss using simulated calcified canals. J Endod 2020;46:1745-1751.
38. Gambarini G, Galli M, Stefanelli LV, Di Nardo D, Morese A, Seracchiani M, *et al*. Endodontic microsurgery using dynamic navigation system: a case report. J Endod 2019;45:1397-1402.

RDE Restorative Dentistry & Endodontics

Research Article

eISSN 2234-7666
Restor Dent Endod. 2026 August;51(3):e33
https://doi.org/10.5395/rde.2026.51.e33

# Impact of bacteriological testing using an anaerobic culture system on the success of nonsurgical endodontic treatment: a retrospective study

**Jun Nakanishi*, Noriko Saito-Nakayama, Shizu Hirata-Tsuchiya, Daisuke Furutama, Ayaka Miyata-Arita, Tomoki Kawayanagi, Takuya Arita, Saki Nishihama, Tomoya Naruse, Wang Chutian, Song Bingxin, Naoki Sadaoka, Tomoki Kumagai, Kazuma Yoshida, Katsuhiro Takeda, Hideki Shiba**

Department of Biological Endodontics, Graduate School of Biomedical and Health Sciences, Hiroshima University, Hiroshima, Japan

## ABSTRACT

**Objectives:** Residual bacteria at the time of root canal obturation significantly influence endodontic treatment outcomes in teeth with apical periodontitis, and confirmation of bacterial elimination from the root canal prior to obturation may improve long-term prognosis. However, the contribution of root canal bacterial culture to treatment outcomes in teeth with infected root canals is debated. This study aimed to retrospectively evaluate treatment outcomes in cases in which root canal obturation was performed after confirming negative bacteriological test results.

**Methods:** The medical records of patients with apical periodontitis or pulp necrosis in whom root canal obturation was performed after confirming a negative bacteriological test result using an anaerobic culture system at the Department of Endodontics and Operative Dentistry at Hiroshima University Hospital between April 1, 2015, and September 30, 2023, were retrospectively reviewed. Treatment outcomes were assessed by comparing dental radiographs obtained before treatment with those obtained during the follow-up, ranging from 3 to 24 months after root canal obturation.

**Results:** This retrospective study included 284 teeth from 218 patients, and the success rate was 89.1%. Tooth type, number of root canals, type of treatment, preoperative radiolucency around the root apex, preoperative root canal obturation material, dentist experience, and postoperative extent of root canal obturation material did not significantly affect treatment outcomes.

**Conclusions:** The findings of this retrospective study suggest that infection control incorporating bacteriological examination of root canals using an anaerobic culture system may contribute to a high success rate of nonsurgical endodontic treatment, regardless of other prognostic factors.

**Keywords:** Anaerobic culture system; Bacteriological examination; Nonsurgical endodontic treatment; Prognostic factor; Treatment outcome

**Received:** October 20, 2025 **Revised:** February 4, 2026 **Accepted:** February 10, 2026

**Citation**
Nakanishi J, Saito-Nakayama N, Hirata-Tsuchiya S, Furutama D, Miyata-Arita A, Kawayanagi T, Arita T, Nishihama S, Naruse T, Chutian W, Bingxin S, Sadaoka N, Kumagai T, Yoshida K, Takeda K, Shiba H. Impact of bacteriological testing using an anaerobic culture system on the success of nonsurgical endodontic treatment: a retrospective study. Restor Dent Endod 2026;51(3):e33.

***Correspondence to**
**Jun Nakanishi, DDS, PhD**
Department of Biological Endodontics, Graduate School of Biomedical and Health Sciences, Hiroshima University, 1-2-3, Kasumi, Minami-ku, Hiroshima, 734-8553, Japan
Email: nakanishijun@hiroshima-u.ac.jp

# INTRODUCTION

Residual bacteria at the time of root canal obturation significantly influence the outcomes of endodontic treatment in teeth with apical periodontitis [1,2]; thus, confirmation of bacterial elimination from the root canal prior to obturation may improve the long-term prognosis of the tooth. The presence of bacterial infection in the root canal can be evaluated using bacteriological culture. Although various bacteria can be detected in the root canal, because the root canal is an anaerobic environment, anaerobes dominate the bacterial flora [3]. Furthermore, approximately 80% of the bacteria in infected dentin, which is caused by bacterial invasion of the root canal walls, are obligate anaerobes [4]. Therefore, anaerobic cultures are considered more appropriate than aerobic cultures for bacteriological examination of the root canal.

Few studies have reported that a negative anaerobic culture result prior to root canal obturation is associated with a favorable prognosis [5,6]. Conversely, other studies have found no significant difference in long-term outcomes between cases with negative and positive anaerobic culture results prior to obturation [7]. Thus, the contribution of bacteriological culture to treatment outcomes in infected root canals remains controversial [8].

Several factors influence the outcome of root canal treatment, including tooth type, number of root canals, type of treatment, presence of preoperative radiolucency around the root apex, type of preoperative obturation material, dentist experience, and the extent of postoperative obturation. However, the effect of these factors on the prognosis of cases in which obturation is performed after confirming a negative anaerobic culture result remains unclear.

This retrospective study analyzed clinical data collected from the medical records of participants who had undergone treatment for infected root canals, including bacteriological examination of root canals using an anaerobic culture system. The aim was to determine whether such examinations are necessary for achieving successful outcomes in nonsurgical endodontic treatment of infected root canals, while accounting for various factors that may influence treatment prognosis.

# METHODS

### Ethics approval

This retrospective study, which used data extracted from previously recorded medical charts, was approved by the Ethical Committee for Epidemiology of Hiroshima University (No. E2023-0206) and conducted in accordance with the principles of the Declaration of Helsinki. As the study used existing clinical data and involved no direct patient intervention, informed consent was obtained using an opt-out approach. Information related to the study and handling of personal data was disclosed on the website of the institution, where patients were given the opportunity to decline participation.

### Study participants and eligibility criteria

Root canal obturation at the Department of Endodontics and Operative Dentistry, Hiroshima University Hospital, is routinely performed only after negative bacteriological results are confirmed using an anaerobic culture system operated by the Center for Oral Clinical Examination of the hospital. In this retrospective study, we reviewed clinical data from patients who underwent infected root canal treatment, including bacteriological assessment with the anaerobic culture system, at the Department of Endodontics and Operative Dentistry between April 1, 2015 and September 30, 2023. Dentists were divided into two groups according to their experience: <5 years and ≥5 years. Patients diagnosed with apical periodontitis or pulp necrosis who had undergone root canal obturation after bacteriological examination of the root canal using the anaerobic culture system and had not refused to participate in this study were included. The exclusion criteria were (i) no follow-up between 3 and 24 months after root canal obturation, (ii) root canal treatment without rubber dam isolation, and (iii) root canal treatment prior to surgical endodontic treatment. Figure 1 shows the study flowchart according to the inclusion and exclusion criteria and the number of cases treated by dentists with <5 years and ≥5 years of experience, respectively.

### Evaluation of treatment outcome

The parameters analyzed were age, sex, tooth type, number of root canals, type of treatment (initial treat-


https://doi.org/10.5395/rde.2026.51.e33

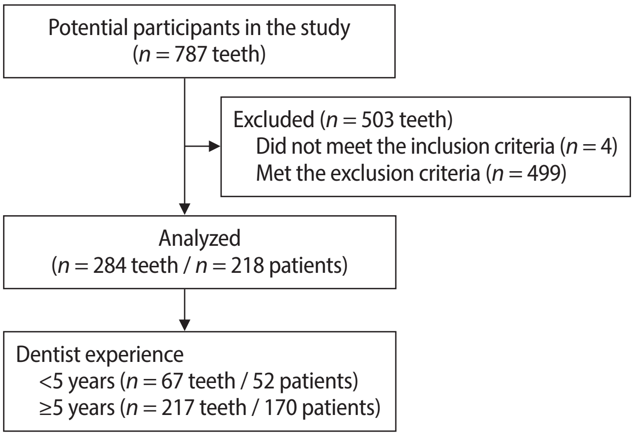


**Figure 1.** Study flow chart.

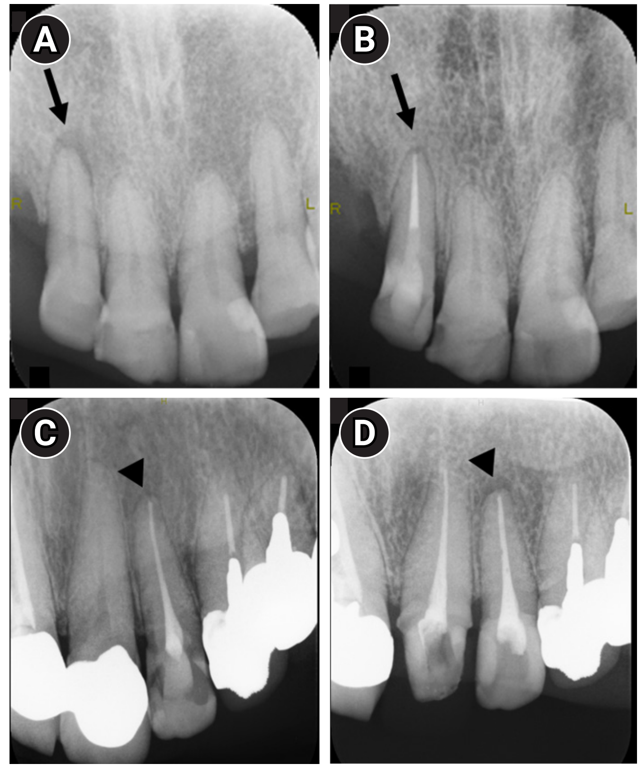


**Figure 2.** Representative pre- and postoperative dental radiographs showing good and poor outcomes. Preoperative (A) and postoperative (B) radiographs of a maxillary right lateral incisor (arrows). The 1-year and 4-month follow-up radiograph demonstrates a good outcome. Preoperative (C) and postoperative (D) radiographs of a maxillary left lateral incisor (arrowheads). The 7-month follow-up radiograph shows a poor outcome.

ment or retreatment), preoperative radiolucency around the root apex, preoperative root canal obturation material, dentist experience (<5 years, or ≥5 years), and pre- and postoperative extension of the root canal obturation material (under, adequate, or over). In this retrospective study, the retreatment group included cases in which patients were referred to the hospital due to poor progress or other reasons, even though retreatment had already been initiated at other hospitals and dental clinics. Treatment outcomes were evaluated by comparing dental radiographs obtained before treatment initiation with those obtained 3–24 months after root canal obturation, using the reduction in lesion size of the apical radiolucency as a parameter. Based on previous studies, good outcomes were defined as disappearance or decrease in bone resorption around the root apex, and when the bone resorption around the root apex remained unchanged or increased, the outcome was defined as poor [9,10]. Clinical symptoms and cone-beam computed tomography images were not used for evaluation. In addition, the outcome was classified as good when the absence of bone resorption at the root apex observed before treatment initiation remained unchanged during the follow-up. In contrast, the outcomes of teeth for which surgical endodontic treatment or extraction was indicated because of poor progress during the follow-up period were classified as poor. All radiographic evaluations were performed by at least two independent evaluators. Figure 2 shows representative pre and postoperative dental radiographs illustrating good and poor outcomes. The kappa coefficient calculated to assess inter-evaluator agreement was 0.789, indicating substantial agreement. The cutoff for number of years of dental experience (5 years) was based on the Japanese Endodontic Association's application requirements for endodontic specialists and the post-licensure training curriculum in Japan.

### Sample collection and anaerobic bacterial culture test

Prior to obturation, all dentists confirmed that the bacteriological tests of the root canal, conducted at the Center for Oral Clinical Examination, Hiroshima University Hospital, using an anaerobic culture system, showed negative results, with no clinical symptoms. The bacterial examination is outlined as follows [11]: the anaerobic culture system comprised an AnaeroPack (Mitsubishi Gas Chemical Co., Inc., Tokyo, Japan), AnaeroPack pouches and sealing clips (Mitsubishi Gas

https://doi.org/10.5395/rde.2026.51.e33

Chemical Co., Inc., Tokyo, Japan), an anaerobic indicator (Mitsubishi Gas Chemical Co., Inc., Tokyo, Japan), sterile cotton swabs, sterile paper points, and culture media that includes Brucella blood agar (Kyokuto Pharmaceutical Industrial Co., Ltd., Tokyo, Japan) and thioglycolate liquid medium (Nihon Pharmaceutical Co., Ltd., Osaka, Japan). Specimens (root canal bacteria) were collected under rubber dam isolation by inserting a sterile paper point moistened with sterile saline into the root canal. The paper point containing the specimen was immediately placed into the liquid medium and suspended. Subsequently, a portion of the liquid medium was inoculated onto blood agar plates using a sterile cotton swab. An anaerobic environment ($N_2$, 80% and $CO_2$, 20%) was established by sealing the blood agar plate containing the specimen, the liquid medium, the AnaeroPack, and the anaerobic indicator within an AnaeroPack pouch, which was incubated at 37°C. Culture evaluation was performed 4–7 days post-initiation. Colony formation on the culture medium surface was considered a positive result, whereas its absence was considered a negative result.

### Nonsurgical endodontic treatment methods

All patients underwent nonsurgical endodontic treatment according to standard protocols [10]. Following completion of root canal preparation, enlargement, and irrigation, bacteriological testing was performed when the operator, based on clinical symptoms, judged it appropriate to proceed with root canal obturation. Root canal obturation was performed using the lateral or vertical condensation technique with gutta-percha points (GC Corporation, Tokyo, Japan) and an eugenol-based root canal sealer (Nishika Canal Sealer; Nihon Shika Yakuhin Co., Ltd., Yamaguchi, Japan) or a non-eugenol-based root canal sealer (Canals-N; GC Showayakuhin Corporation, Tokyo, Japan).

### Statistical analysis

Statistical analysis was performed using JMP Pro software (ver. 17.0; SAS Institute Inc, Cary, NC, USA). The chi-square test and multiple logistic regression analysis were used to compare success rates between the two groups, and statistical significance was set at $p < 0.05$. In the multiple logistic regression analysis, the postoperative extent of root canal obturation material was excluded due to unstable parameter estimates. The chi-square test results showed that for tooth type and postoperative extent of root canal obturation material, cells with expected values below 5 accounted for >20% of the total; therefore, the Fisher exact test was performed for these two groups.

## RESULTS

A total of 787 infected teeth underwent root canal treatment and bacteriological examination of the root canal using an anaerobic culture system during the study period (Figure 1). Of these, 284 teeth with confirmed clinical outcomes between 3 and 24 months after root canal obturation were included (Figure 1). Among these, 67 teeth from 52 patients and 217 teeth from 170 patients were treated by dentists with <5 years and ≥5 years, respectively. The demographic distribution of the patients is shown in Table 1. The treatment success rate in this retrospective study was 89.1% (Table 2). The chi-square test and Fisher exact test show that tooth type, number of root canals, type of treatment, preoperative radiolucency around the root apex, preoperative root canal obturation material, dentist experience, and postoperative extension of the root canal obturation material did not significantly affect treatment outcomes (Table 3). The multiple logistic regression analysis showed no group significantly affects treatment outcomes, consistent with the chi-square and Fisher exact test results (data not shown).

## DISCUSSION

Anaerobic bacteria predominantly form biofilms in the anaerobic environment of the root canal [3,4]. Because elimination of bacteria from the root canal significantly influences the outcome of root canal treatment [1,2], confirming the aseptic condition of the root canal after cleaning and shaping prior to obturation may increase the success rate of root canal treatment. In addition, the elimination of *Enterococcus faecalis*, a problematic facultative anaerobic bacterium, from the root canal is important for improving the success rate of root canal treatment [12–14]. An *in vivo* study in monkeys reported


https://doi.org/10.5395/rde.2026.51.e33

**Table 1.** Demographic distribution of the cases

| Variable | Value |
|---|---|
| Total tooth number | 284 |
| Age (yr) | 62 (48–72) |
| Sex | |
| Male | 73 (25.7) |
| Female | 211 (74.3) |
| Tooth type | |
| Maxillary anterior | 70 (24.7) |
| Maxillary premolars | 44 (15.5) |
| Maxillary molars | 51 (18.0) |
| Mandibular anterior | 27 (9.5) |
| Mandibular premolars | 29 (10.2) |
| Mandibular molars | 63 (22.2) |
| Number of root canals | |
| Single | 150 (52.8) |
| Multiple | 134 (47.2) |
| Type of treatment | |
| Initial treatment | 101 (35.6) |
| Retreatment | 183 (64.4) |
| Preoperative radiolucency around the root apex | |
| Absent | 82 (28.9) |
| Present | 202 (71.1) |
| Preoperative root canal obturation material | |
| Absent | 130 (45.8) |
| Present | 154 (54.2) |
| Preoperative extent of root canal obturation material | |
| Under | 87 (30.6) |
| Adequate | 55 (19.4) |
| Over | 3 (1.1) |
| Postoperative location of root canal obturation material | |
| Under | 25 (8.8) |
| Adequate | 249 (76.8) |
| Over | 10 (3.5) |
| Dentist experience | |
| <5 yr | 67 (23.6) |
| ≥5 yr | 217 (76.4) |

Values are presented as number, median (interquartile range), or number (%).

**Table 2.** Treatment outcomes

| Variable | Value |
|---|---|
| Total tooth number | 284 |
| Treatment outcome | |
| Good | 253 (89.1) |
| Poor | 31 (10.9) |

Values are presented as number or number (%).

**Table 3.** Treatment outcomes according to each characteristic

| Variable | Good | Poor | *p*-value |
|---|---|---|---|
| Tooth type | | | |
| Maxillary anterior | 64 (22.5) | 6 (2.1) | 0.2906 |
| Maxillary premolars | 42 (14.8) | 2 (0.7) | |
| Maxillary molars | 44 (15.5) | 7 (2.5) | |
| Mandibular anterior | 23 (8.1) | 4 (1.4) | |
| Mandibular premolars | 23 (8.1) | 6 (2.1) | |
| Mandibular molars | 57 (20.1) | 6 (2.1) | |
| Number of root canals | | | |
| Single | 134 (47.2) | 16 (5.6) | 0.8869 |
| Multiple | 119 (41.9) | 15 (5.6) | |
| Type of treatment | | | |
| Initial treatment | 93 (32.8) | 8 (2.8) | 0.2292 |
| Retreatment | 160 (56.3) | 23 (8.1) | |
| Preoperative radiolucency around the root apex | | | |
| Absent | 77 (27.1) | 5 (1.8) | 0.0971 |
| Present | 176 (62.0) | 26 (9.2) | |
| Preoperative root canal obturation material | | | |
| Absent | 120 (42.3) | 10 (3.5) | 0.1095 |
| Present | 133 (46.8) | 21 (7.4) | |
| Dentist experience | | | |
| <5 yr | 62 (21.8) | 5 (1.8) | 0.2998 |
| ≥5 yr | 191 (67.3) | 26 (9.2) | |
| Postoperative extent of root canal obturation material | | | |
| Under | 25 (8.8) | 0 (0) | 0.1113 |
| Adequate | 218 (76.8) | 31 (10.9) | |
| Over | 10 (3.5) | 0 (0) | |

Values are presented as number (%).

that treatment outcomes were influenced more by the presence of bacteria in the root canal than by the quality of root canal obturation [15]. Therefore, bacteriological examination of the root canal using an anaerobic culture system is recommended to confirm the absence of bacteria causing apical periodontitis or pulp necrosis. As the Center for Oral Clinical Examination, Hiroshima University Hospital has this culture system, dentists in the Department of Endodontics and Operative Dentistry routinely use it as a standard practice.

The treatment success rate in this retrospective study was 89.1%, which is higher than that previously reported [16–20]. Several factors influence endodontic treatment outcomes [16–25]. Particularly, rubber dam isolation during endodontic treatment significantly influences tooth survival [21] and was performed in all cases in this study. In this study, we evaluated factors that influenced the outcomes of root canal treatment in previous studies (type of treatment, preoperative radiolucency around the root apex, preoperative root canal obturation material, years of dental experience, and postoperative extension of the root canal obturation material). Surprisingly, none of these significantly affected treatment outcomes (Table 3). Particularly, this study highlighted that the dentist's experience did not significantly influence the success rate. Previous studies have reported that treatment planning and technical skills for performing root canal treatment depend on the dentist's experience, and that the success rate of endodontic treatment is significantly higher when performed by specialists than when performed by general dentists [22,26].

The distribution of treatment difficulty remains unclear; however, the success rate in this retrospective study did not vary with the dentist's experience, and a high success rate was achieved. This suggests that bacteriological examination of the root canal using an anaerobic culture system may result in less clinically experienced dentists achieving successful nonsurgical endodontic treatment.

This retrospective study had some limitations, including a small sample size, a wide range of observation periods (3–24 months), a lack of consideration of the type of restoration after root canal obturation, and crown leakage. Additionally, because samples are collected using sterilized paper points inserted into saline-soaked root canals with rubber dam isolation, anaerobic bacterial culture primarily detects bacteria in the main root canal(s) rather than in lateral root canals. Furthermore, the study did not include a comparison of success rates with cases in which root canal obturation was performed after confirming a positive anaerobic bacterial culture test, since the establishment of a positive control group that could potentially lead to poor clinical outcomes for patients was expected to be disapproved by the Ethical Committee for Epidemiology of Hiroshima University. Another limitation is that anaerobic culture results require 4–7 days to become available. Therefore, because an interval is necessary between sampling and obturation, intracanal medicament using calcium hydroxide paste and a tight temporary seal using a double layer of temporary stopping material and glass ionomer cement were routinely applied to minimize the risk of reinfection during nonsurgical endodontic treatment. Previous studies supporting the utility of bacterial culture have shown that, when root canal treatment and obturation were performed on infected canals, prognosis was better when bacterial culture tests were negative prior to obturation than when they were positive [1,6]. Although this study has certain limitations, anaerobic bacterial culture remains an important procedure for achieving favorable outcomes in nonsurgical endodontic treatment.

## CONCLUSIONS

The success rate of root canal treatment in teeth in which obturation was performed after confirming negative anaerobic bacterial culture test results was not influenced by factors conventionally believed to affect treatment outcomes. Notably, the dentist's experience had no impact on treatment outcomes. Based on the findings in this retrospective study, in addition to rubber dam isolation, implementing standardized infection control through bacteriological examination of the root canal using an anaerobic culture system may be considered to achieve high success rates in root canal treatment.

### CONFLICT OF INTEREST

No potential conflict of interest relevant to this article was reported.

### FUNDING/SUPPORT

The authors have no financial relationships relevant to this article to disclose.

### ACKNOWLEDGEMENTS

We are deeply grateful for the financial support provided by Dr. Shunichi Oshima. We also sincerely appreciate the staff of the Center of Oral Clinical Examination at Hiroshima University Hospital for conducting bacteriological tests using an anaerobic culture system.

### AUTHOR CONTRIBUTIONS

Conceptualization, Data curation, Methodology: Nakanishi J, Saito-Nakayama N. Formal analysis: Nakanishi J, Hirata-Tsuchiya S. Investigation: Furutama D, Miyata-Arita A, Kawayanagi T, Arita T, Nishihama S, Naruse T, Sadaoka N, Kumagai T, Yoshida K. Project administration: Hirata-Tsuchiya S. Supervision: Takeda K, Shiba H. Visualization: Nakanishi J. Writing - original draft: Nakanishi J. Writing - review & editing: Hirata-Tsuchiya S, Wang C, Song B, Takeda K, Shiba H. All au-



https://doi.org/10.5395/rde.2026.51.e33

thors read and approved the final manuscript.

## DATA SHARING STATEMENT

The datasets are not publicly available but are available from the corresponding author upon reasonable request.

## DISCLOSURE OF GENERATIVE AI IN SCIENTIFIC WRITING

No generative AI technologies were used in the preparation of this manuscript.

## REFERENCES


1. Sjögren U, Figdor D, Persson S, Sundqvist G. Influence of infection at the time of root filling on the outcome of endodontic treatment of teeth with apical periodontitis. Int Endod J 1997;30:297-306.
2. Zandi H, Petronijevic N, Mdala I, Kristoffersen AK, Enersen M, Rôças IN, *et al*. Outcome of endodontic retreatment using 2 root canal irrigants and influence of infection on healing as determined by a molecular method: a randomized clinical trial. J Endod 2019;45:1089-1098.e5.
3. Sato T, Yamaki K, Ishida N, Hashimoto K, Takeuchi Y, Shoji M, *et al*. Cultivable anaerobic microbiota of infected root canals. Int J Dent 2012;2012:609689.
4. Ando N, Hoshino E. Predominant obligate anaerobes invading the deep layers of root canal dentin. Int Endod J 1990;23:20-27.
5. Yoneda M, Kita S, Suzuki N, Macedo SM, Iha K, Hirofuji T. Application of a chairside anaerobic culture test for endodontic treatment. Int J Dent 2010;2010:942130.
6. Waltimo T, Trope M, Haapasalo M, Ørstavik D. Clinical efficacy of treatment procedures in endodontic infection control and one year follow-up of periapical healing. J Endod 2005;31:863-866.
7. Peters LB, Wesselink PR. Periapical healing of endodontically treated teeth in one and two visits obturated in the presence or absence of detectable microorganisms. Int Endod J 2002;35:660-667.
8. Sathorn C, Parashos P, Messer HH. How useful is root canal culturing in predicting treatment outcome? J Endod 2007;33:220-225.
9. Hoskinson SE, Ng YL, Hoskinson AE, Moles DR, Gulabivala K. A retrospective comparison of outcome of root canal treatment using two different protocols. Oral Surg Oral Med Oral Pathol Oral Radiol Endod 2002;93:705-715.
10. Hirata-Tsuchiya S, Furutama D, Saito-Nakayama N, Naruse T, Kawayanagi T, Nishihama S, *et al*. Increasing the apical sizes of root enlarged for root canal obturation influences the outcome of single-root-canal teeth affected by apical periodontitis. Eur Endod J 2024;9:418-424.
11. Iwata T, Hino T, Kitamoto Y, Shiba H, Ogawa I, Morimoto M, *et al*. Bacterial examination with anaerobic culture system for samples from root canals for the achievement of biological root canal treatment. J Jpn Endod Assoc 2007;28:1-8.
12. Stuart CH, Schwartz SA, Beeson TJ, Owatz CB. Enterococcus faecalis: its role in root canal treatment failure and current concepts in retreatment. J Endod 2006;32:93-98.
13. Alghamdi F, Shakir M. The influence of enterococcus faecalis as a dental root canal pathogen on endodontic treatment: a systematic review. Cureus 2020;12:e7257.
14. Kayaoglu G, Erten H, Bodrumlu E, Ørstavik D. The resistance of collagen-associated, planktonic cells of *Enterococcus faecalis* to calcium hydroxide. J Endod 2009;35:46-49.
15. Fabricius L, Dahlén G, Sundqvist G, Happonen RP, Möller AJ. Influence of residual bacteria on periapical tissue healing after chemomechanical treatment and root filling of experimentally infected monkey teeth. Eur J Oral Sci 2006;114:278-285.
16. Elemam RF, Pretty I. Comparison of the success rate of endodontic treatment and implant treatment. ISRN Dent 2011;2011:640509.
17. Sjogren U, Hagglund B, Sundqvist G, Wing K. Factors affecting the long-term results of endodontic treatment. J Endod 1990;16:498-504.
18. de Chevigny C, Dao TT, Basrani BR, Marquis V, Farzaneh M, Abitbol S, *et al*. Treatment outcome in endodontics: the Toronto study: phases 3 and 4: orthograde retreatment. J Endod 2008;34:131-137.
19. de Chevigny C, Dao TT, Basrani BR, Marquis V, Farzaneh M, Abitbol S, *et al*. Treatment outcome in endodontics: the Toronto study: phase 4: initial treatment. J Endod 2008;34:258-263.
20. Gorni FG, Gagliani MM. The outcome of endodontic retreatment: a 2-yr follow-up. J Endod 2004;30:1-4.
21. Lin PY, Huang SH, Chang HJ, Chi LY. The effect of rubber dam usage on the survival rate of teeth receiving initial root canal treatment: a nationwide population-based study. J Endod 2014;40:1733-1737.
22. Alley BS, Kitchens GG, Alley LW, Eleazer PD. A comparison of survival of teeth following endodontic treatment per-

formed by general dentists or by specialists. Oral Surg Oral Med Oral Pathol Oral Radiol Endod 2004;98:115-118.
23. Ng YL, Mann V, Rahbaran S, Lewsey J, Gulabivala K. Outcome of primary root canal treatment: systematic review of the literature--Part 2. Influence of clinical factors. Int Endod J 2008;41:6-31.
24. Azim AA, Griggs JA, Huang GT. The Tennessee study: factors affecting treatment outcome and healing time following nonsurgical root canal treatment. Int Endod J 2016;49:6-16.
25. Mello FW, Miguel AF, Ribeiro DM, Pasternak B, Porporatti AL, Flores-Mir C, *et al*. The influence of apical extent of root canal obturation on endodontic therapy outcome: a systematic review. Clin Oral Investig 2019;23:2005-2019.
26. Nagi SE, Khan FR, Rahman M. Practice of endodontic re-treatment in four cities of Pakistan. J Ayub Med Coll Abbottabad 2017;29:445-449.


https://doi.org/10.5395/rde.2026.51.e33

RDE Restorative Dentistry & Endodontics

Research Article

eISSN 2234-7666
Restor Dent Endod. 2026 August;51(3):e34
https://doi.org/10.5395/rde.2026.51.e34

# Effect of silane treatment and resin cement type on bond strength to three-dimensional printed restorative resin: an *in vitro* experimental study

**Seul Ji Park[1], Eun Hye Lee[2], Ryan Jin Young Kim[2,*], Joo Hee Shin[1,*]**

[1]Department of Conservative Dentistry, Korea University Guro Hospital, Seoul, Korea
[2]Department of Dental Science, Dental Research Institute, School of Dentistry, Seoul National University, Seoul, Korea

## ABSTRACT

**Objectives:** This study aimed to evaluate the shear bond strength (SBS) of different resin cements to three-dimensional (3D)-printed restorative resins and to investigate the effects of silane treatment and substrate type on bonding performance.

**Methods:** Four resin cements—three self-adhesive and one adhesive—were applied to two types of 3D-printed resins: ODS Permanent Resin (OPR) and Graphy Permanent Resin (GPR). Each substrate was tested with and without silane treatment. SBS was measured, and the failure modes were classified. Scanning electron microscopy (SEM) was used to analyze surface morphology of the 3D-printed substrates. Statistical analyses were performed to determine the effects of cement type, silane application, and substrate type on SBS.

**Results:** Resin cement type significantly influenced SBS, with Clearfil SA (Kuraray) exhibiting the lowest values, while the other cements demonstrated comparable performance. Silane treatment and substrate type did not show statistically significant effects on SBS. SEM analysis revealed smoother surfaces in OPR compared to GPR. Failure mode analysis showed predominantly cohesive failures for OPR, whereas GPR exhibited more adhesive and mixed failures.

**Conclusions:** Resin cement selection plays a crucial role in achieving optimal bond strength to 3D-printed restorative resins. Silane application provided limited benefits for filler-deficient substrates, indicating that alternative surface treatments may be necessary.

**Keywords:** Dental bonding; Permanent dental restoration; Resin cements; Silane; Three-dimensional printing

**Received:** October 19, 2025 **Revised:** January 22, 2026 **Accepted:** February 22, 2026

**Citation**
Park SJ, Lee EH, Kim RJ, Shin JH. Effect of silane treatment and resin cement type on bond strength to three-dimensional printed restorative resin: an *in vitro* experimental study. Restor Dent Endod 2026;51(3):e34.

***Correspondence to**
**Ryan Jin Young Kim, BDS, MSD, PhD**
Department of Dental Science, Dental Research Institute, School of Dentistry, Seoul National University, 101 Daehak-ro, Jongno-gu, Seoul 03080, Korea
Email: ryankim05@snu.ac.kr

**Joo Hee Shin, DDS, MSD, PhD**
Department of Conservative Dentistry, Korea University Guro Hospital, 148 Gurodong-ro, Guro-gu, Seoul 08308, Korea
Email: endoshin@kumc.or.kr

Ryan Jin Young Kim and Joo Hee Shin contributed equally to this work as co-corresponding authors.

## INTRODUCTION

Three-dimensional (3D) printing—also known as additive manufacturing—has emerged as an indispensable tool across diverse fields, notably revolutionizing workflows in dentistry [1]. It enables high precision and personalization in the fabrication of prostheses, surgical guides, orthodontic devices, and customized oral appliances such as mouthguards and splints by constructing each item layer-by-layer from digital models [2–4]. Furthermore, 3D printing facilitates the fabrication of dental restorations, streamlines treatment procedures, and reduces total treatment time. Recent advancements have made this fabrication suitable for producing long-term restorations.

3D-printed restorations rely on dental luting cements for secure bonding to tooth structures, making the bond strength of the cement essential for the durability of the restoration. The use of self-adhesive resin cements in indirect restorations has gained popularity, as they simplify clinical procedures while offering strong and durable bonds to both tooth structures and restorative materials [5]. To further enhance the adhesion of indirect restorations, conventional surface treatments such as etching, sandblasting, and the application of silane and resin bonding agents have been studied [6–8]. For glass-ceramics and resin-based substrates, silane treatment is commonly recommended to enhance the bond strength with resin cement [8,9]. Silane molecules contain two reactive groups that enable chemical bonding with both ceramic and resin materials: hydrolyzable groups bind to silicon hydroxyl groups (Si-OH) on ceramic surfaces, while organic groups interact with adhesive or composite resin monomers. This dual function makes silane a critical agent for strengthening the interface between inorganic and organic components in dental restorations [10].

3D-printing resins have distinct chemical compositions, and their physical and mechanical properties are largely determined by the types and ratios of monomers and fillers used. Unlike conventional dental restorative resins, 3D-printed resins typically contain no or lower filler content to minimize interference with light curing and to avoid excessive viscosity [11,12]. This altered composition may influence the efficacy of silane treatments and affect the bond strength with resin cements. Although previous studies have investigated the bond strength of provisional 3D-printed resins to repair materials or composite resins [7,13–15], no research to date has specifically examined the bond strength between 3D-printed resins and resin cements, or the effect of silane application prior to cementation.

While chemical compatibility plays a key role in bonding, another important factor is the surface wettability of the materials involved. This property is often assessed using contact angle measurements, which provide insight into how well a resin cement can spread across a given surface. In general, lower contact angles are associated with improved wettability, which can lead to improved adaptation and stronger adhesion at the interface [16,17]. Given the differences in filler content and surface chemistry between resin cements and 3D-printed materials, measuring the contact angles can help explain variations in bond strength observed across different material combinations.

Therefore, this study aimed to evaluate the bond strength of four different resin cements on two types of 3D-printed resins designed for permanent restorations both with and without silane treatment. Additionally, contact angle measurements were conducted to assess the wettability of each resin cement and 3D-printed substrate. The null hypothesis was that silane application and the type of 3D-printed resin would not significantly affect the bond strength among the resin cements.

## METHODS

Institutional Review Board approval was not required because this was an *in vitro* study that did not involve human participants, human-derived materials, or identifiable personal information.

### Sample preparation

The workflow of this study is illustrated in Figure 1. A total of 192 3D-printed resin cylinders (15 mm diameter, 15 mm height) were produced using a digital light processing printer (IMC 3D printer; Carmina, Seoul, Korea). All specimens were printed at a 0° orientation to the build platform with a layer thickness of 100 µm. After


https://doi.org/10.5395/rde.2026.51.e34

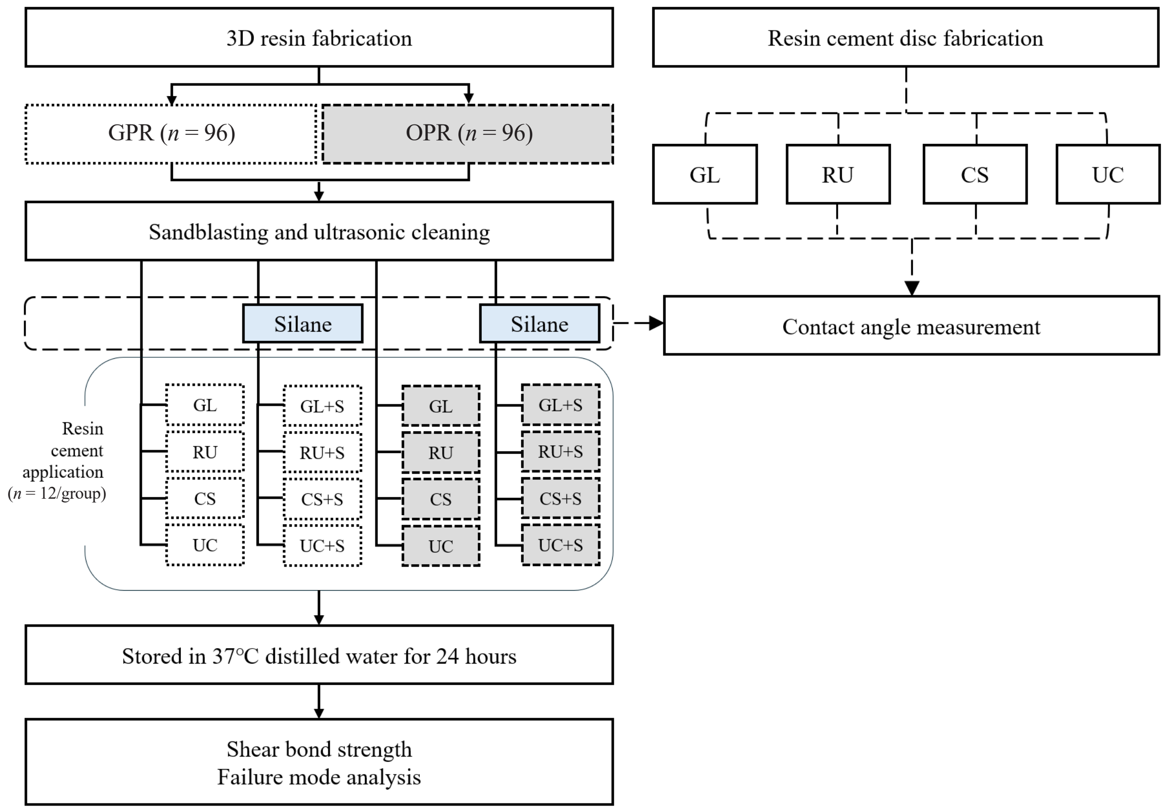


**Figure 1.** Workflow of the study. The full names and manufacturers of the materials are provided in Table 1. The +S notation indicates silane application.

printing, the specimens were cleaned in isopropyl alcohol for 10 minutes (Form Wash; Formlabs, Somerville, MA, USA) to remove residual uncured resin, followed by post-curing for 30 minutes (Form Cure; Formlabs).

The resins used for printing consisted of ODS Permanent resin (OPR; C&B Permanent Resin; ODS, Incheon, Korea) and Graphy Permanent Resin C&B TC-80DP (GPR) (Graphy, Seoul, Korea), with 96 cylinders fabricated from each resin type. For bonding preparation, one side of each cylinder was sandblasted using 50 µm aluminum oxide particles at 0.2 MPa pressure for 10 seconds, followed by a 5-minute cleaning cycle in an ultrasonic unit and thorough air drying. After air abrasion, the surface morphologies of the 3D-printed resin substrates were observed using scanning electron microscopy (SEM; Apreo 2; Thermo Fisher Scientific, Waltham, MA, USA) at an accelerating voltage of 10 kV and 500× magnification. Additional specimens that received silane treatment after air abrasion were also examined.

The GPR and OPR cylinders ($n = 96$ each) were divided into eight subgroups ($n = 12$ per subgroup) according to the type of resin cement used—G-CEM LinkAce (GL; GC Corp., Tokyo, Japan), RelyX U200 (RU; 3M ESPE, St. Paul, MN, USA), Clearfil SA (CS; Kuraray, Okayama, Japan), and RelyX Ultimate Clicker (UC; 3M ESPE)—and the presence or absence of silane treatment. In the silane-treated groups, RelyX Ceramic Primer (3M ESPE) was applied to the air-abraded 3D-printed resin surfaces using a microbrush and allowed to react for 60 seconds, and then air-dried for 15 seconds prior to cementation, in accordance with the manufacturer's instructions. For the GL and UC groups, G-Multi PRIMER (GC) and Single Bond Universal Adhesive (3M ESPE) were applied, respectively, before placement of the corresponding resin cement, following the manufacturers' recommended protocols.

Both the silane and resin cements were prepared according to the manufacturer's instructions. The materials used in this study and their respective compositions are listed in Table 1. For cement application, specimens

**Table 1.** Test materials, manufacturers, and compositions used in the study

| Abbreviation | Type | Materials | Composition | Lot number |
|---|---|---|---|---|
| OPR | Substrate | C&B Permanent Resin A2 (ODS, Incheon, Korea) | Diurethane dimethacrylate, 2-propenoic acid, 2-methyl-, (1-methylethylidene)bis(4,1-phenyleneoxy(1-methyl-2,1-ethanediyl)) ester, 2-hydroxyethyl methacrylate (HEMA), diphenyl(2,4,6-trimethylbenzoyl) phosphine oxide, and additives | OP201221212-143 |
| GPR | Substrate | Permanent C&B - TC-80DP (Graphy, Seoul, Korea) | Urethane acrylate oligomer, bisphenol A ethoxylate dimethacrylate, 2-HEMA, diphenyl (2,4,6-trimethylbenzoyl) phosphine oxide, and additives | 1-B0607K12-003 |
| GL | Cement | G-CEM LinkAce (GC Corp., Tokyo, Japan) | Paste A: Fluoro-alumino-silicate glass, Urethane dimethacrylate (UDMA), dimethacrylate, silicon dioxide, initiator, inhibitor, pigment | 2402091 |
| | | G-Multi PRIMER (GC Corp., Tokyo, Japan) | Paste B: UDMA, dimethacrylate, phosphoric acid ester monomer, initiator, stabilizer | |
| | | | Ethyl alcohol, silane, phosphoric acid ester monomer, dimethacrylate component | 2302221 |
| RU | Cement | RelyX U200 (3M ESPE, St. Paul, MN, USA) | Base: Methacrylate monomers containing phosphoric acid groups, methacrylate monomers, initiators, stabilizers, rheological additives | 8567202 |
| | | | Catalyst: Methacrylate monomers, alkaline fillers, silanated fillers, initiator components, stabilizers, pigments, rheological additives, zirconia/silica fillers. | |
| CS | Cement | Clearfil SA Luting (Kuraray, Okayama, Japan) | Paste A: Bis-GMA, TEGDMA, MDP, hydrophobic aromatic dimethacrylate, silanated barium glass filler, silanated colloidal silica, dl-Camphorquinone, benzoyl peroxide, initiator | B20200 |
| | | | Paste B: Bis-GMA, hydrophobic aromatic dimethacrylate, silanated barium glass filler, silanated colloidal silica, surface-treated sodium fluoride, accelerators, pigments | |
| UC | Cement | RelyX Ultimate Clicker (3M ESPE, St. Paul, MN, USA) | Base: Methacrylate monomers, radiopaque, silanated fillers, initiator components, stabilizers, rheological additives | 8689538 |
| | | | Catalyst: Methacrylate monomers, radiopaque alkaline (basic) fillers, initiator components, stabilizers, pigments, rheological additives, fluorescence dye, dual-cure activator for Single Bond Universal Adhesive | |
| | | Single Bond Universal Adhesive (3M ESPE, St. Paul, MN, USA) | MDP monomer, dimethacrylate resins, HEMA, Vitrebond copolymer, filler, ethanol, water, initiators, silane | 40109D |
| S | Silane | RelyX Ceramic Primer Silane Coupling Agent (3M ESPE, St. Paul, MN, USA) | 3-(Trimethoxysilyl)propyl methacrylate, ethanol, water | 9972485 |

were prepared using a Bonding Clamp and a Bonding Mold Insert (Ultradent Products, Inc., South Jordan, UT, USA). The mold insert was designed to create a space with a 2.38 mm internal diameter and 2.67 mm height for resin cement, which was clamped against the cylinder. Resin cement was incrementally filled into the mold to a height of 2.0 mm. A light-emitting diode (LED) curing light unit (B&Lite S; B&L Biotech, Ansan, Korea) was fixed to the top surface of the mold insert and the resin cement was light-cured for 20 seconds. After removing the molds, the resin cement on the cylinders was light-cured for an additional 40 seconds—20 seconds on each of the two axial surfaces. All specimens were then stored in distilled water at 37°C in an incubator for 24 hours.

### Shear bond strength measurement

All specimens were subjected to shear bond strength (SBS) analysis using a universal testing machine (Shimadzu AG-X Series; Shimadzu Corp., Kyoto, Japan). A vertical loading force was applied to the resin cement immediately adjacent to the bonded area using a knife-edge blade at a crosshead speed of 1 mm/min. The maximum load at failure was recorded, and SBS (MPa) was calculated by dividing the peak load by the bonded surface area of the specimen.

To evaluate the failure modes, each fractured specimen was examined using a stereomicroscope (SZ61; Olympus, Tokyo, Japan) at 20× magnification and classified as adhesive failure when >75% of the failure area


https://doi.org/10.5395/rde.2026.51.e34

was located at the interface between the resin cement and the 3D-printed resin substrate, cohesive failure when >75% of the failure occurred within the 3D-printed resin substrate, or mixed failure when neither mode exceeded 75%, indicating a combination of both adhesive and cohesive failures.

### Contact angle measurement

To evaluate the surface wettability of both the resin cements and the 3D-printed resin substrates, static contact angle measurements were performed using a contact angle goniometer (Phoenix 300; Surface Electro Optics, Suwon, Korea) via the sessile drop method. For the resin cements (GL, RU, CS, and UC), flat disk-shaped specimens (10 mm in diameter and 1 mm in thickness) were fabricated by dispensing each material into a cylindrical mold placed on a glass slide covered with a polyester strip. After resin cement placement, another polyester strip was placed on the top surface to ensure a flat surface and prevent the formation of an oxygen-inhibited layer. The specimens were then light-cured for 20 seconds using the LED curing unit (B&Lite S). Five specimens of each of the four cement types were prepared. Surface pretreatment protocols identical to those used in the SBS tests—namely, GC for GL and Single Bond Universal Adhesive for UC, as recommended by the manufacturers—were applied prior to contact angle measurement.

For the 3D-printed resin substrates, disc specimens of GPR and OPR (10 mm in diameter and 1 mm in thickness) were fabricated, with five specimens prepared for each material using the same sample preparation protocol described above. All 3D-printed substrates were sandblasted with 50 μm aluminum oxide at 0.2 MPa for 10 seconds. In the silane-treated groups, the same silane coupling agent and application protocol used in the SBS test were applied, resulting in four substrate conditions: GPR, GPR + Silane, OPR, and OPR + Silane.

For all groups, a droplet of distilled water was deposited on the surface of each specimen, and the contact angle was measured within 10 seconds of droplet placement. Five measurements were performed for each group.

### Statistical analysis

SBS data were analyzed using IBM SPSS Statistics ver. 25 (IBM, Armonk, NY, USA). A three-way analysis of variance (ANOVA) was performed to evaluate the main effects of resin substrate type, resin cement type, and silane treatment, as well as their interactions. For simple group comparisons, a one-way ANOVA was conducted based on cement type and silane application, followed by Tukey honestly significant difference (HSD) *post hoc* test. For contact angle analysis, one-way ANOVA was applied to compare the surface wettability among the resin cements and 3D-printed substrates, with Tukey HSD *post hoc* test to identify significant differences between the groups.

## RESULTS

### Shear bond strength

The SBS test results are presented in Table 2 and Figure 2. In the OPR group without silane application, the highest SBS was observed for GL, followed by UC, RU, and CS. Although no statistically significant differences were observed among the GL, UC, and RU groups ($p > 0.05$), the CS group exhibited a significantly lower SBS ($p < 0.05$). With the application of silane, RU showed the highest SBS, followed by GL, UC, and CS; however, no statistically significant differences were found between RU, GL, and UC, aside from CS, which showed a signifi-

**Table 2.** Shear bond strength (MPa) of the resin cements

| Substrate | GL | | RU | | CS | | UC | | *F*-value | *p*-value |
|---|---|---|---|---|---|---|---|---|---|---|
| | No silane | Silane | No silane | Silane | No silane | Silane | No silane | Silane | | |
| OPR | $25.75 \pm 2.98^{A}$ | $25.72 \pm 2.72^{A}$ | $25.14 \pm 4.38^{A}$ | $26.20 \pm 4.80^{A}$ | $16.94 \pm 3.13^{B}$ | $17.99 \pm 2.62^{B}$ | $25.20 \pm 4.14^{A}$ | $25.08 \pm 2.23^{A}$ | 13.917 | <0.001 |
| GPR | $23.91 \pm 3.96^{A}$ | $22.99 \pm 2.54^{AB}$ | $25.36 \pm 4.62^{A}$ | $24.87 \pm 4.41^{A}$ | $19.07 \pm 2.95^{B}$ | $18.80 \pm 4.13^{B}$ | $23.82 \pm 3.11^{A}$ | $23.20 \pm 2.93^{AB}$ | 5.538 | <0.001 |

Values are presented as mean ± standard deviation.
The full names and manufacturers of the materials are provided in Table 1.
Different uppercase letters indicate statistically significant differences between resin cements and silane treatment (one-way analysis of variance followed by Tukey honestly significant difference *post hoc* test, $p < 0.05$).

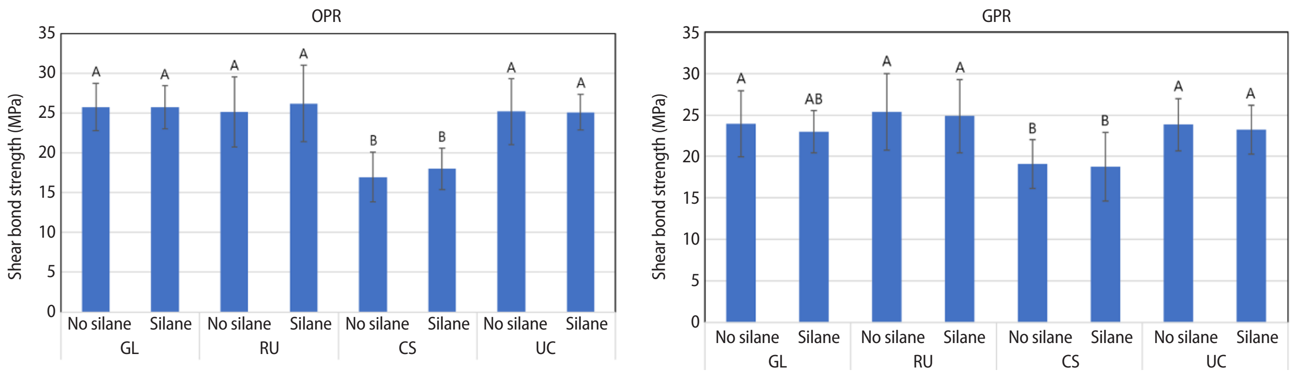


**Figure 2.** Shear bond strength of the resin cements. The full names and manufacturers of the materials are provided in Table 1.

cantly lower bond strength ($p < 0.05$). In the GPR group without silane treatment, the highest SBS was observed for RU, followed by GL, UC, and CS. In the GPR group treated with silane application, RU exhibited the highest SBS value, followed by UC, GL, and CS. Similar to the OPR group, no statistically significant differences were noted between the RU, GL, and UC groups, whereas the CS group showed the lowest SBS ($p < 0.05$). When comparing SBS values between the OPR and GPR substrates under identical conditions (with or without silane), no statistically significant differences were observed for most cement types. According to the results of the three-way ANOVA (Table 3), resin cement type had a significant effect on SBS ($p < 0.001$). In contrast, resin substrate type and silane treatment did not show significant main effects ($p > 0.05$). Furthermore, no significant two-way or three-way interaction effects among resin cement type, resin substrate type, and silane treatment were observed ($p > 0.05$).

In the OPR group, cohesive failure predominated across all subgroups. The GL, GL + S, RU, RU + S, UC, and UC + S exhibited 100% cohesive failures. In contrast, the CS subgroup showed a more varied distribution: 66.7% (8/12) were cohesive, 25.0% (3/12) were adhesive, and 8.3% (1/12) were mixed failures. The CS + S subgroup showed 83.3% (10/12) cohesive failures and 8.3% (1/12) mixed and adhesive failures. By contrast, the GPR group showed a broader distribution overall: 39.6% (38/96) cohesive, 30.2% (29/96) mixed, and 30.2% (29/96) adhesive failures. Notably, the CS subgroup showed no cohesive failures, with an equal distribution

**Table 3.** Three-way analysis of variance results

| Effect | Sum of squares | df | Mean square | *F*-value | *p*-value |
|---|---|---|---|---|---|
| Cement type | 1582.684 | 3 | 527.561 | 41.330 | <0.001 |
| Resin type | 26.948 | 1 | 26.948 | 2.110 | 0.148 |
| Silane treatment | 0.085 | 1 | 0.085 | 0.007 | 0.935 |
| Cement × Resin | 97.054 | 3 | 32.351 | 2.530 | 0.058 |
| Cement × Silane | 7.150 | 3 | 2.383 | 0.190 | 0.905 |
| Resin × Silane | 13.573 | 1 | 13.573 | 1.060 | 0.304 |
| Cement × Resin × Silane | 1.979 | 3 | 0.660 | 0.050 | 0.984 |

df, degree of freedom.

of adhesive and mixed failures (50.0% each). Cohesive failure was most frequently observed in the RU and UC subgroups (66.7%, 8/12, respectively) (Figure 3).

### Contact angle and surface evaluation

Figure 4 shows the contact angle values for the different resin cements and 3D-printed resin substrates. Among the resin cements, CS exhibited the highest contact angle (67.6°), followed by GL (59.2°), RU (51.8°), and UC (43.5°). All resin cement groups differed significantly from one another. For the substrates, GPR with silane treatment (GPR + S) exhibited a significantly higher contact angle (94.4°) than all other conditions. In contrast, GPR (68.8°), OPR (65.7°), and OPR with silane (62.0°) showed no significant differences.

Figure 5 presents representative SEM images (×500) of the 3D-printed resin substrates after air abrasion and silane application. Microcracks were observed on both OPR and GPR surfaces after air abrasion. The OPR surface appeared relatively smooth and uniform, whereas


https://doi.org/10.5395/rde.2026.51.e34

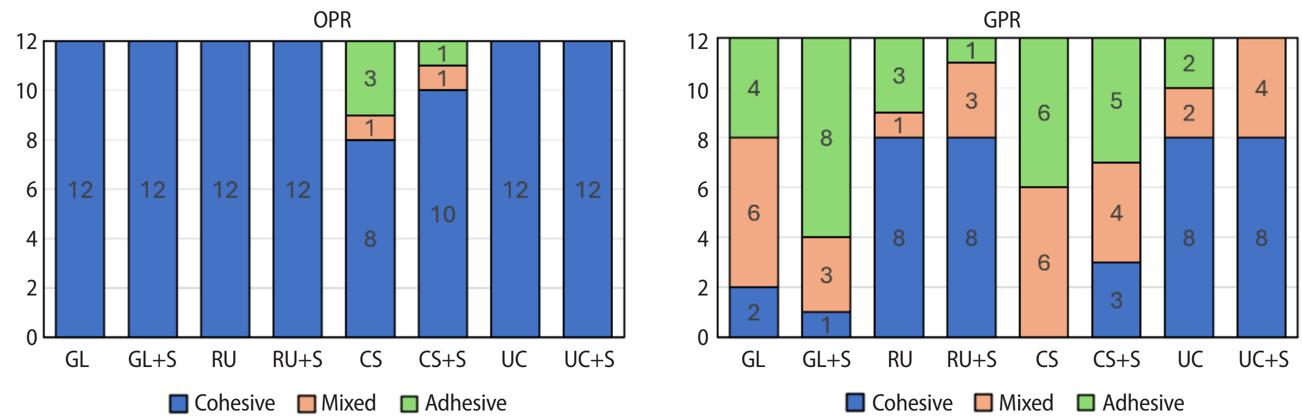


Figure 3. Failure mode distribution. The full names and manufacturers of the materials are provided in Table 1. The +S notation indicates silane application.

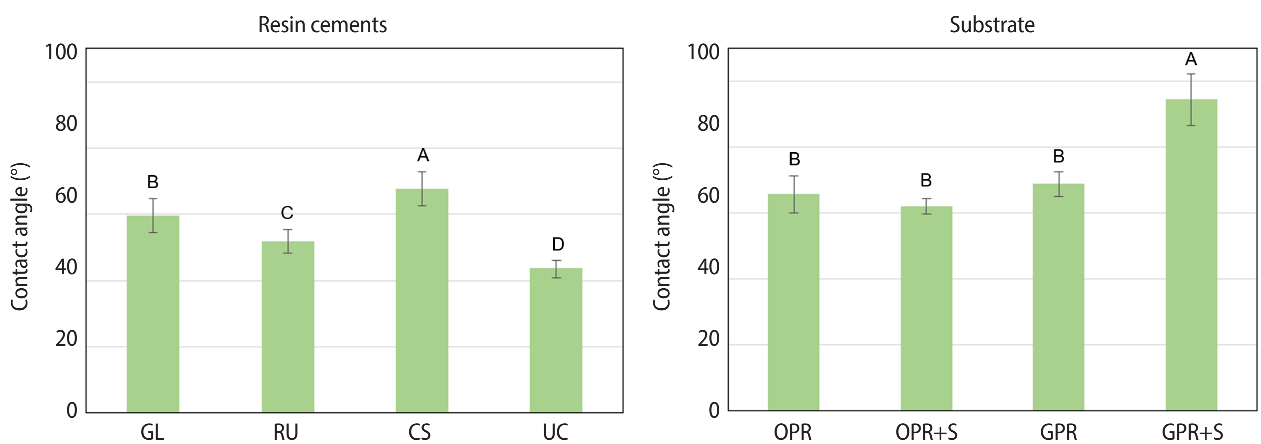


Figure 4. Contact angles among resin cements and three-dimensional printed substrates. The +S notation indicates silane application. Among the resin cements, G-Multi PRIMER and Single Bond Universal Adhesive were applied to GL and UC, respectively. The full names and manufacturers of the materials are provided in Table 1.

the GPR surface exhibited a rougher and more irregular texture with deeper grooves and distinct surface features. Silane application produced minimal visible morphological changes compared to the air-abraded surfaces in both groups at this magnification.

## DISCUSSION

As a form of indirect restoration, 3D-printed dental restorations require durable adhesion to luting cements to ensure clinical success. In this study, the SBS of three self-adhesive resin cements—GL, RU, and CS—and one adhesive resin cement, UC, was compared to two types of 3D-printed restorative resins. The effect of applying a silane coupling agent on bonding performance was also assessed. The null hypothesis proposed that the type of resin cement, use of silane, and type of 3D-printed resin did not significantly influence SBS. Thus, this hypothesis is only partially supported. The results demonstrated that the type of resin cement had a statistically significant effect on the bond strength, whereas the application of silane and choice of 3D-printed resin substrate did not have a significant impact.

In both the OPR and GPR resin groups, CS consistently showed a significantly lower bond strength than the other cements. According to manufacturer data, CS has a film thickness of 19 μm, which is notably greater than that of GL (3 μm), RU (13 μm), and UC (12 μm). A thick-

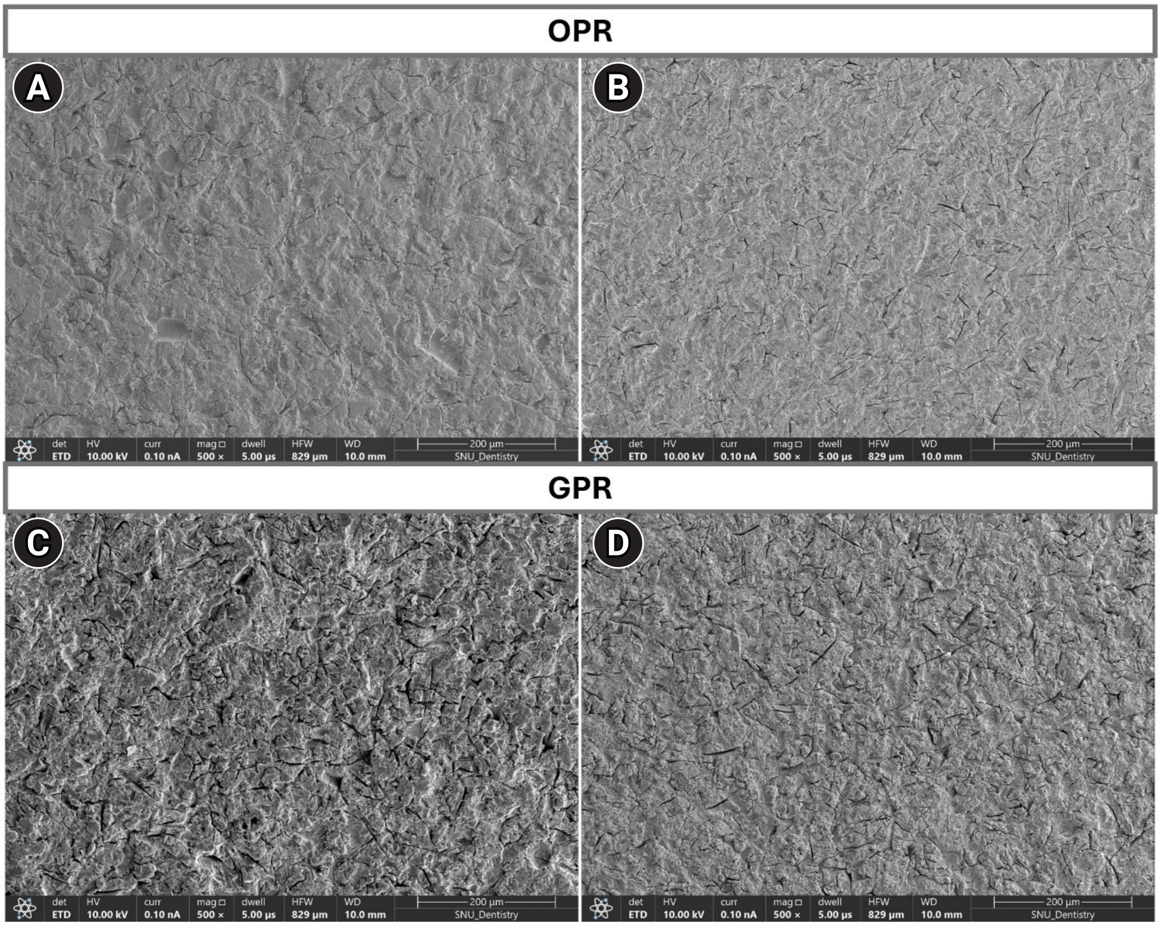


**Figure 5.** Representative scanning electron microscopy images (×500 magnification) of air-abraded and silane-treated OPR and GPR surfaces. (A) OPR after air abrasion without silane application, (B) OPR after air abrasion followed by silane application, (C) GPR after air abrasion without silane application, and (D) GPR after air abrasion followed by silane application. The full names and manufacturers of the materials are provided in Table 1.

er cement layer can compromise mechanical interlocking by introducing interfacial gaps and cause uneven stress distribution during loading [18]. The CS exhibited the highest contact angle among the cements, indicating that its wettability was relatively poor. The combination of greater film thickness and limited wetting ability may have contributed to reduced bonding performance, resulting in a higher incidence of adhesive failure.

RU and UC are produced by the same manufacturer and are intended for different adhesive strategies. UC is an adhesive resin cement requiring the application of a separate bonding agent to achieve optimal adhesion, whereas RU is a self-adhesive resin cement that simplifies the clinical procedure by eliminating the need for additional bonding. Despite the added bonding step, UC did not exhibit superior bond strength compared with RU. The contact angle data further revealed that UC, when used in conjunction with a bonding agent, exhibited the lowest contact angle, indicating excellent wettability. RU also demonstrated relatively good wettability, which may have contributed to its ability to achieve a bond strength comparable to that of UC, despite not requiring an additional adhesive step. In addition to wettability, another possible explanation for the lack of significant difference in bond strength between UC and RU may lie in their inherent chemical composition, which enables effective bonding to the tested substrates, regardless of the bonding protocol used.

Regarding the silane coupling agents, no significant improvement in the SBS between the 3D-printed resins


https://doi.org/10.5395/rde.2026.51.e34

and resin cements was observed. This finding is consistent with previous studies that reported mixed results regarding the effectiveness of silane, often attributed to differences in the chemical composition of the materials being tested [19–22]. The absence of a noticeable bonding enhancement may be due to the unique chemical structure of the 3D-printed resins. Specifically, the types of monomers and fillers used in these materials can significantly influence their mechanical properties and adhesive compatibility with resin cements [23]. Compared to conventional composite resins, 3D printing resins contain different types and ratios of monomers [24], and only a limited number of studies have investigated the chemical composition of commercial 3D-printed resins used for dental prostheses [12,25]. Common monomers found in light-cured dental composites, such as bisphenol A-glycidyl methacrylate (bis-GMA) and urethane dimethacrylate (UDMA), are used in 3D printing resins [26]. Additionally, monomers such as ethoxylated bisphenol A-dimethacrylate (bis-EMA) and triethylene glycol dimethacrylate (TEGDMA) are often incorporated to reduce the viscosity of the liquid resin [24,27]. While monomer composition plays a key role in determining the mechanical properties, ceramic fillers are added to 3D-printed resins to enhance their strength [8,28]. These fillers vary in shape, size, and composition; however, increasing their size or percentage can not only reduce light transmission but also significantly increase viscosity, both of which may lead to undesirable outcomes [11,12]. The 3D printing resins used in this study, OPR and GPR, were urethane acrylate-based materials with no reported filler content. This composition limits the effectiveness of silane, which typically enhances adhesion through chemical interactions with silanol groups present on silica-containing surfaces [10,29]. Silane application on the GPR surface increased the contact angle, indicating reduced wettability and thus showed no clear beneficial effect on the bond strength. Similarly, previous studies reported that silane treatment has minimal or no effect on non-silica-based substrates, highlighting the substrate-dependent bonding mechanism [9,30]. In the present study, a commonly used air-drying protocol was employed to facilitate solvent evaporation from the applied silane; however, variations in drying duration or the use of heat-assisted evaporation may further influence the extent of silane condensation and surface energy. The absence of a significant improvement in bond strength following silane application may therefore be partially attributable to the selected drying protocol, in addition to the filler-deficient, urethane acrylate-based nature of the tested 3D-printed resins.

To further investigate the substrate-related differences in bonding performance, both the SBS results and SEM analysis were examined. Although SBS values between OPR and GPR were not significantly different, noticeable differences were observed in their failure patterns. The OPR groups predominantly exhibited cohesive failures, suggesting that failure occurred within the substrate material rather than at the interface, possibly because of the weaker interlayer cohesion in the OPR. In contrast, the GPR groups exhibited more frequent adhesive and mixed failures, indicating weaker adhesion at the resin-cement-substrate interface. The SEM analysis supports these observations. The OPR surfaces appeared relatively smooth and uniform after air abrasion and silane application, which may have allowed for a more consistent resin adaptation and stress distribution. Conversely, the GPR surfaces exhibited a rougher and more irregular morphology with microcracks, which may have compromised uniform resin infiltration despite the potential for mechanical interlocking. Additionally, the prevalence of cohesive failure in OPR suggests that the interlayer bonding within the printed substrate may be weaker than that in GPR. Although the resin cement achieved good adhesion to the OPR surface, internal structural weaknesses between the printed layers could have served as the primary failure site. In contrast, GPR may have stronger interlayer cohesion but a lower surface affinity for resin cements, as evidenced by the higher rate of adhesive failure. These morphological and structural differences likely contributed to the less favorable interfacial bonding behavior observed in the GPR substrate. These morphological differences also provide a framework for interpreting the contact angle results. The smoother and more uniform surface observed for OPR after air abrasion and silane application may have promoted more homogeneous wetting behavior, resulting in minimal changes in contact angle. In contrast, the rougher and more irregular surface morphology with microcracks observed in GPR may have facilitated non-uniform silane film distribution and possibly localized retention of organosilane components, leading to increased surface hydrophobicity and a higher water contact angle after silane treatment. Furthermore, both OPR and GPR are urethane acrylate-based materials with limited or no reported silica filler content, which restricts effective siloxane coupling. Under such conditions, silane is more likely to function as a superficial surface modifier rather than a true chemical coupling agent, explaining why material-dependent changes in wettability did not translate into significant improvements in bond strength. Therefore, while SBS values alone may suggest similar bonding performance, a more comprehensive evaluation that considers both quantitative bond strength and qualitative failure modes is essential for assessing the true integrity of adhesive interfaces in 3D-printed materials.

The findings of this study demonstrate that the type of resin cement has a significant impact on the SBS of 3D-printed resins, whereas silane treatment does not enhance the bonding performance under the conditions tested. These results suggest that careful selection of resin cement is critical for optimizing bonding to 3D-printed restorative materials with minimal or no filler content. However, this study has several limitations. First, only one silane coupling agent (RelyX Ceramic Primer) was evaluated using a single application and drying protocol. Variations in silane composition, solvent systems, or application methods among different products may influence interfacial chemistry and bonding performance. Therefore, the present findings should not be generalized to all silane agents. Second, thermocycling was not incorporated and should be included in future studies to better simulate clinical conditions and assess the long-term durability of the bond. In addition, only two 3D-printed restorative resins were investigated, both of which are urethane acrylate-based materials that were locally available at the time of the study. This limits the generalizability of the findings to other resin chemistries or commercially available materials in different regions. Furthermore, exploring a wider range of surface modifications, such as varying the air-abrasion pressure and application time, would provide further insights. Addressing these limitations in future research will help establish a more comprehensive understanding of the bonding behavior of 3D-printed resin materials.

## CONCLUSIONS

Within the limitations of this study, it can be concluded that the type of resin cement significantly impacts the SBS to 3D-printed resins. Furthermore, silane treatment does not significantly enhance the SBS for either the OPR or GPR substrates, both of which lack filler content. Additionally, although no significant differences in SBS were found between the OPR and GPR substrates, the two substrates exhibited distinct failure patterns.

### CONFLICT OF INTEREST

No potential conflict of interest relevant to this article was reported.

### FUNDING/SUPPORT

This research was partially supported by Engineering-Dentistry Interdisciplinary Research Grant jointly funded by College of Engineering and School of Dentistry, Seoul National University.

### AUTHOR CONTRIBUTIONS

Conceptualization: Shin JH. Data curation, Investigation: Park SJ, Lee EH. Formal analysis: Park SJ. Funding acquisition: Kim RJ. Supervision: Kim RJ, Shin JH. Writing - original draft: Park SJ, Lee EH. Writing - review & editing: Kim RJ, Shin JH. All authors read and approved the final manuscript.

### DATA SHARING STATEMENT

The datasets are not publicly available but are available from the corresponding author upon reasonable request.

### DISCLOSURE OF GENERATIVE AI IN SCIENTIFIC WRITING

No generative AI technologies were used in the preparation of this manuscript.

## REFERENCES

1. Tian Y, Chen C, Xu X, Wang J, Hou X, Li K, *et al*. A review of 3D printing in dentistry: technologies, affecting factors, and applications. Scanning 2021;2021:9950131.
2. Dawood A, Marti Marti B, Sauret-Jackson V, Darwood A. 3D


https://doi.org/10.5395/rde.2026.51.e34

printing in dentistry. Br Dent J 2015;219:521-529.
3. Abduo J, Lyons K, Bennamoun M. Trends in computer-aided manufacturing in prosthodontics: a review of the available streams. Int J Dent 2014;2014:783948.
4. Goodacre BJ, Goodacre CJ. Additive manufacturing for complete denture fabrication: a narrative review. J Prosthodont 2022;31:47-51.
5. Spitznagel FA, Horvath SD, Guess PC, Blatz MB. Resin bond to indirect composite and new ceramic/polymer materials: a review of the literature. J Esthet Restor Dent 2014;26:382-393.
6. Lee KS, Shin MS, Lee JY, Ryu JJ, Shin SW. Shear bond strength of composite resin to high performance polymer PEKK according to surface treatments and bonding materials. J Adv Prosthodont 2017;9:350-357.
7. Dewan H, Sayed ME, Jundus A, Gharawi M, Baeshen S, Alali M, *et al*. Shear strength of repaired 3D-printed and milled provisional materials using different resin materials with and without chemical and mechanical surface treatment. Polymers (Basel) 2023;15:4284.
8. Kim M, Lee J, Park C, Jo D, Yu B, Khalifah SA, *et al*. Evaluation of shear bond strengths of 3D printed materials for permanent restorations with different surface treatments. Polymers (Basel) 2024;16:1838.
9. Zakir M, Ashraf U, Tian T, Han A, Qiao W, Jin X, *et al*. The role of silane coupling agents and universal primers in durable adhesion to dental restorative materials: a review. Curr Oral Health Rep 2016;3:244-253.
10. Lung CY, Matinlinna JP. Aspects of silane coupling agents and surface conditioning in dentistry: an overview. Dent Mater 2012;28:467-477.
11. Zattera AC, Morganti FA, de Souza Balbinot G, Della Bona A, Collares FM. The influence of filler load in 3D printing resin-based composites. Dent Mater 2024;40:1041-1046.
12. Bora PV, Sayed Ahmed A, Alford A, Pitttman K, Thomas V, Lawson NC. Characterization of materials used for 3D printing dental crowns and hybrid prostheses. J Esthet Restor Dent 2024;36:220-230.
13. Jain S, Sayed ME, Shetty M, Alqahtani SM, Al Wadei MH, Gupta SG, *et al*. Physical and mechanical properties of 3D-printed provisional crowns and fixed dental prosthesis resins compared to CAD/CAM milled and conventional provisional resins: a systematic review and meta-analysis. Polymers (Basel) 2022;14:2691.
14. Yim JH, Shin SY. A study on the shear bond strength between 3D printed resin and provisional resin after thermal cycling. J Dent Rehabil Appl Sci 2021;37:101-110.
15. Nasiry Khanlar L, Revilla-León M, Barmak AB, Ikeda M, Alsandi Q, Tagami J, *et al*. Surface roughness and shear bond strength to composite resin of additively manufactured interim restorative material with different printing orientations. J Prosthet Dent 2023;129:788-795.
16. Wongsue S, Thanatvarakorn O, Prasansuttiporn T, Nimmanpipug P, Sastraruji T, Hosaka K, *et al*. Effect of surface topography and wettability on shear bond strength of Y-TZP ceramic. Sci Rep 2023;13:18249.
17. Noro A, Kaneko M, Murata I, Yoshinari M. Influence of surface topography and surface physicochemistry on wettability of zirconia (tetragonal zirconia polycrystal). J Biomed Mater Res B Appl Biomater 2013;101:355-363.
18. Ling L, Ma Y, Chen Y, Malyala R. Physical, mechanical, and adhesive properties of novel self-adhesive resin cement. Int J Dent 2022;2022:4475394.
19. Nobuaki A, Keiichi Y, Takashi S. Effects of air abrasion with alumina or glass beads on surface characteristics of CAD/CAM composite materials and the bond strength of resin cements. J Appl Oral Sci 2015;23:629-636.
20. Elsaka SE. Bond strength of novel CAD/CAM restorative materials to self-adhesive resin cement: the effect of surface treatments. J Adhes Dent 2014;16:531-540.
21. Stawarczyk B, Stich N, Eichberger M, Edelhoff D, Roos M, Gernet W, *et al*. Long-term tensile bond strength of differently cemented nanocomposite CAD/CAM crowns on dentin abutment. Dent Mater 2014;30:334-342.
22. Frankenberger R, Hartmann VE, Krech M, Krämer N, Reich S, Braun A, *et al*. Adhesive luting of new CAD/CAM materials. Int J Comput Dent 2015;18:9-20.
23. Peskersoy C, Oguzhan A. Evaluation of the mechanical and adhesion characteristics of indirect restorations manufactured with three-dimensional printing. Polymers (Basel) 2024;16:613.
24. Lin CH, Lin YM, Lai YL, Lee SY. Mechanical properties, accuracy, and cytotoxicity of UV-polymerized 3D printing resins composed of Bis-EMA, UDMA, and TEGDMA. J Prosthet Dent 2020;123:349-354.
25. Kim N, Kim H, Kim IH, Lee J, Lee KE, Lee HS, *et al*. Novel 3D printed resin crowns for primary molars: in vitro study of fracture resistance, biaxial flexural strength, and dynamic mechanical analysis. Children (Basel) 2022;9:1445.
26. Yılmaz D, Sabatini GP, Kahveci Ç, Yoon HI, Yilmaz B, Çakmak G, *et al*. Effect of material thickness and coffee thermo-

cycling on the color stability and translucency of additively and subtractively manufactured resin-based materials for definitive restorations. Int J Prosthodont 2024;37:143-150.
27. Kang YJ, Park Y, Shin Y, Kim JH. Effect of adhesion conditions on the shear bond strength of 3D printing resins after thermocycling used for definitive prosthesis. Polymers (Basel) 2023;15:1390.
28. Koenig A, Schmidtke J, Schmohl L, Schneider-Feyrer S, Rosentritt M, Hoelzig H, *et al*. Characterisation of the filler fraction in CAD/CAM resin-based composites. Materials (Basel) 2021;14:1986.
29. Matinlinna JP, Lung CY, Tsoi JK. Silane adhesion mechanism in dental applications and surface treatments: a review. Dent Mater 2018;34:13-28.
30. Han JY, Shin JH, Shim JS, Kim RJ. Effects of dentin bonding agents and silanization on bond strength between 3D printed resin and composite resin. Dent Mater J 2024;43:400-406.


https://doi.org/10.5395/rde.2026.51.e34

RDE Restorative Dentistry & Endodontics

Research Article

eISSN 2234-7666
Restor Dent Endod. 2026 August;51(3):e35
https://doi.org/10.5395/rde.2026.51.e35

# Effect of light-curing modes on degree of conversion and color stability of flowable bulk-fill composites: an *in vitro* experimental study

**Eda Karaaslan**[1], **Sultan Aktuğ Karademir**[2,*]

[1]Department of Restorative Dentistry, Faculty of Dentistry, Niğde Ömer Halisdemir University, Niğde, Türkiye
[2]Department of Restorative Dentistry, Faculty of Dentistry, Ordu University, Ordu, Türkiye

## ABSTRACT

**Objectives:** This study aims to evaluate the impact of light-curing modes on the degree of conversion (DC) and color change (CIEDE2000 color difference, $\Delta E_{00}$) of different flowable composite resins.
**Methods:** A total of 120 specimens ($n = 10$ per group) were prepared from four materials: G-aenial Universal Injectable (GUI; GC), Estelite Bulk Fill Flow (EBF; Tokuyama Dental), Tetric N-Flow Bulk Fill (TNF; Ivoclar Vivadent), and Filtek Bulk Fill Flowable (FBF; 3M ESPE). The specimens were polymerized using an LED light-curing unit under three light-curing modes: standard (1,000 mW/cm², 20 seconds), high-power (1,400 mW/cm², 3 × 4 seconds), and extra-power (3,200 mW/cm², 2 × 3 seconds). The DC was quantified using Fourier transform infrared spectroscopy. Color measurements were performed at baseline, and on the 7th and 14th days after immersion in coffee, using a spectrophotometer. The $\Delta E_{00}$ was calculated using the CIEDE2000 formula. The data were analyzed using IBM SPSS software ($\alpha = 0.05$).
**Results:** Material type and light-curing mode significantly affected both the DC and $\Delta E_{00}$ ($p < 0.05$). All composites exhibited lower DC in the extra-power mode compared to the high-power mode. On day 14, the extra-power mode resulted in significantly greater discoloration in TNF, FBF, and EBF compared to the high-power mode ($p < 0.05$).
**Conclusions:** Although curing with the extra-power mode saves time, it may result in a lower DC and an increase in $\Delta E_{00}$ in flowable composite resin.

**Keywords:** Color change; Degree of conversion; Flowable bulk-fill; Fourier transform infrared spectroscopy; Light-curing mode; Spectrophotometer

## INTRODUCTION

In recent years, advancements in polymer chemistry and technology have led to significant developments in restorative materials. Initially, the term "bulk-fill" referred to a resin composite application technique

**Received:** July 17, 2025 **Revised:** January 21, 2026 **Accepted:** February 22, 2026
**Citation**
Karaaslan E, Karademir SA. Effect of light-curing modes on degree of conversion and color stability of flowable bulk-fill composites: an *in vitro* experimental study. Restor Dent Endod 2026;51(3):e35.
***Correspondence to**
**Sultan Aktuğ Karademir, DDS, MSD**
Department of Restorative Dentistry, Faculty of Dentistry, Ordu University, Cumhuriyet, Mustafa Kemal Blv. No: 254, Altınordu, Ordu 52200, Türkiye
Email: Sultan_721@hotmail.com

that allowed layering in 4–5 mm thicknesses; however, over time, it has been adopted as a new class of material [1]. The use of bulk-fill composites, which allow for the placement of thicker layers resulting in a homogeneous restoration, is advantageous because of their ease and speed of application. The use of additional or more efficient photoinitiators, combined with a reduction in filler content, enhances light transmission and deepens polymerization in bulk-fill composites [2,3].

The degree of conversion (DC) is a fundamental parameter of composite resins, significantly influencing their mechanical performance, polymerization shrinkage, and biocompatibility [4,5]. The DC is affected by various parameters, including the chemical composition of the dimethacrylate monomer, intrinsic elements like the type and quantity of photoinitiators, as well as extrinsic conditions such as the temperature during polymerization. Additionally, the increased viscosity of the polymerizing network and the restricted mobility of reactants due to the presence of filler particles impact the DC [4]. More translucent bulk-fill composite resins facilitate the conversion of monomers to polymers, thereby increasing the DC. Flowable bulk-fill composites, characterized by a low inorganic filler content and a high resin matrix ratio, exhibit higher monomer-to-polymer conversion rates [6]. Nanoparticle fillers have been integrated into new-generation flowable bulk-fill resin-based composites to improve their mechanical properties while preserving low viscosity [7]. However, the polymerization efficiency of these materials must be tested using direct or indirect methods to ensure clinical applicability [8].

Adequate polymerization requires the light source to operate within an appropriate wavelength range, provide sufficient light output, and be used for an effective light-curing time [9]. Recent experimental studies [9–12] have shown that curing kinetics and depth of cure are strongly dependent on light-curing unit (LCU) type, spectral match, and exposure protocol. Although Ajaj *et al.* [8] and Parra Gatica *et al.* [11] reported valuable insights into bulk-fill polymerization efficiency and flowable bulk-fill characteristics, they emphasized substantial heterogeneity in light-curing protocols, material compositions, and evaluation methods. In many studies, higher irradiance has not generally been associated with higher DC because different irradiance intensities combined with varying light-curing times can lead to similar irradiance exposures [11,12]. Although *in vitro* studies argue that sensitivity to changes in irradiance depends on the material and that calculations based solely on total energy are invalid, LCUs continue to increase irradiance intensity. Moreover, manufacturers persistently claim that sufficient polymerization can be achieved with short exposure times (5 seconds or less) at high irradiance levels [6].

The release of residual monomers into the oral cavity and pulp chamber, caused by incomplete polymerization, may compromise the physical integrity and long-term stability of dental materials [12]. Czasch and Ilie [13] reported that this condition leads to problems such as marginal leakage, discoloration, water absorption, and reduced mechanical strength in restorations. Color stability in resin composites is influenced by multiple compositional aspects, encompassing the resin matrix's chemical characteristics, the filler type and load, as well as photoinitiator content. Although restorations are influenced by external factors according to their inorganic filler and surface characteristics, intrinsic discoloration may occur due to oxidation-induced changes in the resin matrix and at the interface between the matrix and fillers [14]. The presence of unreacted carbon double bonds increases material susceptibility to degradation, thereby reducing color stability [15]. Significant discoloration in restorative materials is a primary reason for the replacement of anterior composite resin restorations. The long-term color stability of bulk-fill resin composites remains a critical concern among clinicians [16]. Furthermore, despite the introduction of new photoinitiators and increased irradiance outputs, there is limited evidence regarding (1) the compatibility between recently developed flowable bulk-fill composites and third-generation polywave LCUs, (2) the influence of high-irradiance and short-exposure modes on both DC and color stability, and (3) the relationship between initial polymerization efficiency and post-staining color changes.

The compatibility of the third-generation polywave light-emitting diode (LED) LCU introduced to the market with the addition of new photoinitiators to the materials has not yet been verified with flowable bulk-


https://doi.org/10.5395/rde.2026.51.e35

fills, and the effectiveness of the modes has not been determined [17]. Therefore, this study aims to contribute novel data by evaluating how different polywave light-curing modes affect the DC and color stability of contemporary flowable bulk-fill resin composites, directly addressing the unresolved issues noted in recent reviews.

The null hypotheses of the study were: (1) the DC would not be affected by different light-curing modes and material types and (2) color stability would not be influenced by different light-curing modes, material types, and time.

## METHODS

In this *in vitro* study, three flowable bulk-fill composite resins (Estelite Bulk Fill Flow [EBF; Tokuyama Dental, Tokyo, Japan], Tetric N-Flow Bulk Fill [TNF; Ivoclar Vivadent, Schaan, Liechtenstein], and Filtek Bulk Fill Flowable Restorative [FBF; 3M ESPE, St. Paul, MN, USA]) were evaluated, along with one injectable flowable composite resin (G-aenial Universal Injectable [GUI; GC Corp., Tokyo, Japan]), which served as the control group. The characteristics and specifications of the materials evaluated in this study are summarized in Table 1. The experimental workflow of this study is summarized in Figure 1.

The sample size was determined using G*Power 3.1.9.7 software (Heinrich Heine University, Düsseldorf, Germany), based on data from a previous study [18]. Using one-way analysis of variance (ANOVA) with an effect size of 0.40, corresponding to an expected difference of 2.69 units with a standard deviation of 0.33, a significance level of $\alpha = 0.05$, and a statistical power of $1 - \beta = 0.80$, the required sample size was calculated. A total of 120 specimens—10 for each of the three subgroups of the four composite resins—were deemed sufficient.

### Specimen preparation

Specimens (5 × 4 mm) were prepared using transparent silicone molds placed on glass plates with Mylar strips on both sides. The composites were injected, covered with another Mylar strip and glass plate, and light-cured using a third-generation LED LCU (VALO Cordless; Ultradent, South Jordan, UT, USA) positioned perpen-

**Table 1.** Flowable resin composite materials used in the study

| Material | Resin matrix monomer | Photoinitiator system | Filler system | Shade/LOT and manufacturer | Primary source |
|---|---|---|---|---|---|
| G-aenial Universal Injectable (GUI) | UDMA[a], TEGDMA[a] | CQ | Type: nanofill<br>Size: 0.1 µm<br>Filler loading (wt/vol): 69%/50% | A2 / 230519A<br>GC Corp., Tokyo, Japan | GC SDS/TDS |
| Estelite Bulk Fill Flow (EBF) | Bis-GMA[b], TEGDMA[a], Bis-MPEPP[b] | CQ (Rap Technology) | Type: supranano<br>Size: 0.2 µm<br>Filler loading (wt/vol): 70%/56% | A2 / 163E83<br>Tokuyama Dental, Tokyo, Japan | Tokuyama IFU (the SDS does not list monomers individually) |
| Tetric N-Flow Bulk Fill (TNF) | Bis-GMA[b], UDMA[a], TEGDMA[a] | Ivocerin | Type: nanohybrid<br>Size: 5 µm<br>Filler loading (wt/vol): 68.2%/46.4% | IVA / Z05PHM<br>Ivoclar Vivadent, Schaan, Liechtenstein | Ivoclar Vivadent SDS/TDS |
| Filtek Bulk Fill Flowable Restorative (FBF) | Bis-GMA[b], UDMA[a], TEGDMA[a], Bis-EMA[b], procrylate resins[a] | CQ | Type: microhybrid<br>Size: Undeclared<br>Filler loading (wt/vol): 64.5%/42.5% | A2 / 10264465<br>3M ESPE, St. Paul, MN, USA | 3M ESPE SDS/TDS |

Bis-EMA, bisphenol A dimethacrylate; Bis-GMA, bisphenol A glycidyl methacrylate; Bis-MPEPP, bisphenol A polyethoxy methacrylate; CQ, camphorquinone; IFU, Instructions for Use; SDS, Safety Data Sheet; TDS, Technical Data Sheet; TEGDMA, triethylene glycol dimethacrylate; UDMA, urethane dimethacrylate.
[a]Aliphatic monomer. [b]Aromatic monomer.

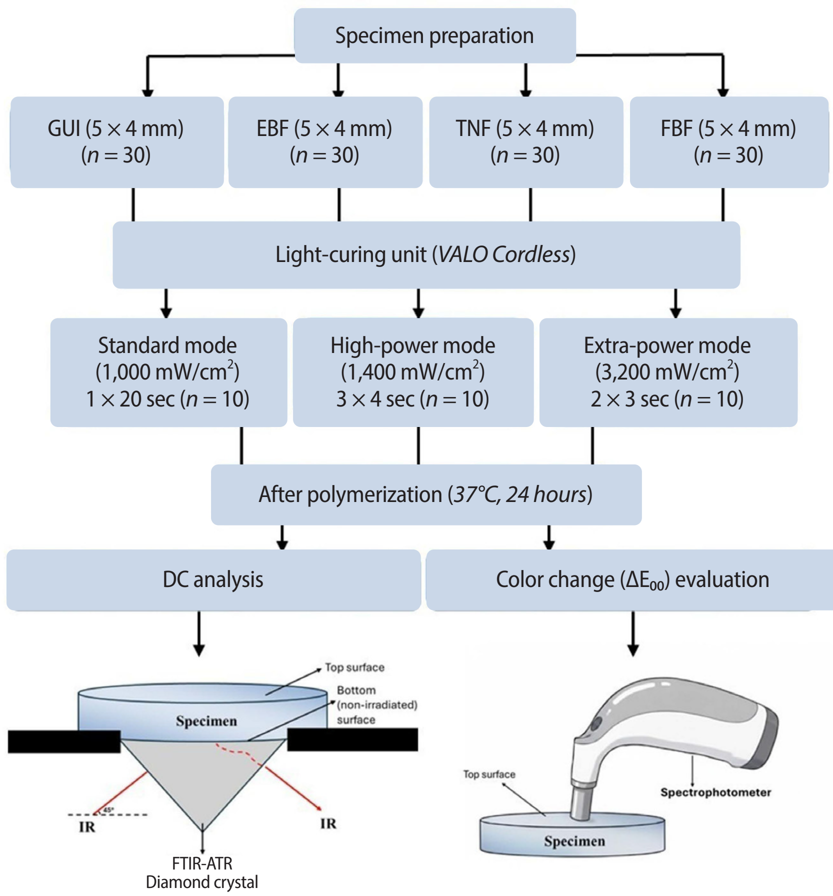


**Figure 1.** Schematic representation of the experimental workflow. ATR, attenuated total reflectance; DC, degree of conversion; FTIR, Fourier-transform infrared; IR, infrared. Material abbreviations and manufacturer information are provided in Table 1.

dicularly with the tip in contact with the glass surface. Polymerization was performed in three modes: standard (1,000 mW/cm$^2$, 20 seconds), high-power (1,400 mW/cm$^2$, 3 × 4 seconds), and extra-power (3,200 mW/cm$^2$, 2 × 3 seconds). Measurements taken at the tip of the device indicated corresponding radiant exposures of approximately 20.0, 16.8, and 19.2 J/cm$^2$, respectively. To determine the irradiance reaching the specimen, measurements were performed at the specimen plane through the interposed glass plate and Mylar strips using a calibrated radiometer (SDI RADII Plus; SDI Limited, Bayswater, VIC, Australia). The corresponding radiant exposures at the specimen plane were calculated as approximately 19.0, 15.8, and 18.1 J/cm$^2$. The output intensity of the LCU was verified before each curing session using a calibrated radiometer to ensure consistency across all specimens.

A total of 120 specimens ($n$ = 10 per subgroup) were fabricated and stored dry in a 37°C incubator for 24 hours to complete polymerization. Finishing and polishing procedures were conducted by a single operator to minimize operator-related variability. Surface standardization was achieved using sequential aluminum oxide discs of coarse, medium, fine, and superfine grits (Sof-Lex Discs; 3M ESPE) applied for 5 seconds each, followed by medium-fine diamond-grit wheels (Clearfil Twist Dia; Kuraray Europe GmbH, Hattersheim am Main, Germany) for 30 seconds each [14,19]. All procedures were performed dry at 10,000 revolutions per minute with overlapping unidirectional strokes to prevent heat and grooves. To ensure consistency, approximately constant manual pressure was applied using only the inherent weight of the handpiece, without extra force; the applied pressure was standardized on a force


https://doi.org/10.5395/rde.2026.51.e35

sensor (Axis, Gdańsk, Poland) at around 1–2 N, consistent with previous reports [20]. Discs were replaced after every three uses, and specimens were rinsed with water for 20 seconds and air-dried for 5 seconds between steps.

Specimen thickness was measured and verified at 4 ± 0.1 mm using a digital caliper (Mitutoyo Corp., Kawasaki, Japan).

### Degree of conversion analysis

The DC was assessed via Fourier-transform infrared (FTIR) spectroscopy (Spectrum One; PerkinElmer, Waltham, MA, USA) equipped with a universal attenuated total reflectance (uATR) accessory featuring a single-reflection diamond crystal (refractive index $n = 2.40$) at a 45° incidence angle. A constant pressure of approximately 70 N was applied using the integrated clamp to ensure consistent specimen–crystal contact. The effective ATR penetration depth was calculated at 1,637 $cm^{-1}$—the wavenumber used for DC analysis—using the standard equation for a 45° diamond ATR crystal. Assuming refractive indices of 1.52 for the composite resin and 2.40 for the diamond crystal, the penetration depth at 1,637 $cm^{-1}$ was estimated to be approximately 1.2–1.4 µm.

Specimens were stored dry for 24 hours prior to evaluation to avoid potential interference of residual surface or absorbed water with ATR-FTIR spectra, and in light-proof containers to prevent polymerization changes. All FTIR spectra were recorded on the same day for consistency. Prior to measurements, the ATR crystal was cleaned with alcohol and background scans were performed for calibration, including void check and linearity confirmation. Spectra were collected in absorbance mode (4,000–650 $cm^{-1}$, 4 $cm^{-1}$ resolution, 32 scans) and processed using Spectrum ver. 5.0.1 software (PerkinElmer) with baseline correction and automatic peak detection. Uncured composites were placed directly on the ATR crystal, while cured specimens (5 × 4 mm) were positioned with the bottom (non-irradiated) surface against the crystal and slightly compressed to ensure proper contact. For reproducibility, three measurements were taken for each specimen, and the averaged data were used to calculate a single DC value. In addition, one representative specimen from each group was analyzed for both top and bottom surfaces to verify polymerization uniformity.

Spectra of each resin were analyzed. Baseline correction in the 1,450–1,700 $cm^{-1}$ region was performed using a straight-line baseline defined between these limits, and peak integration was based on peak height relative to the corrected baseline [21]. The peak height around 1,637 $cm^{-1}$, indicating the absorbance intensities of aliphatic C=C, was calibrated according to Rueggeberg *et al.* [21]. Absorbance at 1,637 and 1,510 $cm^{-1}$, corresponding to the aliphatic and aromatic C=C vibrations, respectively, was recorded (Figure 2). The aromatic band at 1,510 $cm^{-1}$ served as the internal reference [22]. The DC was calculated from the absorbance values of uncured and cured specimens using the equation 1 [4].

(1)

$$DC = \left(1 - \frac{[Abs(aliphatic)/\ Abs(aromatic)]cured}{[Abs(aliphatic)\ /\ Abs(aromatic)]uncured}\right) \times 100$$

### Evaluation of color change

Baseline color measurements ($T_0$) of the post-polymerized specimens were obtained using a VITA Easyshade V digital spectrophotometer (VITA Zahnfabrik, Bad Säckingen, Germany). In accordance with the Commission Internationale de l'Éclairage (CIE) system, the primary color parameters (L*, a*, b*) of each specimen were measured three times against a white background within a light box illuminated by D65 lighting, and the mean values were subsequently calculated. The L* value represents the black/white color range (lightness), a* represents the red (+)/green (–) color range, and b* represents the yellow (+)/blue (–) color range [14].

Specimens that underwent baseline ($T_0$) color measurements were marked on their bottom surfaces and individually immersed in light-proof amber bottles containing coffee solution for 14 days. To prepare the coffee solution, 2 g of coffee (Nescafé Classic; Nestlé, Barcelona, Spain) was dissolved in 200 mL of boiling water, which was subsequently cooled to ambient temperature prior to application. The solution was renewed daily. Prior to each solution change, samples underwent a 60-second rinse using distilled water to eliminate surface residues. Ertaş *et al.* [23] reported that a 7-day coffee immersion simulated approximately 7 months of coffee consumption. Furthermore, given that the

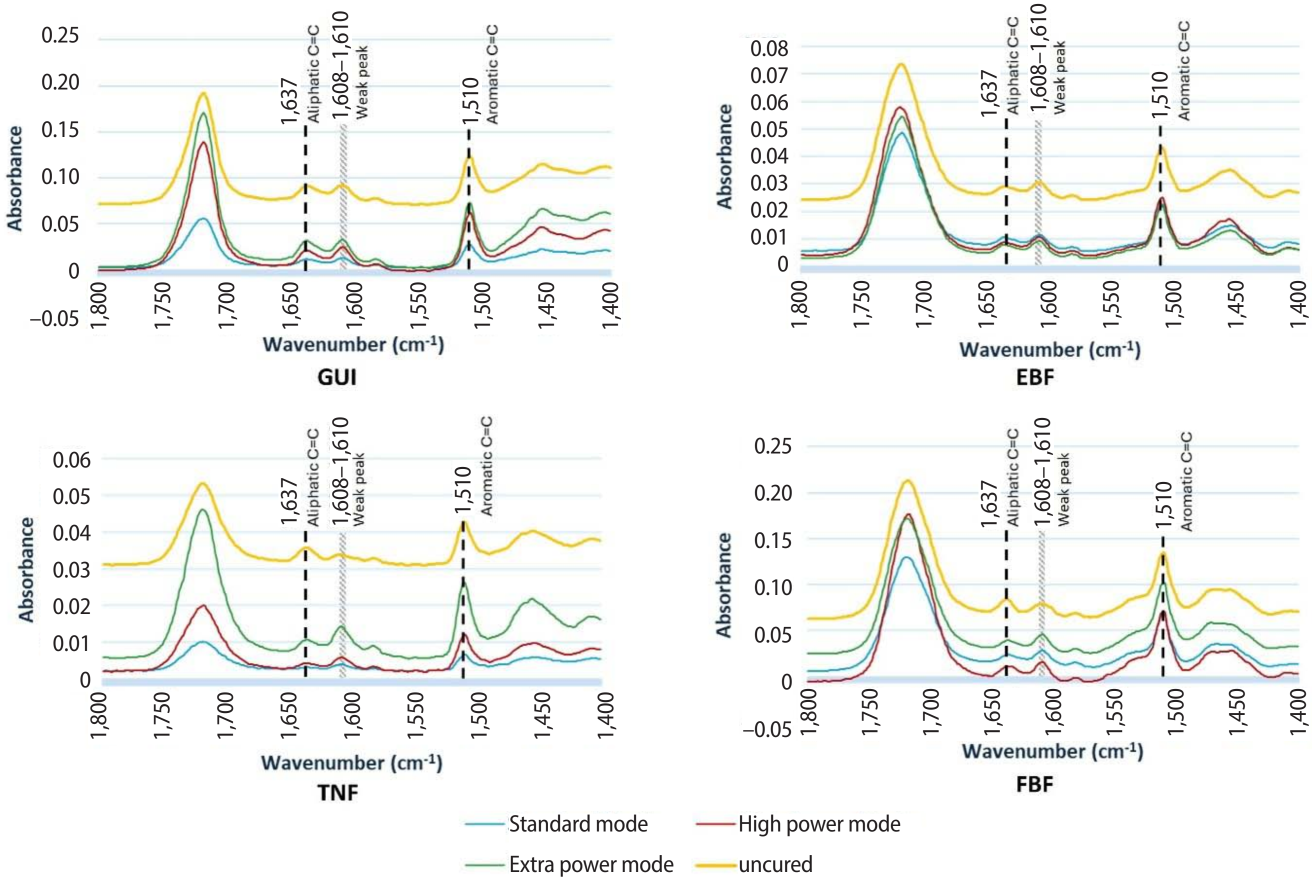


**Figure 2.** Representative FTIR (Fourier-transform infrared) spectra of materials under different curing modes, showing the average absorbance curves. Two reference peaks are indicated: 1,510 $cm^{-1}$ (internal standard aromatic carbon double bond, C=C) and 1,637 $cm^{-1}$ (methacrylate C=C). Material abbreviations and manufacturer information are provided in Table 1.

actual contact time of coffee with oral tissues is shorter during drinking, the 14-day coffee immersion used in this study represents a longer period than 14 months of actual coffee consumption. Color measurements were repeated on day 7 ($T_1$) and day 14 ($T_2$). Color variation (CIEDE2000, $\Delta E_{00}$) was determined using the equation 2 [24].

(2)

$$\Delta E_{00} = \sqrt{\left(\frac{\Delta L}{K_L S_L}\right)^2 + \left(\frac{\Delta C}{K_C S_C}\right)^2 + \left(\frac{\Delta H}{K_H S_H}\right)^2 + R_T\left(\frac{\Delta C}{K_C S_C}\right)\left(\frac{\Delta H}{K_H S_H}\right)}$$

In this formula, $\Delta L$ represents the change in lightness, $\Delta C$ the change in chroma, and $\Delta H$ the change in hue. $S_L$, $S_C$, and $S_H$ are weighting functions used to calibrate for visual non-uniformity. The parametric factors for environmental correction, $K_L$, $K_C$, and $K_H$, were all set to 1. $R_T$ is a rotational function incorporated to compensate for the interaction between chroma and hue differences, particularly in the blue region of the color space.

Color change evaluation was based on a 50:50 perceptibility threshold ($\Delta E_{PT}$) set at 0.8 and a 50:50 acceptability threshold ($\Delta E_{AT}$) defined as 1.8 [24].

### Statistical analysis

Statistical analyses were performed using IBM SPSS ver. 21.0 (IBM Corp., Armonk, NY, USA) at a 95% confidence level ($p < 0.05$). The assumption of normality was tested using the Shapiro-Wilk test, and homogeneity of variances was assessed with the Levene test. The effects of material type and light-curing mode on DC were evaluated using two-way ANOVA. A three-way repeated-mea-


https://doi.org/10.5395/rde.2026.51.e35

sures ANOVA was conducted to evaluate the effects of material and light-curing mode as between-subjects factors, and time (two levels: day 7 and day 14) as the within-subjects factor on color change ($\Delta E_{00}$). Because the within-subjects factor consisted of only two levels, the sphericity assumption was inherently satisfied. One-way ANOVA was performed to compare differences among materials within each light-curing mode, as well as differences among light-curing modes within each material. For pairwise comparisons, Bonferroni or Dunnett's T3 *post hoc* tests were applied depending on the homogeneity of variances. The relationship between DC and $\Delta E_{00}$ was examined through the Pearson correlation and linear regression analyses.

## RESULTS

### Degree of conversion results

The DC results of the tested materials across different light-curing modes are presented in Table 2. A statistically significant difference in DC was found between light-curing modes for all materials except TNF ($p < 0.001$). The highest DC values were observed in the high-power curing mode for all tested materials. FBF exhibited the highest DC in the high-power mode (82.04 ± 9.04), while EBF showed the lowest DC in the standard power mode (43.34 ± 15.10). Polymerization of EBF in the standard mode resulted in significantly lower DC compared to other light-curing modes ($p < 0.05$). For GUI and FBF, the high-power mode produced significantly higher DC values than other curing modes ($p < 0.05$).

The differences in DC among the materials were statistically significant in the standard and high-power curing modes ($p < 0.001$), but not in the extra-power mode ($p = 0.224$). In the standard mode, FBF exhibited significantly higher DC values than GUI and EBF, and in the high-power mode, a statistically significant increase in DC values was observed in this material relative to the others ($p < 0.05$).

According to the two-way ANOVA results, material type, light-curing mode, and the interaction between material type and light-curing mode had a significant effect on the DC ($p < 0.001$) (Table 3).

### Color change results

The color change results of the tested materials across different light-curing modes on days 7 and 14 are presented in Table 4. On day 7, differences in $\Delta E_{00}$ between light-curing modes were not statistically significant for

**Table 2.** Degree of conversion (%) of tested materials in different light-curing modes

| Material | Light-curing mode | | | $\eta^2$ | $p$-value[a)] |
|---|---|---|---|---|---|
| | Standard | High-power | Extra-power | | |
| GUI | 58.79 ± 3.35$^{Aa}$ | 65.09 ± 3.75$^{Ba}$ | 55.81 ± 5.60$^{Aa}$ | 0.46 | <0.001 |
| EBF | 43.34 ± 15.10$^{Aa}$ | 65.41 ± 9.92$^{Ba}$ | 61.50 ± 6.43$^{Ba}$ | 0.45 | <0.001 |
| TNF | 50.57 ± 18.05$^{Aab}$ | 62.76 ± 3.58$^{Aa}$ | 59.08 ± 10.18$^{Aa}$ | 0.16 | 0.089 |
| FBF | 67.01 ± 5.11$^{Ab}$ | 82.04 ± 9.04$^{Bb}$ | 61.39 ± 3.11$^{Aa}$ | 0.68 | <0.001 |
| $\eta^2$ | 0.37 | 0.55 | 0.11 | | |
| $p$-value[a)] | 0.001 | <0.001 | 0.224 | | |

Material abbreviations and manufacturer information are provided in Table 1. Different superscript capital letters in rows and different superscript lowercase letters in columns indicate statistical significance.

[a)]Analyzed by one-way analysis of variance. $p < 0.05$, statistically significant.

**Table 3.** Two-way analysis of variance results for degree of conversion (%)

| Parameter | Sum of squares | df | Mean square | $F$-value | $p$-value | Partial $\eta^2$ | 95% CI for partial $\eta^2$ |
|---|---|---|---|---|---|---|---|
| Material type | 3,461.098 | 3 | 1,153.699 | 14.054 | <0.001 | 0.281 | 0.13–0.42 |
| Light-curing mode | 3,364.717 | 2 | 1,682.358 | 20.493 | <0.001 | 0.312 | 0.19–0.43 |
| Material type × light-curing mode | 2,921.571 | 6 | 486.928 | 5.931 | <0.001 | 0.203 | 0.03–0.41 |
| Error | 8,865.988 | 108 | 82.092 | | | | |

CI, confidence interval; df, degree of freedom.

https://doi.org/10.5395/rde.2026.51.e35

GUI ($p = 0.215$) and TNF ($p = 0.081$), whereas statistically significant differences were identified for EBF and FBF ($p < 0.001$). All materials showed lower $\Delta E_{00}$ values when cured with the high-power mode compared to other modes. The lowest $\Delta E_{00}$ was recorded for GUI in the high-power mode (1.76 ± 0.54), whereas the highest was observed for FBF in the extra-power mode (8.35 ± 1.06).

On day 14, differences in $\Delta E_{00}$ between light-curing modes were statistically significant for all materials except GUI ($p < 0.05$). Although $\Delta E_{00}$ increased over time ($p < 0.05$), the lowest value on day 14 was again observed for GUI in the high-power mode (2.83 ± 0.84). On both days 7 and 14, EBF exhibited significantly higher $\Delta E_{00}$ values in the extra-power mode in comparison with the other modes ($p < 0.05$), whereas FBF showed significantly lower $\Delta E_{00}$ values in the high-power mode in comparison with the others ($p < 0.05$).

At both time points, statistically significant differences in $\Delta E_{00}$ were found among the materials across all light-curing modes ($p < 0.001$).

The three-way repeated-measures ANOVA revealed significant effects of material type, light-curing mode, time, and their interactions on the $\Delta E_{00}$ of the tested materials ($p < 0.001$), except for the three-way interaction (time × material × light-curing mode), which was not significant ($p = 0.136$) (Table 5).

A significant negative association was observed between DC and $\Delta E_{00}$ values on day 7 ($\beta = -0.208$, $p = 0.023$) and day 14 ($\beta = -0.238$, $p = 0.009$). Furthermore, a strong positive correlation was found between the color

**Table 4.** Color change ($\Delta E_{00}$) of tested materials in different light-curing modes

| Light-curing mode | Standard | High-power | Extra-power | $\eta^2$ | $p$-value[a] |
|---|---|---|---|---|---|
| Day 7 | | | | | |
| GUI | $1.99 \pm 0.42^{Ab}$ | $1.76 \pm 0.54^{Ab}$ | $2.11 \pm 0.32^{Ab}$ | 0.10 | 0.215 |
| EBF | $3.88 \pm 0.48^{Aa}$ | $3.52 \pm 0.58^{Aa}$ | $5.58 \pm 0.74^{Ba}$ | 0.70 | <0.001 |
| TNF | $6.32 \pm 0.55^{Ac}$ | $6.08 \pm 0.53^{Ac}$ | $6.77 \pm 0.85^{Ac}$ | 0.16 | 0.081 |
| FBF | $7.74 \pm 0.74^{Ad}$ | $5.42 \pm 0.33^{Bd}$ | $8.35 \pm 1.06^{Ad}$ | 0.74 | <0.001 |
| $\eta^2$ | 0.94 | 0.92 | 0.90 | | |
| $p$-value[a] | <0.001 | <0.001 | <0.001 | | |
| Day 14 | | | | | |
| GUI | $3.10 \pm 0.53^{Ab}$ | $2.83 \pm 0.84^{Ab}$ | $3.61 \pm 0.88^{Ab}$ | 0.16 | 0.091 |
| EBF | $5.57 \pm 0.73^{Aa}$ | $5.02 \pm 0.71^{Aa}$ | $7.80 \pm 0.66^{Ba}$ | 0.76 | <0.001 |
| TNF | $8.02 \pm 0.50^{ABc}$ | $7.57 \pm 0.44^{Ac}$ | $8.71 \pm 0.99^{Ba}$ | 0.33 | 0.004 |
| FBF | $10.15 \pm 0.59^{Ad}$ | $7.31 \pm 0.50^{Bc}$ | $10.95 \pm 1.18^{Ac}$ | 0.80 | <0.001 |
| $\eta^2$ | 0.95 | 0.90 | 0.89 | | |
| $p$-value[a] | <0.001 | <0.001 | <0.001 | | |

Material abbreviations and manufacturer information are provided in Table 1. Different superscript capital letters in rows and different superscript lowercase letters in columns indicate statistical significance.
[a]Analyzed by one-way analysis of variance. $p < 0.05$, statistically significant.

**Table 5.** Three-way repeated-measures analysis of variance results for color change ($\Delta E_{00}$)

| Parameter | Sum of squares | df | Mean square | $F$-value | $p$-value | Partial $\eta^2$ | 95% CI for partial $\eta^2$ |
|---|---|---|---|---|---|---|---|
| Material type (M) | 1,153.197 | 3 | 384.399 | 464.944 | <0.001 | 0.928 | 0.90–0.95 |
| Light-curing mode (L) | 101.908 | 2 | 50.954 | 61.631 | <0.001 | 0.533 | 0.36–0.65 |
| M × L | 93.906 | 6 | 15.651 | 18.930 | <0.001 | 0.513 | 0.33–0.64 |
| Error | 89.291 | 108 | 0.827 | - | - | - | - |
| Time (T) | 186.208 | 1 | 186.208 | 1329.425 | <0.001[a] | 0.925 | 0.89–0.95 |
| T × M | 8.770 | 3 | 2.923 | 20.871 | <0.001[a] | 0.367 | 0.22–0.49 |
| T × L | 4.170 | 2 | 2.085 | 14.886 | <0.001[a] | 0.216 | 0.10–0.33 |
| T × M × L | 1.401 | 6 | 0.233 | 1.667 | 0.136[a] | 0.085 | 0.00–0.18 |
| Error (time) | 15.127 | 108 | 0.140 | - | - | - | - |

CI, confidence interval; df, degree of freedom.
[a]Sphericity assumed results are reported because the within-subjects factor includes only two time points (day 7, day 14).


https://doi.org/10.5395/rde.2026.51.e35

changes measured on days 7 and 14 ($r = 0.974$, $p < 0.001$) (Tables 6 and 7).

## DISCUSSION

The extent of polymerization, expressed as the DC, critically affects the performance and biocompatibility of resin composites. It is influenced by total energy input, which depends on irradiance and curing time [4]. However, no consensus exists on the optimal radiant exposure, as DC varies by material, making total energy-based protocols unreliable [11]. Manufacturers suggest that short, high-intensity exposures may be as effective as standard protocols. In this study, the DC and color changes of flowable bulk-fill composites polymerized using different light-curing modes—each involving varying energy densities and irradiation times—were investigated and compared with an injectable flowable composite resin. Results showed that both light-curing mode and material type significantly affected DC; therefore, the first null hypothesis of the study was refuted.

FTIR, a quantitative method used to measure DC, is considered the gold standard; however, the choice of reference peak may influence calculated conversion values. As an internal standard, the band at 1,608–1,610 $cm^{-1}$ representing the aromatic C=C absorption is commonly used [25]. The availability of this vibrational band depends on the presence of methacrylate monomers containing an aromatic core, such as bisphenol A glycidyl methacrylate (Bis-GMA) and bisphenol A dimethacrylate (Bis-EMA). In composites based on aliphatic monomers, e.g., urethane dimethacrylate (UDMA), the vibrational band at 1,608–1,610 $cm^{-1}$ is absent, and other alternative reference bands are used [25]. According to the manufacturer's Safety Data Sheet information, the tested material GUI contains only aliphatic monomers such as UDMA and triethylene glycol dimethacrylate (TEGDMA), and no aromatic monomer is specified. However, the literature reports that GUI may also contain aromatic dimethacrylates such as Bis-EMA [26]. In the uncured FTIR spectra obtained in this study, it was determined that no distinct peak was present in the 1,608–1,610 $cm^{-1}$ region for the tested materials, and that only very weak signals were observed in some samples. In contrast, the 1,510 $cm^{-1}$ band exhibited a more stable and stronger peak in all four materials (Figure 2). Therefore, the 1,510 $cm^{-1}$ region was preferred as the internal reference for the DC calculations.

Studies investigating the DC in bulk-fill composite resins show considerable methodological variability in terms of both measurement timing and the surface from which DC is assessed. In a network meta-analysis synthesizing the findings of *in vitro* studies, Hatipoğlu *et al.* [5] reported significant differences between top and bottom surface DC values when measured immediately after curing, whereas no significant difference was observed between the two surfaces when measurements were performed 24 hours post-curing. Since bottom-surface DC provides more meaningful and comparable information regarding curing efficiency among materials, DC measurements in the present study were performed on the bottom surfaces of the specimens and at 24 hours after curing. Additionally, to verify polymerization homogeneity, one representative specimen from each group was analyzed on both the top and bottom surfaces, and the top surface was found to exhibit approximately 1.5%–2% higher DC values.

**Table 6.** Pearson correlation analysis between DC and color change

| Variable | r | *p*-value |
|---|---|---|
| DC – $\Delta E_{00}$ (day 7) | −0.208* | 0.023 |
| DC – $\Delta E_{00}$ (day 14) | −0.238** | 0.009 |
| $\Delta E_{00}$ (day 7) – $\Delta E_{00}$ (day 14) | 0.974** | <0.001 |

DC, degree of conversion; $\Delta E_{00}$, color change; r, Pearson correlation coefficient. *$p < 0.05$ (2-tailed); **$p < 0.01$ (2-tailed).

**Table 7.** Linear regression analysis evaluating the association between DC and color change

| Dependent variable | Independent variable | β | SE | Standardized β | *p*-value | 95% CI |
|---|---|---|---|---|---|---|
| $\Delta E_{00}$ (day 7) | DC | −0.038 | 0.016 | −0.208 | 0.023 | −0.070 to −0.005 |
| $\Delta E_{00}$ (day 14) | DC | −0.051 | 0.019 | −0.238 | 0.009 | −0.089 to −0.013 |
| $\Delta E_{00}$ (day 14) | $\Delta E_{00}$ (day 7) | 1.155 | 0.025 | 0.974 | <0.001 | 1.106 to 1.204 |

β, regression coefficient; CI, confidence interval; DC, degree of conversion; $\Delta E_{00}$, color change; SE, standard error.

The present research found that while radiant exposures did not significantly differ between the three curing modes, the high-power mode produced greater DC in every material assessed. Similarly, in a study by Yenidünya *et al*. [27], which examined the effect of different light-curing modes on the DC in various materials, significantly higher DC values were reported under the high-power mode. The higher DC observed in the high-power mode may be attributed to the greater initial irradiance (1,400 mW/cm²) compared to the standard mode. This high irradiance could lead to a greater increase in exothermic heat within the polymeric matrix, enhancing the mobility of polymer chains and consequently increasing the DC [28]. However, relatively lower DC values were recorded in the extra-power mode. Very high irradiance combined with very short curing times accelerates radical generation at the beginning; however, the rapid weight gain leads to early vitrification, which restricts chain mobility. This condition alters the rate of bimolecular termination and, consequently, the final hardness/conversion depending on the material's depth profile [12]. The relatively low DC observed in the extra-power mode in this study may be attributed to the accelerated polymerization rate. On the other hand, in cases where the reaction proceeds at a normal rate, an increase in post-irradiation DC has been reported for most resin matrices [29]. After irradiation, polymerization continues depending on factors such as residual monomer content, cross-linking density, radical concentration, and radical lifetimes [30]. The high-power mode may have generated more free radicals by providing increased photon availability, enhancing post-irradiation polymerization [31].

The viscosity of materials is an important factor affecting the DC. Compared to high-viscosity materials, flowable resin-based bulk-fill composites contain a greater proportion of organic matrix, which may lead to a reduction in the refractive index [6]. The matrices of flowable resin-based composites consist of low molecular weight monomers characterized by increased flexibility and reactivity, which have been reported to augment the number of bonding sites during light curing, consequently improving the DC [6]. In the current study, FBF exhibited a higher DC compared to the other materials across all curing modes, with statistically significant differences noted specifically in the standard and high-power curing modes. FBF contains Bis-GMA, TEGDMA, Bis-EMA, and a procrylate monomer. The procrylate monomer is a high molecular weight monomer similar to Bis-GMA; however, it does not contain pendant hydroxyl groups that contribute to increased viscosity [32]. Dental polymers incorporating Bis-EMA and urethane-based monomers with lower viscosity have been demonstrated to achieve higher DC values relative to conventional Bis-GMA/TEGDMA resins [32]. This may account for the elevated DC observed in FBF relative to the other flowable materials.

Highly translucent resin-based composites offer better curing efficiency due to greater light transmission through the material, allowing light to reach deeper layers [3]. The relatively low DC observed in TNF compared to the other materials may be attributed to its lower translucency. Although TNF contains a photoinitiator system (Ivocerin; Ivoclar Vivadent) that exhibits higher curing activity by absorbing visible light at a wider wavelength range than germanium-based camphorquinone (CQ), it does not fully compensate for the reduced translucency in deeper layers. This finding is consistent with the study by Ilie *et al*. [33].

Although GUI, an injectable composite, is not a bulk-fill composite, it is frequently used in clinical practice at thicknesses exceeding 2 mm. In the present study, considering these clinical conditions, GUI specimens were prepared at a thickness of 4 mm to evaluate critical thresholds for DC. Although there is no consensus on a minimum DC value, values between 55%–65% are generally considered critical for mechanical performance [11]. Notably, this range reflects unreacted C=C bonds, not unpolymerized monomers [15]. GUI showed acceptable DC (55%–65%) despite exceeding the recommended thickness. In contrast, EBF and TNF under standard mode exhibited DC below this range, suggesting suboptimal polymerization. Given that curing efficiency varies with monomer type [34], high-power mode may be more appropriate for EBF and TNF. It should also be noted that due to vitrification or gelation, DC rarely reaches 100% [35].

The present study demonstrated that color change was significantly affected by light-curing mode, material type, and time (Table 5), leading to the rejection of the


https://doi.org/10.5395/rde.2026.51.e35

study's second null hypothesis. The best performance in terms of color stability was observed in specimens polymerized with the high-power mode, while groups cured for shorter durations using the extra-power mode exhibited greater color change. During prolonged polymerization, increased light penetration into deeper layers—similar to that at the beginning of irradiation—explains the limitations of the short exposures in the extra-power mode [12]. The unstable resin matrix and reduced DC caused by the short exposure may contribute to increased discoloration of the materials.

In dental composites, CQ and tertiary amines—used as co-initiators to enhance free radical generation—constitute the most common photoinitiator system [36]. To reduce the disadvantages of this photoinitiator, such as weak bleaching properties, yellowish staining, and toxicity, Rap Technology (radical amplified photopolymerization; Tokuyama Dental), which recycles CQ during initiator production, has been developed [36]. The lower color change observed in EBF compared to FBF can be explained by its reduced CQ content due to Rap Technology. Across all curing modes, GUI exhibited less color change than the other materials, which may be attributed to the full-coverage silane coating technology claimed by the manufacturer to enhance filler-matrix bonding [37].

Staining of composite resins is influenced by the polishing protocol and the resulting surface roughness [38]. Because the presence of water during polishing makes it difficult to accurately assess surface texture and gloss, several authors have recommended dry polishing [39]. In addition, immediate finishing and polishing may lead to plastic deformation, as the material has not yet reached its final hardness due to ongoing polymerization. For this reason, postponing finishing and polishing for 24 hours after light curing has been suggested [38], and the same approach was followed in the present study. However, the heat generated during dry finishing and polishing may cause degradation at the filler-matrix interface or microcrack formation, potentially contributing to increased discoloration. These factors should be considered when interpreting acceptability thresholds, as *in vitro* protocols may not fully replicate clinical conditions. Clinically, perceptibility ($\Delta E_{00}$ = 0.8) and acceptability ($\Delta E_{00}$ = 1.8) thresholds are critical benchmarks for esthetic performance [24]. In this study, all groups exceeded the perceptibility threshold after 7 and 14 days of coffee immersion. On day 7, only GUI polymerized in high-power mode remained within the acceptability limit, whereas all groups surpassed it by day 14. Although continuous coffee exposure without saliva or brushing likely intensified staining, these results highlight that both material formulation and curing parameters directly affect long-term esthetic stability.

Staining of composites is affected by surface roughness, filler characteristics, and the hydrophilicity of the resin matrix [40]. Nanofill composites, with smaller particles, offer smoother surfaces, reduced water absorption, and better filler-matrix integration [41,42]. In this study, GUI, which showed the least color change, is a nanofill composite, while FBF, which exhibited the highest discoloration, is a microhybrid composite. The findings of the present study are in agreement with those reported by Gürdal *et al.* [43].

Materials exhibiting a high DC demonstrate reduced deformation due to increased polymer chain entanglement and elevated cross-linking density, which collectively constrain molecular mobility within the polymeric network [5]. Composites with lower DC release greater amounts of unreacted monomers, such as Bis-GMA and TEGDMA, which may diffuse toward the pulp and induce cytotoxic or inflammatory responses. Moreover, residual monomers can undergo oxidative and hydrolytic degradation, accelerating color instability and surface deterioration [15]. As reported by Sham *et al.* [44], chemical discoloration is primarily attributed to the oxidation of the polymer matrix, the oxidation of residual monomer double bonds that remain unreacted, and the formation of degradation products induced by water diffusion. In the present study, the observed negative correlation between DC and $\Delta E_{00}$ supports that insufficient polymerization may contribute to greater color change in resin composites.

A key limitation of this study is that the 1,510 $cm^{-1}$ band used as the internal reference does not represent a single, chemically isolated vibrational mode. In composites containing Bis-GMA/Bis-EMA, this region primarily reflects the aromatic ring C=C stretching vibration, but it also receives measurable contributions from aromatic C–H in-plane bending. In UDMA-based systems, additional overlap from the amide II mode (a combination of N–H bending and C–N stretching) may further broaden this band [45]. Therefore, the 1,510 $cm^{-1}$ signal should not be interpreted as a structurally invariant and "chemically clean" reference band in the same sense as the conventional 1,608–1,610 $cm^{-1}$ aromatic stretching peak.

Al-Zain *et al*. [46] evaluated both dry and wet storage conditions in terms of DC and reported that, under wet storage, the intermolecular bonds within the polymer system were softened due to the hydrolytic effect of water, resulting in a tendency toward reduced DC. The dry storage condition adopted in the present study to avoid potential FTIR spectral alterations related to water absorption may not fully simulate the clinical scenario in which dental materials are placed and may yield comparatively higher DC values. The use of a single light-curing unit represents another limitation, as potential radiometric inaccuracies and directional variations in light output at a 4-mm depth could have influenced the results. Additionally, the lack of a distilled water control group and a non-polished comparison group limited the ability to distinguish water absorption and surface effects from those caused by staining solutions. Future studies including a distilled water control group, various staining solutions, a non-polished comparison group, thermal aging, simulated brushing, and DC variations after coffee staining in relation to optical properties would enhance clinical relevance and clarify the mechanisms underlying color changes.

## CONCLUSIONS

Within the limitations of this study, the different light-curing modes significantly affected both the DC and the discoloration behavior of the flowable composites. Although the extra-power mode shortens curing time, it may lead to a reduction in DC and an increase in discoloration. The discoloration of the tested composites progressed over time, and color stability was influenced not only by DC but also by the material type and its chemical composition. Clinically, these findings suggest that using excessively high curing intensities for short durations may compromise the long-term color stability and polymerization quality of flowable composites. Therefore, clinicians should balance curing efficiency with adequate polymerization to optimize the esthetic longevity of restorations.

### CONFLICT OF INTEREST

No potential conflict of interest relevant to this article was reported.

### FUNDING/SUPPORT

The financial support of this study was provided by Ordu University Scientific Research Projects Coordination Unit with project number B-2340.

### ACKNOWLEDGMENTS

The authors would like to thank the Scientific and Technological Research Center of Inonu University for their support in the FTIR analysis.

### AUTHOR CONTRIBUTIONS

Conceptualization, Data curation, Funding acquisition, Investigation, Project administration, Resources, Software, Supervision: Karaaslan E, Karademir SA; Formal analysis, Validation: Karademir SA; Methodology, Visualization: Karaaslan E; Writing - original draft: Karaaslan E, Karademir SA; Writing - review & editing: Karaaslan E, Karademir SA. All authors read and approved the final manuscript.

### DATA SHARING STATEMENT

The entirety of the data analyzed in this study has been included in the published article. The datasets used and/or analyzed during the current study are available from the corresponding author on reasonable request.

### DISCLOSURE OF GENERATIVE AI IN SCIENTIFIC WRITING

Artificial intelligence was used solely to assist with the language editing of this article.

## REFERENCES

1. Van Ende A, De Munck J, Lise DP, Van Meerbeek B. Bulk-fill composites: a review of the current literature. J Adhes Dent 2017;19:95-109.
2. Arbildo-Vega HI, Lapinska B, Panda S, Lamas-Lara C, Khan AS, Lukomska-Szymanska M. Clinical effectiveness of bulk-fill and conventional resin composite restorations: systematic review and meta-analysis. Polymers (Basel) 2020;12:1786.
3. Salgado VE, Rego GF, Schneider LF, Moraes RR, Cavalcante


https://doi.org/10.5395/rde.2026.51.e35

LM. Does translucency influence cure efficiency and color stability of resin-based composites? Dent Mater 2018;34:957-966.
4. Al-Ahdal K, Ilie N, Silikas N, Watts DC. Polymerization kinetics and impact of post polymerization on the degree of conversion of bulk-fill resin-composite at clinically relevant depth. Dent Mater 2015;31:1207-1213.
5. Hatipoğlu Ö, Par M, Pertek Hatipoğlu F. Comparison of degree of conversion performance of bulk-fill resin composites: a systematic review and network meta-analysis of in vitro studies. J Dent 2024;149:105289.
6. Lima RB, Troconis CC, Moreno MB, Murillo-Gómez F, De Goes MF. Depth of cure of bulk fill resin composites: a systematic review. J Esthet Restor Dent 2018;30:492-501.
7. Sousa-Lima RX, Silva L, Chaves L, Geraldeli S, Alonso R, Borges B. Extensive assessment of the physical, mechanical, and adhesion behavior of a low-viscosity bulk fill composite and a traditional resin composite in tooth cavities. Oper Dent 2017;42:E159-E166.
8. Ajaj RA, Farsi NJ, Alzain L, Nuwaylati N, Ghurab R, Nassar HM. Dental bulk-fill resin composites polymerization efficiency: a systematic review and meta-analysis. J Compos Sci 2021;5:149.
9. Torres CR, Prado TP, Ávila DM, Pucci CR, Borges AB. Influence of light-curing time and increment thickness on the properties of bulk fill composite resins with distinct application systems. Int J Dent 2024;2024:2123406.
10. Burrer P, Par M, Fürer L, Stübi M, Marovic D, Tarle Z, *et al*. Effect of polymerization mode on shrinkage kinetics and degree of conversion of dual-curing bulk-fill resin composites. Clin Oral Investig 2023;27:3169-3180.
11. Parra Gatica E, Duran Ojeda G, Wendler M. Contemporary flowable bulk-fill resin-based composites: a systematic review. Biomater Investig Dent 2023;10:8-19.
12. Lempel E, Szebeni D, Őri Z, Kiss T, Szalma J, Lovász BV, *et al*. The effect of high-irradiance rapid polymerization on degree of conversion, monomer elution, polymerization shrinkage and porosity of bulk-fill resin composites. Dent Mater 2023;39:442-453.
13. Czasch P, Ilie N. In vitro comparison of mechanical properties and degree of cure of bulk fill composites. Clin Oral Investig 2013;17:227-235.
14. Tekçe N, Tuncer S, Demirci M, Serim ME, Baydemir C. The effect of different drinks on the color stability of different restorative materials after one month. Restor Dent Endod 2015;40:255-261.
15. Durner J, Obermaier J, Draenert M, Ilie N. Correlation of the degree of conversion with the amount of elutable substances in nano-hybrid dental composites. Dent Mater 2012;28:1146-1153.
16. Silva MF, Dias MF, Lins-Filho PC, Silva CH, Guimarães RP. Color stability of bulk-fill composite restorations. J Clin Exp Dent 2020;12:e1086-e1090.
17. Misilli T, Gönülol N. Water sorption and solubility of bulk-fill composites polymerized with a third generation LED LCU. Braz Oral Res 2017;31:e80.
18. Chen S, Zhu J, Yu M, Jin C, Huang C. Effect of aging and bleaching on the color stability and surface roughness of a recently introduced single-shade composite resin. J Dent 2024;143:104917.
19. Gömleksiz S, Gömleksiz O. The effect of contemporary finishing and polishing systems on the surface roughness of bulk fill resin composite and nanocomposites. J Esthet Restor Dent 2022;34:915-923.
20. Heintze SD, Reinhardt M, Müller F, Peschke A. Press-on force during polishing of resin composite restorations. Dent Mater 2019;35:937-944.
21. Rueggeberg FA, Hashinger DT, Fairhurst CW. Calibration of FTIR conversion analysis of contemporary dental resin composites. Dent Mater 1990;6:241-249.
22. Ömeroğlu MK, Ertaş E. Effect of layer thickness on conversion degree and microhardness of bulk-fill composites. Essent Dent 2025;4:1-8.
23. Ertaş E, Güler AU, Yücel AC, Köprülü H, Güler E. Color stability of resin composites after immersion in different drinks. Dent Mater J 2006;25:371-376.
24. Paravina RD, Ghinea R, Herrera LJ, Bona AD, Igiel C, Linninger M, *et al*. Color difference thresholds in dentistry. J Esthet Restor Dent 2015;27 Suppl 1:S1-S9.
25. Tarle Z, Par M. Degree of conversion. In: Miletic V, editor. Chapter 5. Dental composite materials for direct restorations. Cham: Springer International Publishing; 2018. p. 63-85.
26. Çarıkçıoğlu B, Ay Şimşek İ, Arıkan V, Sarıyılmaz E. Color stability of a novel self-cure bulk-fill composite compared to light-cure bulk-fill and injectable composite resins. BMC Oral Health 2025;25:1478.
27. Yenidünya ÖG, Erdem A, Akgül N, Yazkan B, Özcan M. Influence of preheating procedure and polymerization modes on degree of conversion of contemporary resin composites.

Curr Res Dent Sci 2025;35:65-70.
28. Calheiros FC, Kawano Y, Stansbury JW, Braga RR. Influence of radiant exposure on contraction stress, degree of conversion and mechanical properties of resin composites. Dent Mater 2006;22:799-803.
29. Vouvoudi EC. Overviews on the progress of flowable dental polymeric composites: their composition, polymerization process, flowability and radiopacity aspects. Polymers (Basel) 2022;14:4182.
30. Ilie N, Jelen E, Hickel R. Is the soft-start polymerisation concept still relevant for modern curing units? Clin Oral Investig 2011;15:21-29.
31. da Silva EM, Poskus LT, Guimarães JG. Influence of light-polymerization modes on the degree of conversion and mechanical properties of resin composites: a comparative analysis between a hybrid and a nanofilled composite. Oper Dent 2008;33:287-293.
32. Tarle Z, Attin T, Marovic D, Andermatt L, Ristic M, Tauböck TT. Influence of irradiation time on subsurface degree of conversion and microhardness of high-viscosity bulk-fill resin composites. Clin Oral Investig 2015;19:831-840.
33. Ilie N, Keßler A, Durner J. Influence of various irradiation processes on the mechanical properties and polymerisation kinetics of bulk-fill resin based composites. J Dent 2013;41:695-702.
34. Łagocka R, Jakubowska K, Chlubek D, Buczkowska-Radlińska J. The influence of irradiation time and layer thickness on elution of triethylene glycol dimethacrylate from SDR(r) bulk-fill composite. Biomed Res Int 2016;2016:3481723.
35. Cramer NB, Stansbury JW, Bowman CN. Recent advances and developments in composite dental restorative materials. J Dent Res 2011;90:402-416.
36. Kowalska A, Sokolowski J, Gozdek T, Krasowski M, Kopacz K, Bociong K. The influence of various photoinitiators on the properties of commercial dental composites. Polymers (Basel) 2021;13:3972.
37. Ranka S, Rao AS, Shah U, Solanki D, Pawar AM, Reda R, *et al*. Comparative evaluation of two different fiber-reinforced composite materials in class 1 post-endodontic restorations in molars: a randomized clinical study. Materials (Basel) 2022;15:7858.
38. Molaei M, Mohammadzadeh A, Ghasemi A, Badiee M. Effect of dry and wet finishing and polishing on color change and opacity of nanofill and nanohybrid composites. BMC Oral Health 2024;24:287.
39. Yap AU, Sau CW, Lye KW. Effects of finishing/polishing time on surface characteristics of tooth-coloured restoratives. J Oral Rehabil 1998;25:456-461.
40. Nasoohi N, Hoorizad M, Torabzadeh Tari N. Effect of tea and coffee on color change of two types composite resins: nano filled and micro hybrid. J Res Dent Sci 2011;7:18-22.
41. Nasim I, Neelakantan P, Sujeer R, Subbarao CV. Color stability of microfilled, microhybrid and nanocomposite resins: an in vitro study. J Dent 2010;38 Suppl 2:e137-e142.
42. Yu B, Lim HN, Lee YK. Influence of nano-and micro-filler proportions on the optical property stability of experimental dental resin composites. Mater Des 2010;31:4719-4724.
43. Gürdal P, Akdeniz BG, Hakan Sen B. The effects of mouthrinses on microhardness and colour stability of aesthetic restorative materials. J Oral Rehabil 2002;29:895-901.
44. Sham AS, Chu FC, Chai J, Chow TW. Color stability of provisional prosthodontic materials. J Prosthet Dent 2004;91:447-452.
45. Guerra RM, Durán I, Ortiz P. FTIR monomer conversion analysis of UDMA-based dental resins. J Oral Rehabil 1996;23:632-637.
46. Al-Zain AO, Piva E, Pimentel AH, Duarte CG, Valente LL, Isolan CP, *et al*. Impact of storage conditions on the fracture reliability and physical properties of a dental resin-based composite. Braz Oral Res 2024;38:e062.


https://doi.org/10.5395/rde.2026.51.e35

RDE Restorative Dentistry & Endodontics

Research Article

eISSN 2234-7666
Restor Dent Endod. 2026 August;51(3):e37
https://doi.org/10.5395/rde.2026.51.e37

# Influence of occlusal reduction on postoperative pain following single-visit root canal treatment in mandibular molars: a randomized controlled trial

Sathvika Kanesalingavelan, Geeth Deepika KG, Anand Sherwood I*, Pavithra Chandrasekaran, Azhagu Abirami A

CSI College of Dental Sciences and Research, Madurai, Tamil Nadu, India

## ABSTRACT

**Objectives:** Postoperative pain is a frequent complication following root canal treatment, and occlusal reduction (OR) has been suggested as a means to minimize such discomfort. However, existing evidence regarding its effectiveness remains inconclusive. This study aimed to evaluate the influence of OR on postoperative pain following single-visit root canal treatment in mandibular molars. It also examined whether preoperative pain intensity affects the postoperative response to OR.

**Methods:** A total of 280 eligible patients with irreversible pulpitis in their first or second mandibular molars were enrolled and stratified into four groups based on their preoperative pain intensity using the visual analogue scale (VAS): 0, no pain; 1–3, mild; 4–7, moderate; and 8–10, severe. Each group was further allocated into OR or no occlusal reduction (NOR) subgroups using block randomization. Standardized endodontic procedures were performed under rubber dam isolation. Postoperative pain was recorded at 24 hours, 48 hours, and 1 week using the same VAS scale. Data were analyzed using the chi-square tests ($p \leq 0.05$).

**Results:** Overall, a statistically significant difference between OR and NOR was found at the 48-hour interval, favoring OR. Stratified analysis showed significant pain reduction at 24 hours in the moderate pain category and near-significant differences in the severe pain group at both 24 hours and 48 hours.

**Conclusions:** OR reduced early postoperative pain most noticeably in patients presenting with moderate to severe preoperative pain, whereas its effect was minimal in asymptomatic or mildly symptomatic cases.

**Keywords:** Occlusal reduction; Postoperative pain; Randomized controlled trial; Root canal therapy; Visual analogue scale

**Received:** November 28, 2025 **Revised:** January 31, 2026 **Accepted:** March 3, 2026

**Citation**
Kanesalingavelan S, Deepika KG G, Sherwood IA, Chandrasekaran P, Abirami AA. Influence of occlusal reduction on postoperative pain following single-visit root canal treatment in mandibular molars: a randomized controlled trial. Restor Dent Endod 2026;51(3):e37.

***Correspondence to**
Anand Sherwood I, MDS, PhD
Department of Conservative Dentistry and Endodontics, CSI College of Dental Sciences and Research, 29 CMH Compound, E Veli St, Madurai, Tamil Nadu 625001, India
Email: anand.sherwood@gmail.com

## INTRODUCTION

Postoperative pain following root canal treatment (RCT) remains a frequent and significant concern in endodontic practice, with incidence rates reported from 25% to 40% [1,2]. Although the primary goal of endodontic therapy is to eliminate infection and preserve the tooth in a symptom-free state, postoperative discomfort can substantially affect patient satisfaction and the perceived success of treatment [3]. So it is no overstatement when Gupta *et al.* [4] postulated that 'patients might regard postoperative pain and flare-ups as a yardstick by which the operator's abilities are assessed.' Consequently, understanding and minimizing postoperative pain has become an imperative aspect of evidence-based endodontic care.

Single-visit root canal treatment has gained wide clinical acceptance because of its advantages, including reduced chair time, fewer interappointment flare-ups, and greater patient convenience [5–7]. However, since instrumentation, irrigation, obturation, and occlusal loading all occur within a single appointment, the risk of postoperative pain may be influenced by multiple procedural and biological factors occurring in close succession.

Postoperative endodontic pain is multifactorial. It results primarily from acute periapical inflammation triggered by mechanical, chemical, or microbial irritation beyond the apical foramen [8], leading to the release of inflammatory mediators such as prostaglandins, bradykinin, and leukotrienes [9]. Procedural factors including extrusion of debris, over instrumentation, irrigation dynamics, and obturation protocols have all been associated with varying degrees of postoperative discomfort [10].

Among procedural variables, occlusal load has long been proposed to influence postoperative pain. Occlusal reduction (OR) involves the deliberate removal of occlusal contacts—both in centric occlusion and excursive movements—to decrease mechanical loading on a treated tooth. The principle is that after root canal therapy, periapical tissues can become inflamed and sensitized. Therefore, excessive occlusal force may exacerbate this inflammation by mechanically stimulating nociceptors present in the periodontal ligament. OR may also decrease the pressure caused by the inflamed periapical tissues, alleviating the effect of mechanical allodynia [11]. In this context, OR may also be viewed as a form of mechanical or occlusal "unloading," whereby functional occlusal forces transmitted to inflamed periapical tissues are temporarily minimized to reduce postoperative discomfort.

Despite its clinical rationale, the literature remains inconclusive regarding the true benefit of OR. Some authors have reported a significant reduction in postoperative pain [12–14], while others have found no meaningful difference between reduced and unreduced groups [15–17]. This literary equipoise highlights the need for further well-designed clinical trials to clarify whether OR genuinely influences postoperative pain or if it is a myth perpetuated by tradition.

Accordingly, the present study primarily aims to evaluate the influence of OR on postoperative pain following single-visit RCT in mandibular first and second molars with asymptomatic and symptomatic irreversible pulpitis. Its secondary objective is to determine whether preoperative pain intensity affects postoperative pain outcomes and if occlusal relief influences it. The null hypothesis reads as: 'OR has no statistically significant influence on postoperative pain following single-visit RCT, irrespective of preoperative pain intensity.'

## METHODS

This was a single-blinded, prospective, randomized, parallel-group, single-center clinical trial conducted in the Postgraduate Clinic of the Department of Conservative Dentistry and Endodontics at CSI College of Dental Sciences & Research, between February 2025 and October 2025. The study followed the ethical principles of the latest version of the Declaration of Helsinki (2024) and was designed and reported in compliance with the updated CONSORT 2025 guidelines for randomized clinical trials [18]. This study received approval from the Institutional Ethics Committee (CSICDSR/IEC/0301/2024) and was prospectively registered with the Clinical Trials Registry of India (CTRI/2025/01/079047).


https://doi.org/10.5395/rde.2026.51.e37

### Sample size calculation

The sample size was calculated using G*Power software for Windows (ver. 3.1.9.7) with a medium standardized effect size (Cohen's d = 0.50), an α-error probability of 0.05, a power of 0.95, and an allocation ratio = 1 [19], giving us a recommended size of 210 with 105 participants in each group. After accounting for the possibility of dropouts, a final sample size of 280 with 140 participants for each type of intervention was determined.

### Participants and eligibility criteria

Patients who met the following inclusion and exclusion criteria were recruited after obtaining written informed consent. All the participants were required to be able to comprehend and utilize a 10-point visual analogue scale (VAS) for pain assessment and be willing to verbally communicate their symptoms and how they were feeling.

**1. Inclusion criteria**

- Systemically healthy adult patients aged 18–70 years (American Society of Anesthesiologists physical status classification [ASA] I and II)
- Mandibular first and second molars diagnosed with asymptomatic or symptomatic irreversible pulpitis
- Periapical index (PAI) score ≤ 2
- Patients providing informed consent and willing to comply with follow-up
- Patients requiring and willing to receive full coverage crowns following RCT

**2. Exclusion criteria**

- Immunocompromised or systemically compromised patients (ASA > II)
- Re-RCTs or intentional RCTs
- Teeth lacking opposing dentition and with significant malocclusions like crossbite, scissor bite, deep bite, etc.
- Teeth with insufficient occlusal height, where OR would be detrimental to the tooth's dimensions
- Severely curved (>30°) or aberrant root morphology
- Pregnant or lactating women
- Patients with allergies to any of the materials used in the study
- Bruxism or parafunctional habits contributing to excessive occlusal load and lost vertical dimension

If patients were initially recruited for the study but clinically required two visits for precise/sufficient management, they were excluded from the study. New patients were then recruited to replace them.

### Preoperative assessment and stratification

Demographic details and idiosyncrasies were recorded for each eligible patient. Baseline pain intensity was scored using a modified 10-point VAS before local anesthesia was administered on the day of the procedure. Based on their preoperative VAS scores, 280 patients were stratified into four groups: no pain (VAS 0, $n = 70$), mild pain (VAS 1–3, $n = 70$), moderate pain (VAS 4–7, $n = 70$), and severe pain (VAS 8–10, $n = 70$).

These groups were further divided into two subgroups each: OR ($n = 35$) and no OR (NOR) ($n = 35$), such that both interventions were given to every type of preoperative pain category. Across all four groups, there was a total of 140 participants who received the intervention and 140 who did not receive the intervention.

### Randomization and blinding

Patients were recruited into each group based on their preoperative VAS. Further allocation into their intervention group (OR or NOR) was done via block randomization. The randomization sequence was generated using a computer-based random number generation software (Random Allocation Software ver. 2.0) by an independent researcher who was not involved in the clinical procedure or data analysis. The operator who performed all the procedures was aware of the assigned intervention, whereas both the participants and the researcher interviewing them after the procedure remained blinded, rendering the study single-blinded in design.

### Root canal procedure

All the procedures were completed by a single, experienced operator. Single-visit RCT was initiated after administering 1.8 mL of 2% lignocaine with 1:80,000 adrenaline (Lignox; Warren Pharmaceuticals Pvt Ltd., Mumbai, India). Following rubber dam isolation, access opening was done using sterile burs from the Mani Endo Access Diamond Bur kit (MANI Inc., Tochigi, Japan). If patients reported any pain or discomfort during the procedure, they were administered either supplemental injections (intrapulpal or intraligamentary) or an additional inferior alveolar nerve block.

The working length was established using E-Pex Apex Locator (Eighteeth, Changzhou, China) with size #10 K files (MANI Inc.) and was cross-verified radiographically. Initial glide path preparation was performed manually until sizes #20 K or #25 K files. Canal lubrication and smear layer removal were obtained using ethylenediaminetetraacetic acid 10% and carbamide peroxide 15% (Endoprep RC; Anabond Stedman Pharmaceuticals, Chennai, India). Biomechanical preparation was performed using Woodpecker EndoPace Brushless Endomotor (IDS Denmed, New Delhi, India) and the NeoEndo S rotary file system (Orikam Healthcare India Pvt. Ltd., Gurgaon, India) until a size of 25/0.06, 0.5 mm short of the apex.

Intermittent irrigation was performed using copious amounts of saline mixed with 2% w/v povidone-iodine (Puradine; Leeford Healthcare Ltd., Mumbai, India) through a 25-gauge beveled needle (Dispo Van; Hindustan Syringes and Medical Devices, New Delhi, India), positioned 1–2 mm short of the working length, with a controlled flow rate of approximately 1 mL/min to reduce the likelihood of apical debris extrusion. After final irrigation, the canals were dried with paper points and obturated with 25/0.06 single cone Neoendo Gutta Percha Points (Orikam Healthcare India Pvt. Ltd.) and zinc oxide eugenol sealer. The gutta-percha was sheared, and the chamber was dried and disinfected to receive the final post-endodontic restoration.

### Occlusal reduction protocol

Post-endodontic restoration of the cavity was done using the Te-Econom Plus composite system (Ivoclar Vivadent AG, Schaan, Liechtenstein). Participants in the OR group of every preoperative pain category received a standardized reduction of approximately 1.5–2 mm using a high-speed handpiece and an SF-13 bur (Frank Dental GmbH, Hainburg, Germany) under continuous water coolant. The range was to ensure that all the cusps (both functional and nonfunctional cusps, as well as the marginal ridges) were not in contact during both centric and excursive movements. The amount of reduction was cross-verified using the sizes 1.5 mm (blue) and 2.0 mm (green) from the autoclavable MiK PrepGauge Silicone Strips kit (MiK Dental, Mumbai, India). The reduction almost mimicked a crown preparation clearance. All the participants who received OR were recalled according to their convenience after a minimum of 2 weeks, for crown preparation and the placement of full coverage crowns.

### No occlusal reduction protocol

Post-endodontic restoration of the cavity was done until cuspal contacts and anatomy were completely re-established using the same composite system. The restoration was checked for iatrogenic high points and then polished. To ensure that all the patients in every preoperative pain category who received NOR were unaware whether their teeth had been reduced or not, a high-speed handpiece with copious amounts of water was activated inside the patient's mouth without contacting the occlusal surface to simulate the procedure used in the OR group. If iatrogenic high points were present, their elimination was sufficient to recreate the same. If the patients in this category also required full coverage crowns owing to mutilated preoperative clinical conditions, they were recalled after 2 weeks for crown preparation.

### Outcome measures

Pain levels were recorded at 24 hours, 48 hours, and 1 week posttreatment using the same 10-point VAS via structured telephonic interviews. Each patient was reminded of the scale before rating their pain. The nature of pain and a trigger factor (if any) was also recorded and categorized as spontaneous continuous, spontaneous occasional, and stimulus-based (during mastication or thermal stimuli).

All patients were prescribed ketorolac 10 mg (Ketorol DT; Dr. Reddy's Laboratories Ltd., Hyderabad, India) as rescue medication and instructed to take it only in case of considerable pain. Analgesic consumption was to be reported and documented. Alternate phone numbers were also noted so that the participants could be efficiently contacted.


https://doi.org/10.5395/rde.2026.51.e37

### Statistical analysis

Data analysis was performed using IBM SPSS Statistics software ver. 24.0 (IBM Corp., Armonk, NY, USA). The distribution of pre- and postoperative pain scores was assessed using the Shapiro-Wilk test. As the data were non-normally distributed and ordinal in nature (VAS scores), nonparametric tests were employed for all inferential analyses. Between-group comparisons of postoperative pain scores between the OR and NOR groups were performed using the Mann-Whitney *U* test. Within-group changes in postoperative pain scores over time were analyzed using the Wilcoxon signed-rank test. Baseline demographic variables and the prevalence and distribution of postoperative pain triggers were analyzed using the chi-square test. A *p*-value ≤0.05 was considered statistically significant.

## RESULTS

The overall process of participant enrollment, stratification, allocation, follow-up, and analysis has been illustrated in Figure 1. Baseline demographic distribution and clinical characteristics of patients in the OR and NOR groups are presented in Table 1. The two groups

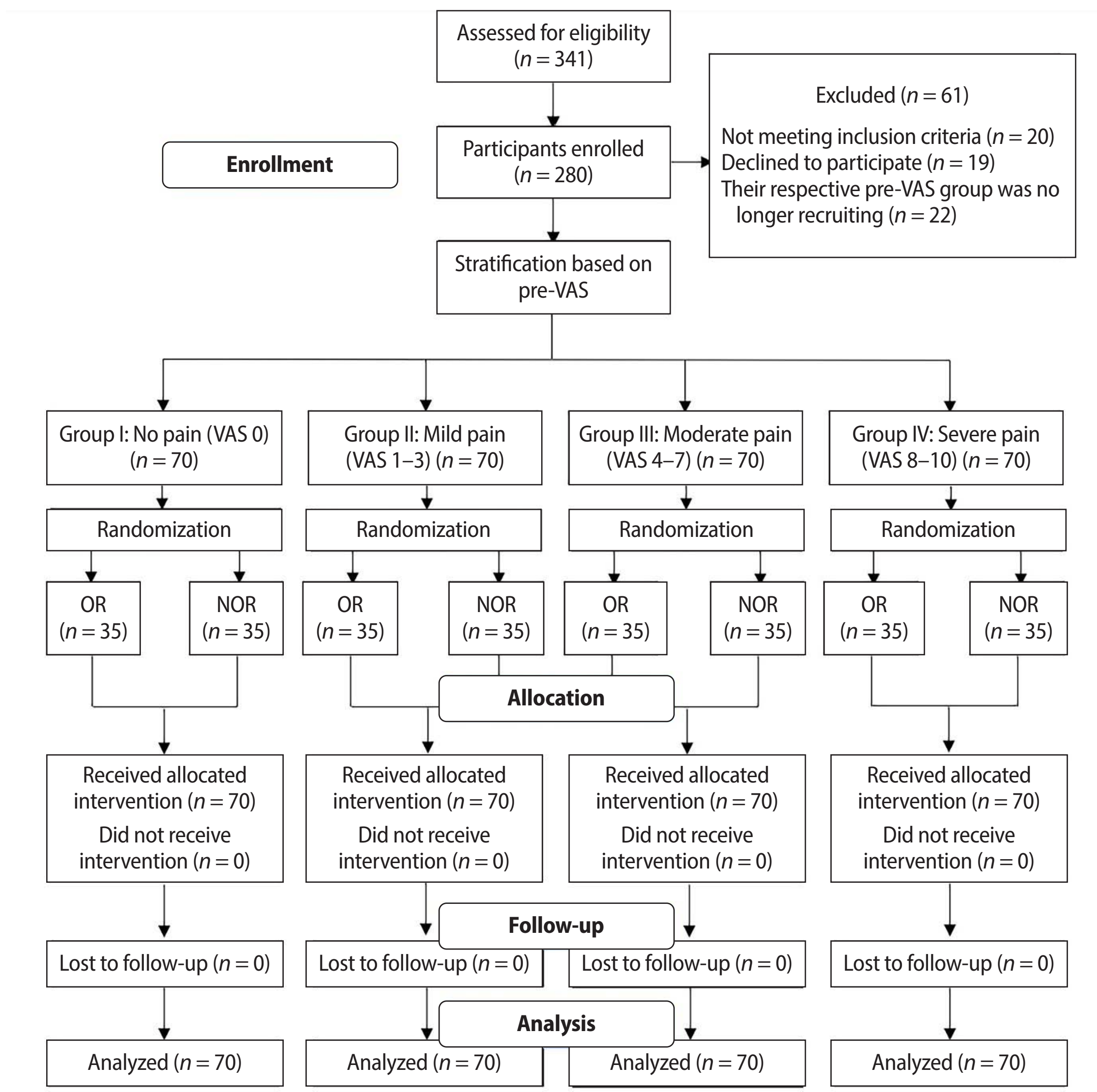


**Figure 1.** CONSORT 2025 flow diagram showing participant enrollment, stratified randomization, allocation, follow-up, and analysis. VAS, visual analogue scale; OR, occlusal reduction; NOR, no occlusal reduction.

were comparable with respect to age, sex distribution, and type of mandibular molar treated, indicating successful randomization and homogeneity between groups.

The comparison of postoperative pain scores between the OR and NOR groups at different time intervals is shown in Table 2. At baseline, no statistically significant difference in preoperative VAS scores was observed between the two groups ($p = 0.959$). At 24 hours postoperatively, mean pain scores were lower in the OR group compared with the NOR group; however, this difference did not reach statistical significance ($p = 0.155$). At 48 hours, patients in the OR group reported significantly lower postoperative pain scores than those in the NOR group ($p = 0.031$). At the 1-week follow-up, all patients in both groups reported complete resolution of pain (VAS 0), with no difference between groups ($p > 0.999$). Within-group comparisons of postoperative pain scores over time are presented in Table 3. Both OR and NOR groups demonstrated a statistically significant reduction in postoperative pain between 24 hours and 48 hours, and between 48 hours and 1 week (all $p < 0.001$). These findings indicate a consistent and significant decline in pain intensity over time.

Between-group comparisons of postoperative pain at 24 hours stratified by preoperative pain intensity are shown in Table 4. In patients with moderate preoperative pain (VAS 4–7), the OR group demonstrated significantly lower postoperative pain scores compared with the NOR group at 24 hours ($p = 0.024$). No statistically significant differences were observed in patients with no pain (VAS 0) or mild pain (VAS 1–3). In patients with severe preoperative pain (VAS 8–10), lower mean postoperative pain scores were observed in the OR group; however, this difference did not reach statistical significance ($p = 0.055$). This suggests that the effect of OR may be more pronounced among patients presenting with higher preoperative pain intensities, particularly during the early postoperative period. Patients with no preoperative pain (VAS 0) or mild pain (VAS 1–3) showed negligible postoperative discomfort regardless of occlusal intervention. Between-group comparisons at 48 hours

**Table 1.** Baseline demographic distribution and clinical characteristics of patients in the OR and NOR groups

| Demographic parameter | OR group | NOR group |
|---|---|---|
| No. of patients | 140 | 140 |
| Sex | | |
| Female | 86 | 84 |
| Male | 54 | 56 |
| Age (yr) | 33.24 ± 12.78 | 28.78 ± 13.29 |
| Type of molar | | |
| First molar | 91 | 99 |
| Second molar | 49 | 41 |

Values are presented as counts or mean ± standard deviation.
OR, occlusal reduction; NOR, no occlusal reduction.

**Table 2.** Comparison of pain scores between the OR and NOR groups

| Group | VAS score | | | |
|---|---|---|---|---|
| | Preoperative | 24 hours | 48 hours | 1 week |
| OR | 4.22 ± 3.41 | 1.42 ± 1.28 | 0.28 ± 0.60 | 0.00 ± 0.00 |
| NOR | 4.19 ± 3.46 | 1.68 ± 1.44 | 0.48 ± 0.81 | 0.00 ± 0.00 |
| *p*-value | 0.959 | 0.155 | 0.031[a] | >0.999 |

Values are presented as mean ± standard deviation.
OR, occlusal reduction; NOR, no occlusal reduction; VAS, visual analogue scale.
[a]Statistically significant difference between the OR and NOR groups at 48 hours (Mann-Whitney *U* test).

**Table 3.** Within-group comparison of postoperative pain scores over time

| Time interval | OR group | | NOR group | |
|---|---|---|---|---|
| | VAS score | *p*-value | VAS score | *p*-value |
| 24 hours vs 48 hours | 1.42 ± 1.28 vs 0.28 ± 0.60 | <0.001 | 1.68 ± 1.44 vs 0.48 ± 0.81 | <0.001 |
| 48 hours vs 1 week | 0.28 ± 0.60 vs 0.00 ± 0.00 | <0.001 | 0.48 ± 0.81 vs 0.00 ± 0.00 | <0.001 |

Values are presented as mean ± standard deviation.
OR, occlusal reduction; NOR, no occlusal reduction; VAS, visual analogue scale.
*p*-values were calculated using the Wilcoxon signed-rank test. All within-group comparisons demonstrated a statistically significant reduction in postoperative pain over time ($p < 0.001$).

**Table 4.** Between-group comparison of pain scores at 24 hours

| Preoperative pain category | 24-hour VAS score | | *p*-value |
|---|---|---|---|
| | OR group | NOR group | |
| VAS 0 | 0.63 ± 1.06 | 0.54 ± 0.85 | >0.999 |
| VAS 1–3 | 0.97 ± 0.79 | 1.00 ± 0.84 | 0.950 |
| VAS 4–7 | 1.69 ± 1.45 | 2.29 ± 1.10 | 0.024[a] |
| VAS 8–10 | 2.40 ± 0.98 | 2.89 ± 1.45 | 0.055 |

Values are presented as mean ± standard deviation.
OR, occlusal reduction; NOR, no occlusal reduction; VAS, visual analogue scale.
*p*-values were calculated using the Mann-Whitney *U* test.
[a]Statistically significant difference between the OR and NOR groups in patients with moderate preoperative pain (VAS 4–7).


https://doi.org/10.5395/rde.2026.51.e37

stratified by preoperative pain intensity are presented in Table 5. Although the OR group consistently demonstrated lower mean pain scores across moderate and severe preoperative pain categories, these differences were not statistically significant ($p = 0.099$ and $p = 0.051$, respectively). Between-group comparison at the 1-week follow-up was not included, as all participants in both groups reported complete resolution of pain (VAS 0), precluding meaningful statistical analysis.

Figure 2 illustrates the distribution of postoperative pain across the four preoperative pain categories at 24 hours and 48 hours. The graphical pattern reflects a progressive decline in reported pain across time for both groups, with visibly lower pain frequencies among OR cases, especially in the moderate and severe pain categories at 48 hours. The 1-week interval was excluded from the graphical representation since all patients reported a VAS score of 0 by that time.

To further explore the clinical relevance of postoperative pain, VAS scores were dichotomized into "pain" (VAS 1–10) and "no pain" (VAS 0) categories, as shown in Figure 3. This approach enabled a clearer distinction between symptom presence and absence by minimizing subjective variability in intermediate scores. At 24 hours postoperatively, pain was reported by 96 patients in the OR group and 100 patients in the NOR group, while 44 patients and 40 patients, respectively, remained pain-free. By 48 hours, the number of patients reporting pain decreased more markedly in the OR group ($n = 29$) compared with the NOR group ($n = 44$), whereas the majority—111 patients in OR and 96 patients in NOR—reported no pain. An alternative dichotomization (VAS 0–1, no pain; VAS 2–10, pain) was also tested to account for borderline responses where a VAS score of 1 may be of significant consideration to some, while others may perceive it as 'no pain/discomfort' (depending on the patient's pain threshold and perception of recovery). The distribution pattern remained consistent under this adjusted model, confirming the robustness of the observed trend.

The prevalence and distribution of postoperative pain triggers were analyzed using the chi-square test to evaluate whether any particular trigger mechanism

**Table 5.** Between-group comparison of pain scores at 48 hours

| Preoperative pain category | 48-hour VAS score | | *p*-value |
|---|---|---|---|
| | OR group | NOR group | |
| VAS 0 | 0.06 ± 0.34 | 0.06 ± 0.24 | 0.581 |
| VAS 1–3 | 0.09 ± 0.28 | 0.11 ± 0.32 | 0.692 |
| VAS 4–7 | 0.43 ± 0.78 | 0.71 ± 0.86 | 0.099 |
| VAS 8–10 | 0.54 ± 0.70 | 1.03 ± 1.04 | 0.051 |

Values are presented as mean ± standard deviation.
OR, occlusal reduction; NOR, no occlusal reduction; VAS, visual analogue scale.
*p*-values were calculated using the Mann-Whitney *U* test.

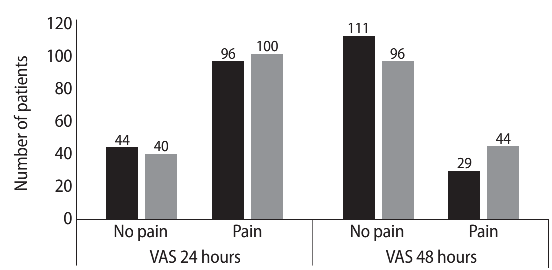


**Figure 3.** Graph depicting the dichotomized postoperative pain trend for both occlusal reduction (OR) and no occlusal reduction (NOR) groups at 24 hours and 48 hours, where a visual analogue scale (VAS) score of 0 was considered as 'no pain' and VAS scores of 1–10 were taken as 'pain.'

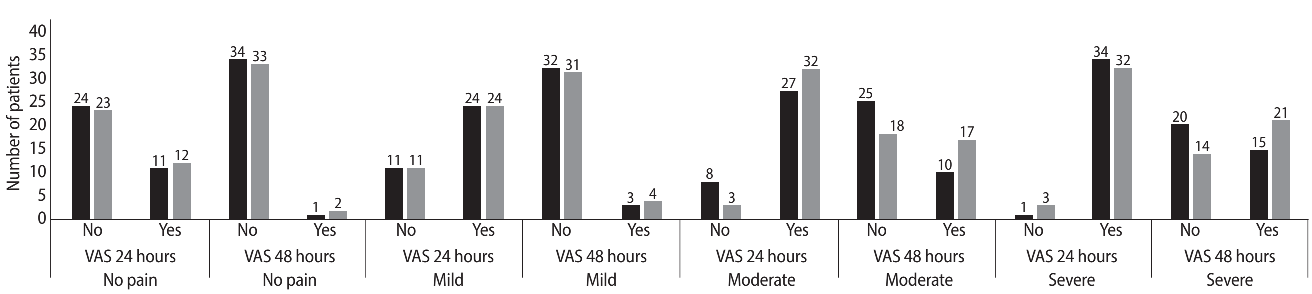


**Figure 2.** Graph depicting the postoperative pain trend across the four categories of pain at 24-hour and 48-hour time intervals. VAS, visual analogue scale; OR, occlusal reduction; NOR, no occlusal reduction.

was significantly associated with postoperative pain (Table 6). Among the 196 patients who reported postoperative discomfort (VAS 1–10), the majority of cases were stimulus-based (78.6%), followed by spontaneous occasional pain (18.9%) and spontaneous continuous pain (2.6%). Although this distribution did not reach statistical significance ($p = 0.078$), the findings indicate that postoperative pain was provoked predominantly by a functional stimulus such as mastication (occlusal contact) rather than occurring spontaneously.

**Table 6.** Overall prevalence of the type of trigger mechanism among the patients who reported postoperative pain ($n = 196$)

| Postoperative pain trigger mechanism | Data |
|---|---|
| Spontaneous continuous | 5 (2.6) |
| Spontaneous occasional | 37 (18.9) |
| Stimulus-based | 154 (78.6) |
| Overall p-value | 0.078 |

*p*-values were calculated using the chi-square test.

## DISCUSSION

This study evaluated the influence of OR on early postoperative pain after single-visit RCTs in mandibular first and second molars. To the best of the authors' knowledge, no previous randomized trial of occlusal adjustment after single-visit RCT has deliberately reserved a distinct arm of pain-free teeth (preoperative VAS = 0) to test whether occlusal manipulation affects the onset of postoperative discomfort in previously asymptomatic cases. This design, therefore, allowed assessment of both prophylactic and therapeutic roles of OR in the same trial population.

Mandibular molars were selected as they represent some of the most clinically demanding teeth. Epidemiologic data identify the mandibular first molar as the most frequently treated tooth endodontically, primarily because it is the first permanent tooth to erupt and thus highly susceptible to decay [20]. They are also subject to the highest occlusal loads during mastication [21], making them suitable for evaluating the influence of OR on postoperative pain. Furthermore, their complex root canal anatomy and multifactorial treatment challenges [22] make the findings more clinically relevant and generalizable than studies limited to single-rooted teeth.

The findings demonstrate that OR produced a transient decrease in early postoperative pain, with statistical significance at 48 hours ($p = 0.031$). The effect was most pronounced among patients with moderate preoperative pain, whereas those with mild or no preoperative symptoms exhibited negligible differences between interventions. In patients presenting with severe preoperative pain, OR was associated with lower postoperative pain scores at both 24 and 48 hours but failed to achieve statistical significance ($p = 0.055$ and $p = 0.051$, respectively). Although these differences did not reach statistical significance, it is noteworthy that the consistently lower pain scores observed suggest a potential biological effect that may warrant further investigation in larger cohorts. This trend aligns with the broader evidence that preoperative pain intensity is one of the strongest predictors of postoperative symptoms [17,23]. Patients presenting with elevated baseline nociceptive drive are more likely to benefit from the mechanical unloading achieved through OR.

The biological plausibility of these findings can be explained through mechanisms of peripheral and central sensitization. Inflammatory mediators and bacterial lipopolysaccharides within the pulp and periapical tissues sensitize nociceptors by up-regulating transient receptor potential vanilloid-1 channels, amplifying peripheral excitability [4,24]. Repeated afferent stimulation of sensitized fibers can subsequently induce central sensitization—a persistent state of hyperexcitability within spinal and trigeminal nociceptive pathways that sustains pain perception even after local inflammation subsides [25]. OR may alleviate peripheral mechanical loading on the inflamed periodontal ligament and periapical tissues, thereby reducing stimulus-driven nociceptive input to the central nervous system. This neurophysiological unloading likely explains why the therapeutic benefit of OR is most evident during the early, stimulus-evoked phase of healing.

The current evidence on OR remains heterogeneous. Rosenberg *et al.* [12] reported that total OR reduced postoperative pain in vital teeth with preoperative tenderness, whereas Parirokh *et al.* [17] observed no significant difference in such cases. A recent systematic review by Nguyen-Nhon *et al.* [11] concluded that OR may reduce postoperative pain in symptomatic teeth


https://doi.org/10.5395/rde.2026.51.e37

but highlighted a substantial heterogeneity among trials. Variations in case selection, irrigation protocols, intracanal medicaments, and timing of definitive restoration likely explain the inconsistent outcomes reported in earlier literature.

Irrigation was performed with sterile saline [26,27] because solutions such as sodium hypochlorite (NaOCl) and chlorhexidine (CHX) can independently influence postoperative outcomes owing to their tissue-damaging capacity and potential cytotoxicity when extruded apically. High concentrations of NaOCl have been linked to an increased incidence of postoperative discomfort [28]. CHX has been shown to reduce the survival rates of fibroblasts, myoblasts, and osteoblasts, thus affecting periapical healing [29]. Although NaOCl and CHX are valued for their abilities of tissue dissolvability and antimicrobial substantivity, using a biologically inert solution like saline ensured that any differences in postoperative pain reflected the mechanical and not the chemical effects of the treatment.

While this approach of removing confounding variables strengthened the study's internal validity, it represents a limitation in terms of external generalizability, particularly in clinical settings where NaOCl and CHX are considered standard irrigants. Similarly, a zinc oxide eugenol-based sealer was used to maintain procedural uniformity and avoid the variable biological responses associated with newer bioceramic sealers. Thus, the findings should be interpreted within the context of the materials used in this study.

Multiple-visit RCTs introduce confounding factors such as interappointment leakage, medicament effects, and downtime. Conducting treatments in a single visit eliminates these factors, ensuring that postoperative pain can be accurately attributed to the variable under investigation. Moreover, it simplifies logistics and follow-up, which likely contributed to the absence of dropouts in the present trial. Our findings support a patient-centered approach to OR rather than a universal rule. For teeth with no or mild preoperative pain, routine OR appears unnecessary. When treating patients with higher pain intensities or those who express elevated anxiety or low pain tolerance, selective occlusal unloading may offer tangible early relief. Allowing patients to participate in the decision aligns with the principles of shared decision-making increasingly advocated in endodontic care.

The term 'occlusal reduction' is conventionally used to describe the removal of occlusal contacts, most often in a restorative or prosthodontic context. When the same procedure is undertaken with the aim of minimizing postoperative discomfort rather than facilitating tooth preparation, the authors suggest that the term 'mechanical-' or 'occlusal unloading' may better reflect its therapeutic intent. From a linguistic and clinical perspective, 'reduction' carries an operative and somewhat aggressive implication, whereas 'unloading' emphasizes the purposeful removal of occlusal stress transmitted to inflamed and sensitized periapical tissues more conservatively. Adopting this terminology could help distinguish between preparative and pain-modulating purposes of occlusal adjustment and align future endodontic literature with the underlying biomechanical rationale rather than the procedural technique.

Pain perception is subjective and shaped by psychosocial and cognitive factors. Dental anxiety, catastrophizing, and prior negative experiences can elevate pain reporting even when objective inflammation is comparable. Consequently, two patients experiencing similar tissue conditions may record markedly different VAS scores [30]. To address potential subjectivity, this study performed dichotomized analyses using two different models: pain (1–10) vs no pain (0), and pain (2–10) vs no pain (0, 1). Both models yielded consistent trends, reinforcing the reproducibility of the findings.

Strengths of this trial include stratified randomization based on preoperative pain intensity, standardized OR of 1.5–2 mm verified using calibrated gauges, and complete follow-up. However, the single-center design, inability to blind the operator, and reliance on self-reported pain scores rather than objective biomarkers represent inherent limitations. Although stratification improved clinical interpretability, subgroup analyses inevitably reduced statistical power, which may explain the absence of statistical significance in the severe pain category despite consistent directional trends. In addition, the study was limited to teeth diagnosed with irreversible pulpitis, excluding cases with necrotic pulp or established periapical pathosis, and other clinical characteristics, such as the nature of the pain, presence of tenderness, and thermal sensitivity, were not independently stratified, potentially contributing to variability in pain perception. Consequently, the findings cannot be extrapolated to all endodontic conditions. Future research should include multicenter designs, other endodontic pathologies, retreatment cases, analgesic consumption patterns, extended follow-up beyond the acute postoperative phase, and exploration of neurophysiological or molecular correlates underlying pain modulation following occlusal unloading.

## CONCLUSIONS

OR following a single-visit RCT in teeth with irreversible pulpitis resulted in a modest but considerable reduction in early postoperative pain, especially in patients with elevated preoperative pain. For asymptomatic or minimally symptomatic teeth, the procedure is unnecessary. When indicated, however, it can be a simple adjunct to improve patient comfort—particularly in individuals who report higher dental anxiety or lower pain thresholds.

### CONFLICT OF INTEREST

No potential conflict of interest relevant to this article was reported.

### FUNDING/SUPPORT

The authors have no financial relationships relevant to this article to disclose.

### ACKNOWLEDGMENTS

The authors would like to acknowledge and thank our peers, colleagues, and mentors for their guidance, support, and supervision.

### AUTHOR CONTRIBUTIONS

Conceptualization: Sherwood IA, Kanesalingavelan S. Data curation: Chandrasekaran P, Abirami AA. Formal analysis, Project administration, Supervision, Validation: Sherwood IA. Investigation, Resources: Kanesalingavelan S. Methodology, Visualization: Kanesalingavelan S, Deepika KG G, Sherwood IA. Writing - original draft: Kanesalingavelan S, Deepika KG G. Writing - review & editing: Sherwood IA, Chandrasekaran P, Abirami AA. All authors read and approved the final manuscript.

### DATA SHARING STATEMENT

The datasets are not publicly available but are available from the corresponding author upon reasonable request.

### DISCLOSURE OF GENERATIVE AI IN SCIENTIFIC WRITING

No artificial intelligence was used for the conception, design, conduct, analysis, interpretation, or reporting of this study. Any assistance was solely to improve grammar, language, and readability of the manuscript.

## REFERENCES

1. Borgo Sarmento E, Guimarães L, Tavares S, Azevedo Batistela Rodrigues Thuller K, Antunes L, Antunes L, *et al.* The influence of sodium hypochlorite and chlorhexidine on postoperative pain in necrotic teeth: a systematic review. Eur Endod J 2020;5:177-185.
2. Jian Y. Preventive and therapeutic effects of semiconductor laser on pain in root canal treatment. Eur J Med Res 2025;30:937.
3. Kumar G, Jena S, Manila N, Fareed M, Karobari MI. Incidence of postoperative pain after single-visit and multiple-visit root canal therapy: a systematic review. BMC Oral Health 2025;25:47.
4. Gupta NK, Mantri SP, Paul B, Dube KA, Ghosh S. Incidence of postoperative pain after single-visit and multiple-visit root canal therapy: a randomized controlled trial. J Conserv Dent 2021;24:348-353.
5. Al-Rahabi M, Abdulkhayum AM. Single visit root canal treatment. Saudi Endod J 2012;2:80-84.
6. Singla R, Marwah N, Dutta S. Single visit versus multiple visit root canal therapy. Int J Clin Pediatr Dent 2008;1:17-24.
7. Geethanjali R, Kumar N, Madhuram K, Leburu A. Single visit endodontics. IP Indian J Conserv Endod 2021;6:147-151.
8. Poorani K, Deepika KG, Sherwood IA, Piriyanga SR. Comparing rotary and reciprocation files for postoperative pain in single-visit root canal treatment: a randomized controlled clinical trial. Endodontology 2025;37:250-256.
9. Gotler M, Bar-Gil B, Ashkenazi M. Postoperative pain after root canal treatment: a prospective cohort study. Int J Dent 2012;2012:310467.
10. Pawar AM, Bhardwaj A, Zanza A, Wahjuningrum DA, Arora S, Luke AM, *et al.* Severity of post-operative pain after instrumentation of root canals by XP-Endo and SAF full sequences compared to manual instrumentation: a randomized clinical


https://doi.org/10.5395/rde.2026.51.e37

trial. J Clin Med 2022;11:7251.

11. Nguyen-Nhon D, Nagendrababu V, Pulikkotil SJ, Rossi-Fedele G. Effect of occlusal reduction on postendodontic pain: a systematic review and meta-analysis of randomised clinical trials. Aust Endod J 2020;46:282-294.
12. Rosenberg PA, Babick PJ, Schertzer L, Leung A. The effect of occlusal reduction on pain after endodontic instrumentation. J Endod 1998;24:492-496.
13. Sheikh H, Ahmed MA, Jouhar R, Choudhry Z. Comparison of post-instrumentation pain in teeth during root canal treatment with or without occlusal reduction. Pak Oral Dent J 2015;35:699-701.
14. Zaman H, Ahmed SS. Effect of occlusal reduction on post instrumentation pain in patients with acute irreversible pulpitis. Pak Oral Dent J 2016;36:119-121.
15. Creech JL, Walton RE, Kaltenbach R. Effect of occlusal relief on endodontic pain. J Am Dent Assoc 1984;109:64-67.
16. Jostes JL, Holland GR. The effect of occlusal reduction after canal preparation on patient comfort. J Endod 1984;10:34-37.
17. Parirokh M, Rekabi AR, Ashouri R, Nakhaee N, Abbott PV, Gorjestani H. Effect of occlusal reduction on postoperative pain in teeth with irreversible pulpitis and mild tenderness to percussion. J Endod 2013;39:1-5.
18. Hopewell S, Chan AW, Collins GS, Hróbjartsson A, Moher D, Schulz KF, *et al*. CONSORT 2025 statement: updated guideline for reporting randomised trials. Lancet 2025;405:1633-1640.
19. Cohen J. Statistical power analysis for the behavioral sciences. 2nd ed. New York: Psychology Press; 2009.
20. Scavo R, Martinez Lalis R, Zmener O, Dipietro S, Grana D, Pameijer CH. Frequency and distribution of teeth requiring endodontic therapy in an Argentine population attending a specialty clinic in endodontics. Int Dent J 2011;61:257-260.
21. Prabahar T, Gupta N, Chowdhary N, Sonnahalli NK, Chowdhary R, Reddy VR. Comparative evaluation of occlusal bite force in relation to the muscle activity in the mixed dentition children of age group 9-12 years: a T-scan analysis. Int J Clin Pediatr Dent 2021;14:S29-S34.
22. Al-Rammahi HM, Chai WL, Nabhan MS, Ahmed HMA. Root and canal anatomy of mandibular first molars using micro-computed tomography: a systematic review. BMC Oral Health 2023;23:339.
23. Alí A, Olivieri JG, Duran-Sindreu F, Abella F, Roig M, García-Font M. Influence of preoperative pain intensity on postoperative pain after root canal treatment: a prospective clinical study. J Dent 2016;45:39-42.
24. Chung MK, Lee J, Duraes G, Ro JY. Lipopolysaccharide-induced pulpitis up-regulates TRPV1 in trigeminal ganglia. J Dent Res 2011;90:1103-1107.
25. Woolf CJ. Central sensitization: implications for the diagnosis and treatment of pain. Pain 2011;152:S2-S15.
26. Evangelin J, Sherwood IA, Abbott PV, Uthandakalaipandian R, Velu V. Influence of different irrigants on substance P and IL-8 expression for single visit root canal treatment in acute irreversible pulpitis. Aust Endod J 2020;46:17-25.
27. Nivedha V, Sherwood IA, Abbott PV, Ramaprabha B, Bhargavi PV. Pre-operative ketorolac efficacy with different anesthetics, irrigants during single visit root canal treatment of mandibular molars with acute irreversible pulpitis. Aust Endod J 2020;46:343-350.
28. Bashetty K, Hegde J. Comparison of 2% chlorhexidine and 5.25% sodium hypochlorite irrigating solutions on postoperative pain: a randomized clinical trial. Indian J Dent Res 2010;21:523-527.
29. Liu JX, Werner J, Kirsch T, Zuckerman JD, Virk MS. Cytotoxicity evaluation of chlorhexidine gluconate on human fibroblasts, myoblasts, and osteoblasts. J Bone Jt Infect 2018;3:165-172.
30. McCormack HM, Horne DJ, Sheather S. Clinical applications of visual analogue scales: a critical review. Psychol Med 1988;18:1007-1019.

RDE Restorative Dentistry & Endodontics

Case Report

eISSN 2234-7666
Restor Dent Endod. 2026 August;51(3):e36
https://doi.org/10.5395/rde.2026.51.e36

# Direct composite injection molding with bilayered three-dimensional-printed clear index: a fully digital workflow case report of post-orthodontic anterior tooth wear

Yuta Utsumi[1], Junji Tagami[2,3], Bas Loomans[4], Nicola Scotti[5], Keiichiro Watanabe[6], Sooha Matsuki[6], Eiji Tanaka[6], Keiichi Hosaka[1,2,*]

[1]Department of Conservative Dentistry, Tokushima University Graduate School of Biomedical Sciences, Tokushima, Japan
[2]Smart Innovations for Preventive and Restorative Dentistry Research Group, Department of Operative Dentistry, Faculty of Dentistry, Chulalongkorn University, Bangkok, Thailand
[3]Cariology and Operative Dentistry, Institute of Science Tokyo, Tokyo, Japan
[4]Department of Dentistry, Research Institute for Innovation, Radboud University Medical Center, Nijmegen, The Netherlands
[5]Department of Surgical Sciences, University of Turin, Dental School Lingotto, Turin, Italy
[6]Department of Orthodontics and Dentofacial Orthopedics, Tokushima University Graduate School of Biomedical Sciences, Tokushima, Japan

## ABSTRACT

This case report describes post-orthodontic direct composite restorations for anterior tooth wear using bilayered, three-dimensional (3D)-printed clear indices with a fully digital workflow. A patient with moderate incisal wear affecting the six maxillary anterior teeth underwent intraoral and facial scanning, followed by the creation of two digital wax-ups. Two sets of bilayered indices were fabricated, consisting of a rigid transparent outer shell for structural stability and a flexible inner liner for precise adaptation. Restoration was performed in two phases: alternate teeth were restored with the skipping-teeth first index, followed by restoration of the remaining teeth using the full-contour second index. The index design facilitated stable seating and controlled composite injection (Clearfil Majesty ES Flow Universal; Kuraray Noritake), which minimized material excess and simplified the finishing process while maintaining the planned morphology. The patient reported high satisfaction with comfort and treatment efficiency. At 15-month follow-up, all restorations remained intact with excellent marginal adaptation, surface quality, and esthetics. Within the limitations of this report, the use of bilayered 3D-printed clear indices suggests a feasible and conservative approach for managing anterior tooth wear.

**Keywords:** Three-dimensional printing; Composite resins; Digital technology; Esthetics, dental; Tooth wear

## INTRODUCTION

Direct composite restoration of worn dentition is supported by a variety of clinical techniques. Several studies have shown that the choice of restorative approach does not significantly influence survival outcomes and

**Received:** November 15, 2025 **Revised:** March 29, 2026 **Accepted:** March 30, 2026

**Citation**
Utsumi Y, Tagami J, Loomans B, Scotti N, Watanabe K, Matsuki S, Tanaka E, Hosaka K. Direct composite injection molding with bilayered three-dimensional-printed clear index: a fully digital workflow case report of post-orthodontic anterior tooth wear. Restor Dent Endod 2026;51(3):e36.
***Correspondence to**
**Keiichi Hosaka, DDS, PhD**
Conservative Dentistry, Tokushima University Graduate School of Biomedical Sciences, 3-18-15 Kuramoto-cho, Tokushima 770-8504, Japan
Email: hosaka@tokushima-u.ac.jp

that direct restorative approaches demonstrate favorable outcomes in the mid- to long-term [1,2]. A recent systematic review further confirmed that direct composite restorations are reliable treatment options, although their clinical execution may be technically demanding [3]. Consequently, new techniques and modifications to established protocols continue to emerge to improve predictability and efficiency.

Among these approaches, direct composite injection techniques have gained increasing attention for their minimally invasive nature [4–7]. This technique enables accurate reproduction of planned tooth morphology, reduces the need for extensive freehand sculpting, and facilitates the simultaneous treatment of multiple teeth. The growing adoption of this technique has been supported by advances in resin composite materials, particularly the development of injectable composites that combine improved flowability with adequate mechanical strength for clinical use. These material developments have expanded the clinical applicability of injection-based restorative procedures [8]. However, in multiunit anterior cases, precise placement and stabilization of the index can still be challenging.

Conventionally, clear silicone indices fabricated from wax-ups on stone models have been used to guide composite placement [9,10]. Although clinically useful, achieving the high level of precision required in contemporary restorative dentistry under high magnification remains a clinical challenge with these indices [11–14]. Digital technologies have therefore been introduced to enhance accuracy, reproducibility, and clinical efficiency. Computer-aided design (CAD) enables virtual wax-ups and the fabrication of silicone matrices [11,12], or fully three-dimensional (3D)-printed indices [15–19], thereby reducing manual steps and improving clinical control.

Despite these innovations, monolithic 3D-printed indices created from a single resin material may present several limitations, including limited translucency, insufficient adaptability, and potential deformation caused by polymerization shrinkage. Similarly, conventional silicone indices may deform when used for multitooth restorations and often require additional stabilization [20]. Although newer approaches, including flexible 3D-printed indices and hybrid stabilization systems [16,17], have provided incremental improvements, an efficient workflow for multiunit anterior restorations is still sought.

As a potential approach to these challenges, the present case report describes a fully digital workflow utilizing a bilayered 3D-printed clear index system. This index design incorporates a rigid transparent outer shell that provides structural stability and a flexible inner liner that passively adapts to the tooth surface. This bilayered configuration is intended to facilitate injection control, reduce excess composite resin, and minimize the risk of unintended interproximal bonding. In addition, the reduced internal volume may help limit 3D deformation associated with polymerization shrinkage. By eliminating the need for stone models and conventional silicone impressions, this workflow aims to simplify the clinical procedure. Therefore, the purpose of this case report was to present a fully digital workflow for direct composite injection molding using bilayered 3D-printed clear indices and to describe their clinical application in the minimally invasive management of post-orthodontic anterior tooth wear.

## CASE REPORT

This case report complies with established ethical standards. Written informed consent was obtained from the patient for the publication of her clinical information and images. This report was prepared in accordance with the CARE (CAse REport) guidelines.

A 31-year-old female patient presented with complaints of masticatory disturbance and esthetic concerns. Clinical examination revealed significant wear of the maxillary and mandibular anterior teeth, which was attributed primarily to long-standing parafunctional activity. Posterior cusp wear was also observed, suggesting occlusal loading concentrated on the molars due to the anterior open bite. The anterior teeth exhibited moderate incisal enamel loss without obvious dentin exposure, corresponding approximately to a Basic Erosive Wear Examination score of 2 [21]. As posterior support and the vertical dimension of occlusion (VDO) were preserved, the overall wear risk was considered low to moderate.

At the initial examination, the patient also presented


https://doi.org/10.5395/rde.2026.51.e36

with anterior crowding (Figure 1). Orthodontic treatment was therefore planned in conjunction with restorative considerations. Because the maxillary anterior teeth were relatively small and space was available for morphological correction, it was anticipated that discrepancies in clinical crown lengths would become apparent once proper alignment was achieved. This possibility was discussed with the patient, and restorative procedures were planned to harmonize crown lengths following orthodontic treatment.

Accordingly, orthodontic tooth movement was directed toward aligning the gingival margins rather than the incisal edges, anticipating subsequent restorative correction of crown height discrepancies (Figure 2A). The patient was diagnosed with a severe anterior open bite, primarily associated with parafunctional habits. To address the skeletal discrepancy, corticotomy was performed on both buccal and palatal aspects of the maxillary molar regions (Figure 2B and C). Orthodontic anchorage was achieved using bilateral anchor plates placed on the zygomatic buttress and a mini screw inserted at the center of the hard palate. Following corticotomy, the bilateral molar segments were intruded by approximately 4.0 mm to correct the open bite.

The total active orthodontic treatment duration was 43 months, resulting in a functionally stable occlusion and improved facial profile. This outcome provided favorable conditions for anterior direct composite resto-

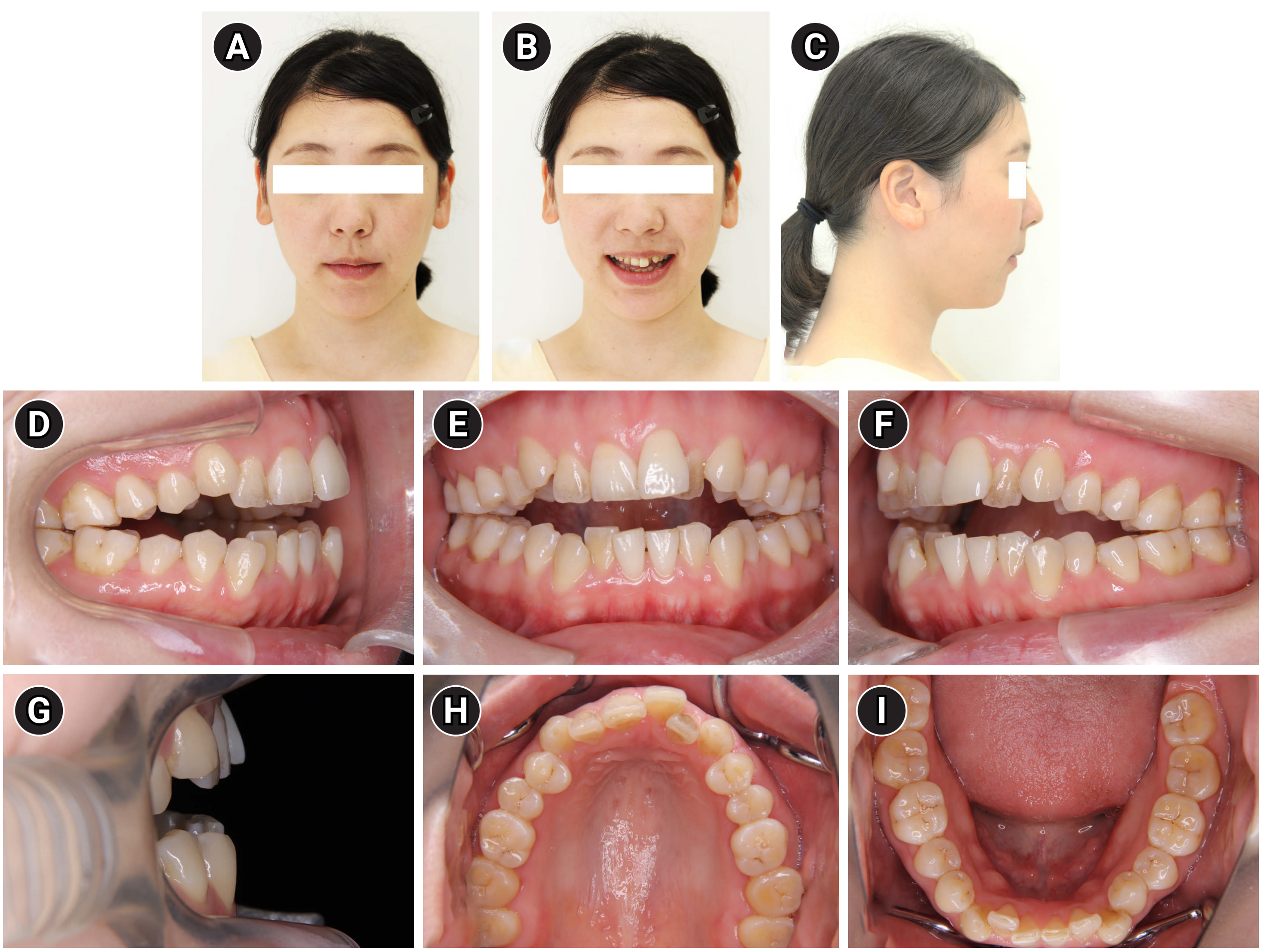


**Figure 1.** Initial extraoral and intraoral photographs at the age of 31 years. (A) Frontal facial view at rest. (B) Frontal facial view during smiling. (C) Lateral facial view. (D–F) Right lateral, frontal, and left lateral intraoral views, respectively. (G) Lateral intraoral view showing the anterior open bite. (H) Maxillary occlusal view. (I) Mandibular occlusal view.

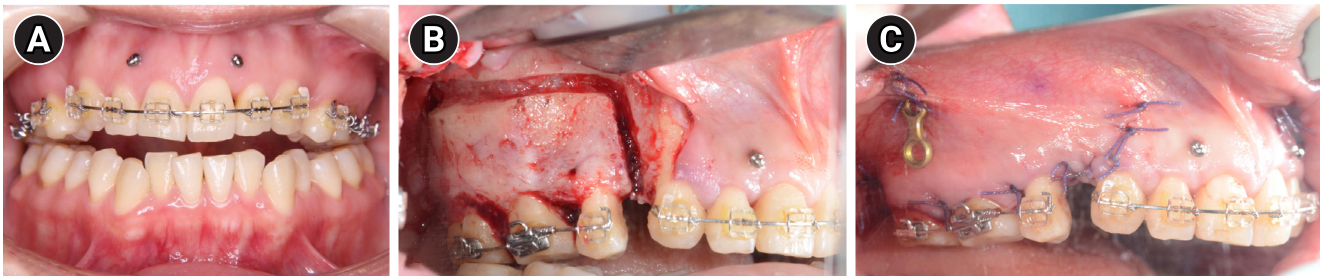


Figure 2. Orthodontic treatment and corticotomy. (A) Frontal intraoral view after leveling and anterior teeth intrusion. (B) Corticotomy on the buccal aspect of the maxillary molar region. (C) After corticotomy and anchor plate placement.

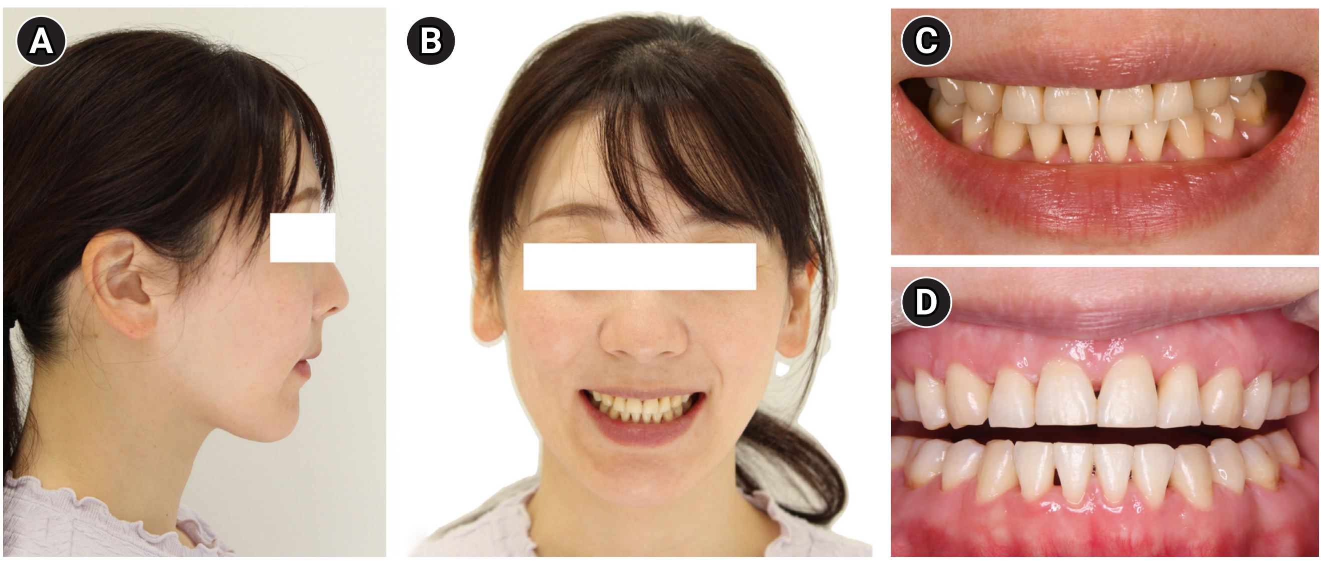


Figure 3. Post-orthodontic condition before restorative treatment. (A) Lateral facial view. (B) Frontal facial view during smiling. (C) Close-up smile view. (D) Frontal intraoral view showing incisal wear and discrepancies in clinical crown length.

rations. Near the completion of orthodontic treatment, the patient requested restorative enhancement. Therefore, fully digital preoperative records were obtained immediately prior to debonding, and minimally invasive definitive procedures were planned on the day of multibracket appliance removal.

Post-orthodontically, the patient presented with moderate incisal wear affecting the six maxillary anterior teeth. Although dentin exposure was not evident, she expressed esthetic dissatisfaction due to slight contour irregularities and incisal shortening. The occlusion remained stable, with maintained posterior occlusal stops and no clinical signs of VDO collapse. Despite the presence of posterior cusp wear, posterior support was preserved, and no reduction in lower facial height was observed. No signs or symptoms of occlusal instability or temporomandibular dysfunction were reported. Given this stable occlusal condition, the patient requested minimally invasive esthetic enhancement limited to the anterior region (Figure 3).

During restorative planning, a slight asymmetry in gingival levels between teeth #12–11 and #21–22 was evaluated. Because the periodontal tissues were healthy and the discrepancy was clinically subtle, periodontal recontouring was not indicated. In keeping with the minimally invasive treatment concept, surgical intervention solely to improve gingival symmetry was avoided. The restorative plan, therefore, aimed to refine anterior guidance and restore natural contours, with an incisal length increase of no more than 1 mm.


https://doi.org/10.5395/rde.2026.51.e36

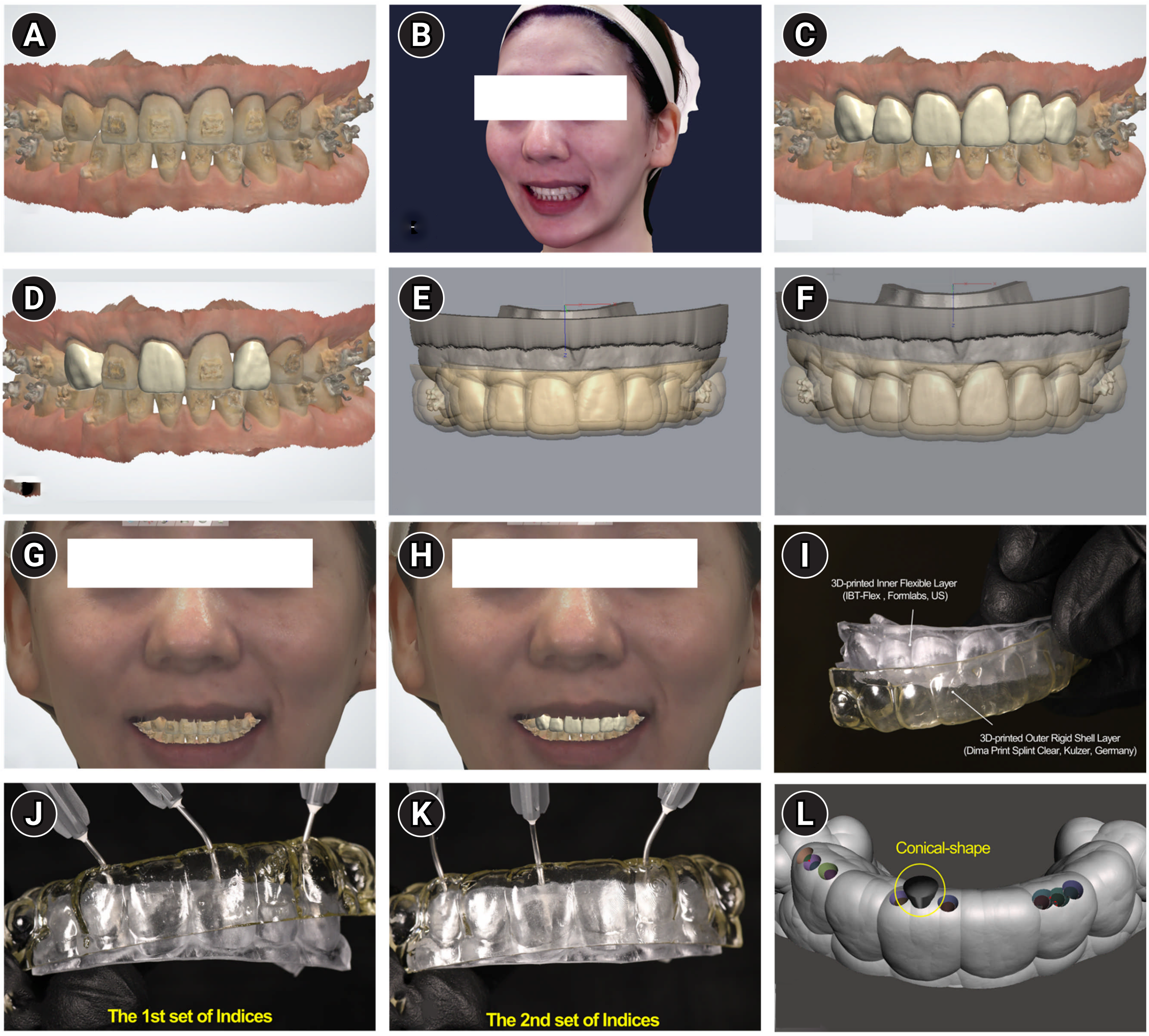


**Figure 4.** Fully digital planning and fabrication of the bilayered clear indices. (A) Intraoral scan. (B) Facial scan. (C) Complete digital wax-up of teeth #13–23. (D) Skip-tooth digital wax-up for the first restorative phase. (E, F) Digital designs of the first and second bilayered indices, respectively. (G, H) Simulated smile views before and after application of the digital wax-up, respectively. (I) Rigid transparent outer shell and flexible semitransparent inner liner of the bilayered index. (J, K) Fabricated first and second sets of bilayered indices, respectively. (L) Conical access and vent-hole design.

A fully digital workflow was employed. Intraoral scans were obtained using an intraoral scanner (Medit i700; Medit Corp., Seoul, Korea) (Figure 4A), and facial scans were captured using the RAYFace system (Ray Co., Ltd., Seoul, Korea) (Figure 4B). The datasets were imported into dental CAD software (3Shape A/S, Copenhagen, Denmark), and a complete digital wax-up was created for all six maxillary anterior teeth (#13–23) (Figure 4C).

To minimize interproximal bonding and improve finishing control, a skip-tooth version of the wax-up was subsequently generated according to the technique reported by Coachman *et al.* [22]. This approach allowed alternate-tooth restoration in two phases: first, teeth #13, #11, and #22, followed by #12, #21, and #23, using separate bilayered indices (Figure 4D–F).

Although no intraoral mock-up was performed prior to index fabrication, the digital design was evaluated with integrated facial scan data, and the patient approved the proposed outcome based on simulated smile previews (Figure 4G and H). Given the additive nature of the restorations and the minimal incisal adjustment required, direct application was considered clinically appropriate.

The bilayered clear index system consisted of a rigid transparent outer shell designed for structural accuracy and a flexible semitransparent inner liner for passive adaptation (Figure 4I–K). Each layer was independently fabricated using 3D printing: the outer shell using Dima Print Splint Clear (Kulzer GmbH, Hanau, Germany) and the inner liner using IBT-Flex resin (Formlabs, Somerville, MA, USA), both printed at a 50-μm layer thickness with a minimum material thickness of 1.5 mm. The indices were digitally designed with conical access and vent holes to enable controlled composite injection and material escape (Figure 4L).

Isolation was achieved using a cheek-lip-tongue retractor (Umbrella; Ultradent Products Inc., South Jordan, UT, USA) in combination with a split rubber dam (Optradam; Ivoclar, Schaan, Liechtenstein), allowing stable and passive seating of the flexible inner liner. The enamel surfaces of teeth #13, #11, and #22 were selectively etched with 37% phosphoric acid (K-etchant syringe; Kuraray Noritake Dental Inc., Tokyo, Japan) for 15 seconds, rinsed thoroughly with water, and air-dried (Figure 5A and B). A universal adhesive (Clearfil Universal Bond Quick 2; Kuraray Noritake Dental Inc.) was then applied following the manufacturer's instructions and light-cured for 10 seconds using an LED curing unit (Pencure 2000; MORITA, Tokyo, Japan) with an output of ≥1,200 mW/cm$^2$.

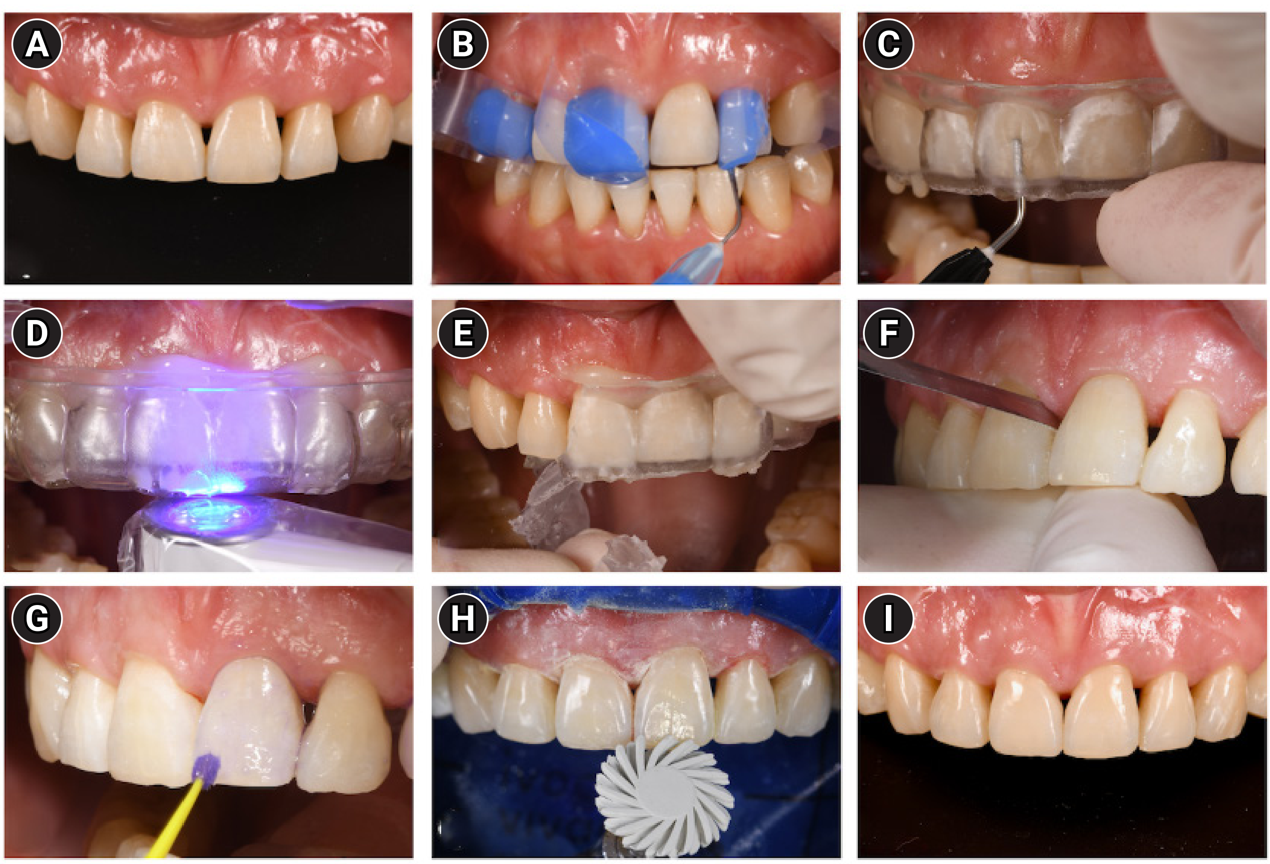


**Figure 5.** Clinical restorative procedure. (A) Preoperative frontal intraoral view. (B) Selective enamel etching of teeth #13, #11, and #22. (C) Injection of composite resin through an access hole of the first index. (D) Light curing through the seated index. (E) Removal of the index after polymerization. (F) Refinement of interproximal excess with an abrasive strip. (G) Cleaning of the restoration surface with Katana Cleaner (Kuraray Noritake Dental Inc., Tokyo, Japan). (H) Finishing and polishing with a silicone point. (I) Immediate postoperative result.


https://doi.org/10.5395/rde.2026.51.e36

Using the first index, a highly filled universal-shade injectable composite resin (Clearfil Majesty ES Flow Universal; Kuraray Noritake Dental Inc.) was injected through the access holes (Figure 5C). The index was fully seated with gentle pressure, allowing excess material to escape through the vent holes. Each restoration was light-cured for 20 seconds (Figure 5D). After polymerization, the index was removed (Figure 5E), and interproximal excess was refined with abrasive strips (New Metal Strips; GC Corp., Tokyo, Japan) (Figure 5F). Following index removal, an additional 20 seconds of light curing was performed for each restoration. The surfaces were then cleaned using a 10-methacryloyloxydecyl dihydrogen phosphate salt-based surface cleaner (Katana Cleaner, Kuraray Noritake Dental Inc.) (Figure 5G).

The second index was subsequently used to restore the remaining teeth (#12, #21, and #23) using the same protocol. Occlusion was verified with 40 µm articulating paper, and minor occlusal adjustments were intentionally performed to refine functional contacts and harmonize lateral movements. This clinical decision prioritized dynamic functional occlusion over the static digital design, resulting in a slight modification of the planned canine morphology for tooth #23. All restorations were finished and polished using silicone points (Jiffy Natural; Ultradent Products Inc.) (Figures 5H and I).

At the 6-month follow-up, all restorations remained intact with excellent marginal adaptation. Anterior guidance was maintained during protrusive movement, while lateral excursions were characterized by stable canine guidance. Functional disocclusion was clinically verified, confirming canine-dominant contact without premolar-only guidance. No fractures or material failures were observed. The slight difference in the incisal morphology of tooth #23 compared with the initial digital plan reflected minor occlusal adjustments aimed at optimizing functional guidance, as well as small discrepancies inherent to the clinical injection procedure (Figure 6A–C).

The patient reported high satisfaction with both esthetic and functional outcomes. Because the tooth wear was associated with parafunctional activity, a maxillary night guard was delivered. Regular recall visits were scheduled at 3-month intervals for occlusal and restorative reevaluation. Clinical findings remained stable during subsequent follow-up visits. The observation period currently extends to 15 months (Figure 6D and E); however, continued long-term monitoring is necessary to evaluate the durability and functional stability of this minimally invasive restorative approach.

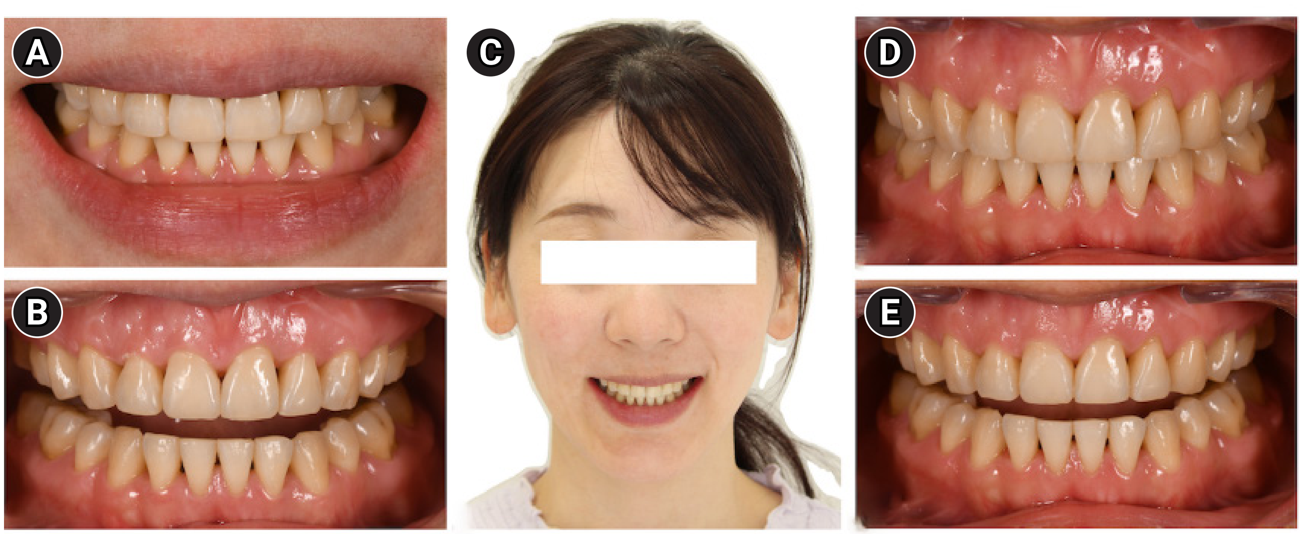


**Figure 6.** Clinical outcomes at follow-up. (A) Smile view at the 6-month follow-up. (B) Frontal intraoral view at the 6-month follow-up. (C) Frontal facial view at the 6-month follow-up. (D, E) Frontal intraoral views at the 15-month follow-up, demonstrating intact restorations and maintained esthetics.

## DISCUSSION

The minimally invasive restoration of anterior tooth wear, particularly in young adults, requires treatment strategies that preserve enamel while providing predictable esthetic and functional outcomes. In the present case, the discrepancy in clinical crown lengths was not primarily caused by orthodontic treatment but was already present at the initial examination. It was anticipated that once proper alignment was achieved, the disharmony of crown lengths would become more evident. Although minor additional incisal wear may have occurred during orthodontic treatment, the main discrepancy reflected the pre-existing condition. This factor was incorporated into the interdisciplinary treatment plan. Orthodontic tooth movement was intentionally directed toward aligning the gingival margins rather than the incisal edges, allowing the correction of crown height discrepancies to be achieved by subsequent restorative procedures.

In the present case, the residual gingival asymmetry was clinically minor and considered acceptable. Complete correction would have required additional orthodontic or periodontal intervention, which would have increased treatment invasiveness without providing meaningful esthetic or functional benefit. Therefore, further correction was not pursued in view of overall facial harmony and the patient's satisfaction with the outcome. This treatment strategy highlights the importance of early interdisciplinary collaboration between orthodontics and restorative treatment planning, ensuring that tooth movement is guided by the anticipated restorative outcome and leading to a more predictable and esthetic result.

Direct composite injection molding using an index-guided approach has emerged as a conservative alternative to indirect restorations [7]. However, conventional workflows often involve multiple manual steps and may provide limited precision when applied to multi-tooth restorations. The bilayered index configuration used in this report was designed to address several of these limitations.

The system incorporates a rigid transparent outer shell that provides structural stability during flowable composite injection and a flexible inner liner that passively adapts to the tooth surface. This dual-layered design may facilitate accurate seating of the index, controlled composite injection, and simplified removal after polymerization. In addition, the reduced internal injection volume may help limit excess composite flow and potentially reduce the risk of unintended interproximal bonding.

Previous designs involving flexible indices typically required auxiliary stabilization devices to maintain positioning [16,17], and earlier bilayered concepts have mainly been reported in limited clinical situations, such as pediatric cases [20]. In contrast, the present configuration was applied to adult anterior restorations within a fully digital workflow. The use of a skip-tooth wax-up design, based on the concept described by Coachman *et al.* [22], further improved control of interproximal contours and facilitated finishing procedures. By restoring alternate teeth in the first phase, sufficient interproximal space was maintained during composite injection, which helped limit unintended interproximal bonding and improved access for finishing and polishing.

From a structural perspective, the current design differs from previously reported indices in several aspects. Technically, structural stabilization and surface adaptation are separated into two independent components. Geometrically, the internal injection volume is intentionally reduced, providing a more controlled pathway for composite flow and potentially limiting deformation associated with polymerization shrinkage. From a material standpoint, the combination of resins with different elastic moduli allows controlled seating while maintaining passive adaptation. Together, these characteristics may distinguish the present configuration from previously reported flexible matrices or monolithic printed indices.

The structural rationale of this concept is supported by a recent *in vitro* study evaluating different index designs using root-mean-square analysis, which demonstrated improved trueness and precision of the bilayered configuration compared with conventional monolayer indices [23]. However, these laboratory findings should be interpreted with caution when extrapolated to clinical situations, and further clinical studies are necessary to confirm these observations. In addition, pre-clinical verification can be performed through a trial composite


https://doi.org/10.5395/rde.2026.51.e36

injection on a 3D-printed model, allowing the injected composite to be compared with the original CAD design. In the present workflow, such verification suggested that dimensional discrepancies appeared to remain within a clinically acceptable range.

Despite these advantages, several limitations should be considered. First, the 3D-printed flexible inner layer may exhibit limited elastic recovery after repeated use, which could potentially affect adaptation. Second, fabrication of the index requires access to CAD software and high-resolution 3D-printing equipment, which may not be available in all clinical or laboratory settings. Third, proper post-processing of the printed index is critical. Incomplete washing or insufficient post-curing of the printed index may leave residual uncured monomer on the internal surface, potentially causing adhesion between the index and the composite resin. Thorough cleaning, typically using isopropyl alcohol, followed by appropriate post-curing under standardized conditions, is therefore essential. Fourth, cost considerations should be acknowledged. The technique requires fabrication of two separate indices, which may increase material consumption and production time compared with single-index approaches. Nevertheless, when compared with indirect ceramic restorations, the technique may represent a conservative and cost-effective alternative, particularly in multiunit anterior cases where preservation of tooth structure is a primary objective.

Although full-arch rubber dam isolation is generally recommended for adhesive procedures, it was not employed in this case because the tension generated during placement could potentially distort the flexible inner liner of the bilayered index. Instead, effective isolation was achieved using a cheek-lip-tongue retractor in combination with a split-dam technique, which provided sufficient control of moisture and visibility. In addition, the use of Katana Cleaner has been reported to efficiently remove contamination from saliva, blood, and temporary materials [24], thereby supporting reliable bonding performance.

While the relatively rigid outer layer of the index may help counteract dam tension and allow seating under compression, future CAD developments may further improve dam adaptation through margin-scalloped designs. Nevertheless, isolation strategies should remain flexible and goal-oriented, prioritizing optimal clinical control rather than strict adherence to a single standardized approach.

As this report describes a single clinical case without quantitative validation, the findings should be interpreted with caution as clinical observations rather than outcomes. Minor deviations from the digital plan may occur due to the inherent variability of the injection procedure or intentional occlusal adjustments to harmonize the restoration with functional guidance. While the short-term outcome was favorable, future prospective studies with larger cohorts and quantitative measurements are required to objectively evaluate the durability, seating accuracy, dimensional stability, and clinical reproducibility of this digital workflow. Nevertheless, this case illustrates the clinical feasibility of the proposed technique and provides a foundation for further systematic investigation.

## CONCLUSIONS

The bilayered 3D-printed clear index system used within a fully digital workflow facilitated precise, minimally invasive restoration of post-orthodontic anterior tooth wear in a single clinical session. This approach enabled controlled composite injection and efficient finishing while maintaining the planned tooth morphology. Within the inherent limitations of this single case study, this technique suggests a potential conservative alternative for the management of anterior tooth wear. Further clinical studies with larger sample sizes and longer follow-up periods are required to confirm its long-term performance and broader applicability.

### CONFLICT OF INTEREST

In compliance with the ICMJE uniform disclosure form, all authors declare the following: Keiichi Hosaka and Keiichiro Watanabe are the Chief Dental Officer (CDO) and Chief Technology Officer (CTO) of Amidex Inc. (Tokushima, Japan), respectively. Junji Tagami is a Scientific Advisory Board member of *Restorative Dentistry and Endodontics* and was not involved in the review process of this article.

### FUNDING/SUPPORT

This research was supported by the Grant-in-Aid for Scientific Research, Grant Number 23K09202 from the Ministry of

Education, Culture, Sports, Science and Technology of Japan and Research Cluster program of Tokushima University, grant number 2402003.

## ACKNOWLEDGMENTS

The authors thank DT Masaya Hashimoto, DT Mayu Watanabe, and DT Yukiko Hashiguchi (Amidex Inc., Tokushima, Japan) for technical assistance in the fabrication of the bilayered clear indices used in this case.

## AUTHOR CONTRIBUTIONS

Conceptualization, Methodology, Supervision: Hosaka K. Data curation: Utsumi Y. Formal analysis: Utsumi Y, Watanabe K, Matsuki S. Validation: Loomans B, Tanaka E, Scotti N, Tagami J. Writing - original draft: Utsumi Y, Hosaka K. Writing - review & editing: All authors. All authors read and approved the final manuscript.

## DATA SHARING STATEMENT

The datasets are not publicly available but are available from the corresponding author upon reasonable request.

## DISCLOSURE OF GENERATIVE AI IN SCIENTIFIC WRITING

During the preparation of this manuscript, the authors used ChatGPT (OpenAI) for English-language editing and improvement of readability. The authors reviewed and edited the output and take full responsibility for the article's content.

## REFERENCES

1. Mehta SB, Crins L, Attin T, Loomans BA. Restorative therapy of erosive tooth wear lesions: direct restorations. Monogr Oral Sci 2025;33:246-260.
2. Utsumi Y, Watanabe K, Matsuki S, Sakamaki T, Tanaka E, Hosaka K. Resin composite injection technique with a digital workflow to reconstruct canine guidance: a two-year follow-up. J Adhes Dent 2025;27:155-161.
3. Alani A, Mehta S, Koning I, Loomans B, Pereira-Cenci T. Restorative options for moderate and severe tooth wear: a systematic review. J Dent 2025;156:105711.
4. Terry DA. Developing a functional composite resin provisional. Am J Esthet Dent 2012;2:56-66.
5. Terry DA, Powers JM. A predictable resin composite injection technique, part I. Dent Today 2014;33:96, 98-101.
6. Terry DA, Powers JM, Mehta D, Babu V. A predictable resin composite injection technique, part 2. Dent Today 2014;33:12.
7. Tolotti T, Sesma N, Mukai E. Evolution of the guided direct composite resin technique in restorative dentistry: a systematic review. J Esthet Restor Dent 2025;37:902-919.
8. Basheer RR, Hasanain FA, Abuelenain DA. Evaluating flexure properties, hardness, roughness and microleakage of high-strength injectable dental composite: an in vitro study. BMC Oral Health 2024;24:546.
9. Ammannato R, Ferraris F, Marchesi G. The "index technique" in worn dentition: a new and conservative approach. Int J Esthet Dent 2015;10:68-99.
10. Ammannato R, Rondoni D, Ferraris F. Update on the 'index technique' in worn dentition: a no-prep restorative approach with a digital workflow. Int J Esthet Dent 2018;13:516-537.
11. Hosaka K, Tichy A, Hasegawa Y, Motoyama Y, Kanazawa M, Tagami J, *et al*. Replacing mandibular central incisors with a direct resin-bonded fixed dental prosthesis by using a bilayering composite resin injection technique with a digital workflow: a dental technique. J Prosthet Dent 2021;126:150-154.
12. Hosaka K, Tichy A, Motoyama Y, Mizutani K, Lai WJ, Kanno Z, *et al*. Post-orthodontic recontouring of anterior teeth using composite injection technique with a digital workflow. J Esthet Restor Dent 2020;32:638-644.
13. Ida Y, Yonekura K, Obayashi S, Muslimah DF, Hasegawa Y, Nakajima M, *et al*. A digitally enhanced transparent silicone index for the direct composite resin injection technique in premolar replacement: a case report. Oper Dent Endodontol Periodontol 2024;4:62-68.
14. Muslimah DF, Hasegawa Y, Antonin T, Richard F, Hosaka K. Composite injection technique with a digital workflow: a pragmatic approach for a protruding central incisor restoration. Cureus 2024;16:e58712.
15. Park SH, Piedra-Cascón W, Zandinejad A, Revilla-León M. Digitally created 3-piece additive manufactured index for direct esthetic treatment. J Prosthodont 2020;29:436-442.
16. Watanabe K, Tanaka E, Kamoi K, Tichy A, Shiba T, Yonerakura K, *et al*. A dual composite resin injection molding technique with 3D-printed flexible indices for biomimetic replacement of a missing mandibular lateral incisor. J Prosthodont Res 2024;68:667-671.
17. Watanabe K, Tichy A, Kamoi K, Hiasa M, Yonekura K, Tanaka E, *et al*. Restoration of a microdont using the resin composite injection technique with a fully digital workflow: a flexible 3D-printed index with a stabilization holder. Oper Dent 2023;48:483-489.


https://doi.org/10.5395/rde.2026.51.e36

18. Zhang Y, Zhang J, Fan L, Yu H. Closing post-orthodontic spaces between anterior teeth using sequential 3D-printed direct composite injection guides. Oper Dent 2022;47:612-619.
19. Zhu J, Wei J, Anniwaer A, Huang C. Esthetic rehabilitation of labial tooth defects caused by caries of the anterior teeth using a composite resin injection technique with veneer-shaped 3D printing indices. J Prosthodont Res 2025;69:127-132.
20. Hosaka K, Tichy A, Yamauti M, Watanabe K, Kamoi K, Yonekura K, *et al*. Digitally guided direct composite injection technique with a bi-layer clear mini-index for the management of extensive occlusal caries in a pediatric patient: a case report. J Adhes Dent 2023;25:211-218.
21. Aránguiz V, Lara JS, Marró ML, O'Toole S, Ramírez V, Bartlett D. Recommendations and guidelines for dentists using the basic erosive wear examination index (BEWE). Br Dent J 2020;228:153-157.
22. Coachman C, De Arbeloa L, Mahn G, Sulaiman TA, Mahn E. An improved direct injection technique with flowable composites: a digital workflow case report. Oper Dent 2020;45:235-242.
23. Muslimah DF, Putra Wigianto AY, Sanon K, Kamoi K, Ida Y, Iuchi T, *et al*. Trueness and precision of composite injection technique: roles of index design, composite flowabilities, and impression workflow. J Dent 2026;166:106325.
24. Toledano M, Osorio E, Espigares J, González-Fernández JF, Osorio R. Effects of an MDP-based surface cleaner on dentin structure, morphology and nanomechanical properties. J Dent 2023;138:104734.

RDE Restorative Dentistry & Endodontics

Retraction Notice

eISSN 2234-7666
Restor Dent Endod. 2026 August;51(3):e38
https://doi.org/10.5395/rde.2026.51.e38

# Retraction of "*Discoloration of teeth due to different intracanal medicaments*" published in *Restorative Dentistry and Endodontics*

**Retracted article:**
Afkhami F, Elahy S, Nahavandi AM, Kharazifard MJ, Sooratgar A. Discoloration of teeth due to different intracanal medicaments. Restor Dent Endod 2019;44(1):e10. https://doi.org/10.5395/rde.2019.44.e10

This article has been retracted by the editorial board of *Restorative Dentistry and Endodontics* (RDE).

Following publication, concerns were raised regarding the reliability of the data reported in this article, including the duplication of Tables 4 and 5. The authors attributed the duplication to a reporting error and submitted a corrected version of Table 5. However, the journal determined that further assessment was necessary and requested the underlying raw data. A post-publication investigation was initiated, and the materials submitted by the authors were reviewed by the Ethics Committee of RDE.

The review identified the following concerns:

(1) Several values reported as standard deviations appeared to represent standard errors of the mean. This apparent systematic reporting error would understate the variability in the data and could affect the interpretation of the findings.

(2) Several values presented in the published tables could not be reproduced from, or reconciled with, the raw dataset. The discrepancies exceeded those reasonably explainable by rounding.

(3) The raw dataset contained duplicate observations and patterns that raised additional concerns regarding data reliability. Although these findings did not constitute conclusive evidence of research misconduct, they further limited confidence in the reported results.

After consideration of the authors' explanations, the raw data, and the independent statistical review, the editorial board concluded that the reliability of the published findings could not be assured. The article is therefore retracted to correct the scientific record, in accordance with the guidance of the Committee on Publication Ethics (COPE).

The corresponding author was informed of this decision and did not agree to the retraction.
The Editorial Board of RDE regrets any inconvenience this may have caused readers.

**Received:** August 11, 2026 **Accepted:** August 11, 2026

*Restorative Dentistry and Endodontics* (*Restor Dent Endod, RDE*) is a peer-reviewed and open-access electronic journal providing up-to-date information regarding the research and developments on new knowledge and innovations pertinent to the field of contemporary clinical operative dentistry, restorative dentistry, and endodontics. In the field of operative and restorative dentistry, the journal deals with diagnosis, treatment planning, treatment concepts and techniques, adhesive dentistry, esthetic dentistry, tooth whitening, dental materials, and implant restoration. In the field of endodontics, the journal deals with a variety of topics such as etiology of periapical lesions, outcome of endodontic treatment, surgical endodontics including replantation, transplantation and implantation, dental trauma, intracanal microbiology, endodontic materials (MTA, nickel-titanium instruments, etc), molecular biology techniques, and stem cell biology. *RDE* publishes research articles, review articles and case reports dealing with aforementioned topics from all over the world.

Manuscripts submitted to *RDE* should be prepared according to the instructions below. For issues not addressed in these instructions, the author should refer to the Recommendations for the Conduct, Reporting, Editing, and Publication of Scholarly Work in Medical Journals (http://www.icmje.org/recommendations/) from the International Committee of Medical Journal Editors (ICMJE).

## Research and Publication Ethics

All of the manuscripts should be prepared based on strict observation of research and publication ethics guidelines recommended by the Council of Science Editors (https://www.councilscienceeditors.org), International Committee of Medical Journal Editors (ICMJE, https://www.icmje.org), World Association of Medical Editors (WAME, https://www.wame.org), and the Korean Association of Medical Journal Editors (KAMJE, https://www.kamje.or.kr/en/main_en).

All studies involving human subjects or human data must be reviewed and approved by a responsible Institutional Review Board (IRB). Please refer to the principles embodied in the Declaration of Helsinki (https://www.wma.net/policies-post/wma-declaration-of-helsinki-ethical-principles-for-medical-research-involving-human-subjects) for all investigations involving human materials. Animal experiments also should be reviewed by an appropriate committee (IACUC) for the care and use of animals. Also, studies with pathogens requiring a high degree of biosafety should pass review of a relevant committee (Institutional Biosafety Committee). The approval should be described in the Methods section. For studies of humans including case reports, state whether informed consents were obtained from the study participants (or from a parent or legal guardian if the participant is unable to provide consent). The editor of *RDE* may request submission of copies of the documents regarding ethical issues.

The *RDE* will follow the guidelines of the Committee on Publication Ethics (COPE, https://publicationethics.org) for the settlement of any misconduct.

## Authorship

Authorship credit should be based on (1) substantial contributions to conception and design, acquisition of data, and analysis and interpretation of data; (2) drafting the article or revising it critically for important intellectual content; (3) final approval of the version to be published; and (4) agreement to be accountable for all aspects of the work in ensuring that questions related to the accuracy or integrity of any part of the work are appropriately investigated and resolved. Authors should meet these four conditions.

**Role of Corresponding Author:** The corresponding author takes primary responsibility for communication with the journal during the manuscript submission, peer review, and publication process. The corresponding author typically ensures that all of the journal's administrative requirements, such as providing the details of authorship, ethics committee approval, clinical trial registration documentation, and conflict of interest forms and statements, are properly completed, although these duties may be delegated to one or more co-authors. The corresponding author should be available throughout the submission and peer review process to respond to editorial queries in a timely manner, and after publication, should be available to respond to critiques of the work and cooperate with any requests from the journal for data or additional information or questions about the article.

**Contributors:** Any researcher who does not meet all four ICMJE criteria for authorship discussed above but contribute substantively to the study in terms of idea development, manuscript writing, conducting research, data analysis, and financial support should have their contributions listed in the Acknowledgments section of the article.

**Changes to Authorship:** Any changes to authorship (the addition, deletion or rearrangement of author names in the authorship of accepted manuscript) needs to be approved by the Editor-in-Chief after a written confirmation by a corresponding author including the reason the name should be rearranged and all the signature of co-authors.

For more information, please refer to the Research and Publication Ethics page on the journal website.

## Copyrights, Open Access, Data Sharing, and Archiving

**Copyright:** Copyright in all published material is owned by the Korean Academy of Conservative Dentistry. Authors must agree to transfer copyright (https://rde.ac/src/author_form.pdf) during the submission process. The corresponding author is responsible for submitting the copyright transfer agreement to the publisher.

**Open Access Policy:** *RDE* is an open-access journal. Articles are distributed under the terms of the Creative Commons Attribution License (https://creativecommons.org/licenses/by-nc/4.0/), which permits unrestricted non-commercial use, distribution, and reproduction in any medium, provided the original work is properly cited. Author(s) do not need permission to use tables or figures published in *RDE* in other journals, books, or media for scholarly and educational purposes.

**Data Sharing:** *RDE* encourages data sharing wherever possible unless this is prevented by ethical, privacy, or confidentiality matters. Authors may deposit their data in a publicly accessible repository and include a link to the DOI within the text of the manuscript.

**Clinical Trials:** *RDE* accepts the ICMJE Recommendations for data sharing statement policy. Authors may refer to the editorial, "Data Sharing Statements for Clinical Trials: A Requirement of the International Committee of Medical Journal Editors," in the Journal of Korean Medical Science (https://doi.org/10.3346/jkms.2017.32.7.1051).

**Archiving Policy:** It is accessible without barrier from PubMed Central (https://www.ncbi.nlm.nih.gov/pmc/journals/2010/), Korea Citation Index (https://kci.go.kr), or National Library of Korea (https://nl.go.kr) in the event a journal is no longer published.

For more information, please refer to the Editorial Policy page on the journal website.

## Article Processing Charge

Authors of accepted articles must pay the following fees:
An Article Processing Charge (APC) of USD 300 shall be levied on Review Articles, Research Articles, and Case Reports submitted on or after May 1, 2026.
Editorials, Letters to the Editor, Open Lectures, and Readers' Forum articles are exempt from the APC.
A transaction fee of 3% may be applied, as applicable, depending on the payment method.

## Submission of Manuscripts

**Copyright Assignment:** Authors submitting a paper do so on the understanding that the work and its essential substance have not been published before and are not being considered for publication elsewhere. The submission of the manuscript by the authors means that the authors automatically agree to assign exclusive copyright to *RDE* if and when the manuscript is accepted for publication.

**Submission:** *RDE* requires electronic submission of all manuscripts. All manuscripts must be submitted to *RDE* through the website (https://www.editorialmanager.com/rde/) with a cover letter to the editor. Manuscripts may be submitted at any time. Authors may send queries concerning the submission process, manuscript status, or journal procedures to the Editor. Please contact the Editor by E-mail at editor@rde.ac.

**Blinded Peer Review Process:** Manuscripts that do not conform to the general aims and scope of the journal will be returned immediately without review. All other manuscripts will be reviewed by experts in the corresponding field (at least two referees). The Editorial Board may request authors to revise the manuscripts according to the reviewer's opinion. The revised manuscript may go through a second review by referees. A final decision on approval of publication of the submitted manuscripts is made by the Editorial Board.

## Manuscript Preparation

### General Requirements

- **Publication types:** Articles falling into the following categories are invited for submission: Research Articles, Case Reports, Review Articles, Editorials, Open Lectures, and Comments for the Reader's Forum.
- **Language:** The language of publication is English. It is recommended that international authors who are not native speakers of English seek help during manuscript preparation. The authors must have the article reviewed by a professional English editorial service before submission and submit the certificate of English proofreading as a supplement. The terminology used should follow the most recent edition of Dorland's Illustrated Medical Dictionary.
- **General text style:** Use Times New Roman 10-point font. Scientific units should be followed by the International System of Units. When non-standard terms appearing 3 or more times in the manuscript are to be abbreviated, they should be written out completely in the text when first used with the abbreviation in parenthesis. For medicine, use generic names. If a brand name should be used, insert it in parentheses after the generic name.
- **Statistical analysis:** Authors are strongly encouraged to consult a statistician for statistical analysis. Manuscripts with inappropriate statistical analysis methods will be returned to the authors without being reviewed.
- **Ethical approval:** All studies using human and animal subjects or specimens obtained from such subjects (such as extracted teeth) should include an explicit statement in the Methods section identifying the review and approval by the ethics committee for each study and provide an approval number. Manuscripts must be accompanied by a statement in the cover letter that the experiments were undertaken with the understanding and written consent of each subject and according to the above-mentioned principles.
- **Permissions:** If all or parts of previously published quotations, tables, or illustrations are used, permission must be obtained from the copyright holder concerned. The authors will be held responsible for failing to acquire proper permission before submission.
- **Reporting guideline:** For specific study designs, such as randomized controlled trials, studies of diagnostic accuracy, meta-analyses, observational studies, and non-randomized studies, we strongly recommend that authors follow and adhere to the reporting guidelines relevant to their specific research design. Randomized controlled trials should be presented according to the CONSORT guidelines (http://www.consort-statement.org). For case reports, authors should follow the CARE guidelines (https://www.care-statement.org). Authors should upload a completed checklist for the appropriate reporting guidelines during initial submission. Some reliable sources of reporting guidelines are EQUATOR Network (https://www.equator-network.org/) and NLM (https://www.nlm.nih.gov/services/research_report_guide.html).
- **Data statement:** Authors should state the availability of data in submission. If you have made your research data available in a data repository, you can link your article directly to the dataset. If the data is unavailable to access or unsuitable to post, authors must indicate why during the submission process, for example by stating that the research data is confidential. The statement will appear with your published article.

## Manuscript Structure and Format

Key features and limits of articles are summarized below. However, the limits are negotiable with the editor.

| Type | Abstract | Reference (max) | Table/Fig (max) |
|---|---|---|---|
| Review Article | · Unstructured<br>· Max 200 words | 70 | NL |
| Research Article | · Structured<br>: Objectives / Methods / Results / Conclusions<br>· Max 250 words | 40 | Total 8 |
| Case Report | · Unstructured<br>· Max 200 words | 30 | Total 6 |
| Editorial | No abstract | 10 | Total 2 |
| Open Lectures | No abstract | NL | NL |
| Comments for the Reader's Forum | No abstract | NL | NL |

NL, no limit.

Units, symbols, figures, tables, and references used must conform to the current issue or the linked article on our website.

- **Title page:** The title page of the manuscript should include the title of the article, the full name of the author(s), academic degrees, institutional affiliations, a running title (of seven or fewer words), correspondence, and declarations.
  - Title: The title should be concise and precise. It should be of 20 or less words, or it should fit within two lines. Only the first letter of the first word of the title should be capitalized.
  - Authors: Listed authors should include only those individuals who have made a significant creative contribution. *RDE* allows multiple authors to be specified as having equally contributed to the article as co-first authors or co-corresponding authors. While the contact information of all the corresponding authors is published in the article, only one corresponding author (the submitting author) is solely responsible for communicating with the journal.
  - Correspondence: The affiliation, address, telephone number, and e-mail address should be given.
  - Declarations: The declarations include conflicts of interest, funding, authors' contributions, ORCID, data availability statement, and acknowledgments.

| | |
|---|---|
| Conflicts of interest | If there are any conflicts of interest, authors should disclose them in the manuscript. Disclosures allow editors, reviewers, and readers to approach the manuscript with an understanding of the situation and background of the completed research. If there are no conflicts of interest, authors should include the following sentence: "No potential conflict of interest relevant to this article was reported." |
| Funding | All sources of funding applicable to the study should be stated here explicitly. |
| Authors' contributions | The contributions of all authors must be described using the CRediT (https://casrai.org/credit/) taxonomy of author roles. |
| | **Author Contributions**<br>Conceptualization: name; Data curation: name; Formal analysis: name; Funding acquisition: name; Investigation: name; Methodology: name; Project administration: name; Resources: name; Software: name; Supervision: name; Validation: name; Visualization: name; Writing - original draft: name; Writing - review & editing: name. (name: the last name and initials; eg, Cho BH) |
| ORCID | All authors are required to provide ORCID identification numbers. Please list the names of all authors and include the corresponding ORCID iD next to each name. |
| | **ORCID**<br>Byeong-Hoon Cho https://orcid.org/0000-0001-9641-5507<br>Kyung-San Min https://orcid.org/0000-0002-1928-3384 |
| Data availability statement | **Data are available in a public, open-access repository:**<br>Please state the repository name, the persistent URL, and any conditions of reuse. All data that are publicly available and used in the writing of an article should be cited in the text and the reference list, whether they are data generated by the author(s) or by other researchers.<br><br>**Data are available upon reasonable request:**<br>Please describe the data (eg, de-identified participant data), who has access to the data, their publishable contact information, and the conditions under which reuse is permitted.<br><br>**All study-related data is included in the publication or provided as supplementary information:**<br>Please ensure this does not include patient identifiable data.<br><br>**Data sharing is not relevant because no datasets were created and/or analyzed for this study:**<br>Please state 'Not applicable' in this section.<br><br>**No data are available:**<br>Please state 'Not applicable' in this section. |

| | |
|---|---|
| Acknowledgments | All persons who have made substantial contributions, but who have not met the criteria for authorship, are acknowledged here. |

- **Abstract:** The abstract should consist of a single paragraph with no more than 250 words for research articles and 200 words for case reports or review articles and should give details of what was done. The structured abstracts of research articles are to contain the following major headings: **Objective, Methods, Results, Conclusion**; and Keywords of no more than six words in alphabetical order. The abstracts of review articles or case reports don't need a structured format, but keywords should be listed. The keywords should be from Medical Subject Headings (MeSH) when possible (https://meshb.nlm.nih.gov/search) but non-MeSH subject headings may be used if deemed appropriate by the authors. Keywords should be written in small alphabetic letters with the first letter in capital. Separate each word by a semicolon.
- **Main text**
  - Introduction: The introduction should briefly review the pertinent literature in order to identify the gap in knowledge that the study is intended to address. The purpose of the study, the tested hypothesis, and its scope should be described.
  - Methods: The explanation of the experimental methods should be concise and sufficient for repetition by other qualified investigators. Procedures that have been published previously should not be described in detail. However, new or significant modifications of previously published procedures need full descriptions. Clinical studies or experiments using laboratory animals or pathogens should mention approval of the studies by relevant committees in this section. The sources of special chemicals or preparations should be given along with their location (name of company, city and state, and country). If the study utilized a commercial product, the generic term should be used and the product name, manufacturer, city, and country should be stated in parentheses. The methods of statistical analysis and the criteria for determining significance levels should be described.

An **ethics statement** should be placed here when the studies are performed using clinical samples or data, and animals. An exemplary is shown below.

| | |
|---|---|
| Human | The study protocol was approved by the Institutional Review Board of OOO (IRB No: OO-OO-OO). Informed consent was obtained by all participants (or the participant's legal guardian) / Informed consent was waived by the IRB. |
| Animal | The procedures used and the care of animals were approved by the Institutional Animal Care and Use Committee at OOO University (approval No. ******). |
| Clinical trial | This is a randomized clinical trial on the second phase, registered at the Clinical Research Information Service (CRIS, https://cris.nih.go.kr), No. *******.<br>* Other international registration is also acceptable. |

Description of participants: Ensure correct use of the terms sex (when reporting biological factors) and gender (identity, psychosocial or cultural factors), and, unless inappropriate, report the sex or gender of study participants, the sex of animals or cells, and describe the methods used to determine sex or gender. If the study was done involving an exclusive population, for example in only one sex, authors should justify why, except in obvious cases (eg, prostate cancer). Authors should define how they determined race or ethnicity and justify their relevance.

  - Results: This section should present only the observations with minimal reference to earlier literature or possible interpretations by the authors. Data must not be duplicated in Tables and Figures. In tables and figures, magnification rates and units should be stated. SI (Le système International d'Unités) units should be used. Tables, figures, and legends of tables and figures may be included in the text or attached as separate pages at the end of the manuscript. Files containing figures and tables must also be submitted as separate files.
  - Discussion: The discussion section should describe the major findings of the study. Both the strengths and the weaknesses of the observations should be discussed. In addition, suggestions for further research topics may be included if needed.
  - Conclusions: A brief conclusion based on the findings of the study and a comment on the potential clinical relevance of the findings should be summarized. The conclusion section should be described in a narrative manner, without numbering.
- **References:** References should be obviously related

to the document. In the text, references should be cited with Arabic numerals in brackets, numbered in the order cited. The reference list should be typed double-spaced on a separate page and numbered in the order the reference citations appear in the text. For journal citations, include surnames and initials of authors, complete title of article, name of journal (abbreviated according to the NLM Catalog; https://www.ncbi.nlm.nih.gov/nlmcatalog/journals/), volume, inclusive page numbers, and year of publication. When books are cited, either inclusive page numbers or chapter numbers should be included. Please note that theses or doctoral dissertations, which have not been published in peer-reviewed journals, should not be cited as references.

If needed, single or double authors should be acknowledged in the text, eg, Ford and Roberts. If there are more than two authors, the first author followed by *et al*. is sufficient, eg, Tobias *et al*.

We recommend the use of EndNote for reference management and formatting. For reference style and format, please refer to the following examples.

| | |
|---|---|
| Journal article | 1. Oh HK, Shin DH. Effect of adhesive application method on repair bond strength of composite. Restor Dent Endod 2021;46:e32.<br>List all authors when six or fewer (ex. reference 1); when seven or more, list six and add *et al*. (ex. reference 2 and 4).<br><br>2. Bergamo ET, Yamaguchi S, Lopes AC, Coelho PG, de Araújo-Júnior EN, Benalcázar Jalkh EB, *et al*. Performance of crowns cemented on a fiber-reinforced composite framework 5-unit implant-supported prostheses: in silico and fatigue analyses. Dent Mater 2021;37:1783-1793.<br><br>3. Shah RA, Hsu JI, Patel RR, Mui UN, Tyring SK. Antibiotic resistance in dermatology: the scope of the problem and strategies to address it. J Am Acad Dermatol 2021 Sep 20 [Epub]. https://doi.org/10.1016/j.jaad.2021.09.024.<br><br>4. Van Meerbeek B, Vargas M, Inoue S, Yoshida Y, Peumans M, Lambrechts P, *et al*. Adhesives and cements to promote preservation dentistry. Oper Dent 2001;(Supplement 6):119-144.<br><br>5. Yoshida Y, Van Meerbeek B, Okazaki M, Shintani H, Suzuki K. Comparative study on adhesive performance of functional monomers. J Dent Res 2003;82(Special Issue B):Abstract 0051, pB-19. |
| Book & Book chapter | 6. Seltzer S, Bender IB. The dental pulp: biologic considerations in dental procedures. 3rd ed. Lippincott; 1984. p400.<br><br>7. Fouad AF, Levin L. Pulpal reactions to caries and dental procedures. In: Hargreaves KM, Cohen S, Berman LH, eds. Cohen's pathways of the pulp. 10th ed. Mosby Elsevier; 2010. p504-528. |
| Website | 8. International Association of Dental Traumatology (IADT). The dental trauma guide [Internet]. IADT; 2014 [cited 2021 Jun 10]. Available from: https://dentaltraumaguide.org |
| Corporate publication | 9. ISO-Standards ISO 4287 Geometrical Product Specifications Surface texture. Profile method: terms, definitions and surface texture parameters. 1st ed. Geneve: International Organization for Standardization; 1997. p1-25. |

- **Tables:** Tables should be included in the text so that they may be edited if necessary. The title of each table should be placed on the top. The first letter of the first word should be capitalized. All abbreviations should be explained in each table. Footnotes should be indicated in superscript as [a), b), c)], and so on.
- **Figures:** Illustrations must be submitted in electronic format with file sizes appropriate for publication. Figures should be submitted as .tif or .jpg files. PowerPoint files are not accepted. All images should be at least 300 dpi and 5 × 5 cm in size, with 500 dpi recommended. If the figures represent a series of related content, it is recommended to present them as panels (A, B, C...) within a single figure. Figure legends should be included as text so that they be edited if necessary. All abbreviations should be explained in each figure. Microscopic images should include the staining method and magnification (eg, hematoxylin and eosin stain, ×400). Figures may use arrows, arrowheads, asterisks, circles, or other indicators as needed for clarity, with each indicated element described in the figure legends.
- **Other types of articles**
  - Review articles: Review articles should be divided into Introduction, Review, and Conclusions. The Introduction section should focus on placing the subject matter in context and justifying the need for the review. The Review section should be divided into logical sub-sections in order to improve readability and enhance understanding. Search strategies must be described and the use of state-of-the-art evi-

dence-based systematic approaches is expected. The use of tabulated and illustrative material is encouraged. The Conclusion section should reach clear conclusions and/or recommendations on the basis of the evidence presented. If a review includes a meta-analysis as part of a systematic review, it should be submitted as a research article.

- Case reports: Case reports should be divided into Introduction, Case Report(s), Discussion, and Conclusions. They should be well illustrated with clinical images, radiographs, diagrams, and where appropriate, supporting tables and graphs. However, all illustrations must be of the highest quality.
- Comments for the Reader's forum: Reader's forum will present various questions, suggestions, and critiques on the subjects of operative dentistry, restorative dentistry, and endodontics from the readers.

## Manuscript Files Accepted

- **Final version:** After a paper has been accepted for publication, the author(s) should submit the final version of the manuscript. The names and affiliations of authors should be double-checked, and if the originally submitted image files were of poor resolution, higher-resolution image files should be submitted at this time. Illustrations must be submitted in electronic format with file sizes appropriate for publication. All images should be at least 300 dpi and 5 × 5 cm in size, with 500 dpi recommended. Symbols (eg, circles, triangles, squares), letters (eg, words, abbreviations), and numbers should be large enough to be legible on reduction to the journal's column widths. All symbols must be defined in the figure caption. When submitted as separate files, name of the author, and illustration number should be stated in the file name. If references, tables, or figures are moved, added, or deleted during the revision process, renumber them to reflect such changes so that all tables, references, and figures are cited in numeric order.
- **Errata and Corrigenda:** To correct errors in published articles, the corresponding author should contact the journal's Editorial Office with a detailed description of the proposed correction. Corrections that profoundly affect the interpretation or conclusions of the article will be reviewed by the editors. Corrections will be published as corrigenda (corrections of author's errors) or errata (corrections of publisher's errors) in a later issue of the journal.

### Contacting the Journal

Editorial assistant: Hye-Young Lee
*RDE* editorial office
The Korean Academy of Conservative Dentistry
B163, Seoul National University Dental Hospital, 101 Daehak-ro, Jongno-gu, Seoul 03080, Korea
Tel: +82-2-763-3818, Fax: +82-2-763-3819, E-mail: editor@rde.ac

### History of the Recommendations

Enacted in March 2, 2012
Modified: August 4, 2023
Last modified: November 4, 2024

# Author's checklist

Authors have written the manuscript in compliance with Instructions to Authors and Recommendations for the Conduct, Reporting, Editing, and Publication of Scholarly Work in Medical Journals (https://www.icmje.org/icmje-recommendations.pdf) from the International Committee of Medical Journal Editors, and the Guideline of Committee on Publication Ethics (https://publicationethics.org).

## Cover letter

☐ Manuscript's title
☐ Statement that your paper has not been previously published and is not currently under consideration by another journal.
☐ Brief description of the research you are reporting in your paper, why it is important, and why you think the readers of the journal would be interested in it.
☐ Contact information for you and any co-authors.
☐ Confirmation that you have no competing interests to disclose.

## Title page

☐ Title page including the title of the article, the full name of the author(s), academic degrees, positions, institutional affiliations, a running title (of 7 or less words), correspondence, and declarations.

## Declaration

☐ Conflicts of interest, funding, authors' contributions, ORCID, data availability statement, and acknowledgments

## Abstract

☐ Original article: <250 words; structured abstract— Objective, Methods, Results, Conclusion
☐ Review article: <200 words; unstructured abstract
☐ Case report: <200 words; unstructured abstract

## Keyword

☐ Keywords should be from MeSH subject headings when possible.

## Main text

☐ Information regarding approval of an institutional review board and obtaining informed consent should be mentioned.
☐ Original article: Introduction/Methods/Results/Discussion/Conclusions
☐ Review article: Introduction/Review/Conclusions
☐ Case report: Introduction/Case Report(s)/Discussion/Conclusions

## Reference

☐ Refer to the reference format in the author's guideline.

## Table

☐ If tables are included, they should be included as text and not as illustrations so that they may be edited if necessary.

## Figure

☐ Figure legends should be included as text and not as illustrations so that they may be edited if necessary.

## Author's form

☐ All authors have completed the Copyright Transfer Agreement and Ethics Concerning Human Subjects.

## Conflict of interest form

☐ All authors have completed the COI Statement.

## Permission

☐ The authors are responsible for obtaining permission from the copyright holder to reprint any previously published material in RDE.

RDE Restorative Dentistry & Endodontics

# Copyright transfer agreement

**Manuscript title** ____________________________________________________________

**Corresponding author name** ________________________________________

**Fax** ____________________ **E-mail** ____________________

The authors of the article hereby agree that the Korean Academy of Conservative Dentistry holds the copyright on all submitted materials and the right to publish, transmit, sell, and distribute them in the journal or othermedia.

## Corresponding author

**Print name** ____________________

**Signed** ____________________ **Date** ____________________

## Co-authors

| | |
|---|---|
| **Print name** ____________ | **Print name** ____________ |
| **Signature/Date** ____________ | **Signature/Date** ____________ |
| **Print name** ____________ | **Print name** ____________ |
| **Signature/Date** ____________ | **Signature/Date** ____________ |
| **Print name** ____________ | **Print name** ____________ |
| **Signature/Date** ____________ | **Signature/Date** ____________ |
| **Print name** ____________ | **Print name** ____________ |
| **Signature/Date** ____________ | **Signature/Date** ____________ |

RDE Restorative Dentistry & Endodontics

# Conflict of interest form

**Manuscript title** ______________________________

As the corresponding author, I declare the following information regarding the specific conflicts of interest of authors of our aforementioned manuscript.

Examples of conflicts of interest include the following: source of funding, paid consultant to sponsor, study investigator funded by sponsor, employee of sponsor, board membership with sponsor, stockholder for mentioned product, any financial relationship to competitors of mentioned product, and others (please specify).

| Author | No conflict involved | Conflict (specify) |
|---|---|---|
| | | |
| | | |
| | | |
| | | |
| | | |
| | | |
| | | |
| | | |

I accept the responsibility for the completion of this document and attest to its validity on behalf of all co-authors.

**Corresponding author (name/signature)** ______________________ ______________________

**Date** ______________________